The Impact of Insulin and Insulin Therapy on Physiology in Critical Illness

Fatanah Mohamad Suhaimi

A thesis submitted in partial fulfilment
of the requirement for the Degree of
Doctor of Philosophy
in
Mechanical Engineering
at the
University of Canterbury,
Christchurch, New Zealand

Acknowledgments

This dissertation would not have been possible without the guidance and the help of several individuals who in one way or another contributed and extended their valuable assistance in the preparation and completion of this study.

First and foremost, my utmost gratitude to my supervisor, Professor J. Geoffrey Chase who has supported me throughout my thesis with his patience and knowledge whilst allowing me the room to work on my own way. One simply could not wish for a better or friendlier supervisor.

My sincere thanks also go to my co supervisor Dr. Geoffrey M. Shaw for the inputs and expertise brought into the research. My sincere thanks also go to Dr. Aaron Le Compte and Dr. Jessica Lin for their inputs. I greatly appreciate their knowledge and guidance throughout my study. They were also very enthusiastic and approachable. This research simply would not be possible without them.

This research has been a great joint effort between many parties to bring it to its current stage. My thanks extend back to all the people ever involved in this research project especially to the people of the Centre for Bioengineering at the University of Canterbury, clinical staffs at the Christchurch Hospital and technical staffs at the mechanical Engineering Department of University of Canterbury.

Many thanks also to Ministry of Higher Education Malaysia, Malaysian Government especially IPPT of USM in providing the funds in doing the research.

I also thank all my loving friends and family who supported me and make my life fulfilling. The deepest thanks go to my parents for their unconditional support and inspiration. They are the people who planted the seed in me that drives me to seek knowledge and solutions. Special thanks to the one above all of us, God, for answering my prayers in giving me the strength in life, thank you so much.

Contents

List of Figures

List of Tables

Nomenclature

Acronyms and abbreviations

AC	Alternating current
ACCP	American College of Chest Physicians
ADC	Analog digital converter
ANN	Artificial Neural Network
APACHE	Acute Physiology and Chronic Health Evaluation
BG	Blood glucose
BMI	Body mass index
CDF	Cumulative distribution function
CF	Clinical feedback
CI	Confidence interval
CRP	C-reactive protein
DC	Direct current
HR	Heart rate
ICU	Intensive care unit
ICING	Intensive Control Insulin Nutrition Glycemic
IL-6	Interleukin 6
IL-8	Interleukin 8
IQR	Inter-quartile range
IR	Infrared
IV	Intravenous
IVGTT	Intravenous Glucose Tolerance Tests
LED	Light emitting diode

MABP	Mean arterial blood pressure
MODS	Multiple organ dysfunction score
MOF	Multiple organ failure
MPC	Model predictive control
MSE	Mean squared error
MSOF	Multiple system organ failure
NPV	Negative predictive value
PCT	Procalcitonin
PID	Proportional integral derivative
PPV	Positive predictive value
R	Red
ROC	Receiver operating characteristic
RR	Respiratory rate
SCCM	Society of Critical Care Medicine
SIRS	Systemic inflammatory response syndrome
SOFA	Sepsis-related organ failure
SPRINT	Specialized Relative Insulin and Nutrition Tables
SSC	Surviving Sepsis Campaign
TGC	Tight glycaemic control
TNFα	Tumor necrosis factor alpha
VOT	Vascular occlusion test

Mathematical variables

α_G	Michaelis-Menten constant for insulin-stimulated glucose removal saturation [L/mU]
α_I	Michaelis-Menten constant for plasma insulin disappearance saturation [L/mU]
CNS	Central nervous system glucose uptake [mmol/min]
d_1	Transport compartment rates [1/min]
d_2	Transport compartment rates [1/min]
D	Dextrose from enteral feeding [mmol/min]
EGP_{max}	Endogenous glucose production at zero insulin [mmol/min]
EGP_b	Basal endogenous glucose production [mmol/min]
G	Total blood glucose level [mmol/L]
I	Blood plasma insulin concentration [mU/L]
I_B	Endogenous insulin production [mU/L/min]
k	Rate of insulin transport and utilisation in the interstitium [1/min]
k_I	Rate of endogenous insulin secretion [min/mU]
n	Plasma insulin decay rate [1/min]
n_I	Diffusion constant of insulin between compartments [L/min]
n_C	Cellular insulin clearance rate from interstitium [1/min]
n_K	Plasma insulin clearance rate at kidney [1/min]
n_L	Plasma insulin clearance rate at liver [1/min]

$P1$	Glucose in the stomach [mmol]
$P2$	Glucose in the gut [mmol]
P_{max}	Maximum enteral feeding [mmol/min]
p_G	Rate of endogenous glucose removal [1/min]
P_t	External nutrition [mmol/min]
Q	Interstitium insulin concentration
S_I	Insulin sensitivity index
$S_I(t)$	Insulin sensitivity profiles [L/mU/min]
u_{ex}	Exogenous insulin input [mU/min]
u_{en}	Endogenous insulin production [mU/min]
V_G	Glucose distribution volume [L]
V_I	Insulin distribution volume [L]
x_L	Fraction of extraction

Abstract

Hyperglycemia is prevalent in critical care, as patients experience stress-induced hyperglycemia, even with no history of diabetes. Hyperglycemia has a significant impact on patient mortality and other negative clinical outcomes such as severe infection, sepsis and septic shock. Tight glycemic control can significantly reduce these negative outcomes by reducing hyperglycemic episode, but achieving it remains clinically elusive, particularly with regard to what constitutes tight control and what protocols are optimal in terms of results and clinical effort.

The model used in this thesis is validated using an independent data and readily be used for different clinical interventions. Moreover, this model also able to accurately predict clinical intervention outcomes given that the model prediction error is very small, which is better than any other reported model. In particular, model-based glycemic control methods is used to capture patient-specific physiological dynamics, such as insulin sensitivity, S_I.

To date, sepsis diagnosis has been a great challenge despite advancement in technologies and medical research. Critically, septic patients are often classified by practitioners according to their experience before standard test results can be assessed, as to avoid delay in treatment. Moreover, several scoring systems have also been widely used to represent sepsis condition and better standardization of sepsis definition across different centers.

In this thesis, insulin sensitivity, S_I, a model-based metric is used to identify sepsis condition based on the finding that S_I represents metabolic

condition of a patient. Additionally, several clinical and physiological variables obtained during patient's stay in critical care are also investigated using mathematical computation and statistical analysis to identify relevant metric which can be accurately use for sepsis interventions. Even though information on S_I, clinical and physiological variables of a patient are insufficient to determine the sepsis status, these informations have brought to a different perspective of diagnosing sepsis.

Microcirculation dysfunction is very common in sepsis. Tracking of microcirculation state among septic patient enable better tracking of patient state particularly sepsis status. The tracking can potentially be done by using a pulse oximeter that can extract additional information related to oxygen extraction level. The processed signals are therefore represent relative absorption of oxyhemoglobin and reduced hemoglobin that can be used to assess microcirculation status.

In addition, this thesis focus on the real challenge of early treatment of sepsis and sepsis diagnosis where several potential metabolic markers are investigated. Microcirculation conditions are assessed using a non-invasive method that is generally used in typical ICU settings. In particular, the concept and method used to assess microcirculation and metabolic conditions are developed in this thesis.

Finally, the work presented in this thesis can act as a starting point for many other glycemic control problems in other environments. These areas include cardiac critical care and neonatal critical care that share most similarities to the environment studied in this thesis, to general diabetes where the population is growing exponentially world wide. Eventually, this added

knowledge can lead clinical developments from protocol simulations to better clinical decision making.

Chapter 1

Introduction

Clinically, hyperglycemia can be a marker of severity of illness and is directly associated with mortality [Krinsley, 2003; Egi et al., 2006; Laird et al., 2004; Jeremitsky et al., 2005]. Hyperglycemia is thus a very serious clinical illness and it is also associated with increases in other negative clinical outcomes, including severe infection [Bistrian, 2001], sepsis and septic shock [Branco et al., 2005; Das, 2003; Oddo et al., 2004], myocardial infarction [Capes et al., 2000], and polyneuropathy and multiple organ failure [Langouche et al., 2005; Van den Berghe et al., 2001].

Landmark studies by Van den Berghe et al [Van den Berghe et al., 2001, 2003] and Krinsley [Krinsley, 2004] focused significant attention and research on managing hyperglycemia and its effects. These studies formed a basis for several additional clinical and model-based studies [Van den Berghe et al., 2006a; Wong et al., 2006b; Chase et al., 2006; Doran et al., 2004b; Goldberg et al., 2004; Laver et al., 2004; Finfer and Heritier, 2009; Brunkhorst et al., 2008; Griesdale et al., 2009; Preiser et al., 2009]. As a result, it has become a significant research area in its own right, and has been recently reviewed by Chase et al [Chase et al., 2007, 2008a, 2010b, 2011b].

The incidence of hyperglycemia is very high globally and great improve-

ment has been documented in recent years with the use of tight glycemic control (TGC) in terms of reducing mortality and morbidity [Chase et al., 2008b; Krinsley, 2004; Van den Berghe et al., 2001, 2006a]. Despite differences in TGC protocol across different centers and studies, many positive outcomes have been documented from some trials. However, several others have found these results difficult to reproduce [Finfer and Heritier, 2009; Brunkhorst et al., 2008; Griesdale et al., 2009; Preiser et al., 2009]. More specifically, different target range of TGC management has been used in clinical trials ranging from 4.4-6.1 mmol/L [Chase et al., 2008b; Pachler et al., 2008; Dortch et al., 2008; Shulman et al., 2007; Juneja et al., 2009; Van den Berghe et al., 2001] and several others with wider or higher target ranges [Krinsley, 2004; Thomas et al., 2005; Preiser et al., 2009; Meynaar et al., 2007; Davidson et al., 2005].

Model-based glycemic control is an emerging treatment approach for managing hyperglycemia in critical illness. In particular, model-based glycemic control methods are able to directly capture the patient-specific physiological dynamics of the human metabolism. The benefits of using model-based glycemic control with TGC are better and adaptive control [Evans et al., 2011] through direct management of patient-specific variability [Lin et al., 2008; Chase et al., 2011b] that thus significantly reduces the risk of hypoglycemia seen using some TGC protocols [Brunkhorst et al., 2008; Preiser et al., 2009; Van den Berghe et al., 2006b; Preiser and Devos, 2007; Vanhorebeek et al., 2007a,b].

This chapter introduces and describes the relation between hyperglycemia, multiple organ failure and sepsis, which are some of the most command and critical problems faced in the ICU. All these issues have resisted

significant improvement despite advances in technology and medicine, and extensive clinical studies. The used of model-based glucose-insulin system models in critical illness enables the real-time identification of patient-specific model parameters that can be used to indicate patient condition. The ability to capture patient-specific model parameters in clinical settings, particularly in real-time, yields significant insight into the physiological condition of critically ill patients. Hence, model-based glycemic control methods offer significant potential to provide further tools to diagnose or guide treatment of other diseases.

1.1 Hyperglycemia in Critical Care

Hyperglycemia is common in acutely and critically ill patients [Capes et al., 2000; McCowen et al., 2001], including those who have not previously had diabetes [Capes et al., 2000; Krinsley, 2003; Van den Berghe et al., 2001]. It is defined as blood glucose concentration higher than a basal level of 4.4-5.5 mmol/L [Mizock, 2001]. For blood glucose concentrations consistently higher than 7 mmol/L, therapy should be initiated as recommended by the American Diabetes Association.

Hyperglycemia is highly associated with insulin resistance in critically ill patients [Wolfe et al., 1979, 1987; Shangraw et al., 1989; Capes et al., 2000] and known to stimulate glucose metabolism [Vander and Luciano, 2001]. Increased counter-regulatory hormone secretion stimulates endogenous glucose production and increases insulin resistance [McCowen et al., 2001; Mizock, 2001], elevating equilibrium glucose levels and reducing the amount of glucose

the body can utilize. Additionally, high glucose content nutritional support regimes can cause an excess of blood glucose that cannot be utilized [Patino et al., 1999; Weissman, 1999; Elia et al., 2005].

Hyperglycemia worsens outcomes, increasing myocardial infarction [Capes et al., 2000], severe risk of infection [Bistrian, 2001], sepsis and septic shock [Das, 2003; Branco et al., 2005; Oddo et al., 2004; Marik and Raghavan, 2004], and other critical illness such as axonal dysfunction and degeneration [Sidenius, 1982], polyneuropathy, and multiple organ failure [Van den Berghe et al., 2001; Langouche et al., 2005; Chase et al., 2010a]. Hyperglycemia also decreases immune function response [Marik and Raghavan, 2004; Weekers et al., 2003; Turina et al., 2005]. According to Weekers et al [Weekers et al., 2003], the immune response is essentially completely ineffective at 10 mmol/L and only ∼33% effective at 8 mmol/L. An ineffective immune response can have obvious significant consequences in terms of fighting off bacterial or viral infections, in addition to other complications noted. Finally, hyperglycaemia can also induce damage at a cellular level including immunosupression, inflammation, thrombosis and increased oxidative stress [Sarikabadayi et al., 2011; Hirsch and Brownlee, 2005; Lelkes et al., 2001; Xi et al., 2011].

Increasing hyperglycemia also correlates with increasing risk of death and increasing length of stay in ICU [Vlasselaers et al., 2009; Jeremitsky et al., 2005]. In addition, hyperglycemia, particularly severe hyperglycemia, is highly associated with increased morbidity and mortality [Krinsley, 2009, 2003; Laird et al., 2004]. Equally importantly, glycemic variability and poor control are independently associated with increased mortality [Krinsley, 2008; Ali et al., 2008; Egi et al., 2006].

Finally, the use of a certain drugs have been recognized to exacerbate hyperglycemia and thus mortality. For example, some steroid-based therapies antagonise insulin action and production, further exacerbating the problem [Pretty et al., 2011; Dimitriadis et al., 1997; Qi and Rodrigues, 2007]. Hence, glycemic level and variability are also at least partly a function treatment and thus, potentially, of patient diagnosis or disease.

From the nutritional input aspect, several studies [Dickerson, 2005; Krishnan et al., 2003; Dickerson et al., 2002; Iyer, 2002] have found that moderate nutrition reductions may reduce mortality. Krishnan and colleagues [Krishnan et al., 2003] showed that feeding over 66% of ACCP recommended rates increased the ICU mortality, as did feeding less than 33%. Reduced enteral nutrition [Elia et al., 2005; Ahrens et al., 2005; Kim et al., 2003] or its carbohydrate content [Patino et al., 1999] and reducing dextrose as a diluent in intravenous medication [Krajicek et al., 2005] can also result in reductions in glycemic levels.

Hence, a number of studies have investigated the effect on patient outcomes when blood glucose levels are controlled with insulin. Several have shown some measurable positive results showing the clear potential of this approach [Lewis et al., 2004; Mowery et al., 2011; Shan et al., 2011; Hasegawa et al., 2011; Arabi et al., 2011; Chase et al., 2008b; Krinsley, 2004; Malmberg, 1997; Van den Berghe et al., 2001, 2003; Finney et al., 2003; Laver et al., 2004]. These studies primarily examined the effectiveness of intensive insulin therapy on mortality, and/or the risk of hypoglycemia and other clinical outcomes. Hence, the use of intensive insulin therapy governed by frequent blood glucose monitoring are useful in improving blood glucose level in critically ill

patients. There is also evidence of significant reductions in the need for dialysis, bacteremia testing and the number of blood transfusions with aggressive blood glucose control using intensive insulin therapy [Van den Berghe et al., 2001, 2003; Krinsley, 2004; Malmberg et al., 1999]. All of these results point towards the conclusion that the control of blood glucose levels in critical care have a significant clinical impact.

In counterpoint, it must also be noted that several studies have not shown benefit [Finfer and Heritier, 2009; Brunkhorst et al., 2008; Preiser et al., 2009], as surveyed by Griesdale et al [Griesdale et al., 2009]. However, several of these studies failed to achieve good control [Chase et al., 2011b] primarily or potentially due to poor protocols and patient metabolic variability. Thus, while there is good evidence, clear and effective protocols are lacking to provide conclusive proof in the field.

1.2 Organ Failure

Infection is one of the worst outcomes of hyperglycemia and if not successfully controlled, it can lead to multiple organ failure (MOF) [Fry et al., 1980]. In MOF, patient may suffers acute respiratory failure, acute renal failure, cardiovascular failure and/or other organ dysfunctions. MOF is the leading cause of ICU mortality, regardless of etiology and cause.

The severity of organ dysfunction and illness on human have lead to the development of therapeutic interventions with the aim of reducing its incidence. However, the therapeutic intervention begins with the definition

for quantifying the degree of organ failure to assess therapies and treatments. Vincent and colleagues [Vincent et al., 1996] describe organ dysfunction as a process, rather than an event, since the process can be seen as a continuum. Table 1.1 lists the variables to describe organ dysfunction.

Table 1.1: Ideal variables for describing organ dysfunction [Vincent et al., 1996].

Objective
Simple, easily, available, but reliable
Obtained routinely and regularly in every institution
Specific for the function of the organ considered
Continuous variable
Independent of the type of patients
Independent of the therapeutic interventions

Several scoring system of organ failure/dysfunction have been developed to better describe the progression of complications such as SOFA (Sepsis-related Organ Failure Assessment), MODS (Multiple Organ Dysfunction Score), the Brussels Score, and MSOF (Multiple System Organ Failure). Most of the scoring systems were developed at a round table conference on clinical trials in sepsis [Sibbald and Vincent, 1995]. The objectives of these scoring systems is to represent and evaluate the increased complexity of disease and its continuum in patients. Specifically, patient risks and level of severity of their condition [Knaus et al., 1991] are the main objectives and to better assess treatment needs. Table 1.2 describes the similarities and differences of these scoring systems.

To date, these scoring systems only define the occurrence of organ fail-

ure and are incapable of prediction. Even though MSOF was designed for prediction, the outcome of clinical trials showed a lack of accuracy in this capability [Hebert et al., 1993]. Overall, SOFA is the most commonly used score in most ICU studies because of its simplicity and effectiveness in describing organ dysfunction [Vincent et al., 1998].

Despite of the various scoring systems used in ICU, the invention of new scoring systems is still taking place. In particular, clinicians and researchers are still looking to find a better system to represent the occurrence of organ failure and disease. Therefore, new scoring systems have been developed in an attempt to meet this challenge. However, the use of a scoring system depends on both its application and its level of complexity. As the system becomes more complex, it may not be effective at the ICU bedside or practicable, even if its predictive performance improves.

1.3 Sepsis

Sepsis is an increasingly common clinical condition defined by the presence of both infection and a systemic inflammatory response. Increasingly severe sepsis is defined by increasing organ failure, linking this condition with organ failure. Overall, sepsis is thus one of the most common and serious medical problems faced in ICU, with a 30-60% mortality rate with 11-15% of all cases defined as severe sepsis events [Angus et al., 2001] from the more than 751 000 cases of severe sepsis reported annually [Li et al., 2011]. In addition, the number of patients with sepsis increases significantly each year and the number of sepsis-related deaths is also increasing [Martin et al., 2003; Parrillo et al.,

Table 1.2: Similarities and differences between SOFA, MODS, Brussels and MOSF Scores.

SOFA Score	Description. Simple and easily calculated. Evaluate morbidity. Individualize degree of dysfunction of each organ. Developed in 1994 at ESICM meeting [Vincent et al., 1996].
MODS Score	Description. Complex. Evaluate morbidity. Individualize degree of dysfunction of each organ. Developed by J. Marshall et al [Marshall et al., 1995].
Brussels Score	Description. Complex. Evaluate morbidity and risk of mortality. Does not individualize degree of dysfunction of each organ. Developed by G. Bernard et al.
MSOF Score	Description. Simple Evaluate morbidity and risk of mortality Individualize degree of dysfunction of each organ Developed by P. Hebert et al [Hebert et al., 1993].

1990; Walkey et al., 2011] despite significant research to better understand the occurrence of this disease.

Sepsis has been classified into several stages according to definitions created by the Society of Critical Care Medicine (SCCM) in 1992 [Levy et al., 2003]. These stages are used for better representation for the occurrence of sepsis and to aid standardization of definitions between different centers. Detailed descriptions of these classifications are discussed in Chapter 5. To date, blood bacteria culture is considered as the only standard method for absolutely confirming an infection. However, this test requires incubation and standard procedures that result in a delayed outcome of 2-3 days preventing real-time monitoring. The delayed outcome consequently delays treatment and can thus worsen patient condition and risk if clinician wait for this result. Equally, $\sim$50% of all sepsis that is clinically defined is "culture negative" [Carrigan et al., 2004]. Hence, there are no ideal definitions nor any real-time definitions.

Several clinical trials [Walkey et al., 2011; Wagner et al., 2011; Cronshaw et al., 2011; Cardoso et al., 2010; Patel et al., 2010; Takahashi et al., 2011; Hirasawa et al., 2009] have examined the risk of death among sepsis patients. The Surviving Sepsis Campaign (SSC) is one of the collaborative initiatives to reduce mortality from severe sepsis and septic shock [Marshall et al., 2010]. This campaign has been supported by professional organizations around the world despite controversial issues around of the protocol used. The SSC provides standard care management guidelines. However, outcomes are varied across different centers [Machado and Mazza, 2010; Cronshaw et al., 2011; Tromp et al., 2011; Cardoso et al., 2010].

Nevertheless, clinical trials on septic patients remains a challenge. Many factors contribute to the difficulties in treating septic patients and designing clinical trials and protocols for effective diagnosis and treatment. However, one significant success has been the reduction in the incidence of sepsis has been observed by implementing a blood glucose control protocol [Van den Berghe et al., 2001; Takahashi et al., 2011; Hirasawa et al., 2009]. There are also some studies suggested different methods such as early administration of antibiotics [Kumar et al., 2006; Micek et al., 2011], fluid resuscitation [Khan et al., 2011; Nguyen et al., 2011], administration of activated protein C [Wagner et al., 2011; Cohen et al., 2011] and early goal-directed therapy [Rivers et al., 2001; Sivayoham et al., 2011; Burney et al., 2011; Turi and Von Ah, 2011; Colin et al., 2011].

However, most current research on sepsis focuses more on finding a better test or method that can confirm the existence of infection, one of the cornerstones of sepsis, as early as possible. Early diagnosis is critical because early interventions have been documented to reduce mortality from 46.5% to 30.5% [Rivers et al., 2001] and thus show significant potential. Moreover, early goal-directed resuscitation is recommended for the septic patient, particularly during the first 6 hours after infection recognition [Dellinger et al., 2004]. Hence, the ability to recognize infection and diagnose sepsis as early as possible will consequently improve mortality outcome and patient condition.

In this thesis in particular, the link between one effective therapeutic approach, glycemic control, and sepsis diagnosis is investigated directly. More specifically, is there a link between model-based metabolic markers and sepsis? Such a link would have potential given the success of model-based glycemic

control [Chase et al., 2007, 2008a, 2010b, 2006].

1.4 The Glucose-Insulin Regulatory System

Immediately after a high carbohydrate meal, nutrients enter the blood and lymph from the gastrointestinal tract as monosaccharides, triglycerides, and amino acids. The glucose absorbed into blood from carbohydrate causes rapid secretion of insulin and consequently increases blood glucose levels. The insulin leads to glucose uptake and storage for later use by almost all the tissues in the body [Guyton, 1991]. Most of the glucose absorbed is stored in the liver in the form of glycogen. When food is not consumed, blood glucose concentration falls and glycogen is transformed to glucose for energy and to prevent low or hypo- glycemia. However, if the amount of glucose absorbed is too high and exceeds the limit the liver can store as glycogen, the excess glucose will be transformed into fatty acids. Figure 1.1 illustrates the overall glucose-insulin regulatory system in which insulin and glucagon play critical functions in glucose homeostasis and serve as acute regulators of blood glucose concentration.

1.4.1 Glucose

Glucose is a simple form of sugar that plays an important role in providing energy to the human body. Glucose is stored mainly in the liver and muscle cells as glycogen. Typically, the blood glucose concentration for normal individual is in a range between 4.4 and 5.0 mmol/L before breakfast and 6.7 to

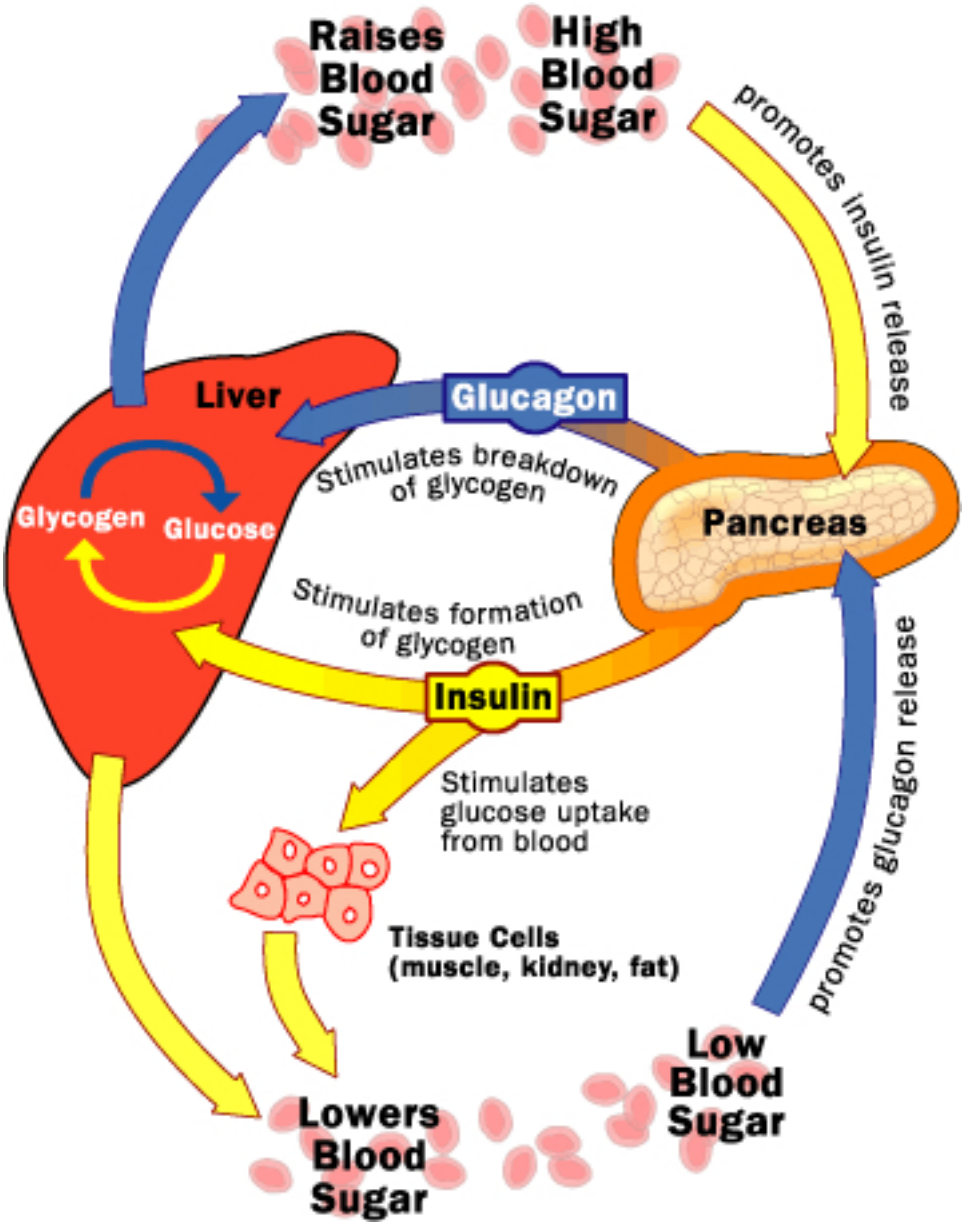

Figure 1.1: Diabetes insulin glucose model system. The schematic shows effect of high and low blood glucose levels on the body. Adapted from health.howstuffworks.com.

7.8 mmol/L after a meal. However, a high glucose intake from carbohydrate of all forms results in high blood glucose levels or extracellular hyperglycemia. When the blood glucose concentration falls, glucagon is secreted by the *alpha* cells of the pancreas to increase blood glucose concentration. Glucagon is a large polypeptide hormone and composed of a chain of 29 amino acids that stimulates EGP or endogenous glucose production from the liver [Guyton, 1991].

1.4.2 Insulin

Insulin is a hormone produced by the *beta* cells in the pancreas [Guyton, 1991]. Insulin can be conceptualized as glucose-regulatory and glucose-counterregulatory hormone [Jefferson et al., 2001]. In particular, insulin secretion increases to lower plasma glucose at high levels of blood glucose. In contrast, insulin secretion decreases to raise plasma glucose at low level blood glucose. Thus, insulin is secreted in response to blood glucose concentrations and has a very important rule in maintaining blood glucose levels.

1.5 Insulin Therapy and Glucose Control

Hyperglycemia, organ dysfunction and sepsis are highly correlated dysfunctions. One of the category in defining sepsis is the presence of organ failure indicating sepsis is severe enough to lead to organ dysfunction [Levy et al., 2003; Bone et al., 1992]. As discussed earlier, organ dysfunction is one of the worst outcomes of hyperglycemia and a leading cause of ICU death. Fur-

thermore, hyperglycemia potentiates the pro-inflammatory response, which is common in sepsis and thus may be partly causal. Therefore, treatment of hyperglycemia consequently reduces the patient's risk of developing organ dysfunction and sepsis, as seen in several studies.

The positive effects of insulin therapy and glucose control observed in studies that achieved good, low variability control suggest that intensive insulin therapy and tight glycemic control (TGC) are necessary to be implemented in critical illness. In addition, intensive insulin therapy and glycemic management reduced mortality in patients with MOF and sepsis, regardless of hyperglycemia [Capes et al., 2000]. Insulin therapy and glucose control can also protect the cardiovascular system, reduce secondary infections, attenuate inflammatory response [Vlasselaers et al., 2009; Hasegawa et al., 2011], and reduce the risk of cholestasis [Van den Berghe et al., 2001].

Relevant to this research, reduces episodes of sepsis can be seen with the implementation of blood glucose control [Hirasawa et al., 2009; Takahashi et al., 2011; Van den Berghe et al., 2001; Marik and Raghavan, 2004]. Similarly, the reduced incidence of sepsis leads to reduced negative clinical outcomes, such as fibrinolytic impairment [Savioli et al., 2009] and the need for mechanical ventilation [Van den Berghe et al., 2001]. Other beneficial effects of insulin therapy and TGC on critical illness that have been previously documented include the prevention of catabolism, acidosis, excessive inflammation, and impaired innate immune function [Weekers et al., 2003; Li et al., 2011; Toft and Tonnesen, 2011].

TGC has thus emerged as a major research focus in critical care due to its potential to simultaneously reduce both mortality and costs [Krinsley,

2004, 2003; Van den Berghe et al., 2001, 2003]. Additionally, TGC reduced the use of resources in intensive care and complications among patients including septicemia and prolonged antibiotic therapy needs. In a randomised controlled study by Vlasselaers and colleagues [Vlasselaers et al., 2009], intensive insulin therapy reduced the duration of stay and need for extended stay in paediatric cohort.

Despite the emerging evidence of TGC on the outcome of septic patients and patients with organ failure, it is still a challenge to reproduce these beneficial effects in the clinical setting. Therefore, treatments for sepsis are more directed and focus on the systemic inflammatory response and infection, rather than controlling blood glucose levels. The recommended protocols used in the Surviving Sepsis Campaign have also created much debate under increasing scrutiny [Barochia et al., 2010; Eichacker et al., 2006; Hicks et al., 2008; Marik and Varon, 2010; Perel, 2008]. However, recent studies still suggest the implementation of early goal-directed therapy for septic patients and clearer operational guidelines in achieving optimal outcomes [Burney et al., 2011; Rivers et al., 2001; Turi and Von Ah, 2011; Colin et al., 2011; Sivayoham et al., 2011; O'Neill et al., 2011].

1.5.1 Model-Based Glycemic Control

To date, most typical practice of glycemic management in the ICU is comprised of ad-hoc protocols based primarily on experience, where relatively large amounts of intravenous insulin, up to 50 U/h, are titrated against glucose measurements variably taken every 1-4 hours. In reality, there are several

circumstances that may exacerbate these situations on a patient by patient, or patient-specific base. For example, unpredictable and sudden metabolic changes, changes in nutritional support administration, and non-standard or non-robust insulin protocols can result in highly variable and poorly controlled blood glucose levels [Chase et al., 2011b].

A physiological model that captures the glucose-insulin system dynamics is thus the basis for more optimally addressing the glycemic control problem [Chase et al., 2011a]. Metabolic modelling of the glucose-insulin system has a very deep history in the published literature. The vast majority of these models have their roots in basic compartment modelling with differential equations [Carson and Cobelli, 2001]. To date, the primary use of metabolic models has been the development of model-based measures to assess metabolic parameters, with a particular focus on measuring insulin sensitivity [Bergman et al., 1981, 1979, 1985; Pacini and Bergman, 1986; Yang et al., 1987; Mari et al., 2001; Mari, 1998; Lotz et al., 2006; Toffolo et al., 1999, 2006].

Implementing TGC includes the increased risk of severe hypoglycemia and difficulty in achieving normoglycemia in critically ill patients [Griesdale et al., 2009]. Because of this issue and uncertainty about the balance of risks and benefits, TGC is used infrequently by some clinicians. Hence, a model for glycemic control needs to be applicable for real-time clinical control, as well as addressing the needs and limitations typical of most ICUs. More specifically, models for glycemic control in the ICU need to satisfy the following basic criteria:

- Accurately capture insulin and glucose pharmacokinetics, and glucose-

insulin pharmacodynamics typical of critically ill patients.

- Feature a simple structure preferably requiring only blood glucose levels as physiological feedback to identify a patient-specific model.

- Address inter- and intra- patient variability over time.

- Have rapidly identifiable patient-specific model parameters.

- Have good accuracy in predicting glycemic outcomes of interventions over 1-3 hour time intervals, to accurately and safely guide therapy.

Given an accurate model satisfying these criteria, model-based glycemic control can offer individualized control adaptable to the critically ill patient's highly dynamic physiological condition. It can also be used as a tool to diagnose a disease in real-time by capturing patient-specific parameters associated with that disease state. Furthermore, such a physiological model may also be used as a patient simulator for protocol development incorporating individual patient-specific parameters [Hann et al., 2005; Wong et al., 2006a; Lonergan et al., 2006; Evans et al., 2011]. Additional knowledge of critically ill population's variable dynamics can further enhance model-based control with more accurate or safer predictive performance [Lin et al., 2008].

1.6 Preface

In summary, sepsis and organ failure are highly associated with hyperglycemia and represent a very serious clinical problem as reflected by their increasing rate of incidence, mortality, and other negative clinical outcomes. Therefore, hyperglycemia can be a marker to represent the severity of illness. Hyperglycemia and sepsis events have been documented to reduce with the implementation of safe, effective TGC in critical illness. However, in few TGC studies [Brunkhorst et al., 2008; Preiser et al., 2009; Vanhorebeek et al., 2007a], septic patients were put at an increased risk due to excessive hypoglycaemia. As a result, some practitioners are reluctant to implement TGC for the critical illness at their centers.

The aim of this research is to investigate the potential of a metabolic model-based parameter to represent the severity of illness of a patient, and to capture sepsis in particular. The model used can capture patient-specific parameters that capture patient-specific physiological condition. The ability of model-based parameters to represent the severity of illness will be helpful for monitoring, controlling and diagnosing patient condition.

Critically, the issue of sepsis is not only limited to the definitions and systems typically used to identify this disease. There are many factors that contribute to the challenge in sepsis diagnosis despite advancements in technologies and medical research. Hence, septic patients are often classified by practitioners according to their experience before standard test results can be obtained or assessed to avoid delay in treatment. Therefore, the ability to treat a septic patient as early as possible has become a real challenge.

Hence, the more specific goal of this research is to develop and examine a model-based bio-marker that can be used to diagnose a disease or condition in critically ill patients. The potential bio-markers need to be clinically practical, incorporate patient-specific parameter(s) that represent dynamic metabolic condition and physiology of a patient, and, importantly, can be identified in real-time for real-time diagnosis. The thesis is organized as follows:

Chapter 2 reviews previous glucose-insulin models that have been extensively applied for controlling glycemia. This chapter also presents an updated glucose-insulin control model that is currently used for real-time glycemic control.

Chapter 3 presents the analysis of two TGC trials for root causes of the differences achieved in control. In this chapter, insulin sensitivity profiles, $S_I(t)$, and stochastic models, are used to assess metabolic condition and variability. Model-based insulin sensitivity, S_I, is therefore defined as a real-time, hour-to-hour patient-specific parameter representing patient metabolic condition.

Chapter 4 presents the overall validation of the glucose-insulin system model and model-based metric, S_I introduced in Chapter 2. Model validation was assessed by using a virtual trials method and simulations run on independent data sets. The end result validates the efficacy of S_I as an independent marker of real-time patient-specific condition.

Chapter 5 reviews current methods used to diagnose sepsis state by analyzing current scoring systems in terms of the definitions and score representation in real-time diagnosis. A different scoring system is also

developed to better classify patients and determine prognosis.

Chapter 6 discusses the use of model-based insulin sensitivity, S_I, as a patient-specific parameter to aid sepsis diagnosis. The relation of S_I and the suggested sepsis score is observed for over hourly intervals for real-time diagnosis using a 30 patient sepsis cohort.

Chapter 7 presents the analyses of potential sepsis predictors by looking at available clinical variables typically gathered for sepsis patients. Artificial neural network (ANN) is used to compute predictive values of sepsis state on hourly basis. Sensitivity and specificity of the tests are compared and examined using mathematical computations to obtain variables that may potentially become a sepsis bio-marker.

Chapter 8 presents the study of sepsis as a disease of the microcirculation. Principles and operation of pulse oximeters are developed as a medium to diagnose microcirculation function.

Chapter 9 validates the concept and operation of pulse oximeters that has been discussed in Chapter 8. In this chapter, pulse oximeters are used to investigate oxygen extraction to the tissues as a potential sensor for diagnosing microcirculation failure in sepsis.

Chapter 10 summarizes the key aspects of the thesis.

Chapter 11 presents the possible future improvements and applications for this research.

Chapter 2

Model Background and Development

This chapter examines several forms of existing metabolic control models that have been used for controlling glycemia in humans. Depending on the type of application, different models have been developed with distinct levels of complexity based on the application and outcome goal. The majority of these models use basic compartmental modelling with differential equations [Cobelli et al., 1984; Carson and Cobelli, 2001]. These approaches vary from second [Ackerman et al., 1965; Lehmann and Deutsch, 1992] to 19th [Parker et al., 1999] order, showing the wide range of possibilities. As the complexity of the models grows, more variables tend to be identified, and more clinical and computational effort are needed. Importantly, a model should be able to accurately describe the physiologically relevant responses, and, for control applications, be clinically applicable, while minimizing mathematical complexity.

Metabolic models have been developed to assess a number of metabolic phenomena. These investigations focused on understanding rather than intervention or control, and center around glucose, insulin, and insulin sensitivity

[Bergman et al., 1981, 1979; Yang et al., 1987; Pacini and Bergman, 1986; Mari et al., 2001; Mari, 1998]. Critically, a physiological model that captures the glucose-insulin dynamics is also the basis of any glycemic control problem. In recent years, metabolic modelling of insulin and glucose has been developed due to a high demand for model predictive control (MPC) [Hovorka et al., 2004] and automated or semi- automated glycemic control [Chase et al., 2007, 2008b; Parker et al., 1999, 2001; Plank et al., 2006; Hovorka et al., 2004]. These are all models for clinical intervention.

2.1 Physiology of a Glucose-Insulin System Model

Early modeling studies [Ackerman et al., 1965; Bolie, 1961] in diabetic individuals have become a basis for analysing glucose-insulin system models in terms of mathematical and physiological identification. Later studies extended to more complicated and nonlinear models, such as the well known Minimal Model [Bergman et al., 1981]. The Minimal Model became popular and forms a basis in most of the models developed despite numerous parameter identifiability issues [Pillonetto et al., 2002, 2003; Caumo et al., 1999; Docherty et al., 2011]. Additionally, other physiological systems have been incorporated in some of the model structure [Cobelli and Mari, 1983] for better representation of human physiology.

Several forms of metabolic system model have been developed, and some have been applied clinically, where various mathematical control algorithms

have been implemented. Some of these models have been used in examining critical care patients and glycemic control [Hovorka et al., 2004; Chee et al., 2003b,a; Parker et al., 1999; Chase et al., 2007]. Besides capturing physiological and metabolic condition, these model must also be designed for clinical applicability and performance. Thus, different models have been developed with different criteria to suit particular applications. In particular, a control model should focus on the ability to predict outcomes of interventions, although many do not [Chase et al., 2011a].

The following sections present a broad cross-section of models to illustrate the range of possibilities. The first model discussed is that of Chee and colleagues [Chee et al., 2003b,a] who introduced a model using an optimised PID form of control. The integral control (Equation 2.1) is implemented when sliding tables do not provide adequate glycemic reduction and the amount of additional insulin is calculated using Equation 2.2, a normalized weighted average of the blood glucose zones using a 2-hour triangular window. Derivative control is implemented using Equations 2.3 - 2.6. Expert control is implemented by keeping an active sliding table and offsetting the recommended sliding table input according to several conditions, based on Equations 2.3 - 2.6. In Equation 2.6, x_{max} and x_{min} represent the maximum and minimum time value in the 30-min window respectively, whereas y_{max} and y_{min} represent maximum and minimum BG value in the 30-min window.

$$\text{Insulin increment} = \begin{cases} 4 \text{ U/hr}, & \text{if } \|\overline{W}_{zone}\| > 4.5 \\ 2 \text{ U/hr}, & \text{if } 3.6 \leq \|\overline{W}_{zone}\| \leq 4.5 \\ 1 \text{ U/hr}, & \text{if } 2.7 \leq \|\overline{W}_{zone}\| \leq 3.6 \\ 0 \text{ U/hr}, & \text{if } \|\overline{W}_{zone}\| < 2.7 \end{cases} \tag{2.1}$$

where:

$$\|\overline{W}_{zone}\| = \frac{1}{\sum_{i=1}^{24} i} \left(\sum_{n=1}^{24} n.W_{zone}[n] \right) \tag{2.2}$$

$$\text{Bolus} = \begin{cases} 6 \text{ U/hr}, & \text{if } \Delta y_{proj} \geq 2 \text{ mmol/L} \\ 4 \text{ U/hr}, & \text{if } 1 \leq \Delta y_{proj} < 2 \text{ mmol/L} \\ 0 \text{ U/hr}, & \text{if } \Delta y_{proj} < 1 \text{ mmol/L} \end{cases} \tag{2.3}$$

$$\Delta y_{proj} = \left(\frac{\sum_{i=1}^{6} X_i Y_i}{\sum_{i=1}^{6} {X_i}^2} \right) \Delta x \tag{2.4}$$

$$X_i = x_i - \tilde{x} \text{ and } Y_i = y_i - \tilde{y} \tag{2.5}$$

$$\tilde{x} = \frac{x_{max} + x_{min}}{2} \text{ and } \tilde{y} = \frac{y_{max} + y_{min}}{2} \tag{2.6}$$

The use of sliding tables and normalized weighted average in this model are incapable of capturing the physiology of glucose-insulin model. Moreover,

expert control is part of the implementation, where keeping and offsetting the recommended sliding input is based on clinical judgement. Hence, any physiology is implicit in this clinical input. It also does not take account for patient variability, as each individual patient has different metabolic condition that can vary with time. Therefore, this model is designed from a control point of view without incorporating the physiological point of view.

The second model is adapted by Hovorka et al from type 1 diabetes control applications. This model is used in critically ill patients, although designed for controlling blood glucose in Type 1 diabetes [Hovorka et al., 2004]. The structure of the model is shown in Figure 2.1 and the model equations are shown in Equations 2.7 - 2.19.

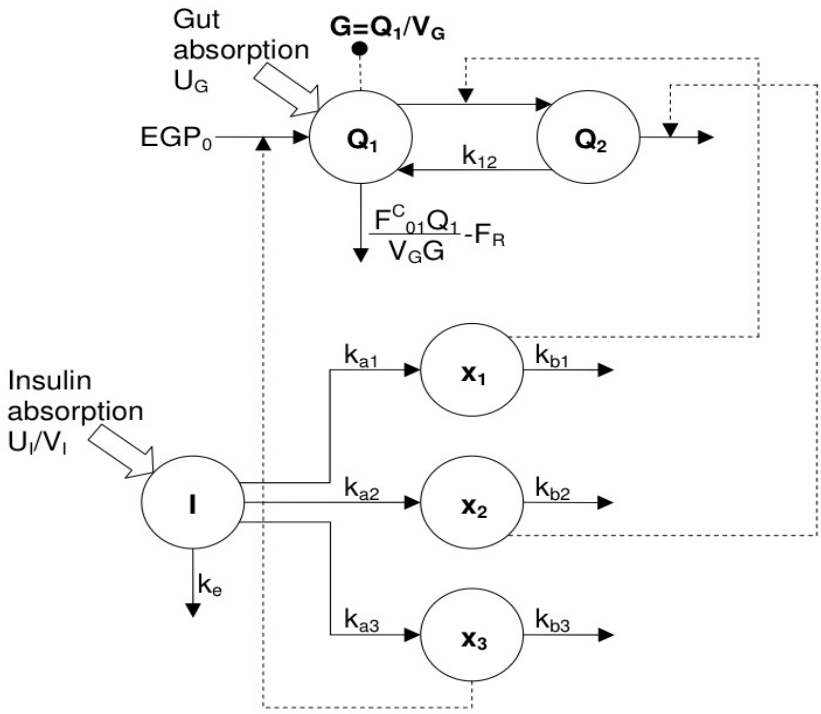

Figure 2.1: Compartment model of glucose-insulin system (Adapted from Hovorka et al. [2002]).

$$\dot{Q}_1(t) = -\left[\frac{F_{01}^c}{V_G G(t)} + x_1(t)\right] Q_1(t) + k_{12} Q_2(t) - F_R + U_G(t) + EGP_0[1 - x_3(t)] \tag{2.7}$$

$$\dot{Q}_2(t) = x_1(t) Q_1(t) - [k_{12} + x_2(t)] Q_2(t) \tag{2.8}$$

$$y(t) = G(t) = Q_1(t)/V_G \tag{2.9}$$

$$F_{01}^c = \begin{cases} F_{01} & \text{if } G \geq 4.5 \text{ mmol/L} \\ F_{01} G/4.5 & \text{otherwise} \end{cases} \tag{2.10}$$

$$F_R = \begin{cases} 0.003(G - 9) V_G & \text{if } G \geq 9.0 \text{ mmol/L} \\ 0 & \text{otherwise} \end{cases} \tag{2.11}$$

$$U_G(t) = \frac{D_G A_G t e^{-t/t_{max,G}}}{t^2} \tag{2.12}$$

$$\dot{S}_1(t) = u(t) - \frac{S_1(t)}{t_{max,I}} \tag{2.13}$$

$$\dot{S}_2(t) = \frac{S_1(t)}{t_{max,I}} - \frac{S_2(t)}{t_{max,I}} \tag{2.14}$$

$$\dot{I}(t) = \frac{U_I(t)}{V_I} - k_e I(t) \tag{2.15}$$

where:

$$U_I(t) = \frac{S_2(t)}{t_{max,I}} \tag{2.16}$$

$$\dot{x_1}(t) = -k_{a1}x_1(t) + k_{b1}I(t) \tag{2.17}$$

$$\dot{x_2}(t) = -k_{a2}x_2(t) + k_{b2}I(t) \tag{2.18}$$

$$\dot{x_3}(t) = -k_{a3}x_3(t) + k_{b3}I(t) \tag{2.19}$$

where Q_1 and Q_2 in Equations 2.7 and 2.8 represent masses of glucose in the accessible and inaccessible compartments. k_{12} represents the transfer rate between the inaccessible and accessible compartments. The distribution volume of the accessible compartment is V_G, the measurable glucose concentration is y and G, and EGP_0 is the endogenous glucose production extrapolated to the zero insulin concentration. F_{01}^C is the total non-insulin-dependent glucose flux corrected for the ambient glucose concentration and F_R is the renal glucose clearance above the glucose threshold of 9 mmol/L. $U_G(t)$ is the gut absorption rate, dependent upon the carbohydrates digested, D_G, carbohydrate bioavailability, A_G, and the time of maximum appearance rate of glucose in

the accessible compartment, $t_{max,G}$. The insulin subsystem is described by Equations 2.13 - 2.19. S_1 and S_2 are a two-compartment chain for absorption of subcutaneously administered rapid-acting insulin, $u(t)$ the insulin input (bolus/infusion), and $t_{max,I}$ the time-to-maximum insulin absorption. $I(t)$ is the plasma insulin concentration, k_e is the fractional elimination rate and V_I the distribution volume. The insulin action subsystem consists of three components, endogenous glucose production, transport/distribution and disposal (x_1, x_2 and x_3). Finally, k_{ai} and k_{bi} (i =1, ..., 3) represent the activation and deactivation rate constant of insulin action, respectively.

Overall, the model uses 9 population values or generic constants, and requires a further 6 patient-specific parameters to be identified. Nonlinearity comes from insulin action on parameters of glucose production, glucose distribution/transport and glucose disposal, and difference in the activation/deactivation profile of the three insulin actions. Consequently, several additional measurements are required to identify patient-specific parameters. However, this model has been used in critical care for glycemic management and achieved promising results [Plank et al., 2006].

Another model used to estimate insulin sensitivity and glucose effectiveness is the Minimal Model [Bergman et al., 1981, 1979]. This classical model of glucose disposal has been constructed by using an iterative numerical algorithms. The minimal model was developed to characterize Intravenous Glucose Tolerance Test (IVGTT) responses. The IVGTT is an insulin sensitivity test that measures the glucose and insulin responses to an intravenous glucose injection. Glucose and insulin kinetics are described by two compartments where parameters have been estimated separately within each compo-

nent. The glucose-insulin system is illustrated by the compartmental model in Figure 2.2 and can be described mathematically, in its most commonly used form, by Equations 2.20 - 2.22.

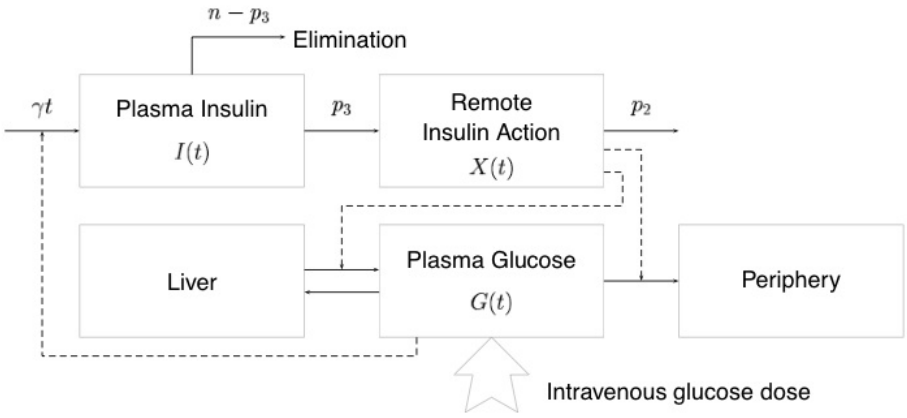

Figure 2.2: Bergman's minimal model describing the glucose and insulin kinetics in an IVGTT study [Bergman et al., 1981].

$$\dot{G}(t) = -p_1(G(t) - G_b) - X(t)G(t) \tag{2.20}$$

$$\dot{X}(t) = -p_2X(t) + p_3(I(t) - I_b) \tag{2.21}$$

where:

$$G(0) = G_o \; ; \; X(0) = 0 \; ; \; I(0) = I_o \tag{2.22}$$

$$S_I = p_3/p_2 \tag{2.23}$$

where $G(t)$ is the plasma glucose concentration at time t, $I(t)$ is the plasma insulin concentration and $X(t)$ is the interstitial insulin. G_b is the basal plasma glucose concentration and I_b is the basal plasma insulin concentration. p_1, p_2, p_3 and G_o are four unknown parameters and S_I represents insulin sensitivity.

This simple model illustrates the basic dynamic of insulin pharmacokinetics, glucose pharmacokinetics and glucose-insulin pharmacodynamics accounting for the removal of glucose that should be captured for any glycemic control problem. It is physiological, but still has too many parameters requiring patient-specific identification. Equally, its predictive accuracy has been called into question [Chase et al., 2006].

2.2 Critical Care Glucose-Insulin Model

Any model used in critical care must effectively account for the fundamental dynamics of the glucose-insulin system, while maintaining clinical applicability. This requirement exists because patients in intensive care units are highly monitored, and insulin and glucose must be carefully administered to achieve homeostasis. Model-based decision support can improve the precision of glycemic control [Wong et al., 2006a; Chase et al., 2006]. However, the model complexity has to be reasonable and, critically, must also account for observed physiological response, dynamics, and inter- and intra- patient variability [Chase et al., 2011a].

There have been several metabolic models used to examine critical care

patients. Chase and colleagues used a model derived from the Minimal Model with additional, physiologically relevant non-linear terms, and a grouped term for insulin sensitivity [Chase et al., 2007; Wong et al., 2006b]. These changes were made because the Minimal Model has significant limitations where it does not accurately capture the dynamics observed in glycemic control [Doran et al., 2004a,b], particularly saturation of glucose removal by insulin [Prigeon et al., 1996; Rizza et al., 1981; Natali et al., 2000; Docherty et al., 2011], saturation of insulin transport [Prigeon et al., 1996; Ellemann et al., 1987], dynamics of insulin receptors and measurable and unmeasurable glucose compartments [Cobelli et al., 1999, 1992]. As a result, a more descriptive model was developed by Chase et al [Chase et al., 2007, 2005].

Figure 2.3 illustrates the schematic of the critical care glucose-insulin model developed by Chase et al. This model has been employed in several critical care glycemic control trials using different control methods, as well as in retrospective analyses [Wong et al., 2006b; Chase et al., 2005, 2007; Lin et al., 2004]. Additional non-linear terms have been introduced to this model that include patient endogenous glucose clearance and insulin sensitivity. The mathematical equations are shown in Equations 2.24 - 2.26, where these equations are the result of several small evolutions as described.

$$\dot{G} = -p_G G - S_I G \frac{Q}{1 + \alpha_G Q} + \frac{P(t) + EGP_{max} - CNS}{V_G(t)} \tag{2.24}$$

$$\dot{Q} = -kQ + kI \tag{2.25}$$

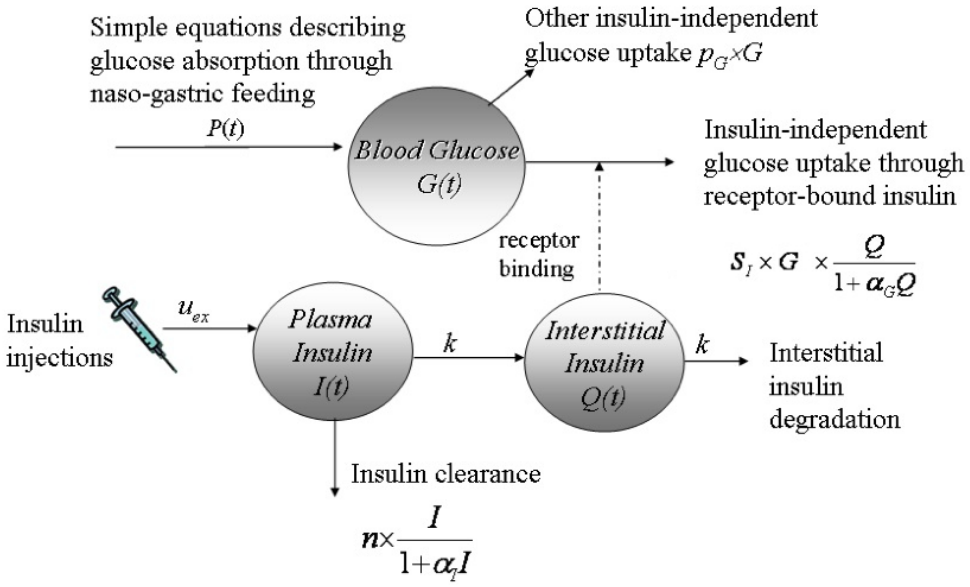

Figure 2.3: Schematic of Critical Care Glucose-Insulin Model adapted from Chase et al.

$$\dot{I} = -\frac{nI}{1+\alpha_I I} + \frac{U_{ex}(t)}{V_I} + e^{-k_I U_{ex}(t)} I_B \tag{2.26}$$

where t [min] is time, the symbols $G(t)$ [mmol/L] denotes the total blood glucose concentration, and $I(t)$ [mU/L] is the plasma insulin resulting from exogenous insulin input, $u_{ex}(t)$ [mU/min]. $Q(t)$ [mU/L] represents the effect of previously infused insulin being utilised over time, with k [1/min] accounting for the effective life of insulin in the system. Patient endogenous glucose clearance and insulin sensitivity are p_G [1/min] and S_I [L/mU/min], respectively. V_I [L] and V_G [L] are the insulin distribution volume and glucose distribution volume, respectively. n [1/min] is the constant first order decay rate for insulin from plasma and external nutrition is $P(t)$ [mmol/min].

Michaelis-Menten functions are used to model saturation, with α_I [L/mU] used for the saturation of plasma insulin disappearance and α_G [L/mU] for the saturation of insulin-dependent glucose clearance. I_B [mU/L/min] and k_I [min/mU] are endogenous insulin secretion, CNS [mmol/min] is central nervous system glucose uptake and EGP_{max} [mmol/min] represents maximum endogenous glucose production at zero insulin.

Patient-specific insulin mediated glucose removal is captured with insulin sensitivity, S_I, which is identified hourly from clinical data as a time-dependent variable that reflects evolving patient condition. Exogenous inputs are glucose appearance $P(t)$ from the carbohydrate content of nutrition infusion via a two compartment model, and intravenous insulin administration $u_{ex}(t)$. The remaining parameters are physiologically defined population constants for transport rates (n, k), saturation parameters (α_G, α_I), endogenous insulin secretion (I_B, k_I) or volumes (V_G, V_I). This model was developed and validated in critical care glycemic control studies [Suhaimi et al., 2010; Le Compte et al., 2009]. All the compartmental transport and utilisation rates are assumed to be constant population values except insulin sensitivity, S_I.

2.3 Intensive Control Insulin Nutrition Glucose Model (ICING)

Finally, another more advanced model used in this study is the ICING Model. This model is the improved version of the model used in critical care, and was recently developed at the University of Canterbury [Lin et al., 2011b]. This

model extensively described the glucose appearance in a patients. Figure 2.4 illustrates the ICING model system. The mathematical formulations used in this model are described in Equations 2.27 - 2.33.

$$\dot{G} = -p_G G - S_I G \frac{Q}{1 + \alpha_G Q} + \frac{P(t) + EGP_b - CNS}{V_G} \tag{2.27}$$

$$\dot{Q} = n_I(I - Q) - n_C \frac{Q}{1 + \alpha_G Q} \tag{2.28}$$

$$\dot{I} = -n_K I - \frac{n_L I}{1 + \alpha_I I} - n_I(I - Q) + \frac{u_{ex}(t)}{V_I} + (1 - x_L)\frac{u_{en}}{V_I} \tag{2.29}$$

$$\dot{P}1 = -d_1 P1 + D(t) \tag{2.30}$$

$$\dot{P}2 = -min(d_2 P2, P_{max}) + d_1 P1 \tag{2.31}$$

$$P(t) = min(d_2 P2, P_{max}) \tag{2.32}$$

$$u_{en}(t) = k_1 e^{\frac{I(t)k_2}{k_3}} \tag{2.33}$$

where G [mmol/L] is the total blood glucose concentration, Q [mU/L] rep-

resents the effect of previously infused insulin being utilised over time and I [mU/L] is the plasma insulin. Patient endogenous glucose clearance and insulin sensitivity are p_G [1/min] and S_I [L/mU/min], respectively. V_I [L] is the insulin distribution volume and V_G [L] is the glucose distribution volume. External nutrition is $P(t)$ [mmol/min], EGP_b [mmol/min] is basal endogenous glucose production and CNS [mmol/min] is central nervous system glucose uptake. α_I [L/mU] is the saturation of plasma insulin disappearance and α_G [L/mU] is the saturation of insulin-dependent glucose clearance. n_I [L/min] is the diffusion constant of insulin between compartments and n_C [1/min] is the cellular insulin clearance rate from interstitium. n_K [1/min] and n_L[1/min] represent plasma insulin clearance rate at kidney and liver, respectively. x_L is the fraction of extraction. u_{ex} [mU/min] and u_{en} [mU/min] are exogenous insulin infusion and endogenous insulin production, respectively.

Equations 2.30 - 2.32 present the gastric absorption of glucose, where $P1$ [mmol] represents the glucose in the stomach and $P2$ [mmol] is for the gut. Transport rates between the compartments are $d1$ [1/min] and $d2$ [1/min]. Amount of dextrose from enteral feeding is $D(t)$ [mmol/min]. Glucose appearance, $P(t)$ [mmol/min] from enteral food intake $D(t)$, is the glucose flux out of the gut $P2$. P_{max} [mmol/min] represents maximum enteral feeding.

The EGP_b term in Equation 2.27 is a constant and represent the theoretical endogenous glucose production for a patient with no exogenous glucose or insulin. Equation 2.33 is a generic representation of endogenous insulin production when C-peptide data is not available from the patient for specific identification of its production. Endogenous insulin production, with the base rate being k_1 [mU/min], is suppressed with elevated plasma insulin levels. The

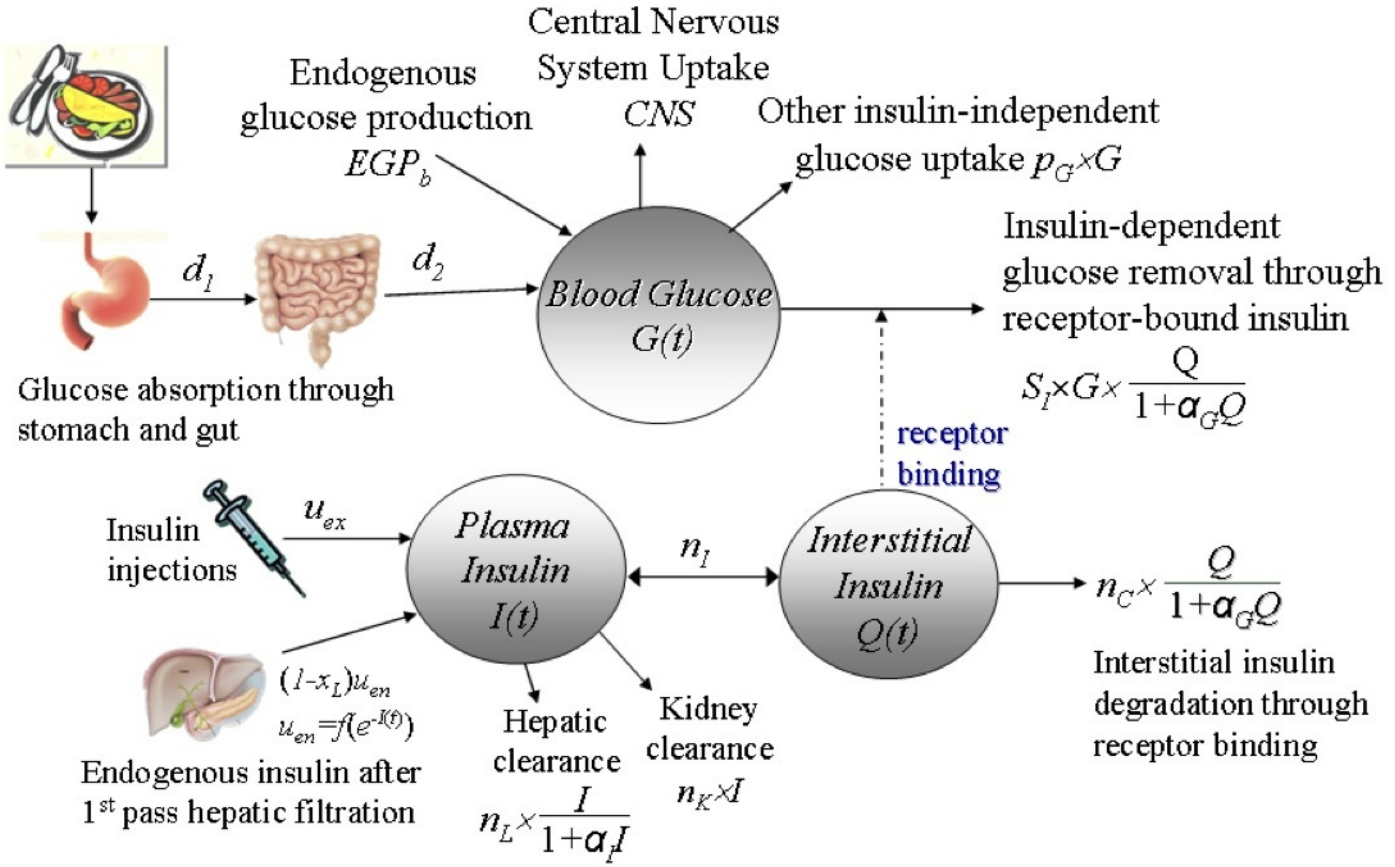

Figure 2.4: Intensive Control Insulin-Nutrition Glycemic Model (ICING) defined in Equations 2.27 - 2.33.

exponential suppression is described by generic constants k_2 and k_3.

2.4 Summary

This chapter discusses the basis of glucose-insulin system models and reviews several forms of model that have been developed and used for glycemic understanding, control and management. These different models have been used clinically for various studies for understanding or intervention. The use for understanding versus intervention require differences in model capability and complexity that may not translate directly from one use to another. However, not all of these models were physiologically complete and some failed to capture inter- and intra- patient variability. The final models presented in this chapter provide an overall measure of a patient's insulin sensitivity, particularly to exogenous insulin and nutrition inputs that guide and determine the metabolic balance in ICU patients. The glucose-insulin models presented are already proven to be suitable for clinical control applicability while accurately accounting for all relevant physiological behavior.

Chapter 3

Successful TGC and Model-Based Metabolic Markers

Tight glycemic control (TGC) can reduce intensive care unit (ICU) patient mortality up to 45%, with glycemic targets from 6.1 to 7.75 mmol/L [Van den Berghe et al., 2006b; Chase et al., 2008b; Krinsley, 2004]. Despite the potential, many ICUs have issues in safely and effectively delivering TGC, particularly in using a fixed protocols (NICE, VISEP, Glucontrol).

This chapter analyses data from two TGC trials for root causes of the differences achieved in control and thus, potentially, in glycemic and mortality outcomes. The two different control trials are Glucontrol [Preiser et al., 2009] and SPRINT protocol [Lonergan et al., 2006]. Specifically, these two protocols vary in terms of clinical practice and nutritional standards, in particular, which both play a major role in BG outcome. Insulin sensitivity profiles $S_I(t)$ of the cohort are generated to assess metabolic condition and stochastic models are used to assess metabolic variability. From the analysis of metabolic condition and TGC interventions, aspects of successful TGC are delineated. Therefore, this chapter provides insight and clearer guidance into the design and implementation of clinical TGC protocols based on metabolic condition.

3.1 SPRINT Protocol

Specialized Relative Insulin Nutrition Titration (SPRINT) is a model-derived protocol [Lonergan et al., 2006; Wong et al., 2006b; Chase et al., 2007] that controls both insulin and (carbohydrate) nutrition inputs. It was implemented at the Christchurch Hospital Department of Intensive Care on August 2005 [Chase et al., 2008b] and has now been used on over 1,000 patients. In SPRINT, the interventions consider current and previous blood glucose measurements, current nutrition rate relative to a patient specific goal rate, and the prior hourly insulin dose to determine a new nutrition and insulin intervention for the coming 1-2 hour measurement interval defined in the protocol [Chase et al., 2008b].

The SPRINT protocol consists of two wheels dedicated to insulin bolus administration and enteral nutrition optimization, as shown in Figures 3.1-3.4. In SPRINT, blood glucose measurements are taken 1-2 hourly at bedside based on the protocol. The approach is patient-specific in nutrition rate and its titration of inputs in response to the patient-specific metabolic condition.

More specifically, SPRINT titrates its insulin and nutrition inputs to achieve a target range of 4-6 mmol/L based on the patient's current insulin sensitivity, which is effectively determined by the response to the insulin and nutrition interventions. More resistant patients receive more insulin and less nutrition (relative to their 100% goal feed rate). Stability and stopping criteria were also based on patient-specific insulin sensitivity. Hence, the protocol explicitly considers glycemic response in the context of both insulin and carbohydrate intake and is thus not blind to carbohydrate intake, which is unique

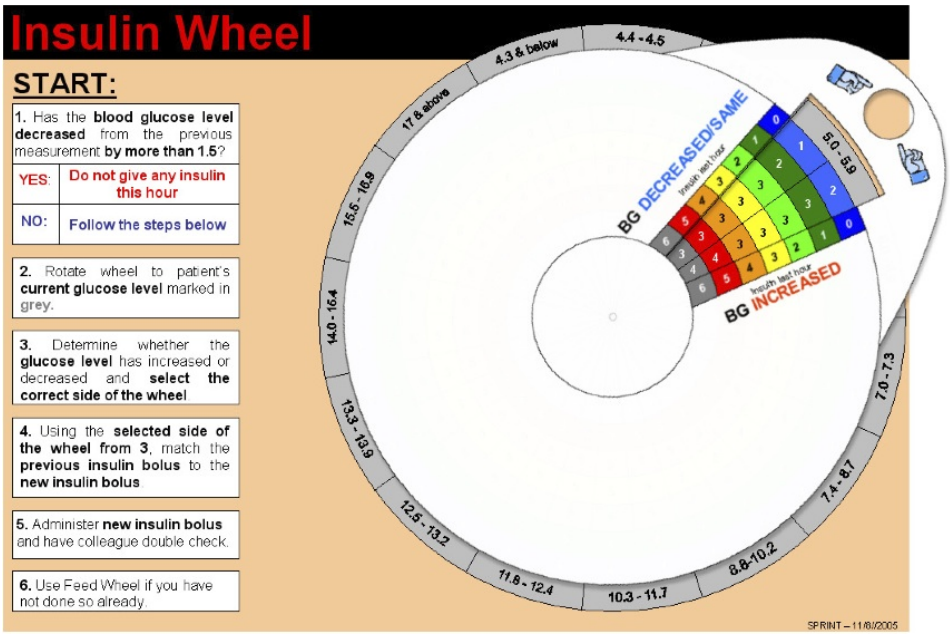

Figure 3.1: The SPRINT insulin wheel with dial [Lonergan et al., 2006].

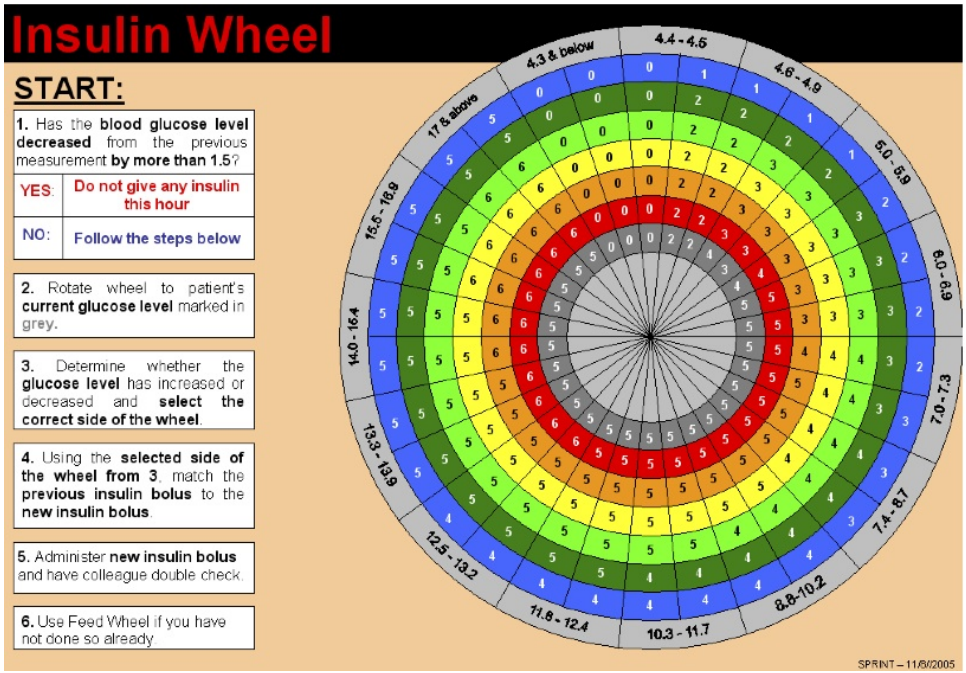

Figure 3.2: The SPRINT insulin wheel without dial [Lonergan et al., 2006].

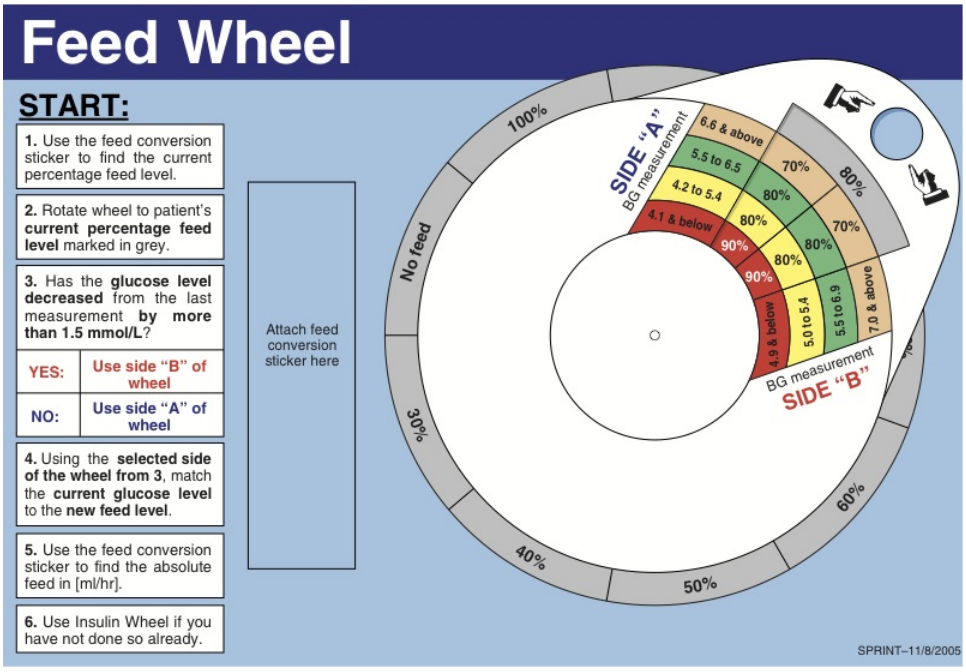

Figure 3.3: The SPRINT feed wheel with dial [Lonergan et al., 2006].

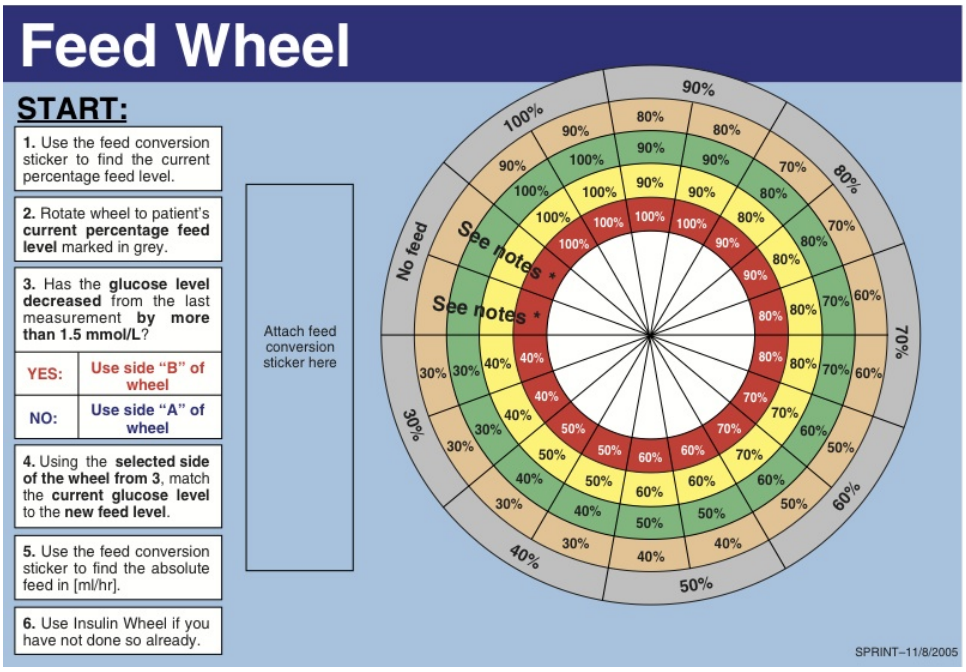

Figure 3.4: The SPRINT feed wheel without dial [Lonergan et al., 2006].

[Chase et al., 2011b]. Virtually all other studies leave nutritional intake to local clinical standards and are thus blind to this critical parameter that directly affects glycemic levels.

A low carbohydrate enteral nutrition formula was also specified for all SPRINT patients, reducing the percentage of carbohydrate calories as a percentage of the total caloric intake. Minimum and maximum nutrition rates are 7.5 and 25 kcal/kg/day respectively, with 2.7 to 9 kcal/kg/day (35-40%) from carbohydrates, which matches ACCP guidelines at the maximum level [Cerra et al., 1997].

Finally, SPRINT uses insulin boluses, limited to 6U per hour to minimize insulin saturation [Chase et al., 2005; Natali et al., 2000; Prigeon et al., 1996]. Boluses also avoid high rates of insulin infusion being left running when clinical staff are occupied, increasing potential safety, which is an important aspect in situations where high insulin infusion rates combined with infrequent measurement can lead to significantly increased hypoglycemic events and variability resulting from acute changes in patient condition and metabolic response. This latter point is critical because, like hyperglycaemia, low BG or hypoglycaemia is also linked to increased mortality [Griesdale et al., 2009].

Overall, SPRINT is a unique TGC protocol among all those published. It was the only TGC protocol to reduce both mortality and hypoglycaemia, where many attempts fail at both [Brunkhorst et al., 2008; Preiser and Devos, 2007; De La Rosa et al., 2008; Van den Berghe et al., 2006b]. Its uniqueness stems from its direct management of insulin and nutrition based on patient-specific, time varying insulin sensitivity. It thus manage inter- and intra-patient variability, and thus glycaemia and hypoglycaemia risk, better than

others [Griesdale et al., 2009].

3.2 Glucontrol Protocol

The Glucontrol protocol is a glycemic control protocol that controls only the amount of insulin given to a patient to change [Preiser et al., 2009]. Hourly measurement was used when the glycemic level was not within the target range. Otherwise, 2-hourly measurement was used in the case of limited variation of glycaemia, defined as less than a, rather large, 50% change from the previous BG in 2-hour range. Finally, 4-hourly measurement was used when the glycemic level was less than 50% of the highest glycaemia of the four last hours. Insulin was administered as a continuous IV infusion. However, nutritional input was left to local and/or clinician standards, and was not explicitly considered in the design or implementation of the protocol.

In the randomised clinical trial of Glucontrol, there were two different insulin targets used, which are defined as intensive insulin therapy and conventional insulin therapy. Patients treated with intensive insulin therapy are known as Group A, whereas patients treated with conventional insulin therapy are known as Group B. Both groups, intensive and conventional, were targeted for different blood glucose levels of 4.4-6.1 mmol/L and 7.8-10.0 mmol/L, respectively. The insulin infusion rates defined by each target protocol are shown in Tables 3.1-3.2 for the Intensive and Conventional protocols.

Table 3.1: Glucontrol protocol for intensive insulin therapy (Group A). (a) Starting insulin infusion rate. (b) Maintenance insulin infusion rates and increments.

a)

Glycemia	Insulin infusion rate
$<$ 110 mg/dl	On hold
110 - 140 mg/dl	1 U/H
140 - 180 mg/dl	2 U/H
$>$ 180 mg/dl	4 U/H

b)

Glycemia	Incremental insulin infusion rate
$>$ 300 mg/dl	+ 3 U/H
180 - 300 mg/dl	+ 2 U/H
140 - 180 mg/dl	+ 1 U/H
110 - 140 mg/dl	+ 0.5 U/H
80 - 110 mg/dl	+ 0 U/H (target range)
40 - 80 mg/dl	Stop insulin, Hourly measurement of glycemia until $>$ 80mg/dl
$<$ 40 mg/dl	Stop insulin, 10gr glucose IVD, Call physician immediately, Hourly measurement of glycemia until $>$ 80 mg/dl

Table 3.2: Glucontrol protocol for intensive insulin therapy (Group B). (a) Starting insulin infusion rate. (b) Maintenance insulin infusion rates and increments.

a)

Glycemia	Insulin infusion rate
< 180 mg/dl	On hold
180 - 250 mg/dl	1 U/H
250 - 300 mg/dl	2 U/H
> 300 mg/dl	4 U/H

b)

Glycemia	Incremental insulin infusion rate
> 300 mg/dl	+ 3 U/H
250 - 300 mg/dl	+ 2 U/H
180 - 250 mg/dl	+ 1 U/H
140 - 180 mg/dl	+ 0 U/H (target range)
80 - 140 mg/dl	Decrease 50% rate insulin
40 - 80 mg/dl	Stop insulin, Hourly measurement of glycemia until > 80mg/dl
< 40 mg/dl	Stop insulin, 10gr glucose IVD, Call physician immediately, Hourly measurement of glycemia until > 80 mg/dl

3.3 Patient Data

In this study, data was used from 350 patients treated using the Glucontrol protocol at CHU de Liege, Belgium, between March 2004 and April 2005. Thus, the Glucontrol data is from only one centre out of the full study [Preiser et al., 2009]. For the purpose of analysis, patients were selected following several considerations.

Figure 3.5 shows the selection of patients used in this model-based analysis, which requires good data density. For the Glucontrol cohort, patients were eliminated from the analysis if they received no insulin for their entire stay, had less than 5 blood glucose measurements over their time in the study or received little or no recorded carbohydrate administration in any form for more than 48 hours of their stay. Out of 350 patients, 211 patients met these criteria. Moreover, all 393 SPRINT patients study met these criteria.

The selection process is crucial in analysing this data as it eliminates biases in comparison to retrospective data that has been obtained from Christchurch Hospital, and to generate virtual patients with sufficient data density. At the end of the selection process, there were 142 patients treated in Group A (Glucontrol) , 69 patients in Group B (Glucontrol) and 393 SPRINT patients.

Table 3.3 compares the SPRINT and Glucontrol patients characteristics, where the latter are separated by tight glycemic control therapy (Groups A and B). Severity of illness over all Glucontrol (A+B) patients, via APACHE II and percentage of male patients were similar ($p > 0.35$). The total Glucontrol cohort (A+B) was slightly older ($p = 0.011$). The distribution of APACHE II

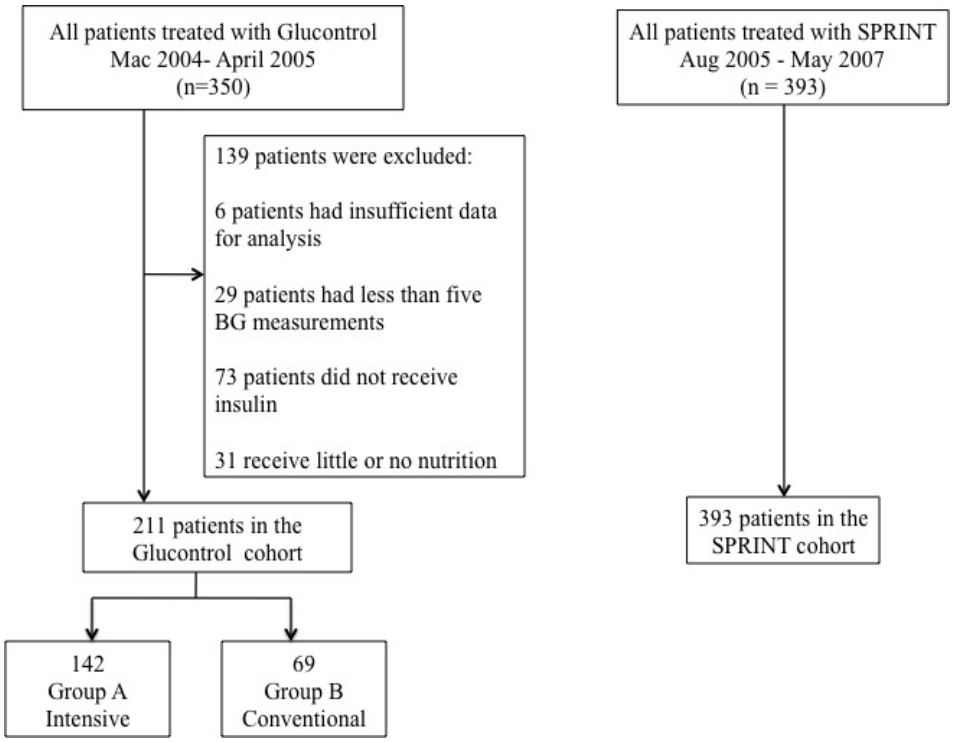

Figure 3.5: Cohort selection for SPRINT and Glucontrol A (Intensive) and B (Conventional) insulin therapy groups.

score among Glucontrol cohort, Group A and Group B, are shown in Figures 3.6 and 3.7. Overall, SPRINT had more hours of control with a total of 49,008 compared to 16,831 and 12,946 for Glucontrol A and B, respectively. SPRINT also had a higher measurement frequency given that total BG measurements were 29,919 for a total of 49,008 hours of control.

Table 3.3: Comparison of Glucontrol and SPRINT cohort characteristics. The P-values are for comparing the Glucontrol A+B cohorts together versus SPRINT.

	SPRINT	Glucontrol A	Glucontrol B	P value
Number of patients	393	142	69	
Percentage of males (%)	62.8	64.8	56.5	0.8531
Age median [IQR]	65 [50 - 74]	71 [61 - 80]	69 [53 - 77]	0.0011
APACHE II score median [IQR]	18[14 - 24]	17 [14 - 22]	17 [14 - 21]	0.3894
Hours of control	49,008	16,831	12,946	
Total blood glucose measurements	29,919	4,571	2,820	

3.4 Insulin Sensitivity as a Model-Based Metric

3.4.1 Model-Based Insulin Sensitivity

The essential model parameter that drives the observed patient-specific glycemic response to insulin and nutrition inputs is insulin sensitivity, S_I. Using the glucose-insulin system model, patient-specific profiles can be generated for time-varying S_I and its hour-to-hour variation as patient condition

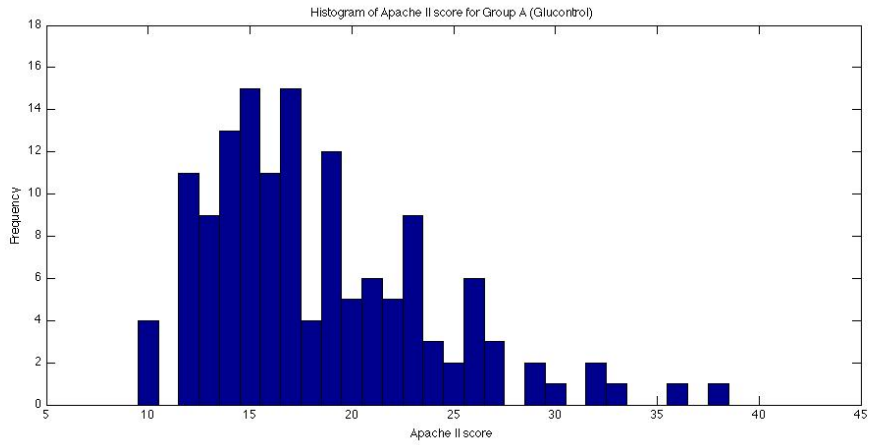

Figure 3.6: APACHE II score distribution for Group A (Glucontrol).

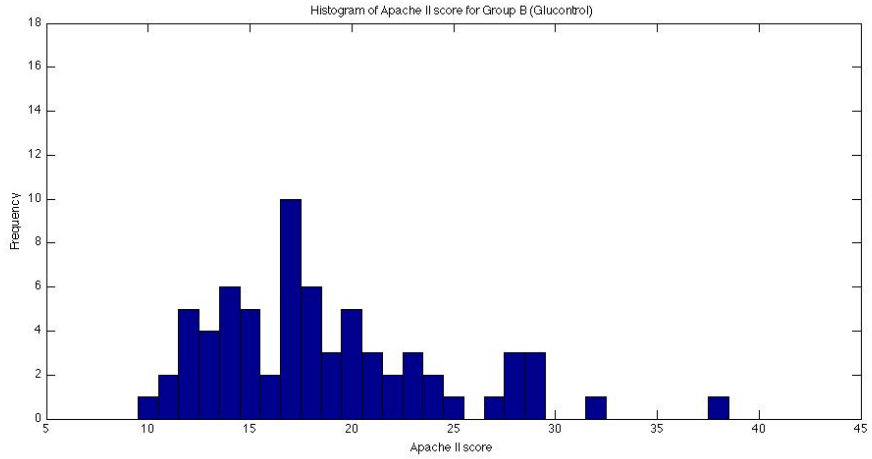

Figure 3.7: APACHE II score distribution for Group B (Glucontrol).

evolves. This task is achieved by fitting the model to retrospective clinical data for blood glucose measurements, insulin and carbohydrate administration input data from the protocols. The resulting insulin sensitivity profile has been validated in correlation to gold standard euglycemic clamp and intravenous glucose tolerance test data [Lotz et al., 2006, 2008], as well as in in silico virtual trials [Lonergan et al., 2006; Chase et al., 2007; Lin et al., 2008; Le Compte et al., 2009].

Figures 3.8 and 3.9 show empirical per-patient CDFs of model-based insulin sensitivity, S_I, for each protocol. The shaded areas show the 90% confidence interval (CI) range and IQR, with the median patient noted by a dashed line. It is clear that the Glucontrol cohort has higher insulin sensitivity at all likelihoods (y-axis) and for all observed percentile patients compared to the SPRINT cohort. It is also clear that the spread or range of insulin sensitivity across the cohort is almost two times wider for Glucontrol, indicating a cohort with far greater inter-patient variability in insulin sensitivity or resistance, and thus one potential reason for its greater outcome glycemic variability given the relatively fixed non-patient-specific structure of the Glucontrol protocol.

3.4.2 Stochastic Model

Insulin sensitivity can evolve both gradually and acutely over time in ICU patients. Stochastic models based on the hour-to-hour variation of this model variable yield distribution of the potential change in insulin sensitivity over 1-4 hours [Lin et al., 2008, 2006]. These distributions then allow the creation of outcome blood glucose confidence bands for a given insulin and nutrition in-

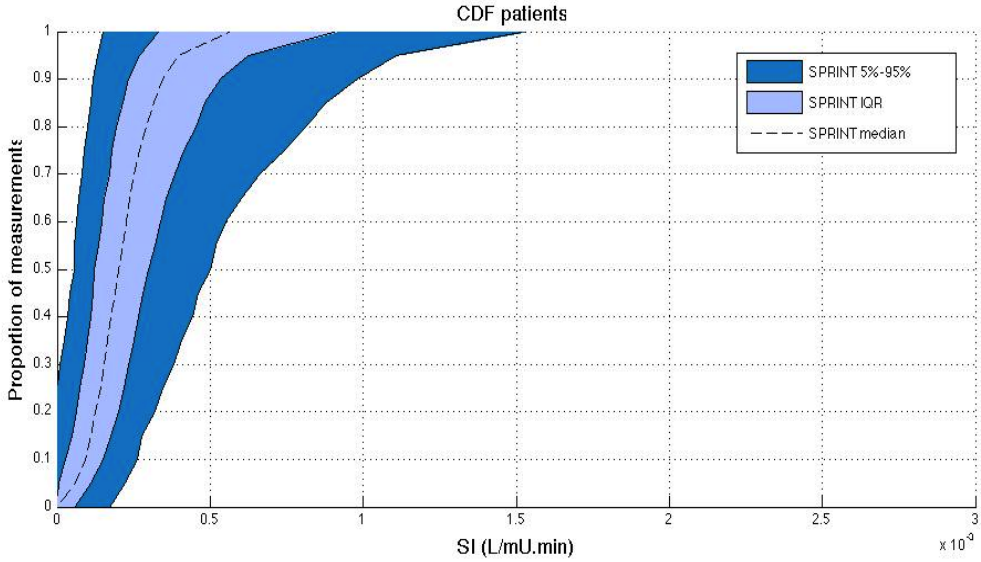

Figure 3.8: Empirical CDFs per-patient of insulin sensitivity on SPRINT.

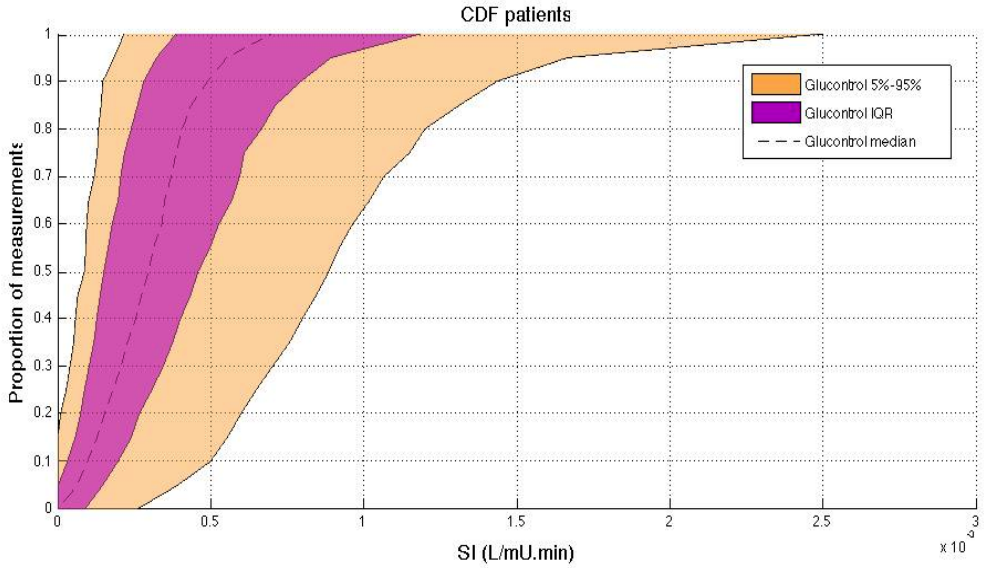

Figure 3.9: Empirical CDFs per-patient of insulin sensitivity on Glucontrol.

tervention [Evans et al., 2011]. Thus, these models also quantify the potential affect on glycemic control of both minor and acute evolutions in patient condition, as a function of current metabolic state and the clinical interventions. As a result, a model-based or adaptive TGC system can optimise interventions to minimise the risk of unexpected glycemic excursion and provide better decision making [Lin et al., 2008; Le Compte et al., 2009].

Knowledge of these dynamic changes provides further metrics of how metabolically dynamic and insulin resistant a given cohort may be. Therefore, they provide another physiologically relevant means of comparing cohorts for similarities and differences relevant to the quality of glycemic control achieved. While details are left to the references, a more dynamic and insulin resistant cohort would expect to have different bounds on this variability, and thus, all else equal, more variable glycemic control. Similarly, a more insulin resistant cohort would be expected to require more insulin to achieve equal glycemic outcomes. Thus, this model based-based parameter and its variation can be used to quantify inter-patient and intra-patient variability for different cohorts, also enabling comparison of metabolic variability (over time and across patients) between cohorts.

This metric is thus a unique, but physiologically and clinically relevant metric not only for glycemic control but also for assessing overall patient-specific stress response to illness. In particular, since the counter-regulatory and acute immune responses of critically ill patients are primary drives of insulin resistance, this metric thus captures their net effect. Hence, S_I is a direct, metabolic-based biomarker of the level of critical illness.

Figure 3.10 shows the distribution and hour-to-hour variation of fitted

S_I over time for all Glucontrol protocol patients, where measurements were 1-2 h apart, enabling the use of the stochastic model of Lin and colleagues [Lin et al., 2008, 2006]. The x-axis shows the S_I value at hour t, and a vertical line shows the distribution of possible S_I values in the next hour, $t+1$ based on the entire cohort's data. The median, IQR and 90% CI lines provide context and indicate the potential variability and the shape of its distribution over the next hour. This plot thus shows the hour-to-hour distribution and likelihood of metabolic intra-patient glycemic variability in response to insulin for the Glucontrol cohorts. Hence, it might be hypothesized that the greater the intra-patient variability in response to insulin interventions, the greater the resulting glycemic variability in response, if not directly managed by the protocol.

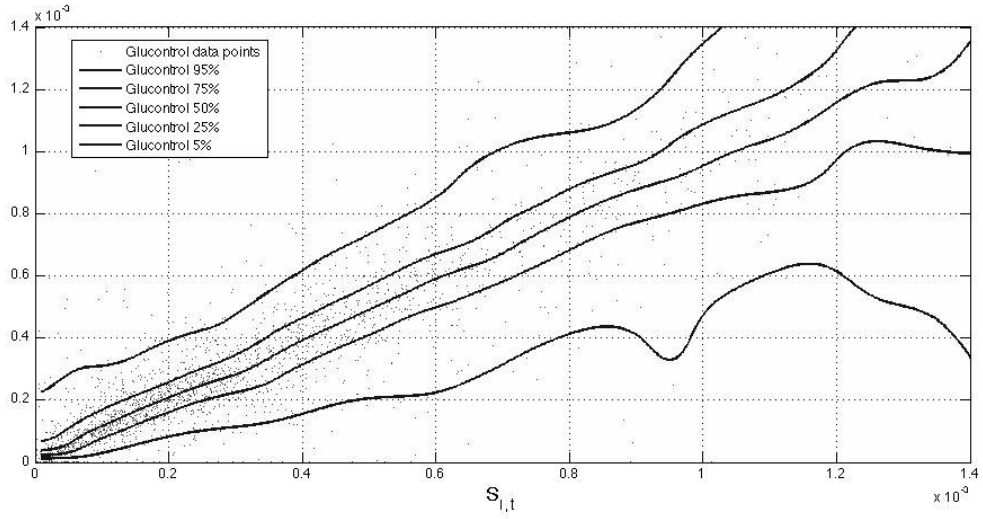

Figure 3.10: Fitted hourly S_I variation and probability distribution function of Glucontrol (1-2 h interval).

Figure 3.11 provides the same data for SPRINT. Figure 3.12 shows the combination of IQR, median and 90% CI from figures 3.10 and 3.11 for both

protocols. Figure 3.12 clearly shows very similar trends of median, IQR and 90% CI, indicating very similar metabolic intra-patient variability, as assessed by this clinically validated parameter.

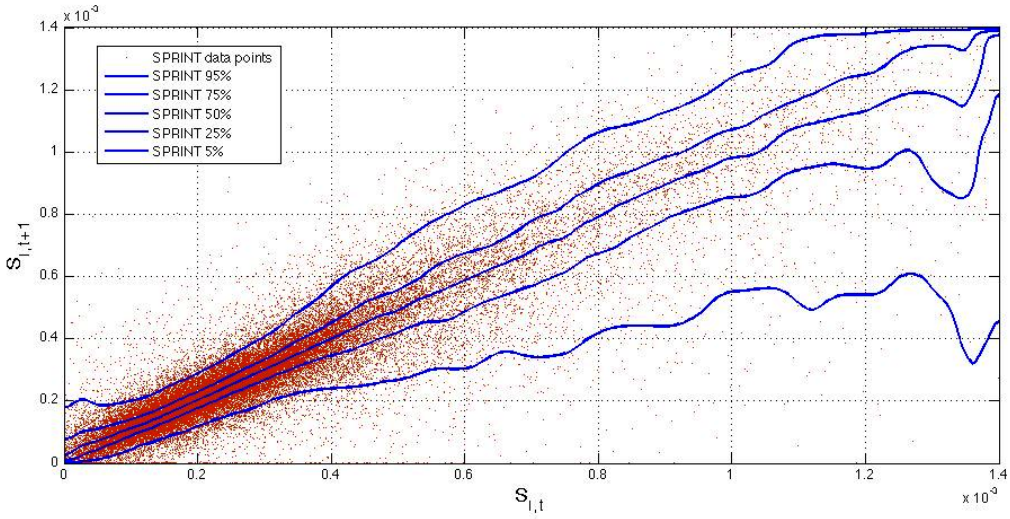

Figure 3.11: Fitted hourly S_I variation and probability distribution function of SPRINT.

Referring to Figures 3.8 and 3.9, its clearly shown that the Glucontrol cohorts span a wider range of insulin sensitivity than the SPRINT cohort with more inter-patient variability. However, their hour-to-hour variation can significantly affect the level of glycemic control, especially in cases with less frequent measurement, where small evolutions over several hours can result in large changes in metabolic status and glycemic outcome for a constant infusion of insulin and nutrition.

Hourly changes are the same for both Glucontrol and SPRINT given the similar plots in Figure 3.12, where one hour variations may be considered significant with respect to glycemic control and interventions when outside a 15%

change from the prior hour [Lin et al., 2008; Chase et al., 2011b]. Thus, despite the different inter-patient variation between SPRINT and Glucontrol in Figures 3.8 and 3.9, the hour-to-hour intra-patient variation between cohorts is, perhaps surprisingly, very similar.

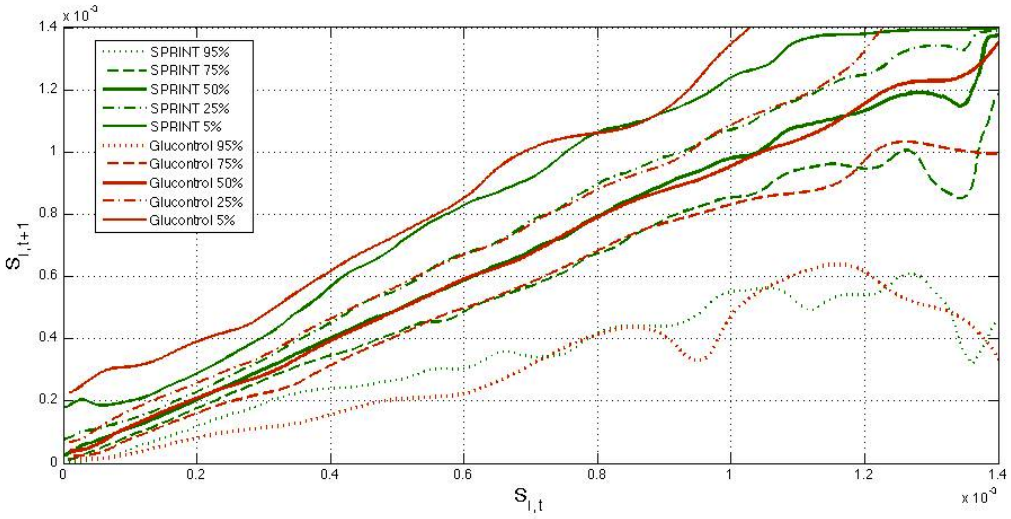

Figure 3.12: Fitted hourly S_I variation and probability distribution function of SPRINT and Glucontrol with a 1-2 h measurement interval.

3.5 Glucose Control Analysis

3.5.1 Glycemic Outcome

Table 3.4 summarizes the control results of SPRINT and Glucontrol. Median blood glucose for groups A and B were 6.3 and 8.2 mmol/L, respectively, as expected, and SPRINT was 5.7 mmol/L, which is close to the Group A value due to their similar glycemic targets. However, variability is much different across these protocols. Median interquartile range (IQR) spread (75th -25th

percentile) was 1.6 mmol/L for SPRINT, but 2.3 mmol/L for Group A and 2.5 mmol/L for Group B over the entire cohorts.

To achieve these results, SPRINT used approximately two times as much insulin as Group A, since the median insulin rate for SPRINT is 2.8 U/h and 1.5 U/h for Group A, noting that both of these groups had similar glycemic target. However, SPRINT used four times more than Group B with 0.7 U/h due, in part, to its higher glycemic target. Since patients who did not receive insulin were eliminated from the Glucontrol cohort examined, the comparison shown is per-protocol patients treated at some point with insulin.

Median nutrition, reported as appearance rate of carbohydrate in the nutritional formulas used, was broadly similar with median rates of 0.3, 0.6 and 0.42 mmol/min for Group A, Group B and SPRINT respectively. However, it is also clear in Table 3.4 that the spread of carbohydrate administration rates is much more tightly controlled by SPRINT with an IQR range of 0.27 mmol/min for SPRINT versus 0.9 mmol/min for Glucontrol groups A and B. Hence, even where there are similar targets, interventions were significantly different.

With respect to variability and safety from hypoglycaemia, SPRINT had increasingly lower percentages of measurements below 4.0, 3.0 and 2.2 mmol/L compared to the similarly targeted Group A. Surprisingly, it also had lower percentages of measurements below 3.0 and 2.2 mmol/L than Group B, which had a much higher glycemic target, indicating that this protocol had significant variability in glycemic response. As a percentage of patients, SPRINT thus had a much lower rate of hypoglycaemia below 2.2 mmol/L with 2% compared to Group A with 7.7% and the higher-targeted Group B

with 2.9%.

Regarding tightness of control, SPRINT had 48.2% of measurements in its target range, which is higher than that for the similarly targeted Group A with 35.8%. In addition, Group B had 40.6% total blood glucose measurement in its target range of 7.8 - 10.0 mmol/L. The results for hyperglycemic measurements (percentage $>$ 8.0 mmol/L) follow similar trends with expected differences for the higher-targeted Group B. Hence, SPRINT was more effective and tighter in its target range indicating better management of inter- and intra-patient variability.

On a per-patient basis, the median patient's median blood glucose was 6.4 mmol/L for Group A, 8.3 mmol/L for Group B, and 5.8 mmol/L for SPRINT, similar to those results for each overall cohort. However, the spread of median glucose levels across patients in each cohort was comparable for SPRINT, with 1.1 mmol/L separating the 25th and 75th percentile patient's median blood glucose value, and Glucontrol, with 1.0 and 1.2 mmol/L spreads for groups A and B, respectively.

Table 3.4: Comparison of Glucontrol and SPRINT control results.

	SPRINT	Glucontrol A	Glucontrol B
Cohort Results			
Blood glucose median [IQR] (mmol/L)	5.7 [5.0 - 6.6]	6.3 [5.3 - 7.6]	8.2 [6.9 - 9.4]
Insulin rate median [IQR] mU/min)	50.0 [16.7 - 50.0]	25.0 [8.3 - 50.0]	11.7 [0.0 - 28.3]
Feed rate of carbohydrate median [IQR] (mmol/min)	0.42 [0.25 - 0.52]	0.30 [0.00 - 0.90]	0.60 [0.10 - 1.00]
Number of patient with blood glucose less than 2.2 mmol/L	8 (2.0 %)	11 (7.7 %)	2 (2.9 %)
Percentage of measurement less than 2.2 mmol/L (%)	0.05	0.4	0.1
Percentage of measurement less than 3.0 mmol/L (%)	0.28	1.3	0.4
Percentage of measurement less than 4.0 mmol/L (%)	3.9	5.3	0.8
Percentage of measurement less than 4.4 mmol/L (%)	9.4	9.4	1.7
Percentage of measurement between 4.4 and 6.1 mmol/L (%)	48.2	35.8	10.4
Percentage of measurement between 7.8 and 10.0 mmol/L (%)	6.2	15.6	40.6
Percentage of measurement greater than 8.0 mmol/L (%)	8.0	20.3	52.5
Per-Patient Results			
Hours of control median [IQR]	53 [19 - 149]	61 [38 - 138]	89 [43 - 229]
Number of blood glucose measurements taken median [IQR]	37 [16 - 97]	19 [11 - 37]	22 [11 - 47]
Blood glucose median [IQR] (mmol/L)	5.8 [5.3 - 6.4]	6.4 [5.9 - 6.9]	8.3 [7.6 - 8.8]
Insulin rate median [IQR] (mU/min)	50.0 [33.3 - 50.0]	25.0 [13.3 - 33.3]	8.3 [0.0 - 16.7]
Feed rate median [IQR] (mmol/min)	0.37 [0.20 - 0.48]	0.1 [0.0 - 0.8]	0.2 [0.0 - 0.7]

All these results indicate that SPRINT maintained far tighter control on a cohort-wide basis, but was comparable for intra-patient glycemic variability when analyzing on a per-patient basis. Figure 3.13 provides cumulative distribution functions (CDFs) for each protocol's entire cohort, where the steeper SPRINT CDF clearly shows the lower variability compared to Glucontrol. The Glucontrol CDFs are similar in slope, but shifted, indicating similar behavior around each glycemic target for each cohort.The crossover of the Group A and SPRINT CDFs at 0.1 y-axis likelihood value shows the higher hypoglycaemia risk in the similarly targeted Group A cohort.

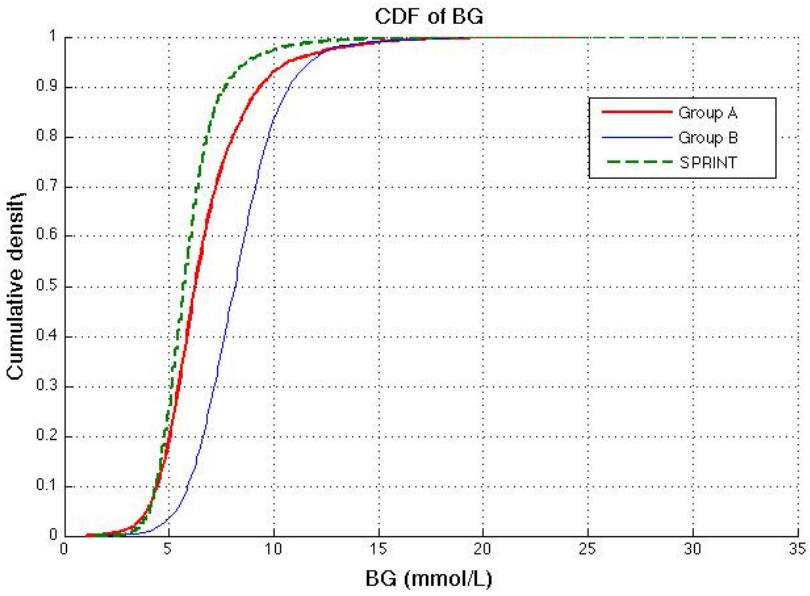

Figure 3.13: Cumulative distribution function of measured blood glucose on cohort basis for SPRINT, Group A and Group B (Glucontrol).

Figure 3.14 shows the same cohort CDFs for insulin delivered and Figure 3.15 for nutritional carbohydrate (all sources) delivery rate. It is clear in Figures 3.14 and 3.15 that SPRINT provides insulin and nutrition far more consistently across the cohort (steeper and less zero-valued CDFS). Thus SPRINT

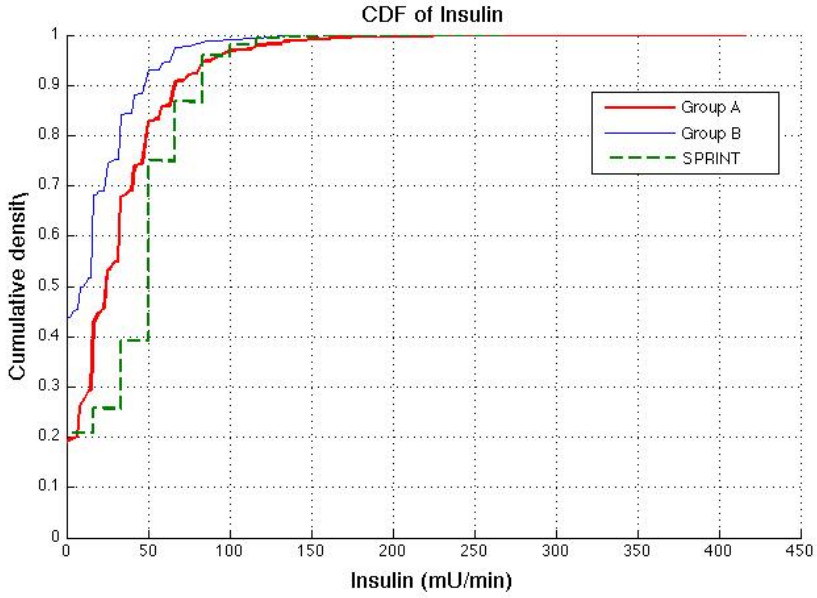

Figure 3.14: Cumulative distribution function for hourly insulin infusion rate on cohort basis for SPRINT, Group A and Group B (Glucontrol).

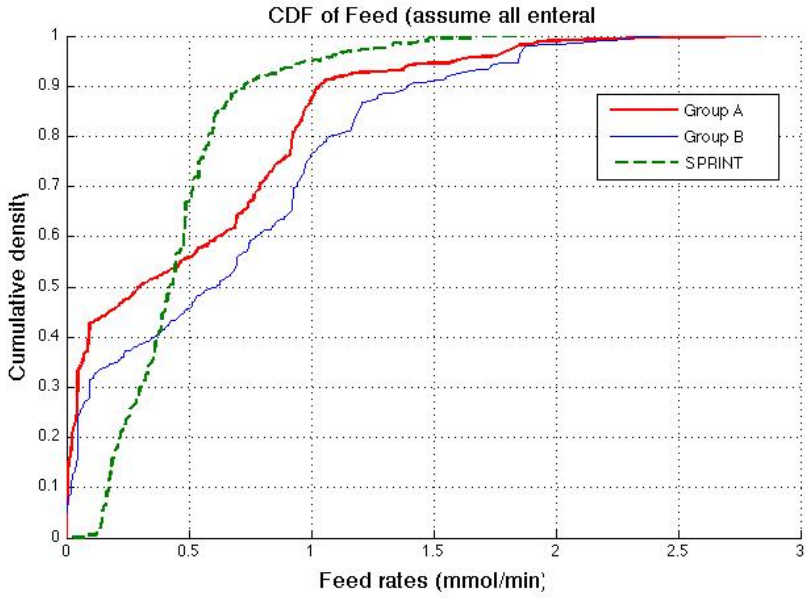

Figure 3.15: Cumulative distribution function of nutrition rate on cohort basis for SPRINT, Group A and Group B (Glucontrol).

provided a more constant nutrition rate in terms of carbohydrate appearance from all sources to balance the insulin given with far less variation in glycemic outcome. Importantly, nutrition rate was not a controlled variable and specified only to local standards in the Glucontrol study, which likely resulted in the greater variability in this input, and thus the greater resulting glycemic variability and greater hypoglycaemia.

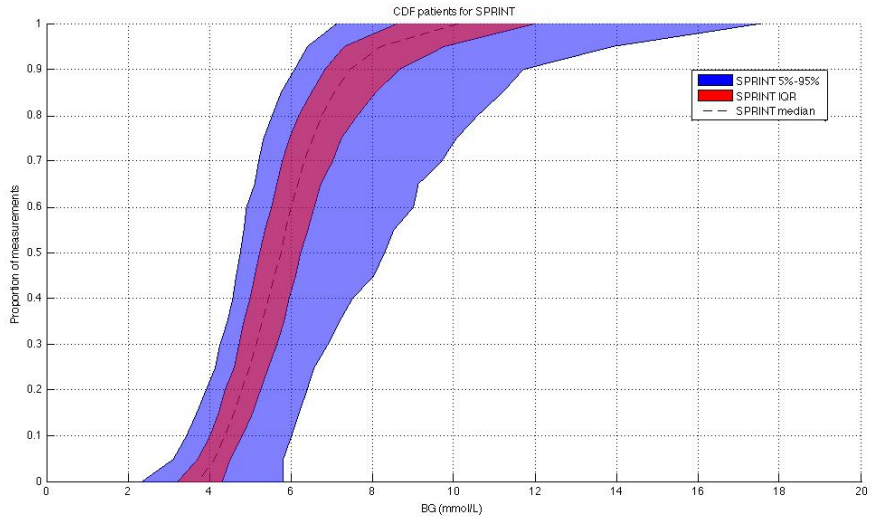

Figure 3.16: Empirical cumulative distribution function of measured blood glucose on SPRINT.

Figures 3.16 - 3.18 illustrate the inter-patient variability in the resulting glycemic outcomes. The curves show the 5th, 25th, 50th (median), 75th and 95th percentile patient responses, and shaded areas show the resulting IQR and 90% confidence interval range, where the x-axes and y-axes show the blood glucose level and proportion of measurements, respectively.

In Figure 3.16, the per-patient CDFs shown reveal a tighter result across patients, particularly over the 25th to 75th percentile IQR patients, for the

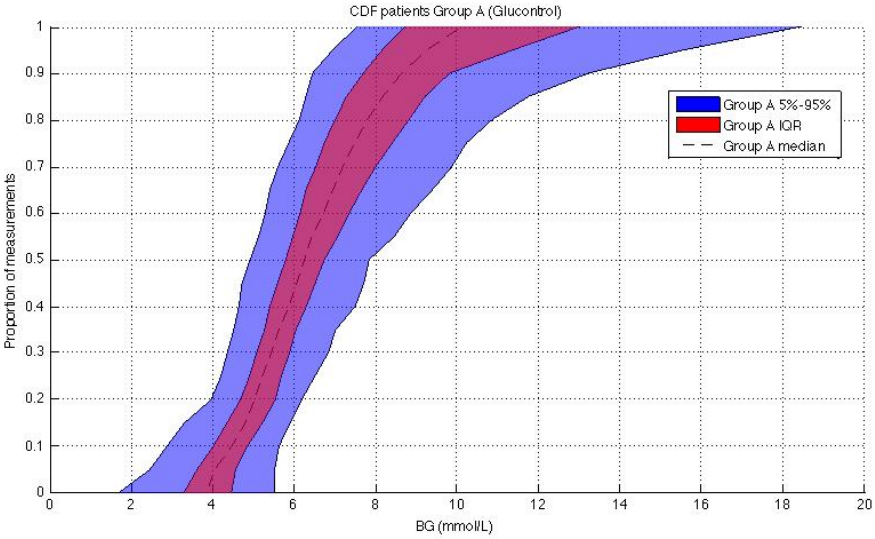

Figure 3.17: Empirical cumulative distribution function of measured blood glucose on Group A of Glucontrol.

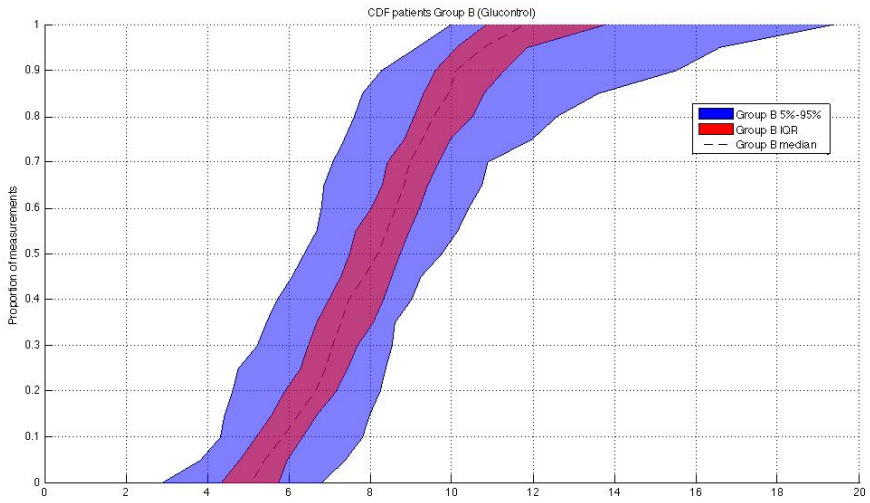

Figure 3.18: Empirical cumulative distribution function of measured blood glucose on Group B of Glucontrol.

SPRINT protocol, despite the differences of variability noted in prior results. The same lower variability seen for SPRINT over the cohort (steeper CDF in Figure 3.13) is also evident for all percentile patients in Figures 3.17 - 3.18, in comparison to the Glucontrol cohorts shown in Figure 3.13.

SPRINT achieved tighter control compared to Glucontrol A or B (for the one center examined) around their respective target glycemic levels, as clearly seen in Figure 3.13. The steeper CDFs indicate the lower, by cohort, glycemic variability. Importantly, the Glucontrol CDFs are very similar, but primarily shifted to their respective target glucose levels, resulting in higher hypoglycaemia for the Group A cohort with the lower target. This result is reinforced by the steeper and less variable per-patient CDFs for the middle 50% of patients (IQR) in each cohort shown in Figures 3.16 - 3.18, which thus indicates the ability of each protocol to manage the inter-patient and intra-patient variability. Notably, intra-patient variability, which determine the per-patient CDF slope, was similar between Glucontrol and SPRINT in Figure 3.12 but resulted in less steep slopes for Glucontrol in Figures 3.16 - 3.18, indicating a protocol failure in managing variability.

The higher incidence of hypoglycaemia for lower percentile patients is clear in Figure 3.17. In particular, Figure 3.17 indicates that the intensive Glucontrol A protocol could not effectively account for the inter-patient and intra-patient variability in metabolic behavior seen in Figures 3.8 - 3.11, despite the wider range of insulin and nutrition inputs used. Hence, some Glucontrol A patients were simply controlled by the protocol to too low glycemic level, resulting in increased risk of hypoglycaemia, which has been commonly reported in other studies [Griesdale et al., 2009].

This outcome clearly indicates that the Group A Glucontrol protocol was not able to fully account for differences between patients or/and intra-patient variability. This outcome was reinforced by the cohort and per-patient results in Table 3.4, which show cohort IQR ranges for glycemic outcomes are much wider in this group than in the similarly targeted SPRINT case. As a result, SPRINT also had far less hypoglycaemia, and thus a significantly decreased risk of death [Bagshaw et al., 2009; Egi et al., 2008; Egi and Bellomo, 2009].

In terms of providing nutrition and insulin, SPRINT has a higher proportion of patients receiving, on average, more insulin than Group A and more consistently as well for Group B (less zero values on the CDF in Figure 3.14). In current thinking, this increased insulin usage should have resulted in similar or greater hypoglycaemia, which was not the case here. However, SPRINT patients also received a more consistent input of carbohydrate administration from all sources compared to Glucontrol Groups A and B , as seen in the relatively very steep CDFs for SPRINT in Figure 3.15 with virtually no zero values.

Considering the carbohydrate intake, note that all sources of carbohydrate includes enteral and parenteral nutrition and intravenous dextrose. This difference in CDFs is critical given that the median and average values are similar across all three cohorts. However, per-patient results for all three cohorts show that the spread of carbohydrate administration rates was much tighter for SPRINT than for either Group A or Group B by a factor of almost 4x for median rates across patients, as seen in Table 3.4.

3.5.2 Insulin and Nutritional Input in Glycemic Control

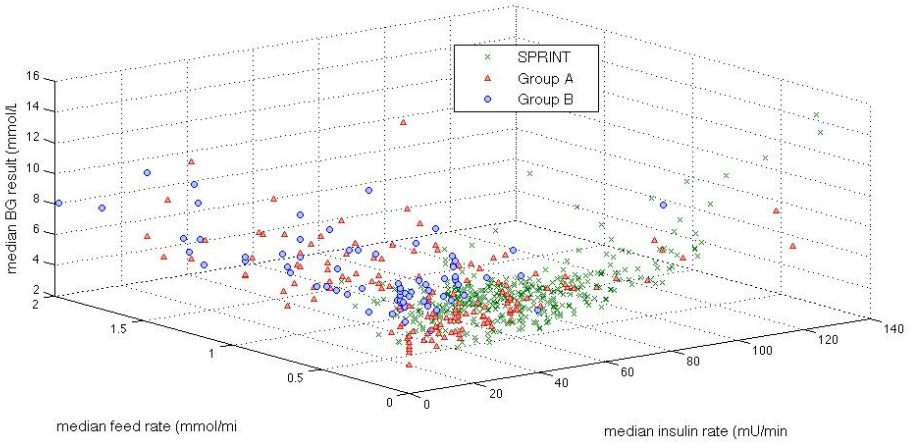

Figure 3.19: Cumulative distribution function of nutrition rate on cohort basis for SPRINT, Group A and Group B (Glucontrol).

Figure 3.19 summarizes the control and metabolic balance delivered by the protocols between carbohydrate administration, insulin administration and resulting glucose levels. It uses three-dimensional plots of median blood glucose, median insulin dose and median carbohydrate administration rates for every patient in all three cohorts. Importantly, these inputs operate on the insulin-glucose balance mediated by S_I and its variability to determine the resulting outcome glycaemia.

For clarity, Figures 3.20 - 3.22 show the decomposition of this three-dimensional plot into two of the dimensions for each parameter. It is clear in Figures 3.20 - 3.22 that the SPRINT data and glycemic outcomes are far less variable and/or more tightly controlled. This result is particularly valid with respect to the median nutrition rate and carbohydrate content versus outcome median blood glucose. In Figure 3.20, both groups had zero feed rates at some

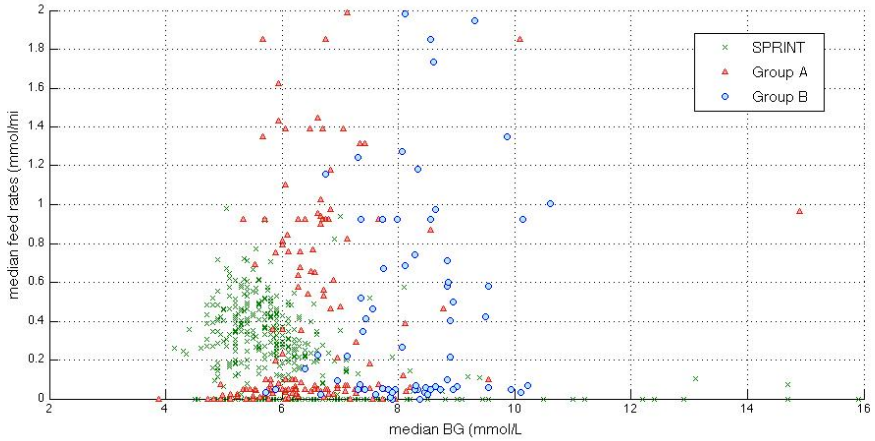

Figure 3.20: Cumulative distribution function of nutrition rate on cohort basis for SPRINT, Group A and Group B (Glucontrol).

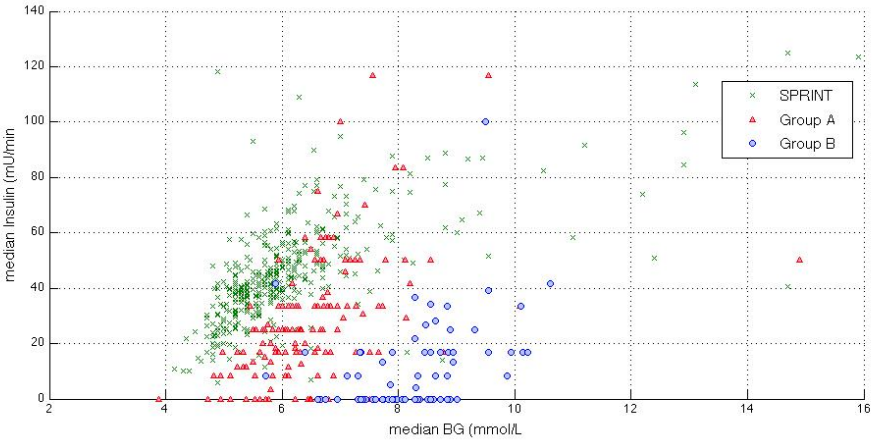

Figure 3.21: Cumulative distribution function of nutrition rate on cohort basis for SPRINT, Group A and Group B (Glucontrol).

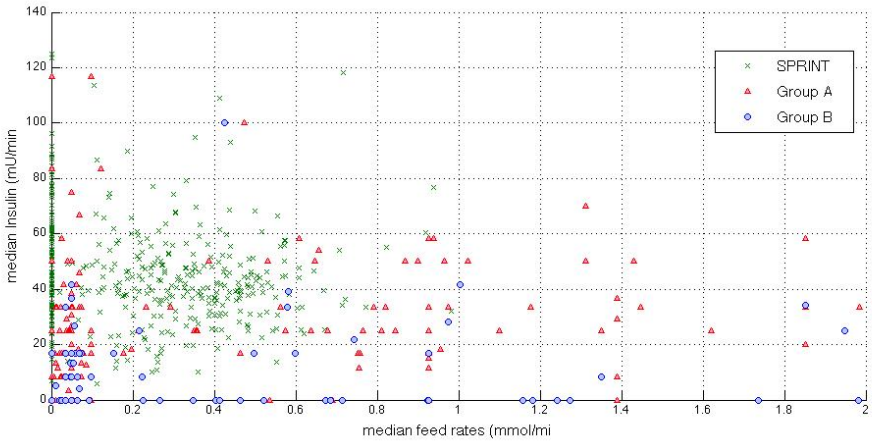

Figure 3.22: Cumulative distribution function of nutrition rate on cohort basis for SPRINT, Group A and Group B (Glucontrol).

portions for very short staying patients. In SPRINT, some patients were not fed, which corresponds to 1-2% of hours with no feed as shown in Figure 3.15. Overall, these plots show the metabolic balance achieved for each patient between insulin and carbohydrate inputs and the resulting glycemic outcome. They also clearly show the outlying patients with unbalanced and/or extreme insulin and nutrition inputs resulting in poor glycemic control to the desired target.

Krishnan and associates [Krishnan et al., 2003] shows that 33-66% of the ACCP guidelines of 25 kcal/kg/day [Cerra et al., 1997] are the optimal rates of carbohydrate administration with respect to mortality outcome. The SPRINT data are thus clustered almost entirely in this range. In contrast, the greater spread in Glucontrol data is due to not controlling this variable, and leaving carbohydrate administration to local clinical practice for that patient cohort. Hence, it may not be unexpected that there was no correla-

tion between mortality and median per-patient carbohydrate administration in SPRINT, but that it was significant considering all Glucontrol patients. Moreover, in Glucontrol study [Preiser et al., 2009], the nutritional inputs were left to local standards of care, which can be quite variable, both between centers and between clinicians in a center. Hence, the failure of Glucontrol to achieve a mortality difference, as well as its increased hypoglycaemia may not be surprising.

These results indicate that the higher insulin usage combined with co nsistent, tightly managed carbohydrate input was balanced in the SPRINT protocol, resulting in less glycemic variation and, for similar target glucose, less hypoglycaemia. More specifically, the SPRINT protocol interventions were both more consistent and within their tighter range, better able to manage the inter and intra-patient variation in their cohort. Overall, hypoglycaemia and tight control are explicit functions of the nutrition and insulin dosing ,leading to the conclusion that explicit knowledge of carbohydrate intake must be accounted for in successful TGC. In particular, without this information, it will be far more difficult, if not impossible, to strike a safe, long term, consistently achieved glycemic balance for such highly variable and dynamic patients.

More importantly, it can be evaluated that clear guidelines for nutrition intake of carbohydrate are essential in TGC protocol design, regardless of the nutritional standards and practices across different countries. In addition, considering frequent and convenient measurement, future protocols should also consider bedside glucose monitoring system for reduced clinical effort and better control. Finally, these recommendations arise from the recognition of

insulin sensitivity and model-based S_I (as defined) as being significant markers of patient metabolic and overall condition.

3.6 Summary

From this analysis, two conclusions may be drawn. Firstly, any protocol must be able to adapt to a given patient's specific level of insulin resistance and its changes with time, thus accounting for inter- and intra-patient variability. It is clear that Glucontrol was potentially unable to manage one or both of these aspects, as per-patient glycemic outcomes were similarly shaped in CDFs across Group A and Group B, with a simple shift due to different glycemic targets. Secondly, to control glycemic levels better, carbohydrate administration must be explicitly accounted for in the protocol design and implementation, which enables assessment or estimation of effective insulin sensitivity in real time in response to interventions. In particular, this data would allow protocols to adapt their inputs to match gradual or acute changes in a patient's metabolic status (insulin resistance or insulin sensitivity, S_I), which is what SPRINT effectively does [Chase et al., 2008b; Lonergan et al., 2006], and thus provide potentially tighter control and more consistent care.

In a nutshell, successful TGC protocols must be able to account for the significant inter-patient and intra-patient variability in insulin resistance (sensitivity) that can be observed in critically ill cohorts. In addition, explicit knowledge of potential control of carbohydrate administration within reasonable limits appears to be a mandatory component in reducing outcome glycemic variability and thus, potentially, in achieving all the benefits of TGC

with minimal risk. It is a factor that is missing from many of the published protocols to date. While inter-patient variability in insulin sensitivity can be quite different between cohorts that are otherwise similar in severity of illness, the evolution and dynamic change or intra-patient variability of this parameter appears to be very similar across the cohorts studied here, which is a unique and potentially valuable insight.

Finally, this chapter highlights the key aspects of TGC trials and data that can be used in developing improved protocols, as well as used for retrospective analysis and comparisons that may have been previously overlooked. It does by identifying a patient-specific marker of patient condition in insulin sensitivity or S_I. As the balance or mediator between insulin and carbohydrate appearance, it thus determines the success or failure of specific TGC protocols. Hence, the main outcome of this chapter is that model-based S_I is a validated means of assessing both patient condition as reflected by the analysis of different TGC protocols on metabolically similar cohorts.

Chapter 4

Model Validation

This chapter presents the overall validation of the glucose-insulin system model on Glucontrol data, a cohort from Belgium Hospital. Model validation was assessed by looking at the ability of producing patient dynamic through a fitting process. Virtual trials method was introduced for better understanding of developing virtual patients process. Simulations are run to capture the behavior of the cohort and protocol, which was different from the data used to replicate the model. Hence, the ability of the model to fit clinical data and physiological parameters validates the dynamics of the model. The overall validation of the model and methods serve to validate the use of model-based metrics in later chapters as representative of patient condition independent of other factors.

4.1 Glucontrol Study

A retrospective analysis using records from a 211 patients subset of the Glucontrol trial taken in Leige, Belgium was used in the Glucontrol study. In the Glucontrol trial [Preiser et al., 2009], patients were randomised into two groups, intensive (Group A) and conventional (Group B) insulin therapy. Both

Group A and Group B were targeted for different levels of BG, which were 4.4-6.1 mmol/L and 7.8-10.0 mmol/L, respectively. They are thus very different treatment regimes, particularly in potential physiological outcome at these different BG level [Chase et al., 2006, 2010a].

In the Glucontrol trial, insulin was administered as a continuous IV infusion [Preiser et al., 2009]. The protocol used hourly, 2-hourly and 4-hourly measurement intervals in obtaining the BG level and determining the resulting insulin treatment. Details of the protocols are shown and discussed in Section 3.2. However, nutritional input was left to local and/or clinician standards, and was not explicitly considered in the design or implementation of the protocol.

Clinical details of the resulting cohorts are shown in Table 4.1. This table provides the baseline variables and results from glucose control on Groups A and B. There were 64.8% of males patient in Group A whereas 56.5% in Group B. Patients in Group A were slightly older than Group B with median age of 71 and 69, respectively. However, there were no significant differences in severity of illness as measured by APACHE II score, weight or BMI. Patients in Group B had a slightly higher initial BG compared to Group A.

The total hours of control for Groups A and B were 16831 and 12946, respectively. There were 7391 total BG measurements, where 4571 measurements were from Group A and 2820 measurements from Group B. Even though more hours of control were required for Group A, a relatively high frequency of BG measurement was also observed for Group B.

Figure 4.1 shows the 5th - 95th percentile range, IQR and median prob-

Table 4.1: Comparison of Group A and B of Glucontrol cohort. *P*-values are computed using chi-squared and Mann-Whitney tests as appropriate.

Glucontrol Cohort	A	B	*P* value
Baseline Variables			
Number of patients	142	69	
Percentage of males (%)	64.8	56.5	0.2460
Median age [IQR]	71 [61 - 80]	69 [53 - 77]	0.0352
Median weight [IQR]	72 [62 - 85]	75 [68 - 81]	0.3802
Median BMI [IQR]	25.4 [22.6 - 29.3]	26.0 [23.2 - 29.3]	0.4577
Median APACHE II score [IQR]	17 [14 - 22]	17 [14 - 21]	0.7605
Median initial BG [IQR]	6.56 [5.56 - 8.56]	6.61 [5.65 - 9.36]	0.5845
Glucose Control			
Total hours of control	16, 831	12, 946	
Total BG measurement	4, 571	2, 820	
Median BG [IQR] (mmol/L)	6.3 [5.3 - 7.6]	8.2 [6.9 - 9.4]	
Median insulin rate [IQR] (mU/min)	25.0 [8.3 - 50.0]	11.7 [0.0 - 28.3]	
Median carbohydrate administration rate (all sources) [IQR] (mmol/min)	0.30 [0.00 - 0.90]	0.60 [0.10 - 1.00]	

ability bounds for stochastic models for Group A and Group B. The distributions indicate the hour to hour metabolic variability in insulin sensitivity is very similar across the majority of the S_I range for both groups, particularly for the middle 50% IQR. Hence, both groups are similar in metabolic variability, which is critical for this validation.

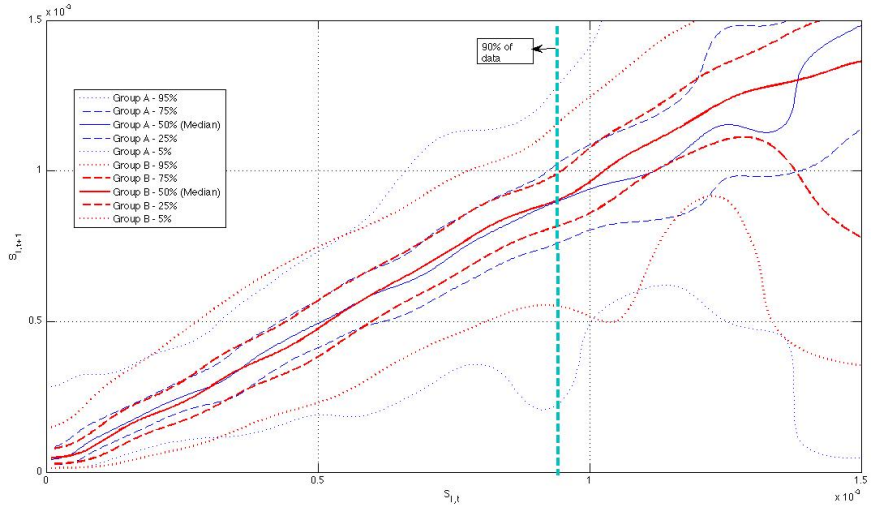

Figure 4.1: Hourly insulin sensitivity distribution for Group A and Group B of Glucontrol cohort.

In particular, 89% - 93% of the data for both groups was in the range of 0.01 x $10^{-3} \leq S_I \leq$ 0.8 x 10^{-3}, which is where there was greatest agreement between the groups. Above this range sparse data had an effect, particularly on the 5% and 95% bounds. Hence, the clinically matched cohorts of Table 4.1 are also similar in metabolic variability, which is significant evidence of similar metabolic response and variability in the context of insulin across patients and cohorts.

Despite significant differences between the two protocols of Glucontrol

A and B, the hour-to-hour intra-patient variation between cohorts is very similar, indicating hour-to-hour changes in insulin sensitivity are patient-specific and protocol independent. The cohorts can thus be considered interchangeable for the purpose of cross-validation. The intra-patient variation helps independently validate the assumption that this model-based insulin sensitivity is independent of the clinical inputs used to identify it, which is important as this assumption is the basis of the virtual trials.

4.2 Virtual Trials Method

Virtual trials are used to simulate a clinical trial using patient-specific data, such as model-based insulin sensitivity, S_I. The insulin sensitivity profile, $S_I(t)$, identified from clinical data captures a patient's time varying glycemic response to insulin and nutrition inputs. Later, this profile can be used to simulate the blood glucose response to other combinations of insulin and dextrose inputs specified by a modified tight glycemic control protocol to obtain a new glycemic response.

The process of developing a virtual patients start by collecting raw clinical data for a set of patients such as blood glucose measurements, insulin rates and enteral and parenteral dextrose rates. The collection of data is then fitted to identify a collection of virtual patients defined by their unique $S_I(t)$ profile. From the fitting process, hourly variation of insulin sensitivity, S_I, can also be assessed.

Figures 4.2 - 4.3 show examples of fitting process output for Patient 186

and Patient 213 from the Glucontrol cohort. The top panels of Figures 4.2 - 4.3 show the blood glucose data fit and measured blood glucose concentration, indicated by solid lines and crosses, respectively. The resulting insulin sensitivity profiles are plotted in the middle panel, and insulin and dextrose data are shown in the bottom panel.

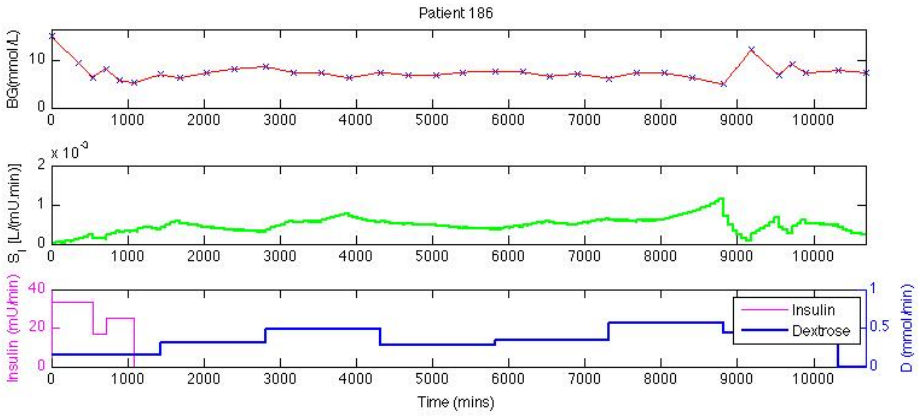

Figure 4.2: Patient 186 blood glucose data fit (top panel, solid line), measured BG (top panel, crosses), corresponding insulin sensitivity S_I (middle panel), and insulin and dextrose (bottom panel).

The next part is the in silico virtual patient simulation. In this process, the collection of virtual patients is simulated using their identified $S_I(t)$ profile with a selected glycemic control protocol. Therefore, simulation results will be based on the protocol applied. The output of the control simulations are insulin rates, dextrose rates, blood glucose response and other relevant performance and safety data. Different controllers will generate different blood glucose responses. Moreover, in silico virtual patient simulation provides the ability to collate and compare blood glucose response between protocols to optimise them before clinical use in a fast and safe manner. Figure 4.4 sum-

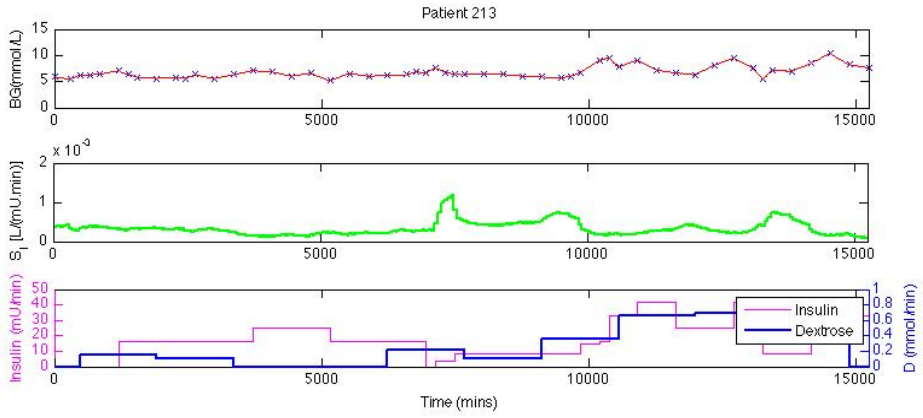

Figure 4.3: Patient 213 blood glucose data fit (top panel, solid line), measured BG (top panel, crosses), corresponding insulin sensitivity S_I (middle panel), and insulin and dextrose (bottom panel).

marizes the method in developing virtual patients and in silico virtual trial simulation method.

4.3 Virtual Trials Validation

In this analysis, two groups of virtual patients were created from clinical data from the Group A and B patients. They are defined by whether they were clinically treated with either the Glucontrol A (intensive) or Glucontrol B (conventional) protocols. Since the patients are clinically matched and metabolically similar, it is possible to compare them for validation purposes.

Three major forms of validation using virtual trials was performed in this study. The first approach is model fit and prediction error where it assesses overall model dynamics by looking at the simulation results and clinical data.

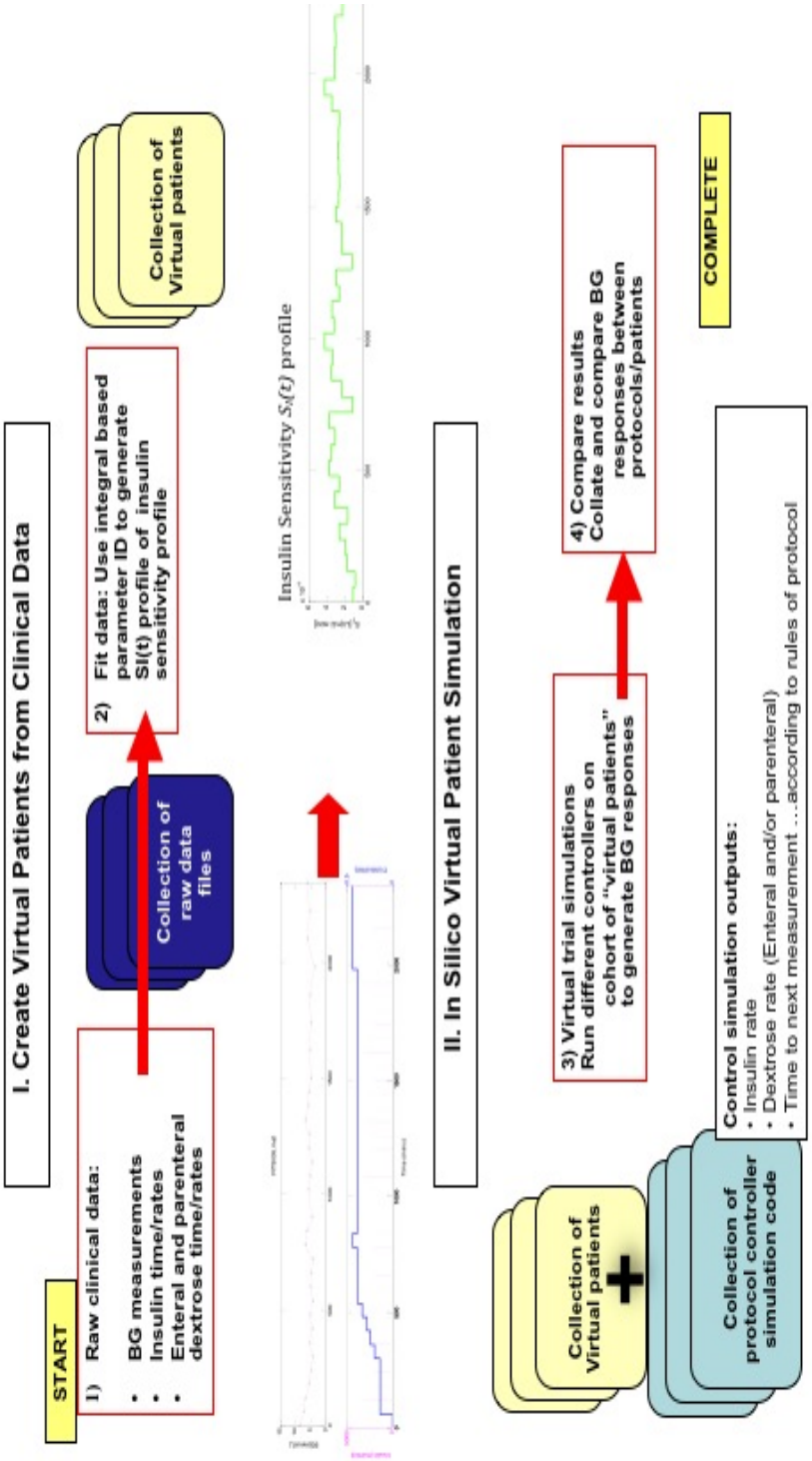

Figure 4.4: Virtual patient development and in silico simulation method.

The other forms of validation are self- and cross- validation. In self-validation, Protocol B is simulated on Group B virtual patients and similarly Protocol A is simulated on Group A virtual patients. These results are compared to clinical results for each group of patients. In contrast, in cross-validation, Protocol A is simulated on Group B virtual patients, and Protocol B is simulated on Group A virtual patients, with results compared to clinical results to see if matched patients treated by one protocol match results when simulated on another.

Figure 4.5 represents the virtual trial validation method used in this analysis. The patient profiles obtained are then used to resimulate the Glucontrol A and Glucontrol B protocols for comparison to the appropriate clinical results. Self-validation assesses the ability of the in silico virtual trials to repeat the clinical data. On the other hand, cross-validation assesses the assumption that the $S_I(t)$ accurately capture patient dynamics, independent of the insulin and nutrition inputs used to create them.

Cross-validation is the critical step in assessing methods and models. Self-validation indicates model errors. Finally, fit and, especially, prediction errors show overall model quality and ability to capture clinically observed dynamics.

4.3.1 Model Fit and Prediction Error

Model fit and prediction error are used to show the ability of the model to fit the data and predict the expected patient state, which is critical for control. Simulations were performed for Groups A and B using the clinically recorded

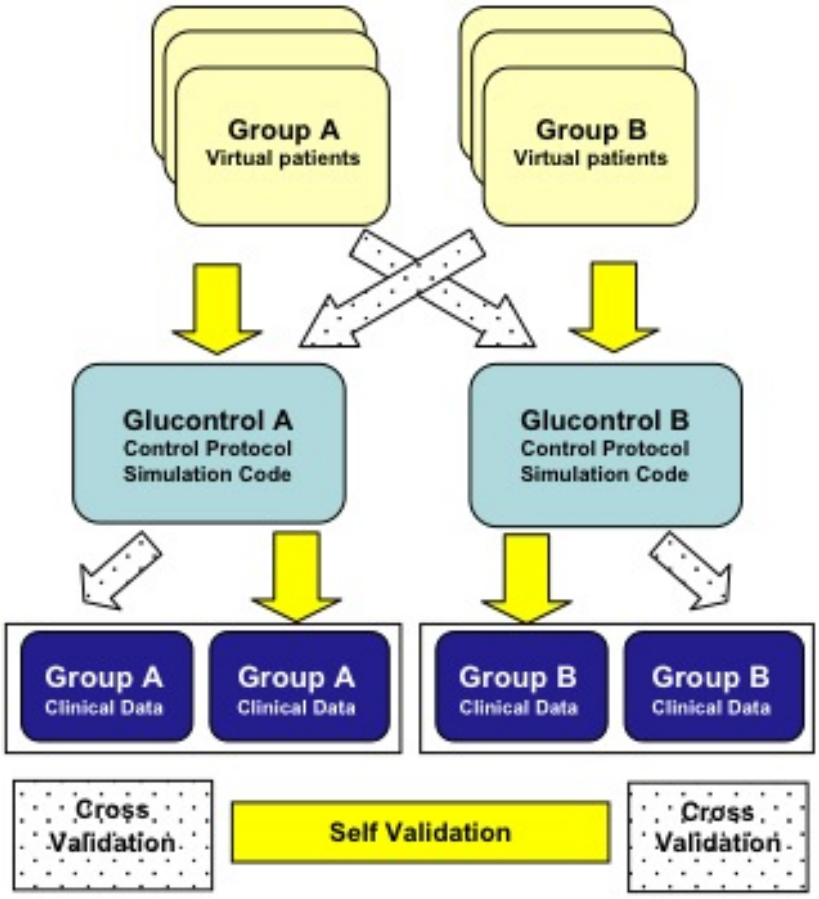

Figure 4.5: Virtual trial validation method.

insulin and dextrose administration rates as model inputs. The simulated BG measurements were compared to clinical BG data.

Prediction errors are a function of hour-to-hour patient variability and ability of the model to accurately capture insulin and glucose dynamics. Prediction results are generated by holding insulin sensitivity, S_I constant for an upcoming hour, for lack of better information, and simulating the blood glucose one hour into the future using the recorded clinical insulin and dextrose inputs. This blood glucose prediction is then compared to the clinically recorded blood glucose or a linear estimate between 2-hourly measurements. Prediction errors thus assess the model's ability to predict the outcome of an intervention in this population.

Figures 4.6 - 4.7 show the example of model generated blood glucose response for two of the same patients shown in Section 4.2. Predictions are generated after each recorded BG measurement assuming a constant S_I over one hour of prediction interval. In Figures 4.6 - 4.7, stars indicate the clinical BG value (input) and crosses indicate the predicted BG value simulated from the model. Dotted and solid lines represent the model BG fit for the input and the simulated BG, respectively. Differences between clinical BG values and simulated BG profiles indicate the prediction error.

Figure 4.8 shows the model fit and prediction errors for the entire Glucontrol cohort (A + B), and separated into Group A and Group B. Results are shown on a cohort and a per-patient basis. Model fit error was consistent across all three groups analysed, with median fit error $< 0.25\%$ in all cases. The model fit errors in Figure 4.8 are relatively very small and almost overlaid for Group A, B and the entire Glucontrol cohort.

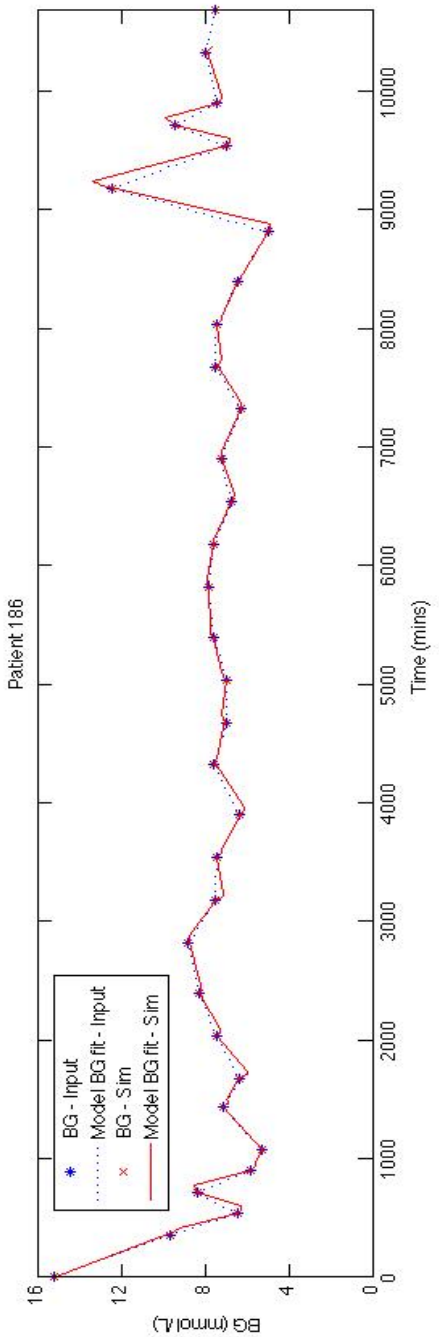

Figure 4.6: Model generated blood glucose response for Patient 186.

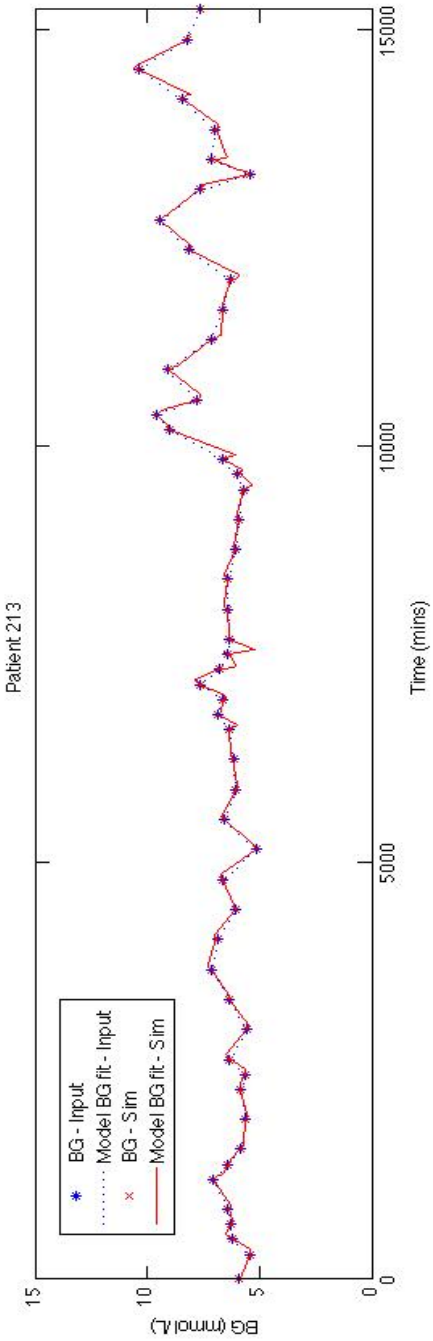

Figure 4.7: Model generated blood glucose response for Patient 213.

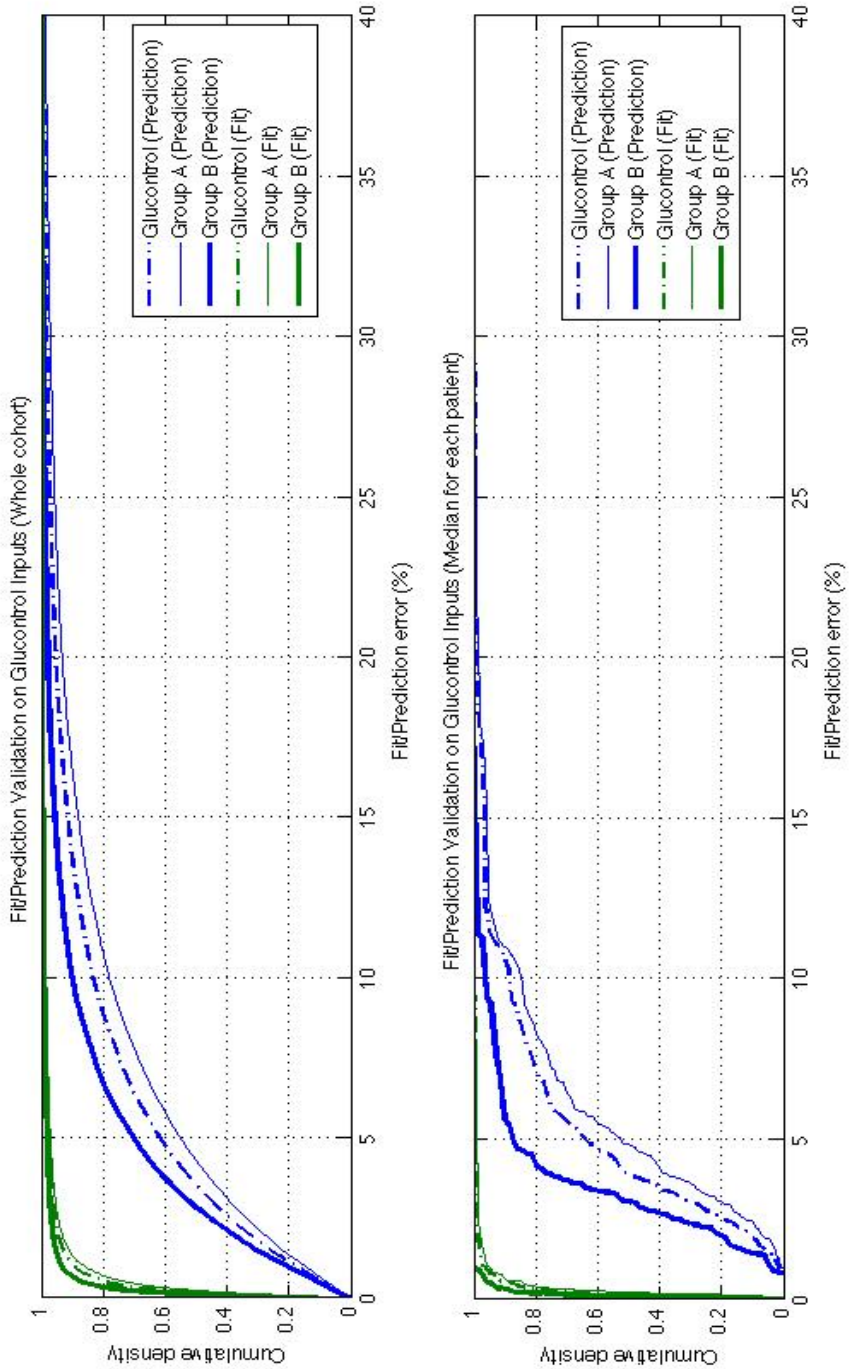

Figure 4.8: Plot of prediction errors for Group A, Group B and entire Glucontrol cohort. Model fit errors essentially overlaid for all 3 cohort groupings.

Group B has the lowest prediction error among these three distributions. The Glucontrol cohort prediction error median value was 3.5%, whereas Group A and Group B were 4.3% and 2.8% respectively. All these median errors are well below sensor errors of 7-12%. Despite the significant differences in clinical insulin usage for Group A and B, the model prediction errors are similar for these patients. This outcome is due to the fact that variability of insulin sensitivity for the cohort is similar, as seen in Figure 4.1.

Furthermore, the model prediction validation results can be seen as an estimate of the variability of insulin sensitivity in this cohort, as well as a sign of model fitness. Low prediction errors were found for both groups. For context, this result suggests the use of model-based targeted BG control will be effective for these cohorts of critically ill patients, as demonstrated for Christchurch ICU cohorts upon whom this model was derived and used. Thus, they also serve as an independent validation of this model using different ICU cohorts.

4.3.2 Self-Validation

In general, self-validation tests the ability of the in silico virtual patient modelling method to reproduce the clinical data from which a virtual cohort was derived. For the self-validation on Glucontrol A, the Glucontrol A protocol defined in Table 3.1 is simulated on Group A virtual patients, and these virtual trial results are compared to the clinical data of Group A. This step was repeated for self-validation on Glucontrol B. The clinically recorded dextrose administration profiles were used for the carbohydrate inputs into the model

in both cases to match the local standard used in the trial, as they were not specified by the protocol.

Differences between clinical and virtual trial results can be ascribed to model errors, and/or lack of perfect compliance in the clinical study versus the perfect compliance and timing in silico. Hence, two self-validation virtual trials were simulated on each group considering:

- The actual measurement timing used in the clinical trials (actual measurement), and

- Measurement timing from the protocol (per-protocol).

Comparing actual and per-protocol measurement timing allows one to assess one aspect of compliance error and its impact on results. For self-validation of actual measurement, the timing used in the virtual trial strictly follows the measurement timing in the clinical trials where the controller selects the proper intervention in response to the blood glucose values at the exact time correspond to its clinical time. In contrast, per-protocol self-validation follows exactly the Glucontrol A and B protocols defined in Tables 3.1 and 3.2 regardless of the measurement timing they had clinically. The controller will still select the intervention according to the current blood glucose values. However, because the Glucontrol protocols modify insulin by increments to a prior infusion rate in Tables 3.1 and 3.2, different measurement timing could significantly change dosing, which would thus indicate the impact of compliance to measurement timing.

Figure 4.9 shows the cumulative distribution function of measured blood

glucose on a cohort basis. This figure compares the distribution of clinical blood glucose for Group A and B to the simulated blood glucose distribution from the virtual trials of the Glucontrol A protocol on virtual patients of Group A and virtual trials of the Glucontrol B protocol on virtual patients of Group B.

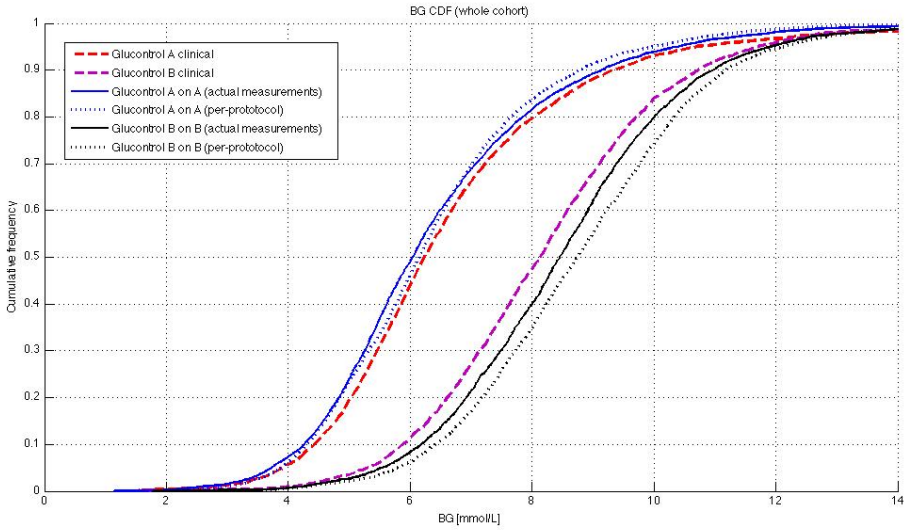

Figure 4.9: Cumulative distribution function of measured blood glucose on a cohort basis for clinical data and self-validation.

The breakdown of distributions shows a clear separation between the protocols for Glucontrol A and Glucontrol B simulations, as expected from the clinical results and Glucontrol trial design. The three distributions for the Glucontrol A protocol show particularly close agreement. The Glucontrol A clinical median blood glucose value of 6.2 mmol/L agrees well with the 6.0 mmol/L and 6.2 mmol/L medians for simulated trials using actual and per-protocol blood glucose measurement timing, respectively.

Blood glucose distributions for the Glucontrol B protocol show a slightly greater spread in results, particularly below the target of 8 mmol/L. However, the median blood glucose value of 8.1 mmol/L still agrees with the medians of 8.5 mmol/L and 8.7 mmol/L for Glucontrol B self-validation with actual and per-protocol measurement frequency, respectively.

Figure 4.10 shows the same results for the cumulative distribution function of the median patient blood glucose levels across all patients in Group A and Group B. This per-patient comparison has the same whole cohort trend in Figure 4.9. Interestingly, and as with the cohort results, the largest gap is between self-validation and clinical data for Glucontrol B. The wider error below 8 mmol/L is due to the fact that the Glucontrol B protocol requires zero exogenous insulin below its target, creating greater reliance on model assumptions and thus creating opportunity for inter-patient variability in these assumptions to play a rule.

4.3.3 Cross-Validation

Cross-validation uses the matched A and B cohorts to determine the ability of the modelling method to reproduce the clinical data on a matched, but independent cohort. For example, protocol A is simulated on virtual patients derived from Group B clinical data. The results of this test are then compared to the clinical data of Glucontrol A. Similarly, protocol B is test on virtual patients of Group A and the results are compared to Group B clinical data. If patients were perfectly, exactly matched the in silico and clinical data would also match. Differences using large matched cohorts can thus be ascribed

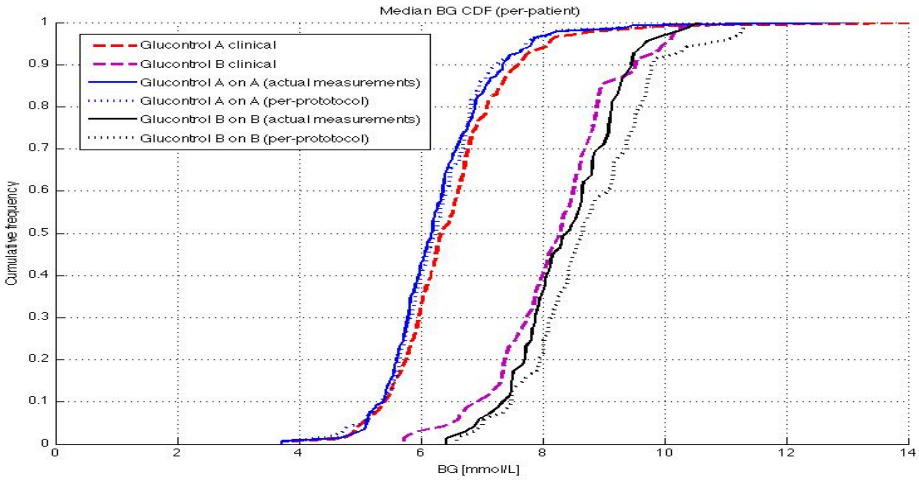

Figure 4.10: Cumulative distribution function of measured blood glucose on a per-patient basis for clinical data and self-validation.

to how well the assumption holds that these virtual patient $S_{I(t)}$ profiles are independent of the clinical inputs used to derive them, which is critical to saying $S_I(t)$ represents patient condition and not other factors.

Figure 4.11 compares the cumulative distribution function of clinical blood glucose for Group A and B to the simulated blood glucose distribution for virtual trials of the Glucontrol A protocol on virtual patients of Group B and virtual trials of the Glucontrol B protocol on virtual patients of Group A. The Glucontrol A clinical median blood glucose value of 6.2 mmol/L agrees well with 6.5 mmol/L for simulated trials of Glucontrol A on Group B virtual patients. In addition, the median blood glucose values for Glucontrol B clinical data and simulated trials of Glucontrol B on Group A virtual patients were 8.1 mmol/L and 8.5 mmol/L, which is less than 5% and quite low compared to sensor errors.

In comparison to the self-validation results for Protocol A and B, the cross-validation results lies between the clinical data and self-validation result indicating it is within the model and/or compliance error. Figure 4.12 shows the same results for the cumulative distribution function of the median patient blood glucose levels across all patients in Group A and Group B.

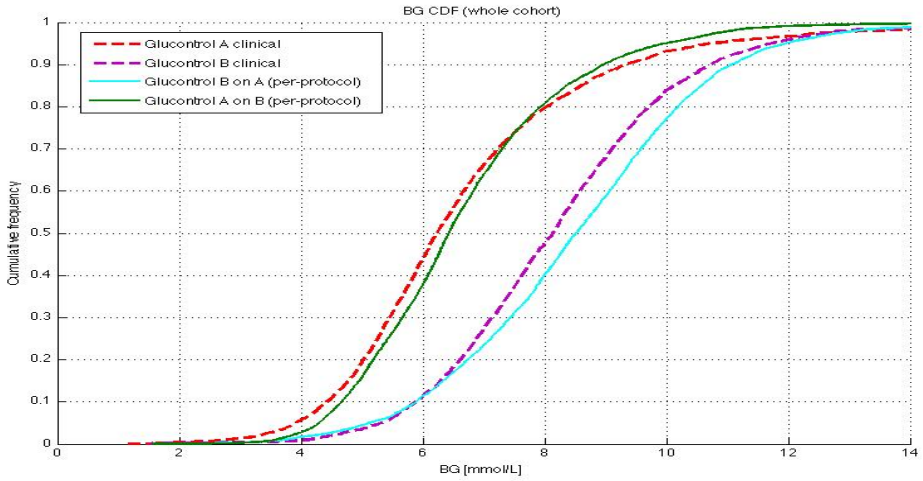

Figure 4.11: Cumulative distribution function of measured blood glucose on a cohort basis for clinical data and cross-validation.

4.3.4 Virtual Trials Results

Details of self-validation and cross-validation results are discussed in this section. Table 4.2 and Table 4.3 show the comparison of clinical trials to the self-validation and cross-validation on Glucontrol A and Glucontrol B, respectively. Results compare per-patient insulin rate, nutrition rate, blood glucose and blood glucose measurement rate.

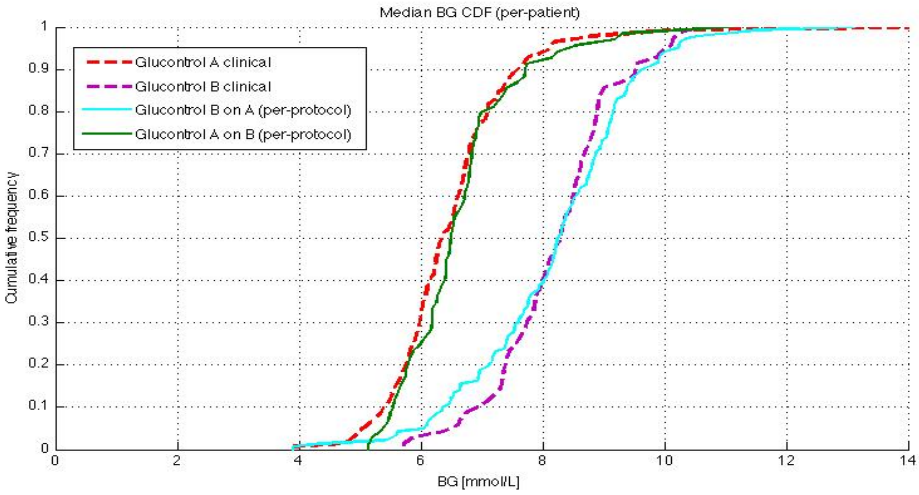

Figure 4.12: Cumulative distribution function of measured blood glucose on a per-patient basis for clinical data and cross-validation.

In Table 4.2, per-patient results show a reasonably close agreement between self-validation per-protocol to the clinical data. However, the insulin rates are higher given the almost 2x higher measurement rate when using the protocol specified rules. Using the actual measurement rate, the insulin rates are similar, indicating the impact on insulin of measurement compliance.

For the cross-validation, the Glucontrol A protocol required almost 3x higher rates of insulin for Group B, compared to the clinical data. However, this result may be a function of the interaction of protocol and measurement frequency where there was a 1.4x difference that results from per-protocol versus actual measurement self-validation, which is significant non-compliance. Equally, the Glucontrol B patients received 2.6x greater carbohydrate input to offset much of this difference in insulin administration showing also a protocol response. Specifically, the cross-validation in Table 4.2 required 3.2x more

insulin to offset 2.6x more carbohydrate administration. Adjusting by 2.5/1.8 the per-protocol versus actual measurement increase in insulin administered yields an estimated 1.4x increase in insulin use to offset this increased carbohydrate administration. Hence, the increased insulin in cross-validation in Table 4.2 is assessed as primarily due to the increased carbohydrate administered to Group B.

Table 4.2: Comparison of per-patient clinical results and virtual trial simulations (self-validation and cross-validation) on Glucontrol A. Median [IQR] is used where appropriate.

		Self-validation		**Cross-validation**
	Clinical	**Actual measurement**	**per-protocol**	**per-protocol**
No. of patients	142	142	142	69
Per-patient results				
Insulin rate (U/h)	1.4 [0.9 - 2.1]	1.8 [1.1 - 2.9]	2.5 [1.5 - 4.1]	4.5 [2.3 - 6.5]
Glucose rate (g/hr)	1.1 [0.5 - 7.6]	1.1 [0.5 - 7.6]	1.1 [0.5 - 7.6]	2.9 [0.7 - 7.4]
BG (mmol/L)	6.4 [5.9 - 6.9]	6.2 [5.7 - 6.8]	6.2 [5.7 - 6.8]	6.5 [6.0 - 6.9]
BG measures	4564	4564	9467	7259
Measurement frequency (measurement/patient/day)	6.52	6.52	13.54	13.48

Table 4.3: Comparison of per-patient clinical results and virtual trial simulations (self-validation and cross-validation) on Glucontrol B. Median [IQR] is used where appropriate.

		Self-validation		**Cross-validation**
	Clinical	**Actual measurement**	**per-protocol**	**per-protocol**
No. of patients	69	69	69	142
Per-patient results				
Insulin rate (U/h)	0.6 [0.3 - 1.2]	0.5 [0.2 - 1.0]	0.6 [0.2 - 1.4]	0.2 [0.0 - 0.8]
Glucose rate (g/hr)	2.9 [0.7 - 7.4]	2.9 [0.7 - 7.4]	2.9 [0.7 - 7.4]	1.1 [0.5 - 7.5]
BG (mmol/L)	8.3 [7.6 - 8.8]	8.4 [7.8 - 9.1]	8.7 [8.1 - 9.5]	8.3 [7.4 - 9.1]
BG measures	2820	2820	4448	5772
Measurement frequency (measurement/patient/day)	5.23	5.23	8.23	8.23

Comparison of clinical trials with self-validation and cross-validation on Glucontrol B is summarized in Table 4.3. Self-validation results show close agreement to the clinical result and for cross-validation lower Group A insulin requirements are reflected by the lower nutrition given that group and the higher target blood glucose under the Glucontrol B protocol, which is similar to the difference in insulin in the cross-validation in Table 4.2, but in the reverse direction. Similarly, virtual trials of Glucontrol B per-protocol have higher measurement frequency compared to the actual measurement indicating significant non-compliance. Thus, the actual measurement case indicates closer agreement with the insulin given and glycemic outcomes, as with the Glucontrol A results.

Differences in measurement rate and insulin dose can be ascribed to non-compliance and due to the design of Glucontrol, where the rate of change of insulin dose is tied to blood glucose measurement frequency. In particular, the clinical and actual measurements were taken 52.0% of the potential per-protocol specified times based on in silico glycemic results for Glucontrol A and 63.5% for Glucontrol B in Table 4.3. Note that Glucontrol B had a higher compliance rate (% of per-protocol measurement) likely due to its higher glycemic target, which allowed 4 hour measurements to start sooner than for Glucontrol A. Thus, it could be construed that Glucontrol A clinical staff were less compliant to a potentially burdensome protocol in this regard.

Figure 4.13 shows the combination of all the cumulative distribution function of measured blood glucose in a cohort basis. The distribution compares the clinical data of Group A and B, self-validation using actual measurement and per-protocol and cross-validation. The per-patient results of

cumulative distribution function of measured blood glucose is illustrated in Figure 4.14.

The distribution of clinically measured blood glucose values shows a very clear difference between Glucontrol protocol A and B, as expected. The virtual trials results are within 5% of the clinical results for both the self-validation and cross-validation. Referring to Figure 4.13 the obvious separation between two protocols indicates the inter-protocol differences are, as expected, much larger than any inter group differences thus supporting the fundamental assumption behind this virtual trials approach. The close correlation of self- and cross-validation results to clinical data validates the idea that these in silico virtual trial simulations can accurately predict the expected clinical results of a tight glycemic control protocol prior to clinical implementation.

Figure 4.13 illustrates some variation between clinical data and virtual trials. Glucontrol A results are closer to the clinical data compared to Glucontrol B. The major difference is that Protocol B uses much less insulin given its higher glycemic target. Therefore, the impact of intrinsic and potentially variable patient-specific dynamics, such as endogenous insulin production I_B and k_I and endogenous glucose production EGP_{max}, are more pronounced with respect to the far lesser exogenous insulin given to Group B, especially at blood glucose levels below 8.0 mmol/L. As these metrics are unidentifiable and thus, by necessity, assumed population constants, some of the Group B simulation errors may reflect errors in these population values.

Comparing Glucontrol B results, the clinical results for Glucontrol B have most mismatched line compared to the simulation results. The fact that the clinical data are lower than the simulations in this region could indicate

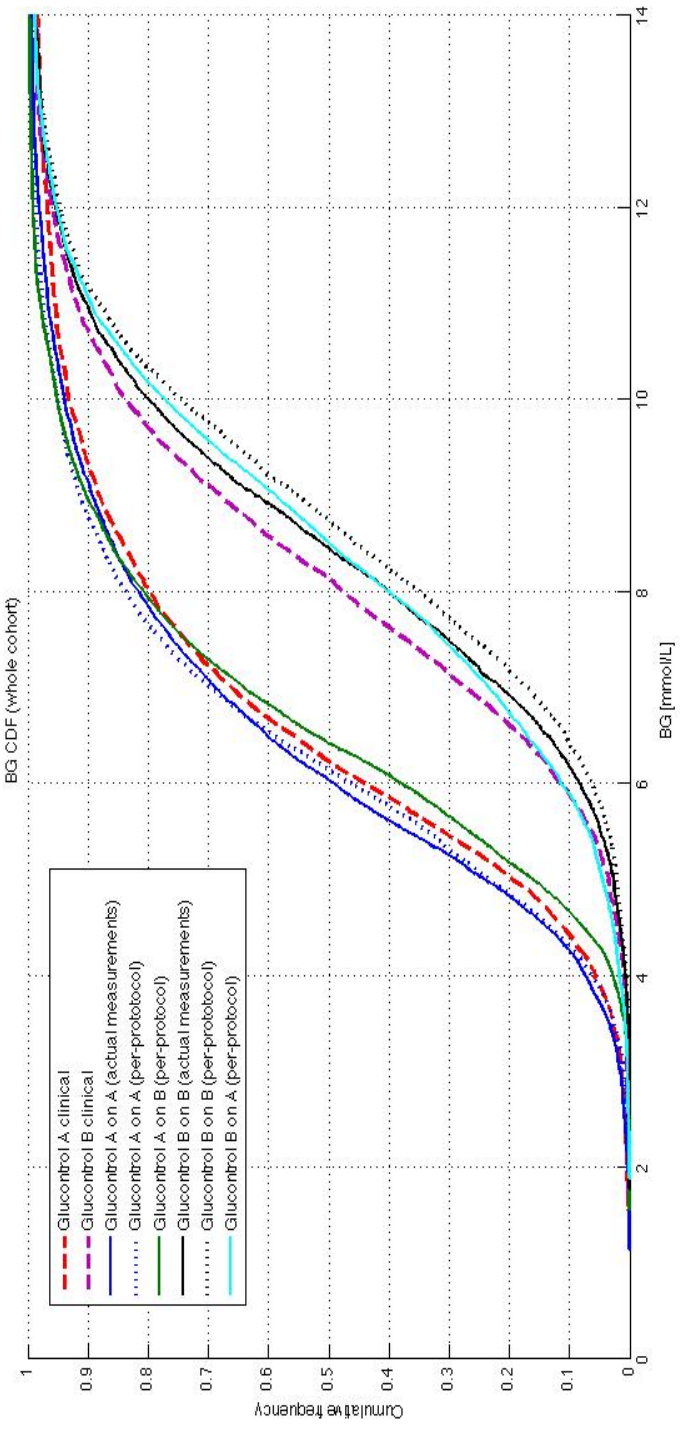

Figure 4.13: Cumulative distribution function of measured blood glucose on a cohort basis for clinical data, self-validation and cross-validation.

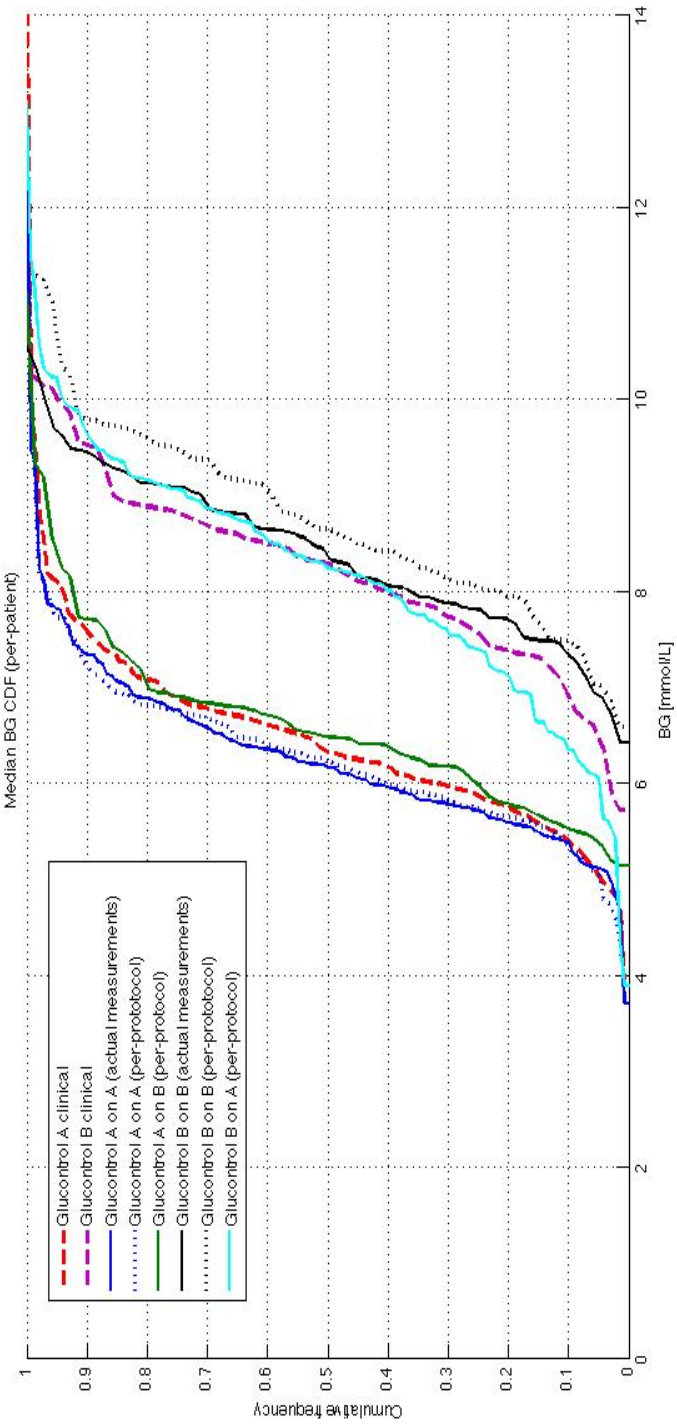

Figure 4.14: Cumulative distribution function of measured blood glucose on a per-patient basis for clinical data, self-validation and cross-validation.

non-compliance in timing or dosing of insulin, or simple overriding of the protocol recommendations by clinical staff. Computer simulations will always follow protocols exactly as instructed. Hence, the self-validation error captures both model and compliance errors, which are clearly evident in Table 4.3 where insulin doses and protocol-specified measurement frequency are very different from the actual measurement case. Reducing measurements in the B protocol would not reduce insulin as fast as the per-protocol case, resulting in lower clinical blood glucose levels. The actual measurement self-validation simulation for Glucontrol B is much closer to the clinical data, having accounted for this effect.

Overall, the gap between the self-validation using actual measurement timing and clinical data indicates the possibility of compliance error. In contrast, the difference between self-validation simulations using exact protocol-specified timing and the clinical data shows one possible indication of model error. However, it may also suggest that the conventional, lower intensity Group B protocol may not have been followed as strictly with respect to dosing.

For the cross-validation, Protocol A on Group B is a very good match with errors similar to the self-validation results for Group A. In addition, Protocol B on Group A virtual patients is within a similar range as the Group B self-validation and close to the slope and trends of the clinical data. Thus, the insulin sensitivity independence assumption behind this virtual trials approach holds, independently validating the concept and the virtual trial method based on this model.

Differences between self- and cross-validation results are ascribed to re-

maining differences between patient groups, despite clinical matching. The main notable difference pointed out in the results and Tables 4.2 - 4.3 is the difference in nutrition given in each cohort. The virtual trials approach treats each group as being treated differently, including the carbohydrate and glucose infusions administered. These infusions were patient specific and specified based on local and individual clinician standards, rather than per a protocol of any type. Thus, they were kept for each patient. As a result, Glucontrol B patients with the higher target had 2.6x higher glucose administration, which in cross-validation was offset by 3.2x more insulin in the virtual trials. Differences in insulin rates between per-protocol and per actual measurement rates makes these differences almost equal at 2.6x higher glucose administration and 2.4x greater insulin required to achieve the almost identical glycemic outcome. Hence, the patients display similar overall insulin sensitivity, and the virtual trials took independently treated, matched patients and achieved the same outcome despite different initial treatments in the clinical data used to create the virtual patient. More specifically, nutritional treatment differences, within reason, did not affect or influence the results outside of expectations.

4.4 Summary

The clinical data in this study was independent from the Christchurch Hospital ICU data used in prior development and clinical validation of the model employed. More importantly, there are two cohorts matched by severity of illness, weight and sex, as well as metabolic variability which is a key parameter in this case, which had significantly different glycemic targets and glycemic

control therapies.

The small model fit errors and low prediction validation results can be seen as an estimate of the variability of insulin sensitivity in this cohort, as well as a sign of model fitness. Moreover, self-validation indicated a clinically insignificant error in these virtual patient methods due to the model and/or clinical compliance. They also showed the impact of some none-compliance independent of model error. In contrast, cross-validation clearly showed that the virtual patient methods and models enabled by patient-specific $S_I(t)$ profiles are effective and the assumption that the $S_I(t)$ profiles are independent of the clinical inputs used to generate them holds.

Therefore, virtual patients and in silico virtual trial methods are validated in their ability to accurately simulate, in advance, the clinical results of an independent tight glycemic control protocol, directly enabling rapid design and optimisation of safe and effective tight glycemic control protocols with high confidence of clinical success. In conclusion, model-based data driven in silico methods has the potential and capable to aid protocol design, as well as providing accurate, safe and effective real time tight glycemic control.

Importantly, as a result, model-based metric, S_I, is effectively validated as an independent metric indicating patient-specific response to condition. Therefore, it can be used as a marker to represent metabolic condition as a response to patient-specific counter-regulatory and immune system (inflammatory) responses that are major parts of the etiology of sepsis in ICU cohorts.

Chapter 5

Sepsis and Sepsis Diagnosis

Treating sepsis as early as possible may reduce mortality in intensive care [Rivers et al., 2001; Bone et al., 1989]. Currently, it is almost impossible to diagnose a patient at the onset of sepsis due to the lack of real-time metrics with high sensitivity and specificity. Patient condition is mostly determined by clinician experience and observation of patient reaction to treatment. In addition, the ability to compare protocols or evaluate different therapeutic interventions is difficult since there are few guidelines in investigating and diagnosing sepsis.

This chapter discusses and analyzes current methods used to determine sepsis condition. Typically, a sepsis score is calculated according to several criteria to determine the level of sepsis to differentiate between severe sepsis, septic shock and refractory septic shock. The different scores are created with the aim of helping clinicians with treatment decisions, and to better classify patients and determine prognosis.

5.1 Sepsis Definition

Severe sepsis and septic shock are common and highly associated with substantial mortality. Sepsis is an increasingly common cause of morbidity and mortality, particularly in elderly, immunocompromised, and critically ill patients [Balk and Bone, 1989; Ayres, 1985; Wheeler and Bernard, 1999]. The incidence of sepsis or septic shock and the related mortality rates are substantially higher in elderly persons than those in younger persons. By the year 2020, the projected growth of the elderly population in the United States will contribute to an increase of 1.5 percent of incidence per year, yielding an estimated of 1,110,000 cases [Angus et al., 2001]. In addition, sepsis has been reported to be the most common cause of death in the noncoronary intensive care unit [Parrillo et al., 1990].

Sepsis is a clinical syndrome defined by the presence of both infection and a systemic inflammatory response (SIRS). In 2001, infection was defined as a pathologic process caused by the invasion of normally sterile tissue or fluid or body cavity by pathogenic or potentially pathogenic microorganisms [Levy et al., 2003]. This definition was created by the 2001 International Sepsis Definitions Conference. However, frequently, infection is strongly suspected without being able to be microbiologically confirmed for several reasons creating so-called "culture negative" sepsis [Carrigan et al., 2004].

Systemic Inflammatory Response Syndrome (SIRS) is an inflammatory state affecting a person's body. It is frequently associated to a response of the immune system to infection, but that is not necessarily always the case. SIRS is also related to organ dysfunction and organ failure [Bone et al., 1992; Levy

et al., 2003], which also occur frequently with and without sepsis. According to the American College of Chest Physicians/Society of Critical Care Medicine, SIRS is considered to be present when patients have more than one of the following clinical conditions [Bone et al., 1992]:

- Body temperature less than 36 °C or greater than 38 °C,
- Heart rate greater than 90 beats per minute,
- Hyperventilation evidenced by a respiratory rate of greater than 20 breaths per minute or an arterial partial pressure of carbon dioxide less than 32 mmHg,
- White blood cell count greater than 12 x 10^9 cells/L or less than 4 x 10^9 cells/L or the presence of greater than 10% immature granulocytes.

The SIRS criteria are summarized in Table 5.1. However, the presence of SIRS may, or may not, represent the presence of sepsis. The SIRS concept is valid to the extent that a systemic inflammatory response can be triggered by a variety of infectious and noninfectious conditions, because, signs of systemic inflammation occur in the absence of infection among patients with burns, pancreatitis and other disease states. Hence, alone, SIRS has limited diagnostic potential for sepsis.

Figure 5.1 shows the interrelationship between SIRS, sepsis and infection. The figure implies that a similar or even identical SIRS response can arise in the absence of infection. For example, a frequent complication of SIRS is the development of organ system dysfunction, including acute lung injury, shock, renal failure and multiple organ dysfunction syndrome. These effects

Table 5.1: SIRS criteria.

Score	Criteria	
+1	Temperature	≤ 36 °C, ≥ 38 °C
+1	Heart rate	≥ 90/min
+1	Respiratory rate or $PaCO_2$	≥ 20/min, ≤ 32 mmHg
+1	White blood cell count	≤ 4 x 10^9/L or ≥ 12 x 10^9/L or presence of $> 10\%$ immature granulocytes

too occur with or without infection. Hence, the diagnosis of sepsis and SIRS are inter-related, but not exclusive.

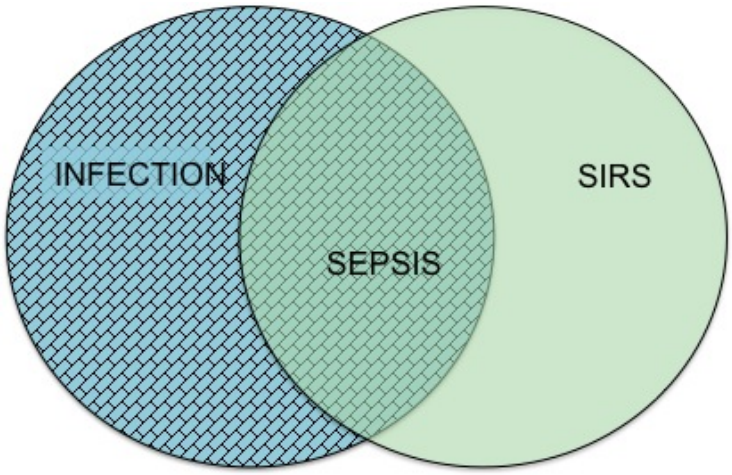

Figure 5.1: The interrelationship between systemic inflammatory response syndrome (SIRS), sepsis and infection.

The occurrence of sepsis can be classified into several stages. Sepsis is a condition where the systemic response to infection is manifested by two or more SIRS criteria as a result of infection. Severe sepsis is a sepsis condition that is also associated with organ dysfunction, hypoperfusion or hypotension. Septic shock is defined as severe sepsis with arterial hypotension, despite adequate fluid resuscitation.

Despite the definition for sepsis, severe sepsis and septic shock, these terms do not precisely characterize patient's stage and condition and may be confounded by a number of issue. More specifically, sepsis, in all levels, is a syndrome or collection of conditions. Grouped together as "sepsis" they categorize patients with a significantly increased risk of death. Hence, unfortunately perhaps, sepsis is a much of a patient category as it is a specific physiological condition. This issue makes sepsis diagnosis quite difficult.

5.1.1 Scoring System

The most accepted sepsis score is calculated following criteria classified by American College of Chest Physicians (ACCP)/Society of Critical Care Medicine (SCCM) definitions of 1992 and 2001 [Levy et al., 2003]. The criteria calculate a sepsis score including Systemic Inflammatory Response Score (SIRS) and Sepsis-related Organ Failure (SOFA) score [Bone et al., 1992]. Details of the criteria are shown in Tables 5.1 - 5.3. Table 5.2 shows the criteria in determining the organ failure score as a component in calculating the sepsis score.

The rationale for using a scoring system is to ensure that the increased complexity of disease in patients currently being treated is consistently represented in evaluations and descriptions. Therefore, clinicians can more accurately monitor patient condition and therapy can be more precisely determined. However, it is apparent that if one waits for the emergence of SIRS or organ failure then clinicians are thus treating more severely ill patients at a later stage of illness.

Referring to Table 5.3, the level of sepsis score is a hierarchical process, where a tick indicates a necessary criterion that must be present to achieve the sepsis score labeled. For example, if a patient had SIRS > 2, an infection during stay without an organ failure, and received fluid and inotropes, the patient is classified as having sepsis, where the sepsis score is 1 instead of septic shock, where the sepsis score is equal to 3. This apparently contrasting outcome occurs because the patient does not meet the criteria for organ failure. Each criteria in defining a sepsis level must be met before classifying the patient's condition.

5.2 Retrospective Cohort Analysis

A collection of clinical data was obtained from the Intensive Care Unit (ICU) of Christchurch Hospital, Christchurch, New Zealand. There were a total of 30 patients that had sepsis during their hospital stay and were selected in this study. They were identified by having positive blood culture results and by the judgement of experienced senior intensive care clinicians. This study was approved by the Upper South Regional Ethics Committee, New Zealand.

Initially, there were 104 patients admitted to the ICU. SIRS is recorded every hour for all of the patients. Patients with SIRS > 2 or suspected to have sepsis were selected to participate in this study. The background information of the retrospective cohorts is shown in Table 5.4.

Table 5.5 summarize the demographics, where 60% of the cohort is male with a median age of 63 years. The severity of illness was defined by calculating

Table 5.2: Organ failure criteria.

Score	System	Criteria	
+1	Cardiovascular	Mean arterial pressure or need for inotropes	$\leq$ 60 mm Hg
+1	Respiratory	PaO_2/FiO_2	$\leq$ 250 mm Hg $\leq$ 200 mm Hg with pneumonia
+1	Renal	Urine output	$<$ 0.5 ml/kg/hr
+1	Blood	Platelets	$<$ 80 x 10^9/L or 50% drop in 3 days

Table 5.3: Sepsis score criteria.

Sepsis score		SIRS $\geq$ 2	Infection during stay	Organ failure $\geq$ 1	Fluid resuscitation	Inotrope present	High dose inotrope
0	Normal						
1	Sepsis	√	√				
2	Severe sepsis	√	√	√	√		
3	Septic shock	√	√	√	√	√	
4	Refractory septic shock	√	√	√	√	√	√

Table 5.4: Retrospective patient cohort background information.

Patient ID	Medical Subgroup	APACHE II Score	Age	Sex	Mortality
BSL002	Septic shock	19	49	F	
BSL010	Septic shock	17	55	F	
BSL012	Pneumonia	18	60	F	
BSL013	Otitis	18	43	F	
BSL017	Pneumonia	15	64	M	Y
BSL022	CAP	17	61	F	
BSL027	CAP	22	74	M	
BSL030	Multiple trauma	19	63	F	
BSL031	CAP	23	52	F	
BSL032	Pneumonia	20	64	M	Y
BSL033	CAP	23	75	M	
BSL035	Pneumonia	21	75	M	
BSL038	Pneumonia	27	70	F	
BSL039	GBS	8	43	M	
BSL044	CAP	24	80	M	
BSL047	Pneumonia	25	71	M	
BSL051	Pneumonia	10	30	F	
BSL052	ARDS	11	63	M	
BSL055	Respiratory failure	17	76	M	Y
BSL056	Type 1 DM	29	46	M	Y
BSL063	Type 2 DM	19	78	F	
BSL069	COPD	17	54	M	
BSL078	CAP	24	88	M	Y
BSL079	Sepsis	19	64	F	
BSL080	Gastrectomy	12	49	M	
BSL083	Pneumonia	18	56	M	
BSL095	Sepsis	16	67	F	
BSL100	COPD	13	55	M	
BSL101	Pneumonia	15	78	M	
BSL104	Sepsis	29	59	M	

the sepsis score for each patient according to clinical data available. Sepsis score is then calculated for every hour using the method mentioned in Section 5.1.

Table 5.5: Summary data for Sepsis cohort taken in ICU, Christchurch Hospital.

Baseline characteristics of the patients	
Variable	
Number of patients	30
Percentage of male	60 %
Age	63 [54 - 74]
Apache II score	19 [16 - 23]
Total hours in ICU	7624
Length of stay (days)	10.5 [6 - 15]
Entry criteria	
Temperature (°C)	36.6 [36.0 - 37.6]
Heart rate (beats/min)	97 [87 - 110]
Mean arterial pressure (mm Hg)	73 [67 - 83]
White cell count (per Liter)	11.6 [7.9 - 20.4]
Partial pressure of carbon dioxide (mm Hg)	47.5 [39.0 - 58.0]
Partial pressure of oxygen (mm Hg)	90 [72 - 113]
Baseline laboratory values	
Creatinine (μmol/L)	110 [82 - 221]
Bilirubine (mmol/L)	11 [5 - 17]

Figure 5.2 shows the distribution of sepsis scores for the 30 identified sepsis patients during their entire stay in the ICU. The histogram shows the distribution of sepsis score for day 1, day 2, day 3 and the final days of their stay. There were 13 patients with a sepsis score of 1 when they were admitted to the ICU. Two patients had 0 sepsis score, 8 patients had sepsis score of 2,

4 patients had sepsis score of 3, and 3 patients had the maximum score of 4.

Note that the sepsis score is not calculated when patients were admitted. Therefore, a patient may or may not have sepsis on the first day they were admitted into the ICU. In addition, length of stay varies between patients. The figure shows an improving pattern of sepsis score from day 1 to the final day of patient stay in the ICU, as expected in many cases, with more patients having a lower sepsis score compared to their early stay.

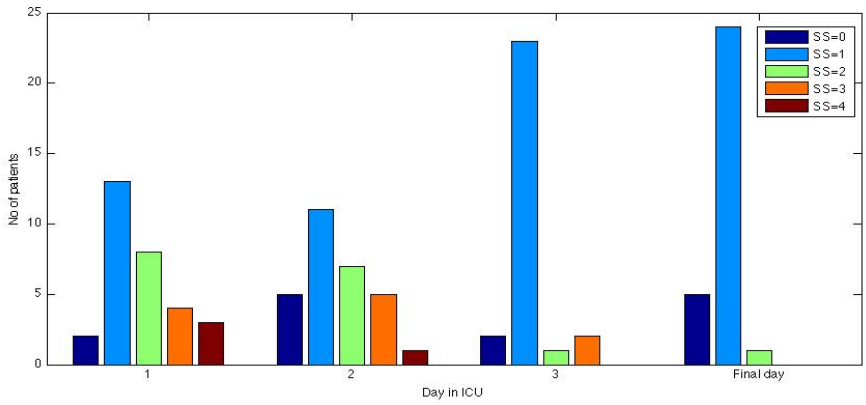

Figure 5.2: Sepsis score distribution for 30 patients during their stay in ICU.

Figures 5.3 - 5.6 show the hourly distribution of sepsis score for the whole length of stay for four patients randomly selected from the sepsis cohort. These plots suggest that sepsis scores vary and may change rapidly over an hourly interval. For example in Figure 5.3, Patient 002 had a sepsis score of 3 at minute 1680, then it decreased to 0 at 1740 minutes and changed back to 3 at 1800 minutes.

Similarly, in Figure 5.4 Patient 012 had a rapid change from 3 to a score of 1 and vice versa over a short time interval. Although the plot in Figure 5.5 shows a more stable and less variable sepsis score, there are times when

the score of Patient 063 changes effectively instantly, with a difference of two levels of sepsis score, as seen at minutes 1620 to 2160. In Figure 5.6, it is observed that the sepsis scores highly variable between a score of 0 and 1 for most of the stay of Patient 079.

Overall, from the whole length of stay for this sepsis cohort, the sepsis scores are fluctuating even over one hour intervals. Generally, the condition of a patient may change, either getting better or worse after several hours of treatment. Similarly, sepsis scores are expected to change by either increasing or decreasing over time. However, the change should be much more stable than seen here, with a much more infrequent rate of change over short intervals.

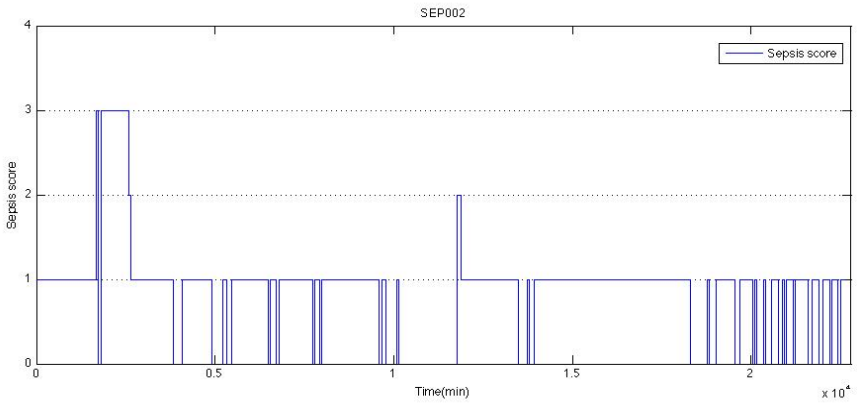

Figure 5.3: Hourly plot of sepsis score for Patient 002.

By definition, sepsis exists by the presence of SIRS and infection. However, the frequent change and irregular sepsis score pattern shown in Figures 5.3 - 5.6 suggest that these patients may have had an on and off condition. It is almost impossible to report that a patient had an infection at this hour and was free from infection at the next hour, especially if the condition oscillates frequently.

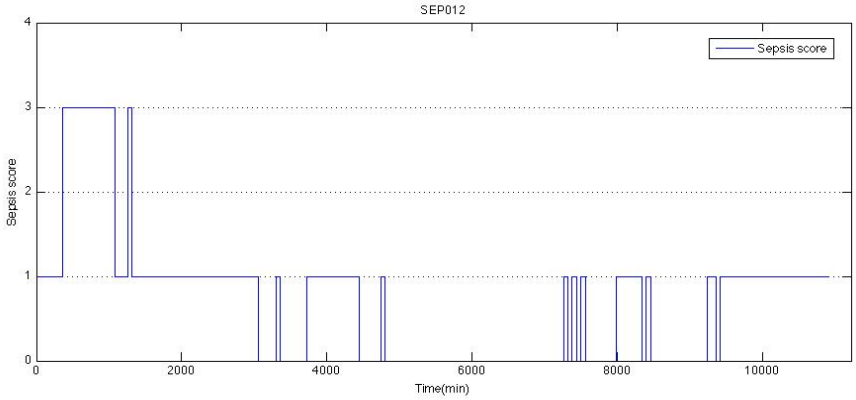

Figure 5.4: Hourly plot of sepsis score for Patient 012.

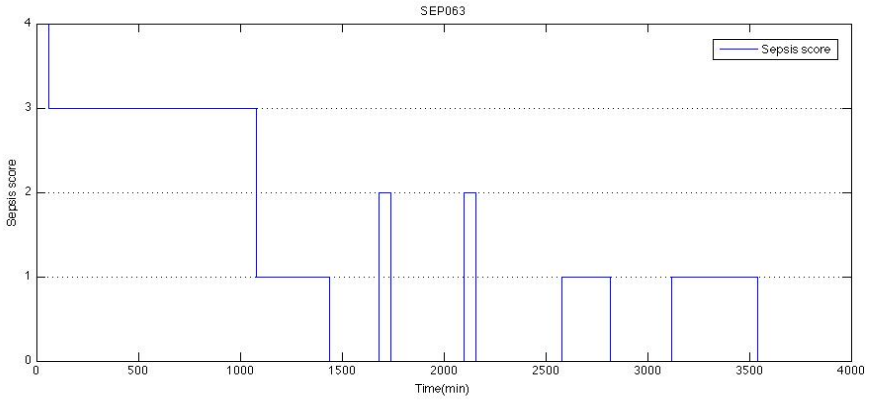

Figure 5.5: Hourly plot of sepsis score for Patient 063.

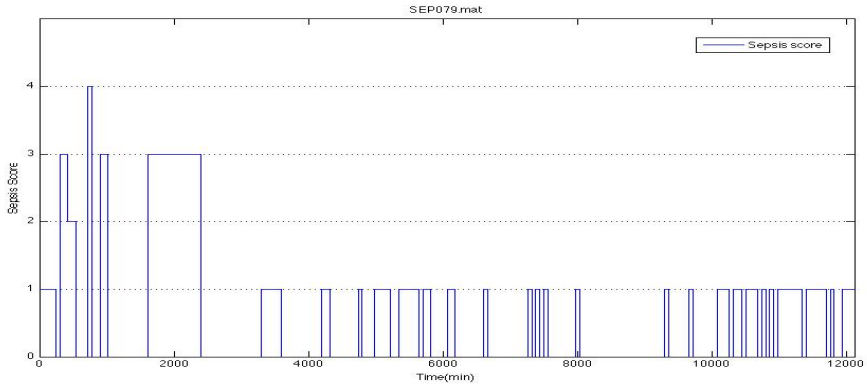

Figure 5.6: Hourly plot of sepsis score for Patient 079.

In contrast, SIRS does have a higher likelihood of changing rapidly since it has several components that may change abruptly. Equally, SIRS symptoms are treated, such as high temperature. Thus, the treatment modifies the SIRS score, causing an apparent change of state.

From a clinical point of view, the patient condition should be aligned with the level of a sepsis they have. If a doctor were treating a patient according to their sepsis score level, the doctor might want to treat based on a stable protocol and assessment. However, rapid changes in score would create a challenge to determining suitable treatments necessary for a patient.

A more stable sepsis representative score are thus required, which is more suitable for hourly, instead of daily evaluation. In particular, the original ACCP/SCCM score was designed for daily use, using a worst or average daily score for each component. Thus, one aspect of the variability seen is simply this metrics unsuitability for hourly assessment without modification.

5.3 Scoring System Analysis

To obtain a useful score that can be used by a clinician to guide diagnosis and treatment, the current score is considered for improvement. The following section discusses the effectiveness aspects of the current sepsis score, and evaluates if any specific component is the cause for the fluctuation and variability in sepsis score. It then creates a near more realistic score suitable for hourly use.

Figure 5.7 shows the classification for calculating SS1, a scoring system that uses the same individual components in determining a current sepsis score. SS1 is determined by calculating the summation of individual component scores used to calculate the current sepsis score. In contrast, the original sepsis score is determined by following the hierarchy component, as shown in Table 5.3.

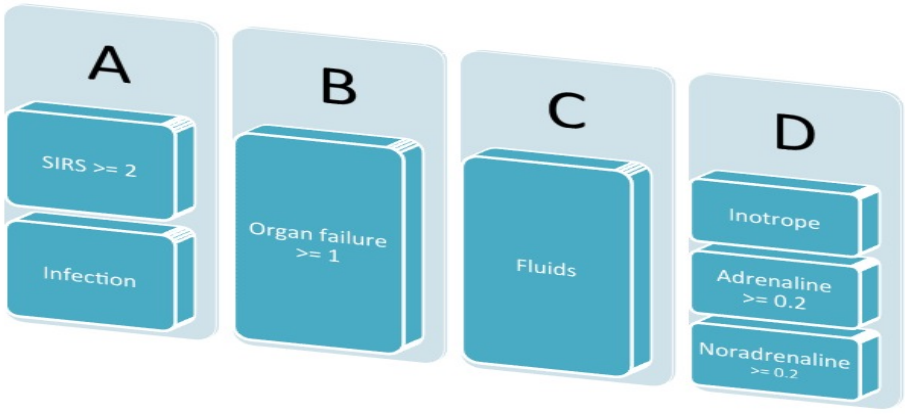

Figure 5.7: Individual components for determining SS1 score.

In Figure 5.7, components A, B, C and D have a value of 1 if they are true. For example, at time t, if a patient had SIRS $\geq$ and had an infection,

the score for A will become 1. If the patient had SIRS ≥ 2 but was free from infection, the score for A is 0. Moreover, if the patient had an organ failure, defined by SOFA ≥ 1 for at least one SOFA score component, at time t, B will become 1, otherwise it is 0. The same method is applied to the criteria in C and D. C and D represent fluid resuscitation and inotrope usage, respectively. Finally, the SS1 value is then calculated by summing the values of A,B,C and D, as shown in Equation 5.1. The range of SS1 is 0 - 4; and there is no hierarchy involved.

$$SS1 = A + B + C + D \tag{5.1}$$

Figure 5.8 illustrates the population of SS1 for 30 patients during their whole stay in ICU. Overall, there were a total of 7624 hours of treatment where patients had SS1 = 2 for the most hours (43%). There were 25.9%, 9.8% and 2.6% of hours where patients had a SS1 score of 1, 3 and 4, respectively. The remaining 18.7% of the total hours are where patients had SS1 = 0.

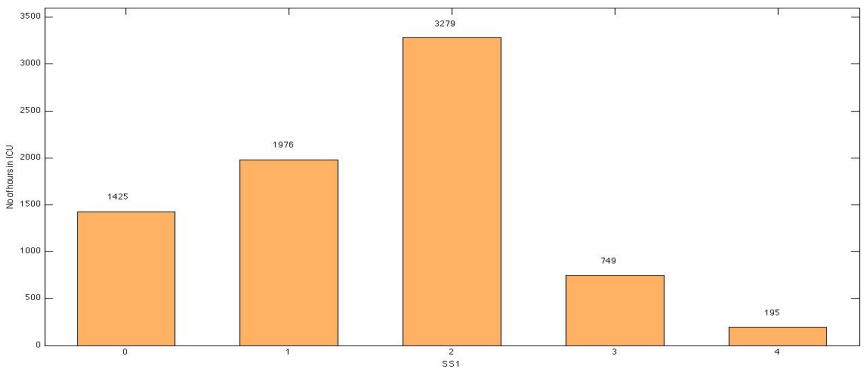

Figure 5.8: Distribution of SS1 for 30 patients in sepsis cohort during their stay in ICU.

Figures 5.9 - 5.12 show an hourly distribution of sepsis score and SS1 for the entire stay of the same four patients selected from the sepsis cohort. The right panel of y-axes represents SS1 and left panel of y-axes represents the original sepsis score. From all the plots, it can be concluded that SS1 add more noise to the sepsis score given that the occurrence of fluctuation is more.

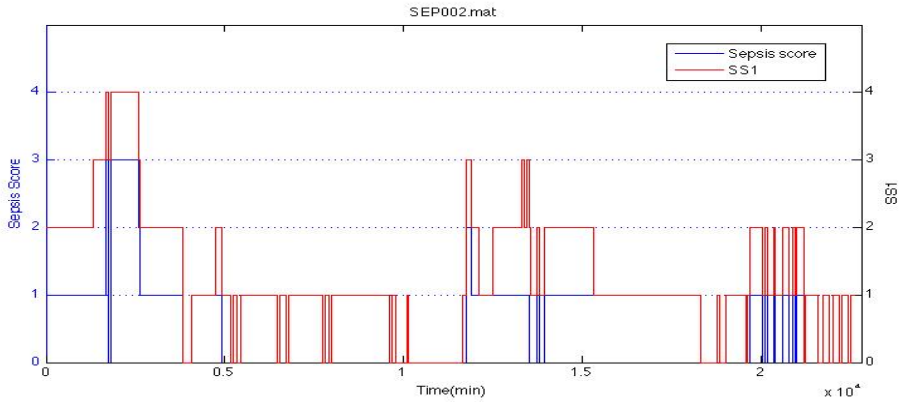

Figure 5.9: Hourly plot of sepsis score and SS1 for Patient 002.

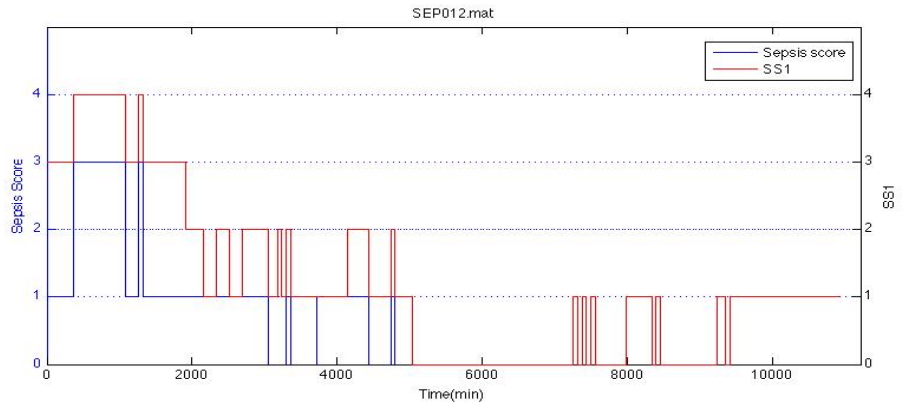

Figure 5.10: Hourly plot of sepsis score and SS1 for Patient 012.

Referring to Figure 5.9, most of the time during the stay Patient 002 had a higher score for SS1 compared to the original sepsis score. Similarly, with Patient 012, a higher score of SS1 has been observed in Figure 5.10 with

a fluctuating score in the second half of the stay. However, Patient 063 had a similar pattern of SS1 compared to the original sepsis score with a shifted score seen for SS1. As seen in Figure 5.12, the SS1 of Patient 079 is also more variable, unlike the plot of the original sepsis score.

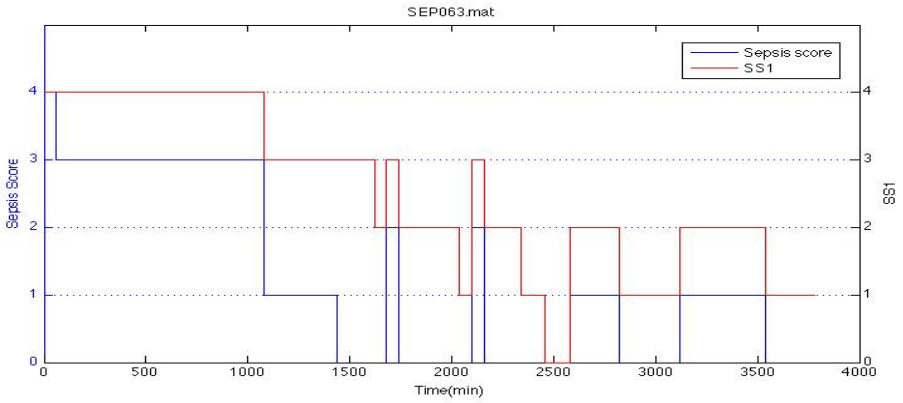

Figure 5.11: Hourly plot of sepsis score and SS1 for Patient 063.

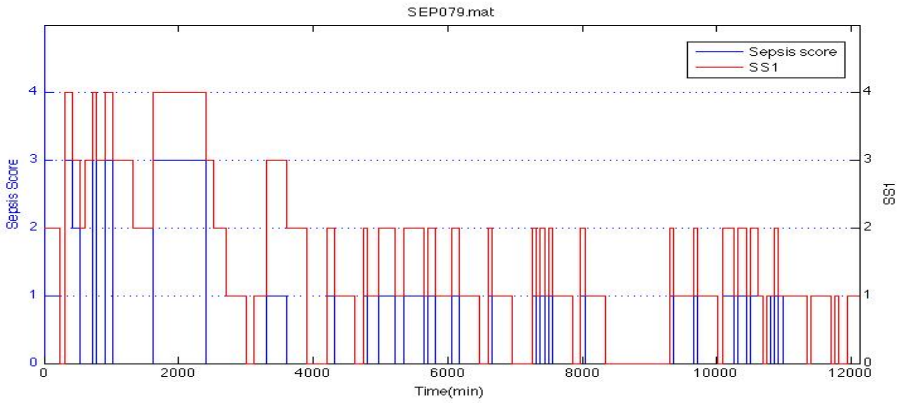

Figure 5.12: Hourly plot of sepsis score and SS1 for Patient 079.

The change in SS1 is happen regularly for most of the patients in the sepsis cohort. In comparison to sepsis score, SS1 adds more noise and changed inconsistently over time. Since SS1 is calculated based on each component in determining sepsis score, it can be observed that the plot of SS1 indicates

the factor contributing to the sepsis score itself. It can be either SIRS, organ failure, fluid resuscitation, inotrope dosing or combination any of these factors.

Figure 5.13 represents the cumulative data points of A, B, C and D when SS1 = 1. There were 1976 measurement of SS1 = 1 during the stay for all 30 patients in the cohort. A has the highest frequency followed by B, D and C. Referring to Figure 5.13, A dominates the total measurement of SS1 at score 1 with a 56% (1086) of total measurements. B is recorded as the second major factor with a total of 690 measurements, followed by D and C with 104 and 96 measurements respectively.

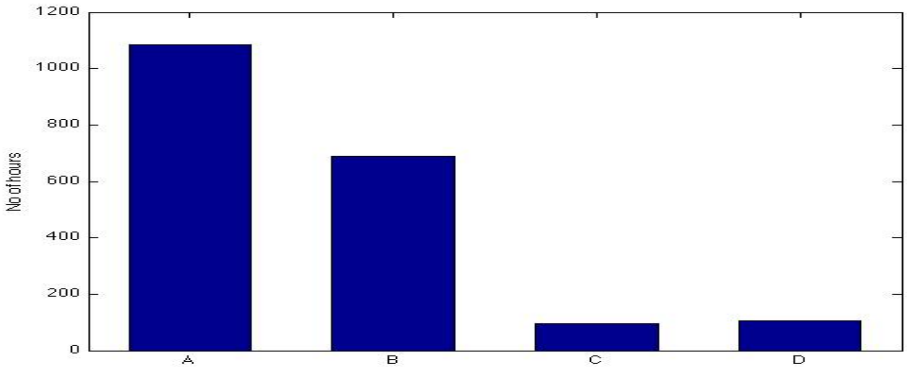

Figure 5.13: Comparison of A, B, C and D score for SS1 value of 1.

The high frequency for A proved that SIRS is the leading factor in developing the SS1 score. In addition, looking at the individual patient plots, it can be observed that the score was on and off between 0 and 1 for most of the time. Therefore, SIRS is the factor contributing to the fluctuation seen in the SS1 scoring system.

Therefore, another sepsis score is introduced, called SS2. In SS2, the SIRS factor is eliminated to obtain a more comprehensive and stable scoring

for diagnosing sepsis. The equation used is shown in Equation 5.2. Since SS2 eliminates the A value of Figure 5.7, maximum and minimum scores are 3 and 0, respectively.

$$SS2 = B + C + D \tag{5.2}$$

Figures 5.14 - 5.17 compare the hourly distribution of SS2 and the original sepsis score for the same four different patients in sepsis cohort. Significant improvement can be seen in Figure 5.14, particularly at minutes 500 to 1000. Less fluctuation and no drastic change has been observed compared to the original sepsis score, which is indicated by the dashed line. Figure 5.15 clearly shows that SS2 improves the scoring system with less oscillation in the first half of stay and a stable score in the second half.

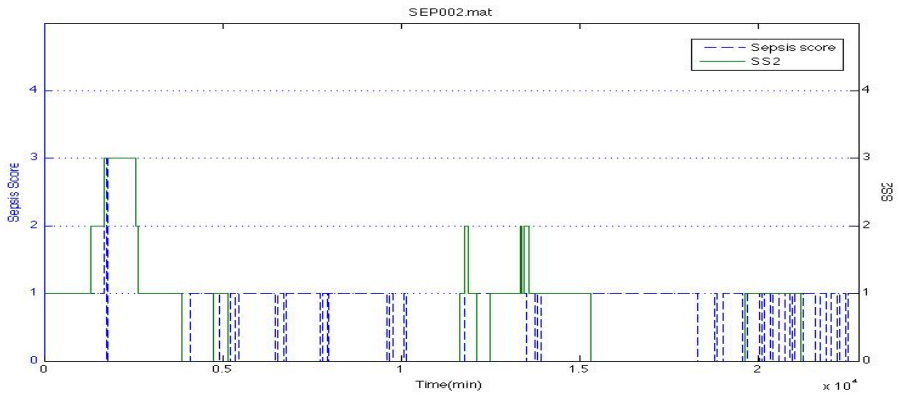

Figure 5.14: Hourly plot of sepsis score and SS2 for Patient 002.

Similarly, Patient 063 also has a better, more physiological and clinically relevant pattern indicated by less frequency of on and off changes in SS2. In Figure 5.16, the original sepsis score changed dramatically from 3 to 1

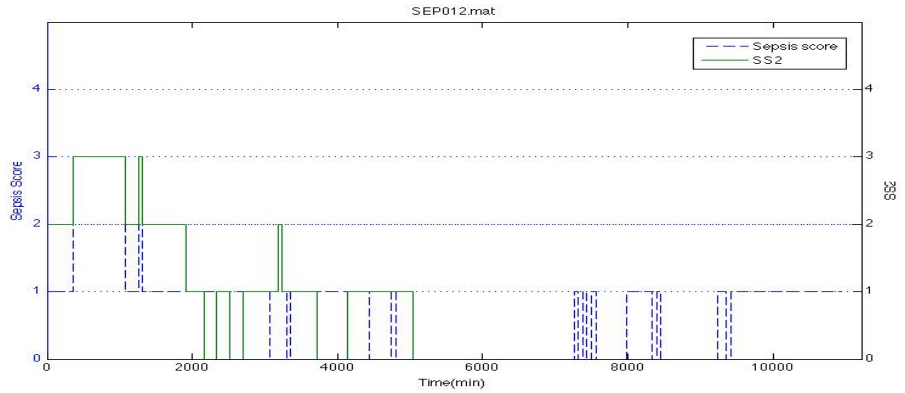

Figure 5.15: Hourly plot of sepsis score and SS2 for Patient 012.

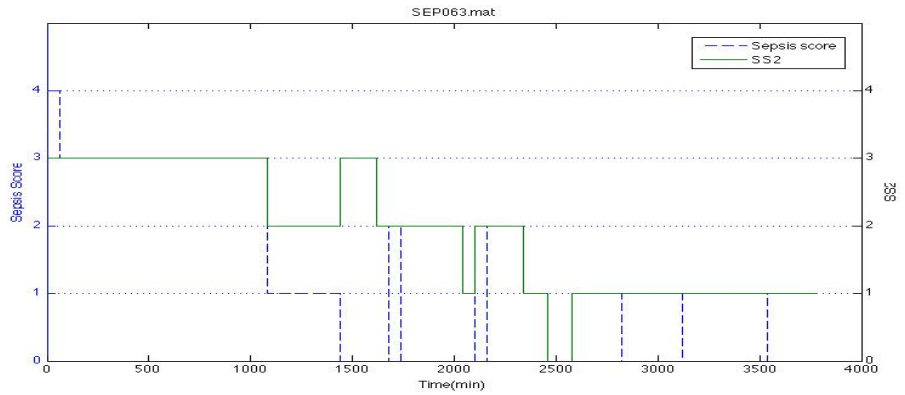

Figure 5.16: Hourly plot of sepsis score and SS2 for Patient 063.

at minutes 1020 to 1440. However, SS2 demonstrates a more reliable score with a single step change at a time. Finally, Figure 5.17 illustrates that SS2 exhibits an improving pattern of sepsis score even though it changes relatively frequently.

Overall, SS2 plots are more stable and had less non-physiological variability in comparison to the original sepsis score and SS1. By eliminating the SIRS component, the resulting sepsis score is more stable and less fluctuation

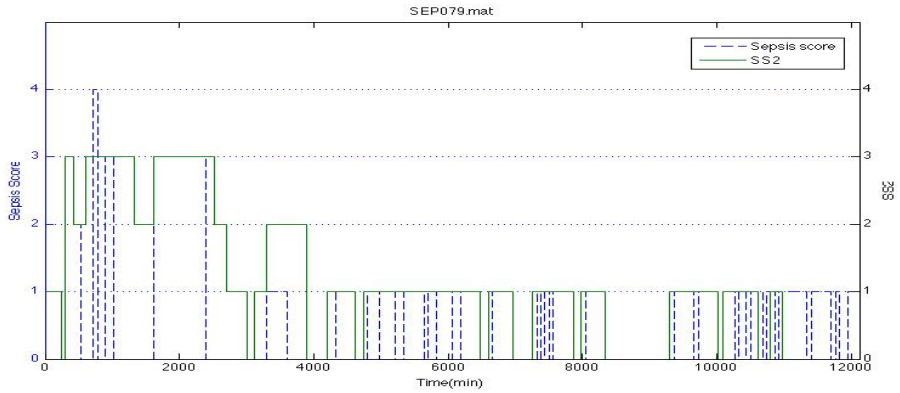

Figure 5.17: Hourly plot of sepsis score and SS2 for Patient 079.

occurs during the stay. Although some patients had frequent changes in SS2, it may suggest that the pattern is caused by the condition of the patient itself. From the overall plot, it may suggest that SS2 can be used as a marker for a clinician to determine a suitable treatment given that SS2 varies somewhat in the level of sepsis, and thus enhance stability for an hourly metric to help guide diagnosis and treatment.

5.4 Challenges in Diagnosing Sepsis

Currently, diagnosing sepsis in critical care has many challenges. It is almost impossible for a clinician to determine the best treatment due to the long (1-3 day) process of getting blood culture results. Therefore, the inability to guarantee accurate, early diagnosis affects treatment selection, patient condition and mortality outcome.

According to Rivers and colleagues [Rivers et al., 2001], early goal-directed treatment of sepsis reduced mortality from 46.5% to 30.5%. More-

over, severe sepsis and septic shock have high incidence and high mortality rates in the intensive care unit. Clinical studies by Rivers et al. [Rivers et al., 2001] observed lower mortality rates in patients with septic shock assigned to early goal-directed therapy (42.3%) than in those assigned to standard therapy (56.8%). Even survive, sepsis usually reduces quality life for those who suffer this disease [Chen et al., 2008; Perl et al., 1995; Heyland et al., 2000; Buysse et al., 2007] and especially if not specifically treated, driven primarily by the body's inflammatory response.

Separately, and in addition, the syndrome and condition of sepsis itself covers a wide range of illness including organ failure, inflammatory response and infection, which result in a complex diagnostic situation. More often systemic inflammatory respond syndrome (SIRS) manifest in critically ill patients and thus reduce the ability to distinguish between SIRS and sepsis. On the other hand, infection is frequently suspected without being microbiologically confirmed [Levy et al., 2003] and hence affecting treatment selection which usually take place beforehand. Thus, sepsis is a condition that requires timely intervention, but is difficult to diagnose [Vincent et al., 1996; Wheeler and Bernard, 1999; Wiersinga, 2011].

Additionally, antibiotic therapy has been widely accepted in the course of an infection due to its effectiveness in reducing morbidity and mortality [Kumar et al., 2006; Micek et al., 2011]. There have been several study [Roberts et al., 2011; Taccone et al., 2011a; Gonzalez de Molina and Ferrer, 2011; Textoris et al., 2011] that describe and potentially recommend for an effective dosing of antibiotics therapy. This is due to the high demand in prescribing an appropriate antibiotic regimen. However, starting an antibiotic therapy to

a patient may escalate the rates of antibiotic resistance [Taccone et al., 2011b; Bassetti et al., 2011; Micek et al., 2011; Hemels et al., 2011] especially before confirming the infection. Pharmacokinetics of antibiotics are commonly altered in sepsis patients which consequently may result in insufficient drug concentrations, even when the concentrations used was recommended [Dickinson and Kollef, 2011; Taccone et al., 2011b].

What is needed is the means to evaluate sepsis based on clinical variables that are easily and routinely measured in the ICU. These variables should be independent of the therapy used since therapeutic management may vary from one institution to another. Development of sepsis bio-markers is therefore important to provide an indicator for sepsis intervention and thus improve patient outcome by enabling effective treatment as early as possible.

5.5 Summary

Sepsis is an increasingly common condition and a leading cause of ICU mortality. It represents a major healthcare problem as affected patients have a high morbidity and mortality leading to high direct and indirect costs [Angus et al., 2001]. The mortality rates of 40% to 60% have not changed significantly in the past 20 years, despite intense research advances in treatment.

Current sepsis scores show a irregular patterns with high oscillation when applied or evaluated hourly. In reality, the existence of sepsis in a patient cannot just disappear within an hourly interval and appear again the next hour. Similarly, patient condition takes some time to improve after being

treated. Hence, the existing sepsis scores are seen to be ineffective when evaluated hourly rather than from a daily average or worst case score.

Individual components of the original sepsis score are evaluated to identify the cause of the observed fluctuations. As a result, a different scoring system has been introduced. The revised scoring system simplifies the way the sepsis score is calculated and eliminates the hierarchical concept.

The new scoring system, denoted SS2, shows an improving more physiological and clinically relevant pattern. SS2 eliminates the effect of SIRS score, which has been found to be the main factor of the fluctuations observed in the original sepsis score. Overall, SS2 is more stable and changes reasonably in a clinical and physiological sense with less occurrence of on and off within an unrealistic short time interval. This stable scoring system will be evaluated as a tool to more accurately aid in the diagnosis of sepsis in real-time.

Chapter 6

Insulin sensitivity and sepsis

The use of metabolic markers in addition to other clinical variables is emerging area of study [Lin et al., 2011a; Chase et al., 2008a; Blakemore et al., 2008]. The main goal is increasing the positive predictive diagnosis of sepsis. However, like many decisions made in the ICU sepsis diagnosis and treatment are largely based on clinical experience and broad standard guidelines. Development of a physiological bio-metric to help diagnose sepsis, particularly as early as possible, could reduce the high mortality rate of this disease and likely reduce the cost of treatment.

This chapter discusses the use of model-based insulin sensitivity, S_I, as a patient-specific parameter to aid sepsis diagnosis. It has the advantage of being readily available every hour at the bedside. Equally, it reflects the counter-regulatory and inflammatory status of the patient, which are significantly augmented in sepsis [Cavaillon and Adib-Conquy, 2007; Marik and Raghavan, 2004; Andersen et al., 2004]. Hence, it could prove to be an ideal bio-marker for early, real-time diagnosis.

Several studies [Lin et al., 2011a; Blakemore et al., 2008] have shown that S_I accurately represents the patient's metabolic condition. S_I is very low, relative to healthy individuals, in patients in critical condition, and decreases

further as condition worsens [Chase et al., 2008a]. As noted, S_I is available hourly via computer analysis. Therefore, it is possible to be used for real-time diagnosis where current sepsis scores [Levy et al., 2003; Bone et al., 1992] are based on daily or 12-hourly assessments. Hence, it is likely to be able to produce a much earlier diagnosis, if successful. Finally, it has the advantage that it is noninvasive and no additional testing is required to obtain this value in real-time.

6.1 Insulin sensitivity

Insulin sensitivity is defined as the dependance of fractional glucose disappearance on plasma insulin. S_I represents the effective insulin sensitivity of a specific patient and it is uniquely independent of insulin transport and saturation. As discussed in Chapter 5, S_I is an independent parameter that represents metabolic condition of a patient, independent of the treatment given [Chase et al., 2010b].

S_I can be determined using parameter compartment models that have been extensively validated clinically [Chase et al., 2010b, 2007; Lonergan et al., 2006; Le Compte et al., 2009]. This model has been used to develop blood glucose protocols for critically ill patients [Chase et al., 2007; Lonergan et al., 2006]. Hence, the S_I value is readily available for most if not all sepsis patients, as these patients have exacerbated hyperglycemia due to sepsis.

For this analysis, insulin sensitivity profiles $S_I(t)$ of a patient are generated using the ICING model discussed in Chapter 2. The model is fitted to

retrospective clinical data for blood glucose measurements, and insulin and carbohydrate administration input data from the protocol used in ICU. With this model, patient specific profiles can be generated for time varying S_I and its hour to hour variation as patient condition evolves.

This model-based S_I has been observed to indicate the severity of illness and is therefore capable of capturing a patient's metabolic status. In particular, Blakemore et al [Blakemore et al., 2008] have shown that insulin sensitivity of a patient decreased as the patient condition worsen. In addition, it has been previously documented that S_I decreases with worsening condition and increases with improvement in patient condition [Chase et al., 2008b; Langouche et al., 2007].

Finally, sepsis induces a counter-regulatory hormone response causing the reduction in S_I [Agwunobi et al., 2000; Virkamaki and Yki-Jarvinen, 1994]. The use of glucocorticoids may exacerbate this situation [Dimitriadis et al., 1997; Qi and Rodrigues, 2007; Pretty et al., 2011], and are commonly used in the treatment of severe sepsis [Dellinger et al., 2004]. Sepsis induces a strong pro-inflammatory acute immune response that worsens hyperglycemia and reduces insulin sensitivity further [Weekers et al., 2003; Fernandez et al., 2011]. Hence, the fact that insulin sensitivity and patient metabolic condition are strongly linked, suggest that S_I is capable of becoming a marker for real-time diagnosis of sepsis.

6.2 Insulin sensitivity of retrospective cohort

Clinical data of retrospective sepsis cohort was collected during their stay in ICU. The data is then used with the model to identify insulin sensitivity profiles, $S_I(t)$, for all 30 patients. These profiles provide an hour-to-hour trajectory for each patient, before, during and after sepsis. Figure 6.1 illustrates the cumulative distribution function (CDF) of 30 patients in the cohort, where the shaded area indicates the 90% confidence interval range and dotted line represents the median distribution. The interquartile range (IQR) is the area between two continuous lines, which are closer to the median line.

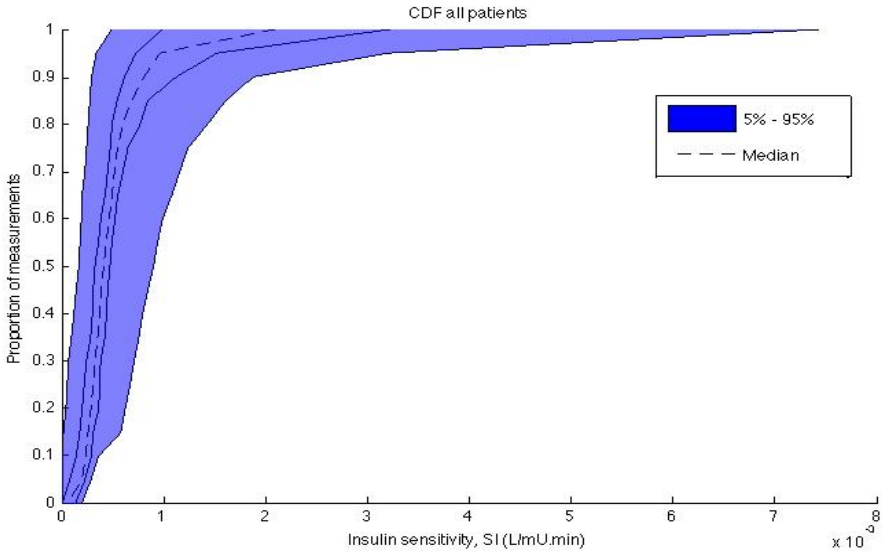

Figure 6.1: Cumulative distribution function of insulin sensitivity for 30 patients in the sepsis cohort.

CDFs of S_I on a per-patient basis are shown in Figure 6.2. Most of the patients in the cohort had similar S_I distribution. However, a few patients had a slightly higher or lower S_I distribution. Clearer distribution of S_I on each patient is illustrated in Figure 6.3. In this figure, the x and y-axes

represent patient number and insulin sensitivity, respectively. The plot shows the median, IQR and 90% range plus out less for each patient. Overall, most of the patients have the same range of S_I and only 10% of the total patients have significantly slightly higher or different ranges of S_I.

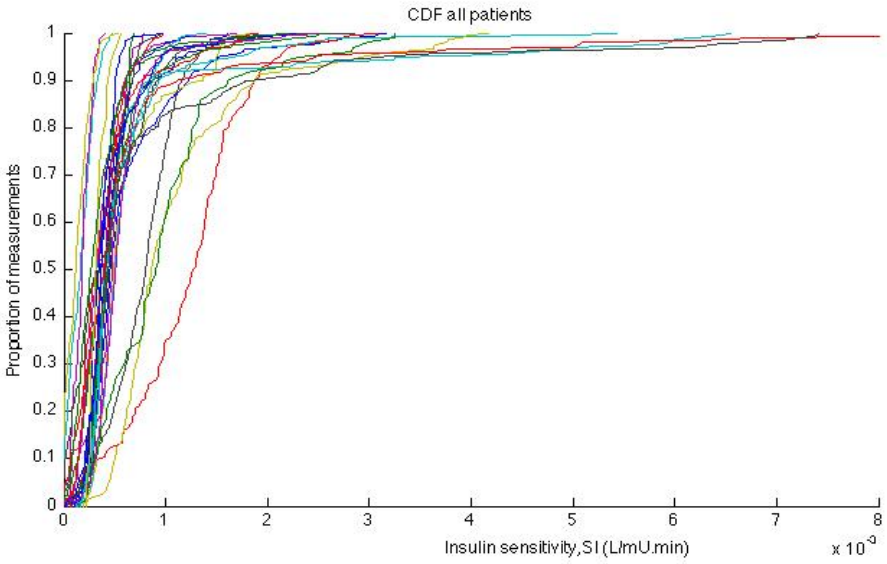

Figure 6.2: Per patient cumulative distribution function of insulin sensitivity for 30 patients in the sepsis cohort.

Table 6.1 represents the median S_I, minimum and maximum S_I, median change in insulin sensitivity (ΔS_I) and percentage of change in insulin sensitivity (% ΔS_I) across patients and the cohort. Maximum S_I values are highly variable across patients. The highest S_I value in the cohort is 0.00927337 L/mU.min, seen in Patient 079.

Median S_I of the cohort is 100 times larger compared to the median ΔS_I, where ΔS_I describes an hour-to-hour change. Most of the patients had similar ranges of ΔS_I, as seen in Table 6.1. Higher median ΔS_I has been observed on Patients 063, 078 and 095. However, the median $\%\Delta S_I$ is observed to be in

Table 6.1: Insulin sensitivity and its variation among 30 patients in the sepsis cohort.

Patient ID	Median S_I (10^{-4})	Minimum S_I (10^{-4})	Maximum S_I (10^{-4})	Median ΔS_I (10^{-6})	Median ΔS_I (%)
002	4.5273	0.0010	32.1552	3.7108	1.084
010	4.4329	1.5402	6.8967	-7.0100	-1.261
012	12.8269	0.6251	31.6565	4.0684	0.471
013	1.6572	0.0010	4.8695	5.3074	3.349
017	4.7024	0.3252	7.9057	-1.0718	-1.021
022	4.9273	1.9004	19.2340	2.8245	0.562
027	8.0113	1.4104	24.1765	-1.6763	-0.255
030	3.6736	0.1142	16.2012	6.6803	1.531
031	3.4392	0.0010	23.2900	4.6365	1.255
032	4.0259	0.0010	19.6549	5.6550	1.597
033	5.0168	1.2815	58.9588	7.9494	1.819
035	3.2228	0.0010	17.8042	7.2160	1.967
038	8.5881	1.9173	42.5266	0.0720	0.012
039	4.3789	1.0615	35.3386	-0.0195	-0.004
044	4.0768	0.8462	13.8395	9.3274	2.705
047	4.1755	1.6226	25.7384	1.9691	0.573
051	3.1187	0.6704	9.6912	7.5956	3.226
052	4.1005	1.5885	66.0763	0.0972	0.003
055	1.7864	0.0010	4.1691	2.8621	1.118
056	1.1706	0.0010	5.7676	6.5147	4.243
063	3.3369	0.0010	9.8669	20.9228	4.554
069	3.3996	1.0894	10.2203	8.6194	2.053
078	9.0696	0.2302	32.5296	48. 2037	5.682
079	3.9202	0.0010	92.7337	17.9259	7.999
080	4.1192	1.1815	15.9559	3.8445	0.972
083	5.0928	0.8300	25.0050	2.8515	0.883
095	3.1732	2.2407	5.5890	-20.5320	-6.079
100	4.1031	0.2632	74.2105	7.5893	0.845
101	3.6671	0.2169	23.7300	2.1505	0.460
104	2.6532	0.0010	21.9804	3.3809	1.132
Cohort	4.1931	0.0010	92.7337	4.2534	1.114

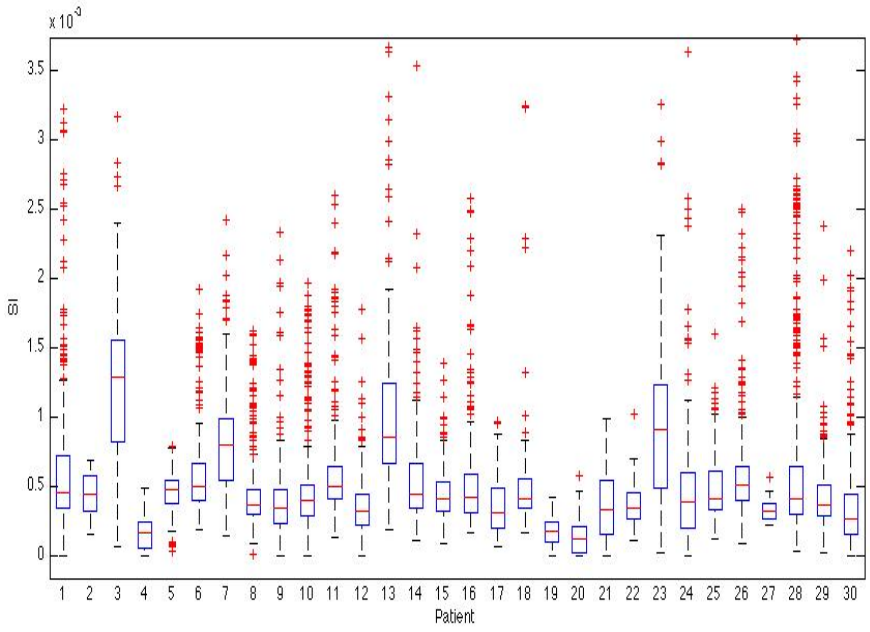

Figure 6.3: Insulin sensitivity distribution for 30 patients in the sepsis cohort.

similar range for the whole cohort given that $\%\Delta S_I$ for the cohort is 1.114%. This latter result indicates similar variability across patients when normalized by current S_I value as a percentage.

Figure 6.4 shows the 5th - 95th percentile range, IQR and median probability bounds for the hour-to-hour stochastic model of 30 patients in the sepsis study based on the models developed by Lin et al [Lin et al., 2006, 2008]. The distribution indicates the hour to hour patient metabolic variability in S_I. The variation distributions are plotted as $S_{I(n+1)}$ on the y-axis against S_{In} on the x-axis.

The dynamic change in S_I from hour to hour also provides information on metabolic dynamics and insulin resistance in this cohort. Importantly,

the variability of S_I over any given hour is dependent on its current value. Therefore, the stochastic model represents the transition of S_I from one hour to the next and changes in variability may be indicative of changes in patient condition, creating a further potential bio-marker.

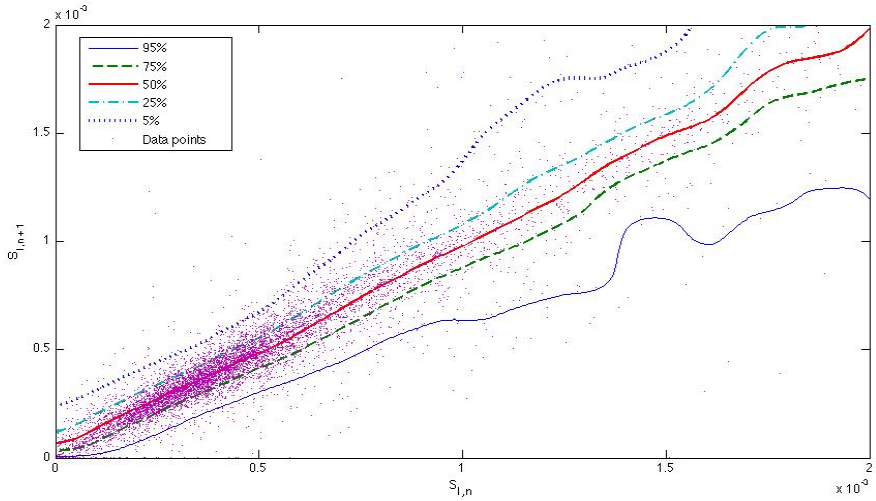

Figure 6.4: Hourly insulin sensitivity distribution for sepsis cohort.

6.3 Insulin sensitivity in diagnosing sepsis

CDFs of S_I on the SS2 score basis is shown in Figure 6.5. SS2 is determined hourly as discussed in Chapter 5. SS2 = 0 has the highest S_I distribution followed by patients with SS2 = 1, SS2 = 2 and SS2 = 3. However, the S_I distribution for SS2 = 0, 1 and 2 are almost overlaid. S_I reduces as the patient condition worsens, as hypothesized. However, the discrimination while significant ($p < 0.05$), is not large. The p-values computed using Mann-Whitney test are shown in Figure 6.5. The obvious separation between these three groups at SS2 = 3 implies that, in the very worst condition for sepsis (SS2 =

3), the S_I profiles of a patient are much lower and much more distinguishable. However, early diagnosis would rely on discrimination at lower scores of SS2.

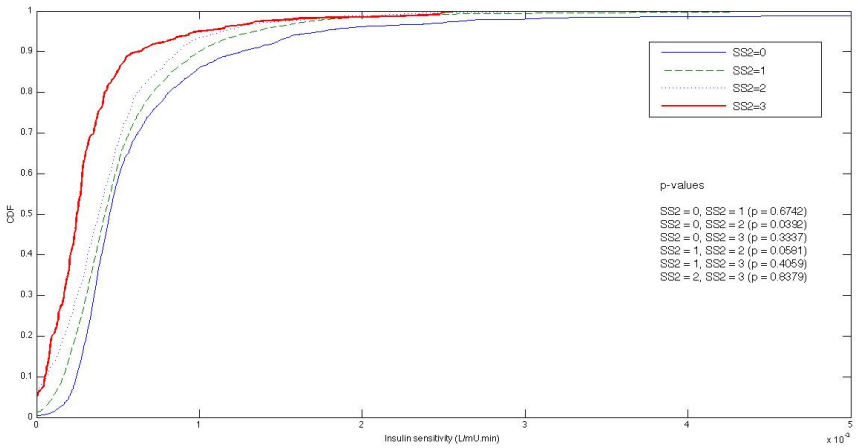

Figure 6.5: Cumulative distribution function of insulin sensitivity grouped by SS2. P-values are computed using Mann-Whitney test.

Figures 6.6 - 6.9 show the hourly distribution of insulin sensitivity, S_I, changes in insulin sensitivity (ΔS_I), percentage of changes in insulin sensitivity ($\%\Delta S_I$) and SS2 for four patients in the cohort. These four patients are the same patients as selected in Chapter 5. These figures are used to describe the issues schematically.

Referring to Figure 6.6, Patient 002 has an increasing value of SS2 at the early stage of the stay to the maximum score of SS2. In contrast, S_I is slowly decreasing and marginally low at the beginning. At 15000 minutes, S_I changes dramatically. At this stage, SS2 decreases gradually from 2 to 0. The ΔS_I value at the early part of the patient's stay is almost constant and more fluctuations are seen in the second half of the stay. Similarly, constant $\%\Delta S_I$ has been observed mostly throughout the stay, showing no real response to

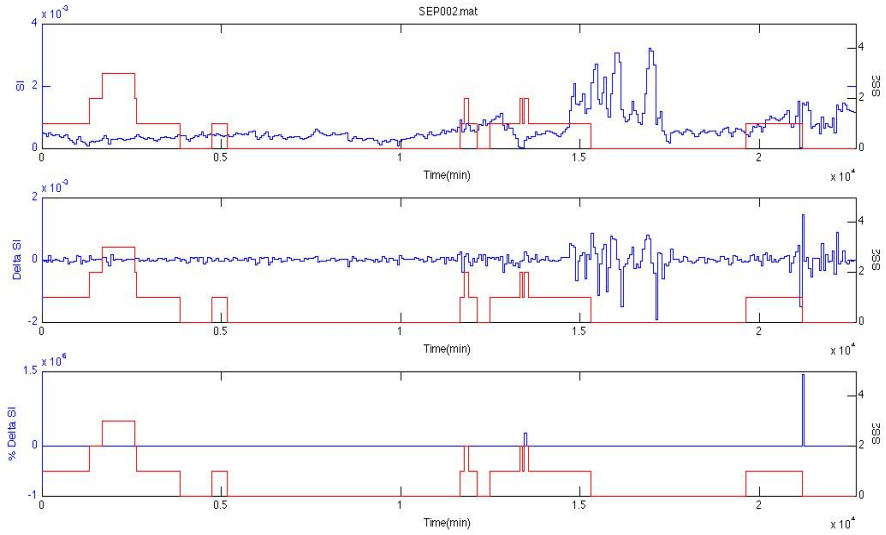

Figure 6.6: Hourly plot of insulin sensitivity, ΔSI, %ΔSI and SS2.

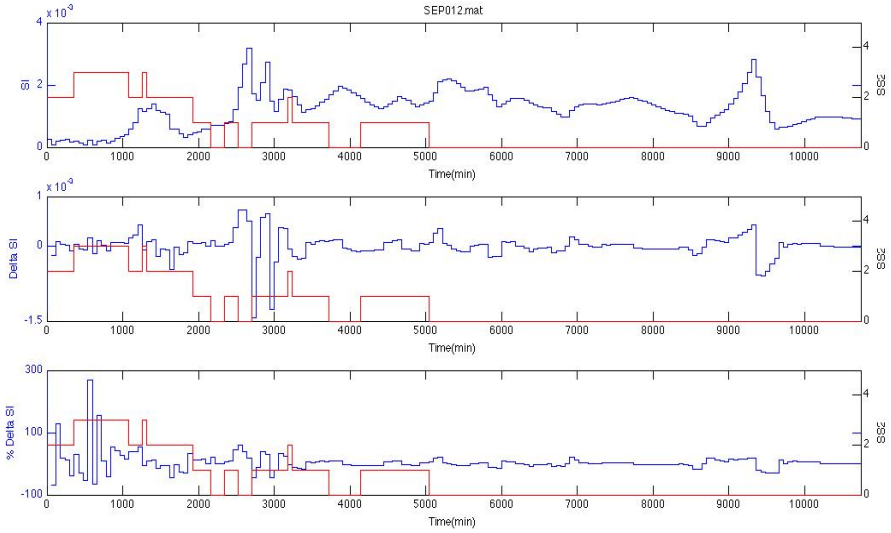

Figure 6.7: Hourly plot of insulin sensitivity, ΔSI, %ΔSI and SS2.

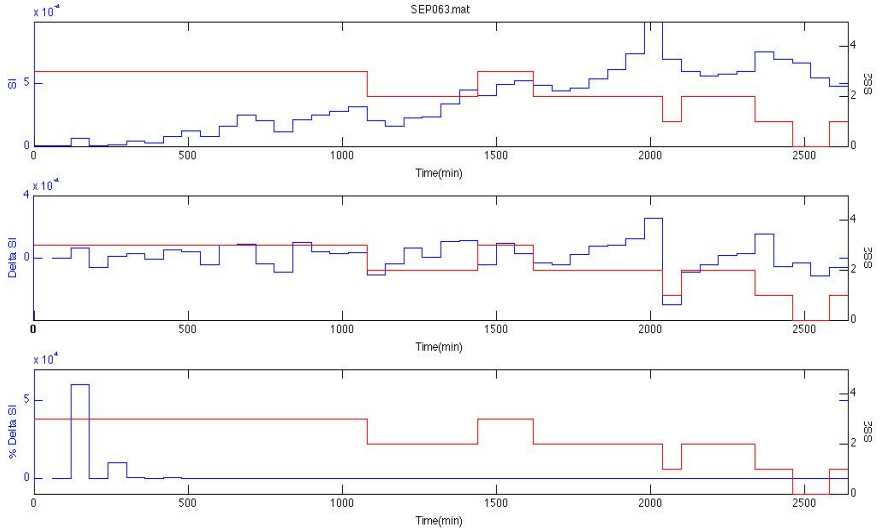

Figure 6.8: Hourly plot of insulin sensitivity, ΔSI, %ΔSI and SS2.

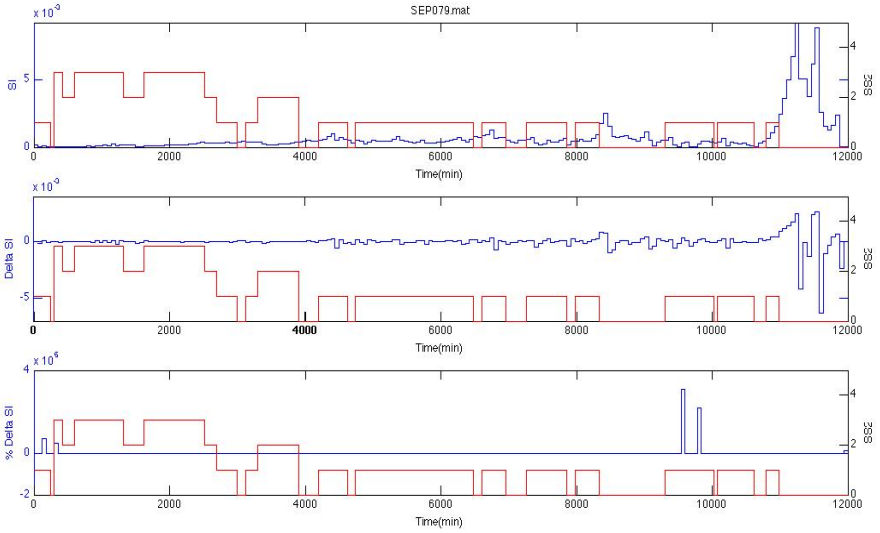

Figure 6.9: Hourly plot of insulin sensitivity, ΔSI, %ΔSI and SS2.

SS2 value.

The hourly plot of Patient 012 is shown in Figure 6.7, where Patient 012 also has higher SS2 and low S_I at the beginning of the stay. As time goes by, it is observed that S_I increases and SS2 keep reducing to a minimum level. For the second half of the stay, SS2 maintains a minimum level. Even though S_I decreases for some time in the second half of the stay, the S_I amount is relatively higher compared to S_I at the early stay. At minute 2500, ΔS_I starts to fluctuate until minute 3000. However, SS2 does not change during this time. In the bottom plot, $\%\Delta S_I$ varies at the beginning of the stay and remains almost constant for the remainder of the stay.

Figure 6.8 shows the S_I, ΔS_I, $\%\Delta S_I$ and SS2 distribution during the stay of Patient 063. Patient 063 has a maximum level of SS2 (SS2 = 3) when admitted into the ICU and has very low S_I. Later, the insulin sensitivity improves as the patient reacts to treatment and therefore the SS2 level decreases, as well and as expected. In the early part of the stay, ΔS_I changes slightly and then slowly increases and follows the S_I pattern. However, $\%\Delta S_I$ shows constant value throughout the stay with an obvious change only at the beginning.

A similar pattern of S_I and ΔS_I is observed on Patient 079 shown in Figure 6.9. S_I is at minimum level at first, then increases gradually over time. On the other hand, $\%\Delta S_I$ is constant during the entire stay. Equally, $\%\Delta S_I$ changes slightly at the early stay and at minute 9500.

Overall, Figures 6.6 - 6.9 imply that SS2 decreases with increases in insulin sensitivity, S_I, given that S_I is above a certain threshold. However,

patients might have different patient-specific thresholds or baseline values to indicate changes in their metabolic condition. Similarly, changes in S_I may also vary between patients. Some patients may have a huge change in S_I when shifting metabolic condition, while others may experience much smaller changes for the same event. Nevertheless, ΔS_I and $\%\Delta S_I$ do not show a significant correlation to the SS2, and thus may not serve as a bio-marker. Equally, these results show that S_I is an effective bio-marker, but patient-specific thresholds make automated diagnosis difficult without external data.

In particular, the relation of insulin sensitivity, S_I to SS2 may suggest S_I as a significant marker in determining sepsis level in critical illness. In addition, the insulin sensitivity profile of a patient is able to be captured as early as possible by computer. Therefore, the possibility of early treatment and diagnosis of sepsis would be enabled conveniently. However, the change in insulin sensitivity, ΔS_I and $\%\Delta S_I$ do not correlate well with SS2 profiles. Thus, information on S_I of a patient is potentially a good marker to diagnose sepsis, but its variability is not.

Figure 6.10 shows the receiver operating characteristic (ROC) curves where x-axis represents (1-specificity) and y-axis represents sensitivity. Plotted lines lay in a sequence according to the SS2 value. As expected, higher SS2 values yield the best possible prediction and the plots show a similar trend for all categories of SS2. There is a small gap between SS2 ≥ 1 and SS2 ≥ 2, and large gap has been observed between SS2 ≥ 3 to the rest.

Figure 6.10 also conveys that at low value of SS2, S_I may be insignificant in aiding sepsis diagnosis. However, at higher value of SS2 (SS2 ≥ 3), which represents the worst condition, such as septic shock, insulin sensitivity shows

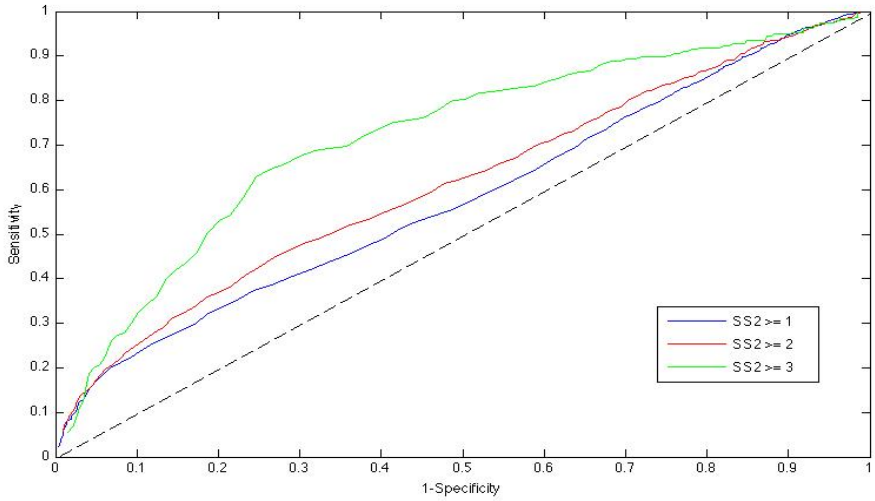

Figure 6.10: Receiver operating characteristic (ROC) plot showing the sensitivity and specificity relation of SS2 and insulin sensitivity.

a significant response with increase in sensitivity. Hence, early diagnosis is unclear, but positive predictive value with this marker alone is not significant without further information. These results are largely due to the fact that S_I lags condition, resulting in S_I values that do not match SS2 score when sepsis state is changing. The end result is a loss of diagnostic power largely due to the hourly nature of assessment and this lag.

6.4 Summary

Early identification of an inflammatory response to infection will enhance the understanding of the cellular and immunologic mechanisms that can cause sepsis. Moreover, early detection and treatment of sepsis may increase chances to recover and consequently decrease mortality rates. However, early detec-

tion and treatment is a challenge due to the lack of physiological information accessible in real-time that is relevant to infection, organ failure and sepsis.

Several studies clearly show that S_I represents metabolic condition of a patient. In addition, this chapter shows that information on S_I can be highly related to SS2, a modified sepsis scoring system indicating sepsis degree. SS2 increases with a decrease in S_I and vice versa. However, other information derived from S_I do not show any direct relation to SS2, particularly in the study of this cohort.

Even though S_I shows a directly proportional relation to SS2, the change in S_I is highly variable and patient-specific especially at low value of SS2. Patient-by-patient analysis shows clear trends and discrimination, but at patient-specific levels that are not easily automated to diagnostic guidelines. Thus, at low S_I, it is almost impossible to differentiate the resulting sepsis condition of a particular patient from other acute conditions. In particular, different patients develop from different S_I baseline values and at different rates, confound the situation. Equally, lag between SS2 score and resulting impact on metabolic bio-markers further confuses automation of diagnosis.

In a nutshell, the use of S_I as a marker may potentially aid the process of diagnosing sepsis. However, information on S_I is insufficient to determine the exact sepsis condition of a patient particularly at moderate sepsis levels (eg SS2=1) which are important for early diagnosis as the condition develops. Other physiological or clinical variables will have to be incorporated with S_I to provide better information for sepsis diagnosis in real-time. More concisely, the impact of sepsis on metabolic markers, like S_I, is clear. However, patient-specific levels and thresholds confound this positive result in trying to

automate its use as an effective diagnostic.

Chapter 7

Predicting Sepsis in Critical Illness

This chapter investigates using one or a series of potential sepsis bio-markers to detect (early) and thus effectively predict the existence of sepsis. Currently, there are no reported studies that successfully predict the existence of sepsis in a patient admitted in a hospital. Since there are many factors that may limit the ability to diagnose emerging sepsis, clinicians focus on treating patients according to their judgement and experience. Confirmative and definitive diagnosis by blood culture results usually take about 1-3 days which is too long a delay. More specifically, early treatment of sepsis has been shown to reduce mortality and improve patient condition [Rivers et al., 2001]. However, the lack of clear information and objective, accurate methods to diagnose sepsis at an early stage makes this has become a significant challenge.

In this chapter, a series of data taken during a specific sepsis study from the Intensive Care Unit (ICU) of Christchurch Hospital is used to analyze and determine if there exists a potential viable bio-marker that is reliable as a sepsis predictor. Several available clinical parameters were tested to obtain a suitable parameter or parameter set that can be used as a marker.

Insulin sensitivity, a patient metabolic parameter is also tested to analyze its potential in assessing sepsis status based on its reflection of the metabolic response to the inflammation and immune response actions concomitant with sepsis [Blakemore et al., 2008]. The overall goal is to determine if a viable hour-to-hour marker exists that is better than clinical experience. Currently, no such metric exists and identifying one would be a major step forward.

7.1 Neural Network Time Series Analysis

Artificial neural networks (ANN) are flexible mathematical structures capable of identifying complex, nonlinear relationships between one or more inputs and outputs. It composed of interconnecting artificial neurons and processing elements that can exhibit and capture complex global behavior, as determined by the numerically weighted connections between the processing elements and specific element parameters. The use of ANN models, particularly in a system where the characteristics are unable to describe by physical equations, have been found to be useful in many areas [Chiu et al., 2005; Hsu et al., 1995]. These black-box models are especially useful in cases, as with sepsis, where the input-output relationships are not fully defined or known, or are highly variable or non-linear.

A sequence of data points, known as a time series of data, is typically measured at successive times spaced at a uniform time intervals. Time series analysis comprises methods for analyzing time series data to extract meaningful characteristics from the data. In time series analysis, forecasting is possible by using a model to forecast future events based on known past events and

patterns as a prediction before the point is measured. Ideally, an hourly prediction of a diagnostic sepsis score can be generated using a model configured by data from one or more previous hours.

Properly trained, ANNs thus can be used to find complex patterns with predictive capability that are not necessarily obvious or clearly evident. Sepsis diagnosis is complex and based on a series of interacting and potentially confounding variables. Hence, even clinical experience is far from perfect. These features make ANNs potentially valuable approach to find patterns and relations that are not clinically evident directly.

In this analysis, a flexible, non-linear auto-regressive technique is implemented. Figure 7.1 illustrates the concept used in getting information about Y, the predictive values. The equation used is shown in Equation 7.1, where Y is the variable of interest. In this case, Y is the sepsis score and X is the externally determined or measured variable(s). The information about X is combined using several weights in predicting Y. Prior values of Y itself can also be used, where L represents the lag of the network system in utilizing prior values of Y. The use of time lags in neural networks in this way can improve forecasting accuracy [Samarasinghe, 2007]. Figure 7.2 shows the schematic decomposition of hidden layer functions represented as F in Figure 7.1.

The first layer of the hidden layer contains 10 neurons, where the second layer has 1 neuron. The net product of the first layer, H_1 is the summation of weighted input, weighted output feedback and biases. The net product of the first layer is then applied to a transfer function to obtain an output for the first layer. The net product of the second layer, H_2 is the summation

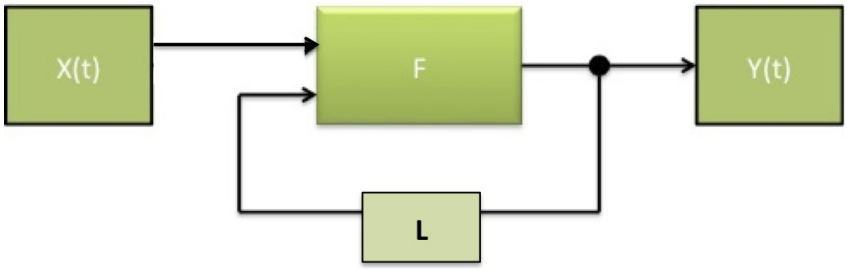

Figure 7.1: Block diagram of nonlinear auto regressive technique.

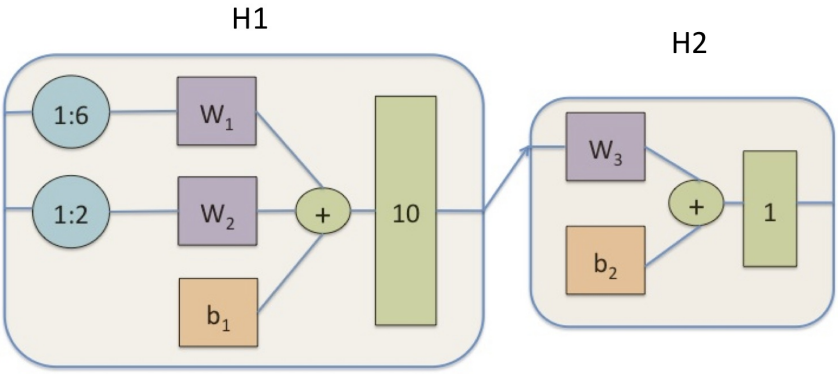

Figure 7.2: Hidden layer parts used in neural network system, the block or layer labelled "10" indicates a hidden layer of 10 neurons.

of the weighted output from first layer and biases. This net product will go through a second transfer function to determine the final output. This process continues until a final value of the input parameter has been entered. The equations used for hidden layer functions, H_1 and H_2 are shown in Equations 7.2 - 7.3.

$$Y_t = F(Y_{t-1}, Y_{t-2}, Y_{t-3}, ..., X_t, X_{t-1}, X_{t-2}, X_{t-3}...) + \in_t \tag{7.1}$$

$$H_1 = F({W_1}^T \cdot X_1 + {W_2}^T \cdot X_2 + b_1) \tag{7.2}$$

$$H_2 = F({W_3}^T \cdot H_1 + b_2) \tag{7.3}$$

The model in this analysis is a general complex structure since there is no clear relationship between the input parameters used and desired output ($Y =$ SS2 values). The uncertainty of the relationship between SS2 and the input parameters requires the used of a non-linear auto-regression model that is suitable for a model with complex structure and unknown dynamics, exacting matching the sepsis diagnosis case. ANNs are also considered superior to conventional models in applicability in these cases where the system and its relationship are not fully understood.

More specifically, in this analysis, the non-linear auto-regressive model is used on time series data because of its advantages over other type of neural network architectures. In particular, it has better computational properties,

storage and learning processes and time-series forecasting properties. It thus provides a better opportunity to develop a model describing the underlying unknown relationship in a sequence of event outcomes [Samarasinghe, 2007]. Finally, 6 prior data points and 2 prior predicted values, also known as lags, were selected as an input variables to encode knowledge of past events. Therefore, the forecast value of SS2 in this architecture is also dependent on past events.

The overall goal is to test several potential bio-markers and sets of common clinical data used in sepsis diagnosis. The ANN is used to determine their predictive ability both individually and in groups. Successful outcomes will provide useful diagnostics, and those sets that do not succeed indicate data for which no clear pattern or diagnostic efficacy exists.

7.2 Data Collection

In this study, prospective data collection was undertaken for several patients as part of a clinical trial. This data consists of sepsis-related clinical data, such as body temperature, respiratory rate and urine output, blood glucose levels, blood culture results, and further laboratory results including white blood cell count. These metrics are related to immune response to infection (temperature, HR and RR) and organ failure (MABP and urine output); which are the core aspects defining sepsis (see Chapter 5). It also includes the model-based insulin sensitivity profiles, which are known to broadly correlate with some aspects of sepsis in prior studies [Blakemore et al., 2008]. Ethics approval to collect, audit and use this data under informed consent was obtained from the

Upper South Regional Ethics Committee, New Zealand.

A total of 7505 data points were gathered from 30 patients in a selected sepsis cohort. These 7505 data points represent a total of 7505 hours of monitoring sepsis patients in the ICU. The data is then divided into 5 groups, Group A, B, C, D and E. Therefore, the test set is independent of the training set. The sampling method used is shown in Figure 7.3. These five groups are then rearranged to obtain 5 sets of data that are used for neural network training and testing processes. For example, in set 1, Groups B, C, D and E were combined to form a training set, and Group A is used for testing the resulting ANN. For every set of tests, there were 6004 of data points in the training set, and 1501 data points used for testing, an 80:20 split.

In neural networks, the training set is used repeatedly to determine the estimation of biases and weight for a candidate ANN design. The known desired output (Y = SS2) is also used in the training process. It is then validated by estimating the performance error of the candidate ANN design. The training process stops when the validation error stops decreasing. In contrast, the testing set is used only once on the best ANN design to obtain an unbiased estimate for the predicted error of unseen non-training data. Thus, data in the test set is independent of the data in the training set [Masters, 1995]. More specifically, in the test set, no information on the output is available, and this knowledge is only used to assess the accuracy of the resulting ANN performance.

Figure 7.4 shows the sequence for developing the hourly prediction of SS2 (see Chapter 5), where the input data is applied to the network system. In Figure 7.4, S_I is used as an input parameter, in this example. In this

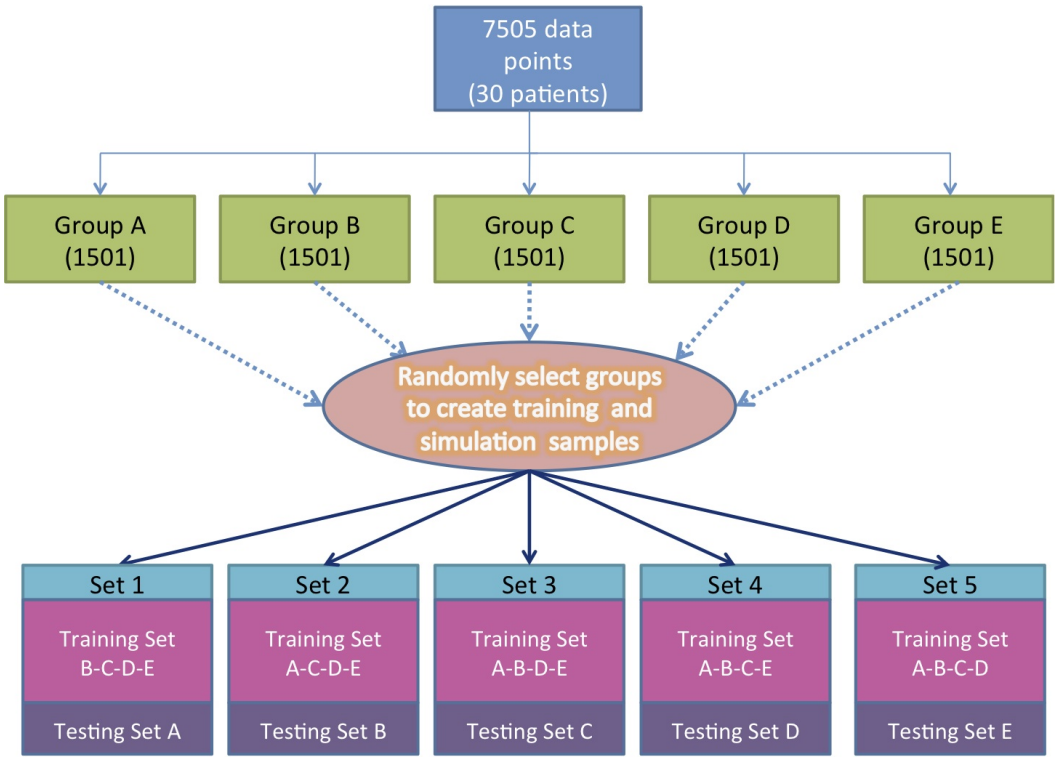

Figure 7.3: Group selection for training and testing.

analysis, 10 neurons were used. These neurons receive one or more input parameters depending on input selection and sum of the weighted inputs was process with a sigmoid function to produce the output.

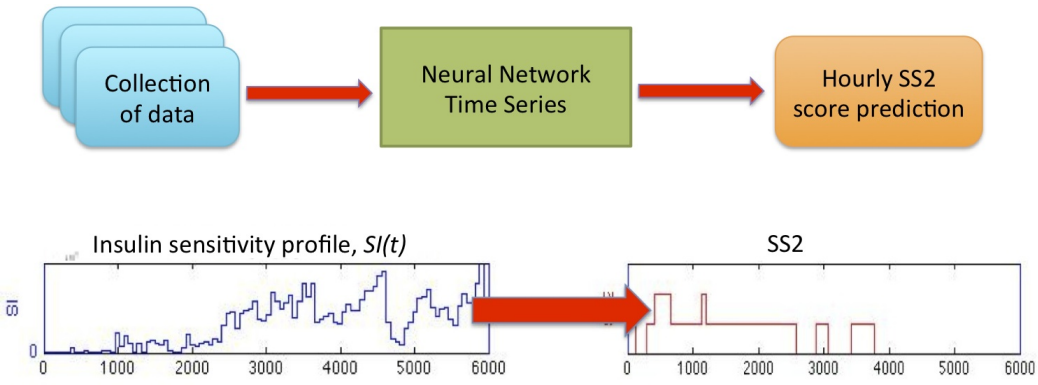

Figure 7.4: Development of desired output from available parameter.

7.3 Identifying Significant Parameters

There were several different clinical data available for the total of 7530 control hours in ICU. These data include: temperature, heart rate, respiratory rate, urine output and BG concentration. The full set is listed in Table 7.1. The variables are tested either individually or combined with other variables to determine the influence of each variable. Sensitivity and specificity for each test set is presented for comparison. This analysis is divided into three categories, which are patient-specific profiles, clinical variables and incorporating or adding the use of prior clinical feedback.

Table 7.1: Clinical data set used for ANN training and testing.

Clinical variables	Nomenclature
Heart rate	HR
Temperature	-
Urine output	-
Blood glucose	BG
Respiratory rate	RR
Mean arterial blood pressure	MABP

7.3.1 Insulin Sensitivity (S_I)

S_I, a patient-specific parameter is tested on the neural network system to investigate the ability of this parameter to predict SS2. In this test, the system processes 6 prior data on S_I and 2 prior SS2 outputs to predict SS2 for the next hour. Table 7.2 shows the confusion plot for the testing process of sets A, B, C, D and E. Blue cells indicate the matched cell between the output and the target. Two different colors of percentage, red and green, represent the percentage of true predictions and percentage of wrongly identified predictions, respectively.

Referring to Table 7.2(a), most of the true identified scores are at target and output of SS2 = 1, where it covers 39.4% of overall data points in Set A. However, most of the data points (49.3%) provide inaccurate results (1 instead of 0). Thus, 40% of data is correctly identified compared to 60% that is wrongly identified. Similarly, in Table 7.2(b), 54% and 46% of data

Table 7.2: Confusion plot for testing process of a) Set A, b) Set B, c) Set C, d) Set D and e) Set E for the case where input and output are insulin sensitivity and SS2, respectively.

a)

Output(SS2) \ Target (SS2)	0	1	2	3	
0	0 0.0%	0 0.0%	0 0.0%	0 0.0%	- -
1	740 49.3%	591 39.4%	65 4.3%	28 1.9%	42% 58%
2	17 1.1%	56 3.7%	4 0.3%	0 0.0%	5% 95%
3	0 0.0%	0 0.0%	0 0.0%	0 0.0%	- -
	0% 100%	91% 9%	6% 94%	0% 100%	40% 60%

b)

Output(SS2) \ Target (SS2)	0	1	2	3	
0	8 0.5%	20 1.3%	9 0.6%	0 0.0%	22% 78%
1	327 21.9%	787 52.4%	320 21.3%	6 0.4%	55% 45%
2	0 0.0%	11 0.7%	13 0.9%	0 0.0%	54% 46%
3	0 0.0%	0 0.0%	0 0.0%	0 0.0%	- -
	2% 98%	96% 4%	4% 96%	0% 100%	54% 46%

c)

Output(SS2) \ Target (SS2)	0	1	2	3	
0	0 0.0%	4 0.3%	0 0.0%	0 0.0%	0% 100%
1	701 46.7%	617 41.1%	135 9.0%	44 2.9%	41% 59%
2	0 0.0%	0 0.0%	0 0.0%	0 0.0%	- -
3	0 0.0%	0 0.0%	0 0.0%	0 0.0%	- -
	0% 100%	99% 1%	0% 100%	0% 100%	41% 59%

d)

Output(SS2) \ Target (SS2)	0	1	2	3	
0	8 0.5%	1 0.1%	6 0.4%	3 0.2%	44% 56%
1	333 22.2%	706 47.0%	127 8.5%	65 4.3%	57% 43%
2	6 0.4%	70 4.7%	143 9.5%	30 2.0%	57% 43%
3	3 0.2%	0 0.0%	0 0.0%	0 0.0%	0% 100%
	2% 98%	91% 9%	52% 48%	0% 100%	57% 43%

e)

Output(SS2) \ Target (SS2)	0	1	2	3	
0	4 0.3%	3 0.2%	0 0.0%	0 0.0%	57% 43%
1	315 20.9%	1066 71.0%	55 3.7%	58 3.9%	71% 29%
2	0 0.0%	0 0.0%	0 0.0%	0 0.0%	- -
3	0 0.0%	0 0.0%	0 0.0%	0 0.0%	- -
	1% 99%	99% 1%	0% 100%	0% 100%	71% 29%

points in Set B are correctly and wrongly identified, respectively. The highest percentage of matched output and target is 52.4% at input and target SS2 = 1. At target SS2 = 1, 96% of data is truly identified. Set C shows a slightly different result in comparison to Sets A and B, given that majority (99.7%) of data points lay on output SS2 = 1 as seen in Table 7.2(c). In addition, more than half (59%) of data in Set C is wrongly identified and 41% is truly predicted. Table 7.2(d) shows the confusion plot on Set D. 57% of data points in Set D is correctly identified whereas 43% is wrongly predicted. In Set D, the data is more scattered and a higher percentage are seen at target and output SS2 = 2, where other data sets show smaller percentages at target and output SS2 = 2. Finally, the confusion plot for Set E is shown in Table 7.2(e). The percentage truly and wrongly predicted are 71% and 29%, respectively. The highest percentage of correctly identified is at target and output SS2 = 1.

Overall, Table 7.2 indicates that most of the output of the network system lay at output SS2 = 1 and SS2 = 2. The percentage of true prediction is very low across all the testing sets. These results suggest that either the network system could not account for the variability in the input applied or the variability of the input itself, specifically in S_I, are the cause of the inability to correctly identify and forecast the value of SS2.

Table 7.3 summarizes the testing results using S_I as an input parameter. The hourly prediction of SS2 is based on 6 hours prior data on S_I and 2 hours prior estimated output. As seen in Table 7.3, the MSE for Sets B and E are marginally lower compared to other data sets. NPV values are relatively small across all data sets. Interestingly, all sets have high sensitivity

($> 90\%$) indicating a high proportion of actual positives that are correctly identified. However, very low specificity across all data sets, which is less than 10%, means this sensitivity comes from an inability to correctly identify the proportion of actual negatives.

Table 7.3: Testing results on SS2 using S_I as an input parameter. MSE, PPV and NPV represent mean squared error, positive predictive value and negative predictive value respectively.

Data set	MSE	PPV	NPV	Sensitivity	Specificity
Set A	0.765	49.6	-	100.0	0.0
Set B	0.462	77.7	21.6	97.5	2.4
Set C	0.697	53.2	0.0	99.5	0.0
Set D	0.691	76.9	44.4	99.1	2.3
Set E	0.387	79.0	57.1	99.7	1.3

Note that these high sensitivity and low specificity results match a lot of clinical practice. Typically, clinicians use experience and intuition, and, importantly tend to err on the side of caution. They thus diagnose and treat, with antibiotics, likely sepsis more often than confirmed by blood test. Typically, $\sim$50% of all sepsis is culture negative [Martin et al., 2003], indicating sensitivity of 80 - 100% but much lower specificity. Very similar to these results, hence, what is seen is not a failure, but a failure to exceed current clinical practice.

Variability among data sets can also be clearly seen in Table 7.3. PPV

values are similar and more consistent across data sets. However, NPV is more variable and inconsistent. Note that, the output obtained from simulation for each data set is highly dependent on the input of the data set, the prior output, and their weights.

From these results, it can be concluded that S_I alone is not capable of improving sepsis diagnosis and becoming an hourly sepsis predictor despite the potential of representing patient metabolic condition in earlier, less in depth, studies [Blakemore et al., 2008]. Therefore, other information is necessary to predict sepsis status. Hence, several combinations of clinical inputs need to be tested to see if a more ideal diagnostic system exists using typical clinical data.

Figure 7.5 illustrates the distributions of BG across the SS2 values of the cohort. The axes are left unmodified for a clearer picture of individual distribution according to their SS2 values. Additionally, Figure 7.6 shows the comparison of BG distribution for different SS2 value. At SS2 = 0 and SS2 = 1, where a high density of measurements has been observed compared to SS2 = 2 and SS2 = 3. Surprisingly, the ranges of BG are almost similar for all the different SS2 values, indicated by the overlapping of the normal distributions in Figure 7.6. Thus, BG may not be a good discriminator on its own, particularly where, as well with these patients on SPRINT [Chase et al., 2008b], BG control is effective across all patients.

Similarly, Figure 7.7 presents the individual distributions of SOFA scores according to SS2 value. Figure 7.8 shows the distributions of SOFA scores across the SS2 values of the cohort. Referring to Figure 7.8, there is a clear separation dividing the SS2 scores into two groups. SS2 = 0 and SS2 = 1 are

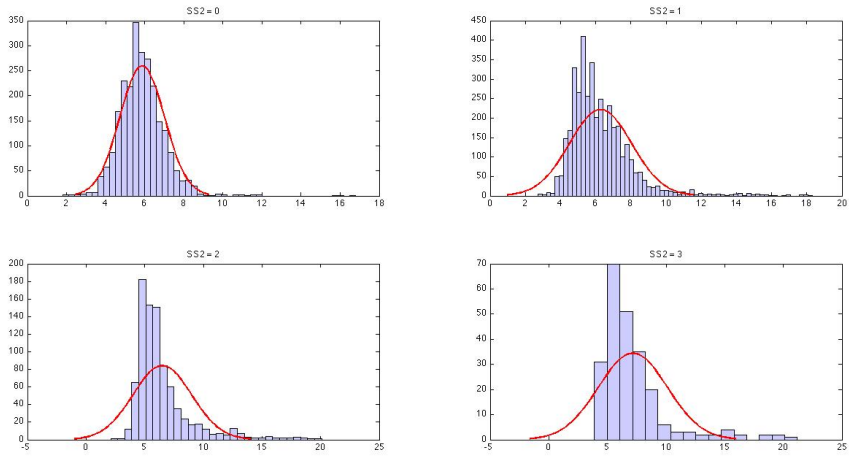

Figure 7.5: Distribution of BG according to SS2 value.

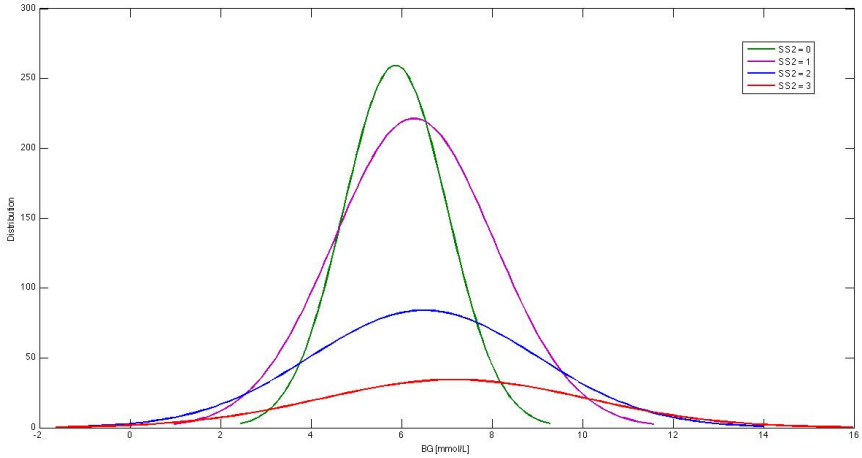

Figure 7.6: Distribution of BG for different SS2 values.

closer and less well separated. Whereas SS2 = 2 is closer to SS2 = 3. These results separate severe sepsis from an early sepsis and no sepsis.

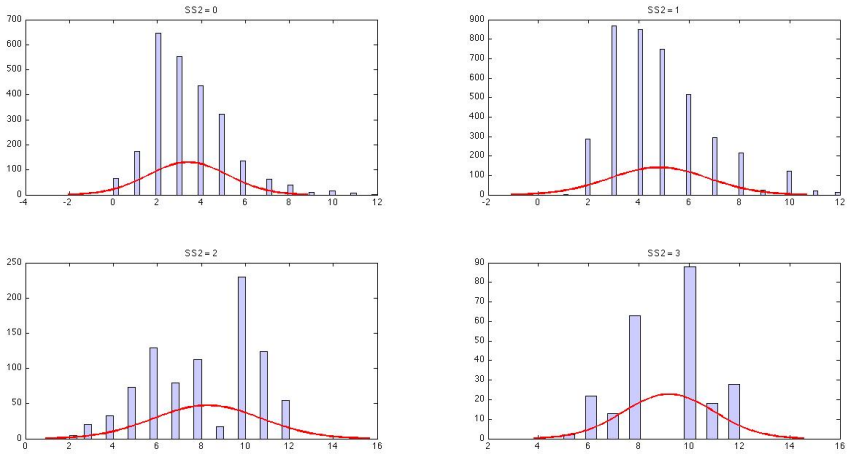

Figure 7.7: Distribution of SOFA score according to SS2 value.

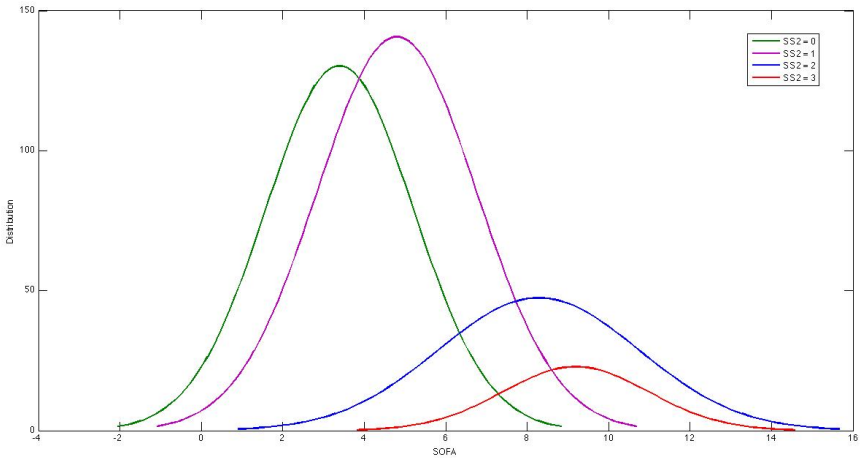

Figure 7.8: Distribution of SOFA score for different SS2 values.

Table 7.4 summarizes the results of the testing process on SS2 using several combinations of input parameters such as S_I, blood glucose measured (BG) and SOFA. Adding BG to S_I as input parameter does not show sig-

nificant improvement on sensitivity and specificity. However, combining S_I and SOFA shows some improvement on specificity and MSE as compared to S_I alone. In contrast, and as expected, adding BG to S_I and SOFA does not show any further improvement in discrimination. In particular, MSE, PPV, and NPV decrease slightly. Similarly, slight changes have been seen in sensitivity and specificity for most of the data sets.

Table 7.4: Testing results on SS2 using several combinations of input parameter. MSE, PPV and NPV represent mean squared error, positive predictive value and negative predictive value respectively.

Input variables	Data set	MSE	PPV	NPV	Sensitivity	Specificity
S_I, BG	Set A	0.872	49.6	100.0	100.0	0.4
	Set B	0.468	77.6	0.0	99.6	0.0
	Set C	0.693	52.9	7.1	98.4	0.1
	Set D	0.664	78.0	74.4	99.1	8.3
	Set E	0.654	79.8	38.1	95.6	10.0
S_I, SOFA	Set A	0.582	62.4	86.5	92.9	45.0
	Set B	0.351	83.0	82.1	98.1	30.1
	Set C	0.560	60.0	67.2	85.3	34.5
	Set D	0.664	81.2	74.8	97.3	26.2
	Set E	0.448	82.5	28.3	68.9	45.8
S_I, SOFA, BG	Set A	0.606	61.1	70.6	78.5	50.9
	Set B	0.512	82.8	69.9	96.2	30.4
	Set C	0.562	59.6	68.0	86.4	33.1
	Set D	0.600	82.3	56.9	91.8	35.3
	Set E	0.478	82.7	29.4	71.1	44.8

Results in Table 7.4 indicate that BG is not suitable to be a meaningful

part of a bio-marker for sepsis diagnosis and more potential can be seen for SOFA as a bio-marker. This outcome occurs because SOFA gives more impact by improving specificity values compared to BG and is more directly associated with sepsis and its definition as infection plus organ failure. In addition, BG is more a function of control than of condition and thus may not reflect sepsis well. This latter point is particularly valid in this cohort, which was on the SPRINT protocol [Chase et al., 2008b] and provided consistent control regardless of condition. These outcomes are visible when noting that the BG distribution for this cohort is very similar across all the different SS2 scores, as shown in Figure 7.6.

7.3.2 Impact of Clinical Variables

Additional tests using ANNs are used to investigate if any of the other readily available clinical parameters in Table 7.1 can potentially improve the results. These variables are tested individually and in groups to identify their relation with SS2 and their potential in creating and improved diagnostic marker.

Table 7.5 shows the results of the testing process using temperature, urine, HR, RR, and MABP as input parameters. Significant improvement is seen for the whole data set, particularly in specificity, as compared to using S_I alone in Table 7.3. However, NPV across the data sets are much smaller compared to using S_I and SOFA. Potentially, not all the clinical inputs used were beneficial for predicting sepsis on an hourly basis. Therefore, each variable is tested individually.

Table 7.6 presents the analysis results on the network system using dif-

Table 7.5: Testing results on SS2 using all available clinical input parameters. MSE, PPV and NPV represent mean squared error, positive predictive value and negative predictive value respectively.

Data set	MSE	PPV	NPV	Sensitivity	Specificity
Set A	0.647	60.6	75.9	85.3	45.4
Set B	1.201	81.2	65.2	96.6	22.4
Set C	0.837	58.4	55.8	70.1	43.1
Set D	0.867	80.7	45.5	88.9	30.5
Set E	0.510	85.4	33.1	69.9	55.5

ferent individual input parameters. PPV and sensitivity are a major challenge to analyze since the values are mostly similar across the data sets and different input variables. In contrast, NPV and specificity are much more variable, and very low specificity has been observed for example using RR with zero specificity for four data sets. Interestingly, Set D has the most promising result, even when using different input variables. In contrast, Set A has been observed for having relatively worst result throughout the testing process. These results reflect smaller differences in the specific patients in each set.

Table 7.7 summarizes the results of individual input tests by looking at the mean average of the testing process across the data sets. As previously mentioned, MSE, PPV, and sensitivity are almost similar across all the input variables. Additionally, HR, temperature and urine show an acceptable NPV value for individual testing of 60.3, 40.3 and 49.9, respectively. As noted

Table 7.6: Testing results on SS2 using several clinical input parameter. MSE, PPV and NPV represent mean squared error, positive predictive value and negative predictive value respectively.

Input variables	Data set	MSE	PPV	NPV	Sensitivity	Specificity
Temperature	Set A	0.833	48.2	17.2	93.5	1.3
	Set B	0.472	77.9	39.1	98.8	2.7
	Set C	0.792	50.9	39.1	87.6	3.7
	Set D	0.661	79.4	71.1	97.9	16.8
	Set E	0.447	81.3	35.1	87.5	25.1
RR	Set A	0.625	49.6	-	100.0	0.0
	Set B	0.469	77.7	0.0	99.9	0.0
	Set C	0.682	53.2	0.0	99.8	0.0
	Set D	0.676	76.9	83.3	99.9	1.4
	Set E	0.403	78.8	-	100.0	0.0
HR	Set A	0.990	54.1	90.7	98.1	18.1
	Set B	0.448	84.5	57.9	91.3	41.8
	Set C	0.612	57.3	89.2	98.3	16.5
	Set D	0.772	76.3	12.5	96.3	1.7
	Set E	0.402	80.8	51.1	96.1	15.0
Urine	Set A	0.641	49.7	66.7	99.6	0.8
	Set B	0.478	77.0	40.0	99.2	01.8
	Set C	0.672	53.4	100.0	100.0	0.4
	Set D	0.707	76.8	29.4	97.9	2.8
	Set E	0.472	78.0	13.4	89.6	6.0
MABP	Set A	0.619	49.6	50.0	99.9	0.1
	Set B	0.595	77.6	0.0	99.7	0.0
	Set C	0.730	53.3	-	100.0	0.0
	Set D	0.998	76.3	22.5	73.4	25.4
	Set E	0.580	76.1	7.7	80.8	6.0

previously, these might be similar to clinical capability. However, RR has the smallest specificity followed by urine, MABP, temperature and HR.

Table 7.7: Mean average testing results on SS2 using individual clinical input parameter. MSE, PPV and NPV represent mean squared error, positive predictive value and negative predictive value respectively.

Input variables	MSE	PPV	NPV	Sensitivity	Specificity
Temperature	0.641	67.5	40.3	93.1	9.9
HR	0.645	70.6	60.3	96.0	18.6
RR	0.571	67.2	16.7	99.9	0.3
Urine	0.594	67.0	49.9	97.3	2.4
MABP	0.704	66.7	16.0	90.8	6.3

Figure 7.9 shows the cdfs for the clinical variables on different SS2 values. Referring to Figure 7.9, the temperature, RR and HR distributions are almost overlaid for different value of SS2. The separation between different SS2 values can be seen in the urine output and MABP variables. The urine distributions follow the sequence of SS2 values with highest urine output for SS2 = 0 and lowest urine output for SS2 = 3. However, MABP distributions are separated into two groups which are SS2 $>$ 1 and SS2 $\leq$ 1. A summary of the clinical variable distributions are shown in Table 7.8.

Overall, the tests of clinical variables on predicting SS2 suggest that clinical data, such as hourly urine output, MABP, temperature, RR and HR add value, but cannot create a significantly improved bio-marker. In partic-

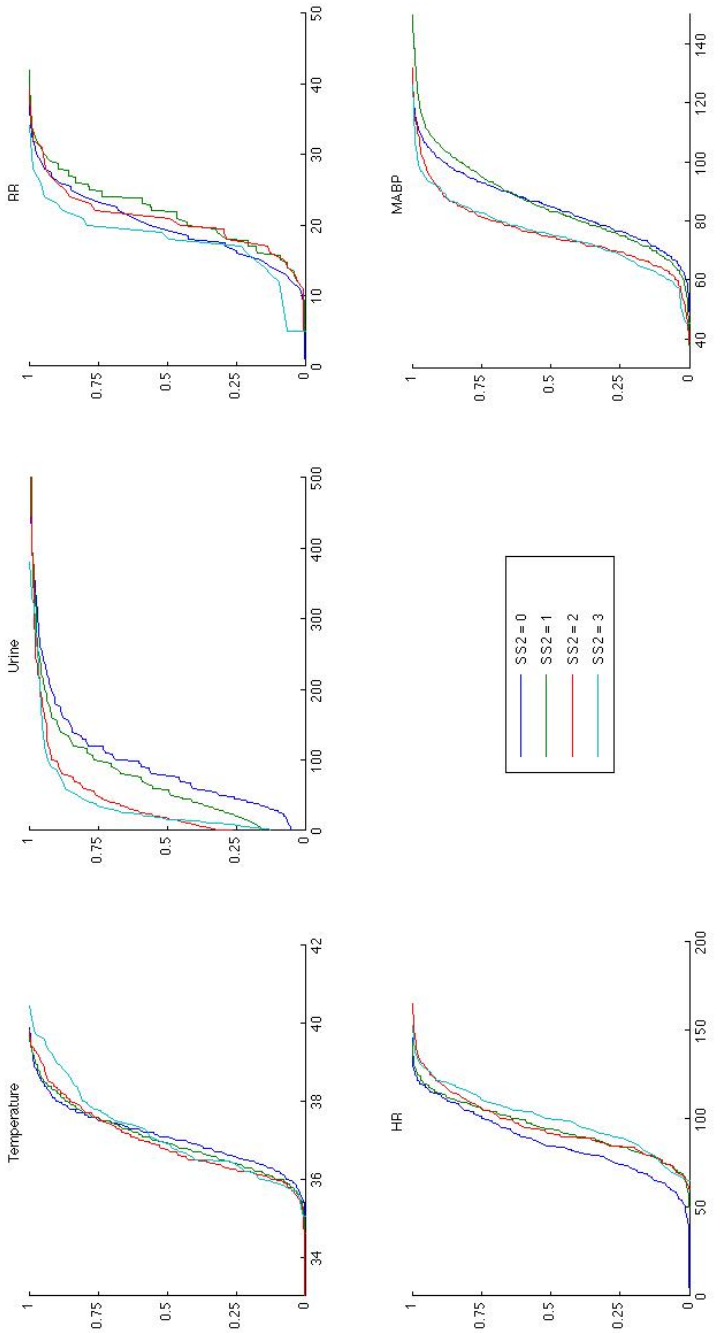

Figure 7.9: Cumulative distribution functions of temperature, urine output, RR, HR and MABP on different SS2 value of the sepsis cohort.

Table 7.8: Clinical variables distribution of sepsis cohort on different SS2 values.

Input variables	SS2 = 0	SS2 = 1	SS2 = 2	SS2 = 3
Temperature	37.1 [36.6 - 37.5]	36.9 [36.4 - 37.6]	36.8 [36.3 - 37.6]	37.0 [36.4 - 37.8]
HR	85 [75 - 102]	95 [85 - 107]	92 [85 - 106]	100 [90 - 112]
RR	20 [17 - 24]	22 [18 - 25]	22 [18 - 22]	19 [18 - 20]
Urine	80 [45 - 120]	60 [20 - 100]	18 [0 - 50]	17 [8 - 35]
MABP	85 [77 - 93]	83 [75 - 95]	75 [70 - 82]	76 [69 - 83]

ular, while PPV values were 66.7 - 70.6%, NPV values of 16.0 - 60.3% mean that sensitivity and specificity do not exceed 99.9% and 18.6%. These values are not much better than clinical experience.

It should be noted that the clinical variables recorded may change because of several factors. For example, changes in patient condition or patient reaction towards treatment such as drugs and inotropes, unrelated to sepsis, cleared the issue significantly. Moreover, clinical variables may not change at the same rate for every patient, as their condition evolves. Therefore, and as seen from the results, the recorded clinical variables are, at least sometimes, potentially misaligned to the hourly sepsis score.

7.3.3 Clinical Feedback Factor

Despite all the results shown above, clinical feedback is another final parameter, which may prove interesting to be analyzed. This parameter is of interest because most of the decisions made in treating sepsis in the ICU are based on clinical experience. Importantly, they are also not made in a vacuum, but are, in fact, based on recent past observations and conclusions made by the attending clinical staff, and not just a one-stop analysis. In this test, clinical feedback of the true value was obtained for every 6 hours. Table 7.9 shows the testing results on SS2 using clinical feedback and several other input parameters.

Referring to Table 7.9, using clinical feedback as an input parameter improves the sensitivity and specificity. Sensitivity is slightly improved while specificity is almost doubled compared to the best specificity obtained using

clinical variables in Table 7.5. The mean average sensitivity and specificity are 0.918 and 0.840, respectively. S_I and SOFA are also tested with clinical feedback and similarly, sensitivity and specificity improve dramatically compared to previous tests discussed in Section 7.3.1. However, the improvements are largely due to the influence of clinical feedback, which merely reflects current practice, but does not significantly improve it.

From all the tests conducted, clinical feedback has the most promising results with higher sensitivity and specificity observed compared to other several tests. Moreover, adding S_I, SOFA, and even both of these parameters made no improvement.

7.3.4 Per-Patient Analysis

Additional analysis was done using the same network architecture on a per-patient data input parameters such as S_I and other clinical variables. However, overall results did not show additional improvement compared to whole cohort data analysis. Generally, very few patients in the cohort have a promising results for different test sets and it is either the sensitivity or the specificity and not for both simultaneously. Most of the sepsis patients (90%) have lower sensitivity and specificity compared to sensitivity and specificity when using clinical feedback input. In addition, 36% and 18% of test sets have higher sensitivity and higher specificity, respectively compared to sensitivity of 86.3% and specificity of 74.4%.

The lower results on sensitivity and specificity observed on per-patient analysis indicate no significant difference when selecting per-patient data ver-

Table 7.9: Testing results on SS2 using several combinations of input parameter. MSE, PPV and NPV represent mean squared error, positive predictive value and negative predictive value respectively.

Input variables	Data set	MSE	PPV	NPV	Sensitivity	Specificity
CF	Set A	0.204	88.2	86.8	86.3	88.6
	Set B	0.143	94.8	86.4	96.3	81.5
	Set C	0.187	92.9	88.7	89.7	92.2
	Set D	0.307	92.2	76.8	93.1	74.4
	Set E	0.164	95.4	78.4	93.8	83.1
CF, S_I	Set A	0.225	85.7	86.3	86.2	85.9
	Set B	0.139	95.0	87.6	96.7	82.4
	Set C	0.250	82.2	87.3	90.1	77.7
	Set D	0.328	91.6	76.9	93.4	72.1
	Set E	0.154	95.1	78.9	94.1	81.8
CF, SOFA	Set A	0.211	85.3	87.5	87.6	85.2
	Set B	0.198	91.0	79.8	95.1	67.2
	Set C	0.172	91.7	89.0	90.1	91.0
	Set D	0.285	91.8	80.6	94.7	72.4
	Set E	3.822	77.1	20.1	39.8	56.1
CF, SOFA, S_I	Set A	0.233	84.1	86.5	86.7	83.9
	Set B	0.157	92.2	86.0	96.7	71.6
	Set C	0.193	91.6	88.9	90.1	90.6
	Set D	0.311	91.1	77.6	93.8	70.1
	Set E	0.329	93.6	82.0	95.5	75.5

sus using the cohort data. Although the sensitivity and the specificity observed were slightly better, most of the patients tend to have better predictions only for one of the categories, either specificity or sensitivity and not for both.

7.4 Factors in Defining a Successful Sepsis Bio-Marker and Diagnostic

Insulin sensitivity, S_I has shown a significant relation to metabolic condition and therefore can be used to rule out the presence of sepsis (high NPV) in the critically ill. Blakemore et al [Blakemore et al., 2008] showed that S_I provides a negative predictive diagnostic for sepsis with a sensitivity and specificity of 78% and 82%, respectively. In addition, Lin et al [Lin et al., 2011a] on a different cohort shows that S_I is potentially a good sepsis bio-marker, particularly for diagnosis of only severe sepsis, achieving a 50% sensitivity and 76% specificity. However, in this study, S_I does not correlate well with SS2, particularly as an hourly predictor to SS2.

The use of clinical variables as a tool for hourly sepsis diagnosis is also unsuccessful compared to current clinical capability, for this cohort, and may be due to the fact that clinical symptoms frequently exist even if the patient is free from infection or sepsis. It is thus a challenge to look at clinical variables, such as temperature, MABP and RR, as these values may change due to several factors changing in a particular patient and not just due to sepsis. In addition, the change in variables may be different between patients for the

same degree of sepsis, creating further difficulty in beating clinical practice.

To date, there is no specific bio-marker developed that can represent or predict (early) the occurrence of sepsis with any better accuracy than found here. Blood culture tests are still considered the gold standard for confirmation of infection. However, even there, only 51% of sepsis cases are positively identified [Martin et al., 2003]. Automated culturing systems are also used for bacteria detection in sepsis diagnosis by determining the solution pH or the the presence of CO_2. However, this method requires 11-31 hours for detection [Carrigan et al., 2004], and is thus neither earlier than clinical practice nor real-time.

Other bio-markers that have been used for sepsis diagnosis are procalcitonin (PCT), C-reactive protein (CRP), tumor necrosis factor-α (TNFα), interleukin 8 (IL-8) and interleukin 6 (IL-6) [Lavrentieva et al., 2011; Schuetz et al., 2011; Tsalik et al., 2011; Ravishankaran et al., 2011; Povoa et al., 2011; Salluh and Lisboa, 2011; Schrag et al., 2011; Uusitalo-Sepp L et al., 2011; Suberviola et al., 2011]. Commonly, these methods require incubation and consequently lead to a minimum of 2 - 3 hours delay for diagnosis. Moreover, most of these markers struggle with the issue of accuracy level [Carrigan et al., 2004]. Additionally, the outcome of a diagnostic marker is evaluated by analyzing the ROC curve, sensitivity and specificity at a specified cutoff value of the marker. Current protein bio-marker research focuses on PCT and several interleukins for detecting infection, since PCT achieves mean sensitivity and mean specificity of 81% and 73%, respectively [Carrigan et al., 2004]. In addition, studies conducted by BalcI and colleagues [BalcI et al., 2003] shows that PCT can discriminate between SIRS and sepsis, and therefore may become a

diagnostic parameter. However, many lesser performances for PCT are also reported [Tsalik et al., 2011; Bele et al., 2011; Kibe et al., 2011].

While more research is conducted to evaluate the use of protein biomarkers for sepsis diagnosis, real-time diagnosis is still a major and important interest. Delayed diagnosis has been shown to increase patient's risk of infection and mortality [Rivers et al., 2001]. In addition, inappropriate antimicrobial treatments due to delayed diagnosis may create future patient resistance to treatment [Carrigan et al., 2004] and consequently increase patient risk.

Importantly, criteria of a successful bio-marker of sepsis must be accountable for diagnosis at a quick rate with a reasonable sensitivity and specificity that exceeds the ∼80% (each) of an experienced clinician [Holub and Zavada, 2011]. Additionally, capturing and analyzing typical ICU data for a diagnostic is a second requirement for a real-time diagnosis, rather than relying on laboratory testing that may take up to 48 hours. Moreover, additional criteria for a bio-marker is to have a reasonable cost. Since the estimated annual healthcare cost of sepsis is nearly US$17 billion in the US alone [Angus et al., 2001], the test should be low cost but does not have to be negligible. Finally, considering patient condition and the risk of mortality, an invasive diagnostic procedure would also be suitable.

7.5 Summary

Limited diagnostic methods have prevented significant improvement in early diagnosis and treatment. Thus, it limits the ability to reduce mortality and

cost. Currently, an experienced clinician is the best diagnostic and best able to consider, accurately, all the relevant data. Only a blood culture test is considered a gold standard test in determining sepsis, but over ∼50% of diagnosed sepsis is culture-negative [Lin et al., 2011a]. Equally, blood culture tests require 1- 3 days to obtain the result, which is also far too slow.

In this chapter, several available model-based and clinical parameters are tested using neural networks to investigate the influence level of each parameter towards predicting SS2, a scoring system used to classify sepsis state. From all the tests conducted, none could exceed current clinical practice. Thus, clinical feedback is the only parameter that resulted in higher sensitivity and specificity in this format, hence, confirming this initial conclusion. In this analysis, hourly input data are tested to evaluate their ability for real-time diagnosis of sepsis. The main issue is that the data is not necessarily perfectly correlated to SS2 or highly discrimination of sepsis.

In conclusion, this study analyzed the potentiality of several available parameters captured in typical ICU settings as possible bio-markers for sepsis diagnosis. A flexible neural network framework showed that none, either alone or in combination, provided an improvement over current conditions and capability. Hence, it may be initially concluded that either a more powerful framework is needed to detect and discriminate sepsis status, or that a more optimal bio-marker is still needed.

Chapter 8

Sepsis, Microcirculation, and Pulse Oximetry

The microcirculation is a critical physiological pathway through which oxygen diffuses to tissues and waste products are returned to be processed by the circulation. Microcirculation dysfunction is one of the most common conditions suffered by critically ill patients with organ dysfunction. Clinically, microcirculatory dysfunction affects organs, such that tissues receive insufficient amounts of oxygen or other substrates.

Sepsis is characterized as a disease of the microcirculation and thus information about microcirculation dysfunction could enable better and more accurate tracking of patient state and sepsis status. This chapter presents a non-invasive potential method to directly assess microcirculatory function that might be used to monitor critically ill patients. In this study, a pulse oximeter is used to assess microcirculation function via extraction. Extraction is the rate or level of exchange of oxygen and other products by the microcirculation. In sepsis, extraction is very low.

Pulse oximeters measure the absorption of red and infrared light by blood and tissues as the light passes through an individual's finger. The raw

red and infrared signals are processed to represent the relative absorption of reduced hemoglobin and oxyhemoglobin. From this concept, oxygen saturation and extraction can potentially be derived and thus can be used to assess the status of the microcirculation. This use is a significant extension from the use of pulse oximetry to measure oxygen saturation in tissues. In particular, in this study, the changes in red and infrared signals are specifically being investigated separately unlike the standard pulse oximeter that combines all these signals into a single, calibrated oxygen saturation metric.

8.1 Sepsis is a Disease of the Microcirculation

The microcirculation consists of the smallest blood vessels, those with less than 100 micrometers diameter, and consists of arterioles, capillaries, and venules. A schematic illustration is shown in Figure 8.1. It connects the arterial and venous systems taking arterial blood to the arterioles, to capillaries, to venules, and back to the heart via the venous circulation.

Microcirculation transports oxygen and nutrients to tissue cells and also helps ensure adequate immunological function. It also acts as a medium for delivering therapeutic drugs to target cells [Ince, 2005]. The main cell types constituting the microcirculation are the endothelial cells, smooth muscle cells, red blood cells, leukocytes, and plasma components in blood. These different types of cells each have individual roles in controlling the mechanisms of microcirculatory perfusion. Specifically:

Endothelial cells are responsible for part of immune response, coagulation,

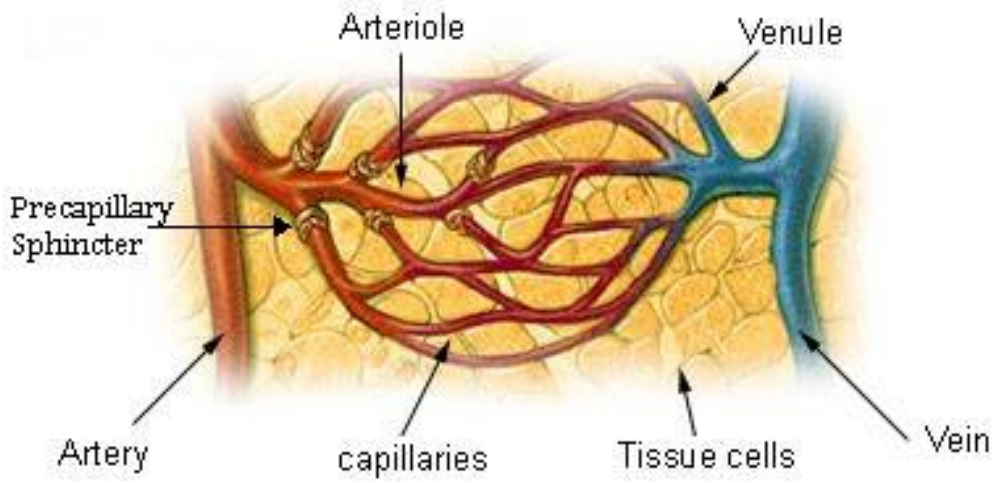

Figure 8.1: Human microcirculation schematic indicating arterioles, capillaries, and venules. Adapted from biology.about.com.

growth regulation, production of extracellular matrix components. It functions as a modulator of blood flow and blood vessel tone [Sumpio et al., 2002].

Smooth muscle cells line the arterioles and help regulate perfusion.

Red blood cells transport hemoglobin, which carries oxygen from the lungs to the tissues. It also catalyzes the reaction between carbon dioxide and water, and is responsible for most of the buffering power of blood [Guyton and Hall, 1996].

Leukocytes provide a rapid defense against infection by localizing at infection sites. Leukocytes are formed partially in the bone marrow and partially in the lymph tissue. The life span is normally 4-8 hours in the blood when released from the bone and another 4-5 days in the tissues. However, life spans are shortened to a few hours in the tissue in infection

[Guyton and Hall, 1996], making leukocytes function a key element of the microcirculation and its function in sepsis.

Plasma helps carry antibodies that are secreted into the lymph and carried to the circulating blood.

The microcirculation plays an important role by providing oxygen to the tissue cells and therefore ensures organ function. Sakr et al [Sakr et al., 2004] found that microcirculatory distress is the only independent factor for predicting patient outcome if it is not treated within 48 hours. In a worst case scenario, microcirculatory dysfunction drives the pathogenic effects of sepsis and results in organ failure [Ince, 2005] and increased risk of death [Spronk et al., 2004].

Sepsis patients normally suffer microcirculatory dysfunction [Spronk et al., 2004]. It is characterized by heterogenous abnormalities particularly in blood flow and under-perfused capillaries. There are several aspects of sepsis that affect microcirculatory function, which thus affect coagulation and immune function, which, in turn, increase the risk of a more severe infection. The overall result can be a spiral of worsening infection and microcirculation dysfunction. Hence, sepsis, organ failure, infection, and microcirculation failure are all related.

In particular, microcirculatory units become hypoxic, a deficiency in the amount of oxygen reaching the tissue, which is common in sepsis patients [Lam et al., 1994; Goldman et al., 2004; Ince and Sinaasappel, 1999]. As a result, the tissues and organs begin to fail. The end consequence is increased risk of the organ failure that defines sepsis.

In addition, signal transduction pathways and electrophysiological communication are disturbed in sepsis rendering endothelial cells unable to function properly. This outcome decreases the efficacy of immune response to the infection at the root of sepsis [Vallet, 2002]. Hence, the infection and resulting microcirculation dysfunction are unchecked and grow worse.

Other severe conditions associated with sepsis patients are reduced adrenergic sensitivity and reduced tone of smooth muscle cells [Price et al., 1999], high rate of aggregation and less deformable red blood cells [Baskurt et al., 1997; Piagnerelli et al., 2003; Reggiori et al., 2009], and the formation of reactive oxygen species by leukocytes activated by septic inflammation or oxidative stress. Oxidative stress and reactive oxygen, in particular, affect microcirculation function by destroying microcirculatory formation, cellular interactions, and coagulatory function [Martins et al., 2003; Victor et al., 2004, 2009]. Furthermore, massive increases in reactive oxygen species consequently damage mitochondrial respiratory dysfunction as indicated by reduced levels of ATP and oxygen consumption [Victor et al., 2009]. The end result is a further increased risk of organ failure and worsened infection.

Therefore microcirculation function plays a very important and central role in the evolution of sepsis. Hence, it is well understood that sepsis directly and broadly affects microcirculatory function by reducing microcirculatory oxygen transport and tissue oxygen utilization. Therefore, analyzing oxygen transport and utilization can potentially be done by using independent signals from pulse oximetry to assess oxygen saturation and extraction.

8.1.1 The Concept

The overall goal is to use this marker to assess microcirculation function, and its changes over time. More specifically, the absorption of red and infrared light provides information on the amount of oxyhemoglobin and reduced hemoglobin concentrations, respectively. Variation over time can be used to represent the time-varying absorption of oxygen into the tissue and its rate of extraction. Thus, processed correctly, the signals commonly used in pulse oximetry may contain significant additional information relevant to sepsis via the assessment of oxygen transport and the microcirculation.

8.2 Pulse Oximeter: Principles and Operation

In general, a pulse oximeter is a device used to monitor heart rate and oxygen saturation. Pulse oximeter operation is based on measuring the absorption of red and infrared light passed through a patient's finger or ear lobe. Background, such as fluid, tissue and bone, are factored out of the measurement by monitoring the steady state of absorption from bone tissue, venous blood and arterial blood. It measures periodic variations produced by arterial pulsation. The periodic variations are an alternating current (AC) component, which is very small relative to the steady state direct current (DC) component. In normal use, the change in the AC signal relative to the DC signal measured represents the absorption of oxygen into tissue. Specifically:

DC component represents the absorption of light by the tissue bed, includ-

ing venous blood, capillary blood and nonpulsatile arterial blood.

AC component represents the absorption of light due to the pulsatile expansion of the arteriolar bed with arterial blood.

Figure 8.2 illustrates the different components of pulsatile and nonpulsatile absorption when light passes through the finger. The principle of pulse oximetry is based on the assumption that the only pulsatile absorption between the light source and the photodetector is that of arterial blood. The light source incorporated in the oximeter probe consists of two light-emitting diodes (LEDs) that emit light at known wavelengths, specifically 660 nm (red, R) and 940 nm (infrared, IR). These two wavelengths are used because oxyhemoglobin and reduced hemoglobin have different absorption spectra at these particular wavelengths, as shown in Figure 8.3. In the red region, oxyhemoglobin absorbs less light than does reduced hemoglobin, while the reverse is true in the infrared region. However, the difference in absorption in the infrared region is much smaller compared to the red region. To measure oxygen saturation, the pulse oximeter uses the ratio of red and infrared pulsatile components as a percentage of the DC component. Specifically, it uses $(AC_R/DC_R)/(AC_{IR}/DC_{IR})$ with a special calibration table to assess the level of oxygen saturation in pulsatile blood.

8.3 Signal Acquisition and Processing

Generally, the red and infrared LED's on the probe are alternately pulsed in a controlled fashion. The output from the photodiode of the finger probe

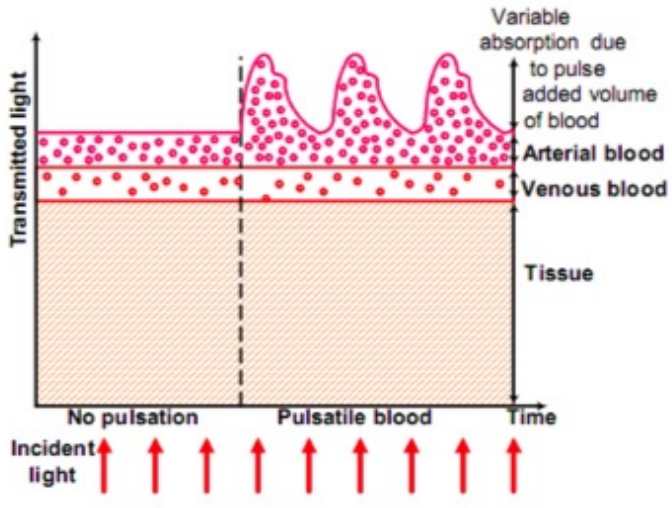

Figure 8.2: Light passing through the substances of a finger. Adapted from cypress.com.

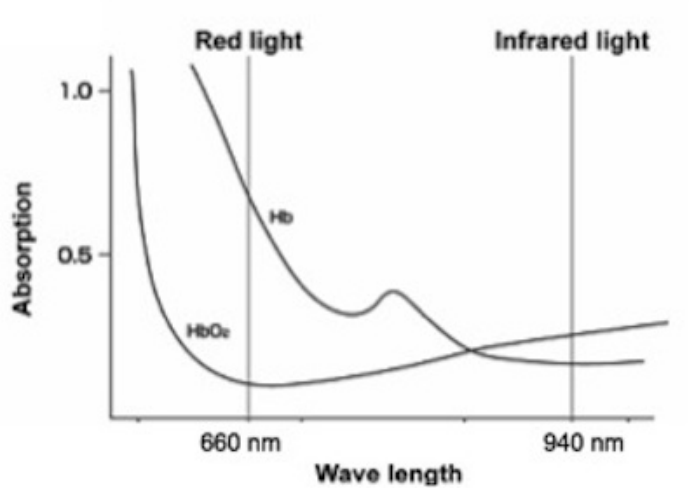

Figure 8.3: Transmitted light absorbance spectra of oxyhemoglobin and reduced hemoglobin.

is passed through a current-to-voltage converter. The intensity of the IR and R LED is controlled by the LED intensity control block to keep the photo-receiver sensors within specification. The raw voltage converted signal is amplified using a second stage amplifier. The signals from these two stages are fed to two different channels of ADC. Figure 8.4 shows the example of AC and DC components for red and infrared output signals, from the experimental pulse oximeter built for this study because commercial devices do not permit this specific data to be accessed.

The sampling rate used in this experiment is approximately 70 Hz. The output data is captured from a serial port and stored in the PC. The DC component at the top panel of Figure 8.4 is obtained by determining a 32 point moving average of the raw signal, while the AC on the bottom panel is the remainder of the signal with the DC portion removed. The red signal is represented by the red color, while the infrared signal is in blue color.

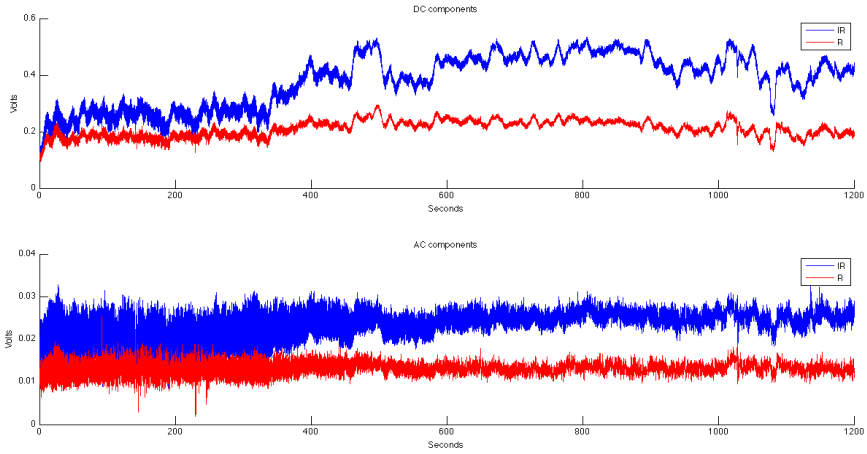

Figure 8.4: Sample of a signal indicate separation between R and IR output with DC components on the top panel and AC components on the bottom panel. The y-axis is in volts and the x-axis is in seconds.

8.4 Data Processing

8.4.1 Intensity Adjustment

The raw signal measured from the finger probe is directly related to the amount of the light received at the photodetector. The raw signal received for the R wavelength is used to control the intensity control of R LED. Similarly, the raw signal received for IR wavelength is used to control the intensity control of IR LED. However, the absorption of R and IR light can vary depending on several factors, such as dyshemoglobins, ambient light, nail polish, skin pigmentation, dyes, low-perfusion state and motion artifacts [Jubran, 2004, 1999].

Figure 8.5 shows an example of the raw DC and AC signals in volts and light intensity in counts of R and IR. In this figure, higher values of the DC and AC components indicate more light received at the photodetector and vice versa. To eliminate the intensity change factor, the raw signal was adjusted according to the average intensity during a baseline period. Baseline is thus defined as the initial stabilization period during the tests.

Figure 8.6 shows the resulting DC and AC components and light intensity after the process of standardizing the intensity for each LED's intensity. Adjusted DC and AC components in y-axes are in volts and adjusted intensity is in counts. This adjustment is important as relative levels of R and IR DC and AC signals are related to the extraction rate to be assessed. Thus, comparable magnitudes must be used.

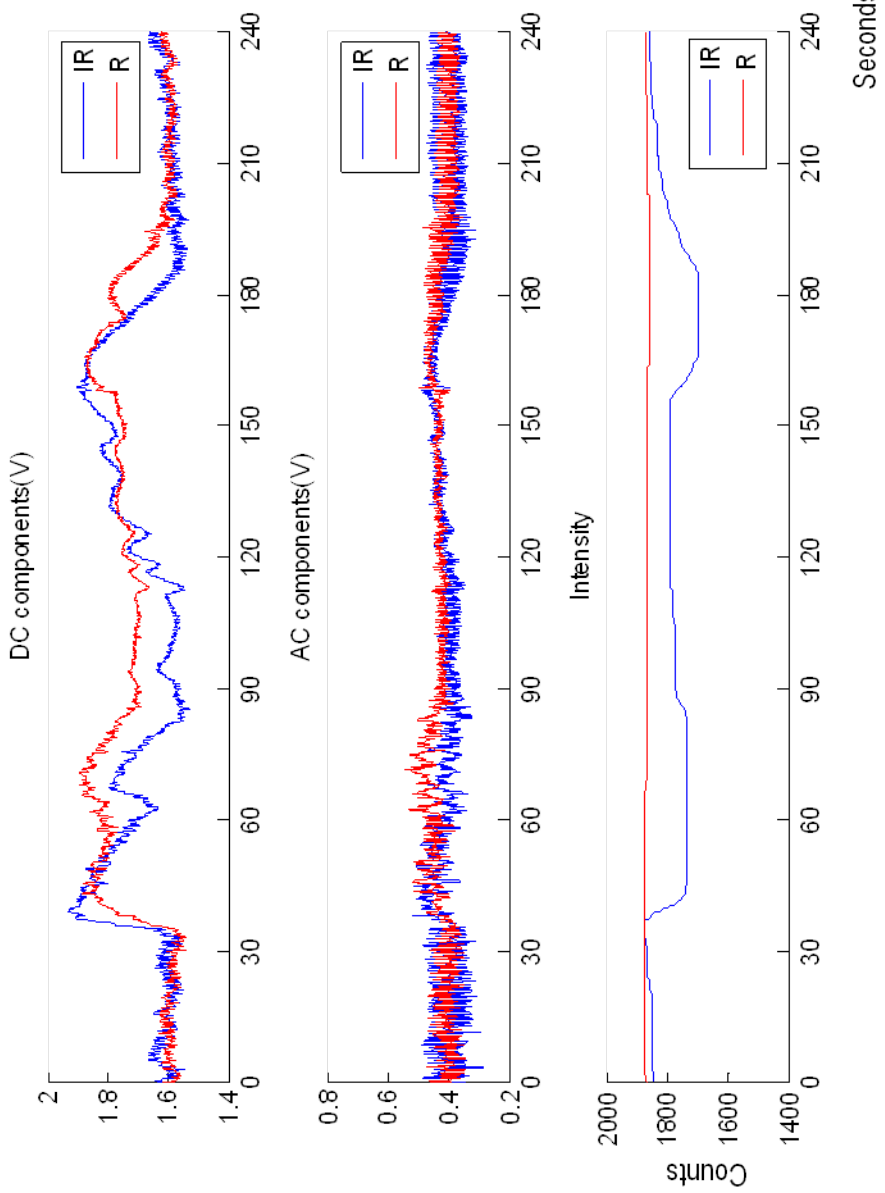

Figure 8.5: Raw signal of DC components (top panel) and AC components (middle panel), and light intensity of R(red) and IR(blue) on the bottom panel.

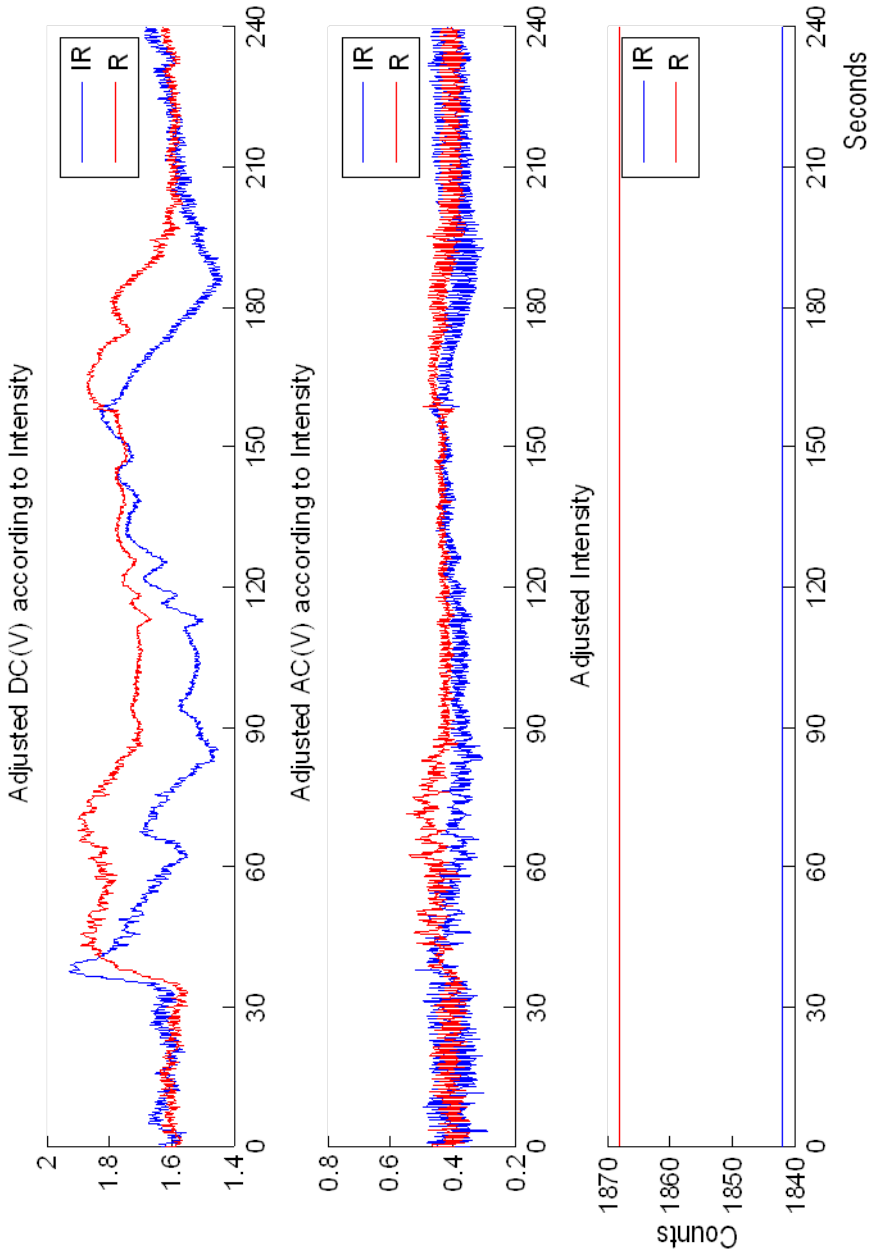

Figure 8.6: Adjusted DC components (top panel), adjusted AC components(middle panel) and light intensity of R(red) and IR(blue) on the bottom panel using a 30 second average of R and IR intensity.

8.4.2 Baseline Coordination

For each test, a baseline measurement was recorded for approximately 30 - 60 seconds. The baseline measurement was used to observe the initial condition of the subjects before proceeding with any test and to indicate stability of the test subjects. During this period, subjects were asked not to move their hand or arm, and were in a resting position.

Figure 8.7 shows the comparison of the DC component of R and IR before and after normalization using an average of 30 seconds during the baseline. The average value computed is subtracted from the other recorded values to find the respective measurements. The bottom panel represents the resulting plot of R and IR AC components with respect to the x-axis as the average baseline measured. Therefore, the change in wavelength can be seen as a comparison to the baseline measurements.

8.4.3 Conversion of Intensity to Absorption

The raw signal measured is the processed output from the detector and represents the amount of light received by the photodetector. Therefore, a higher amount of light detected at the receiver indicates less light being absorbed by tissue and vice versa. To aid clinical interpretation, the plots are therefore inverted, as shown in Figure 8.8, as an example. The inverted plot (bottom panel) represents the inverse amount of light absorbed by a finger. Thus, a higher value in this modified plot represents more light being absorbed for the red or infrared signals and thus less light detected. More light absorbed means greater number of cells or oxygen at that wavelength.

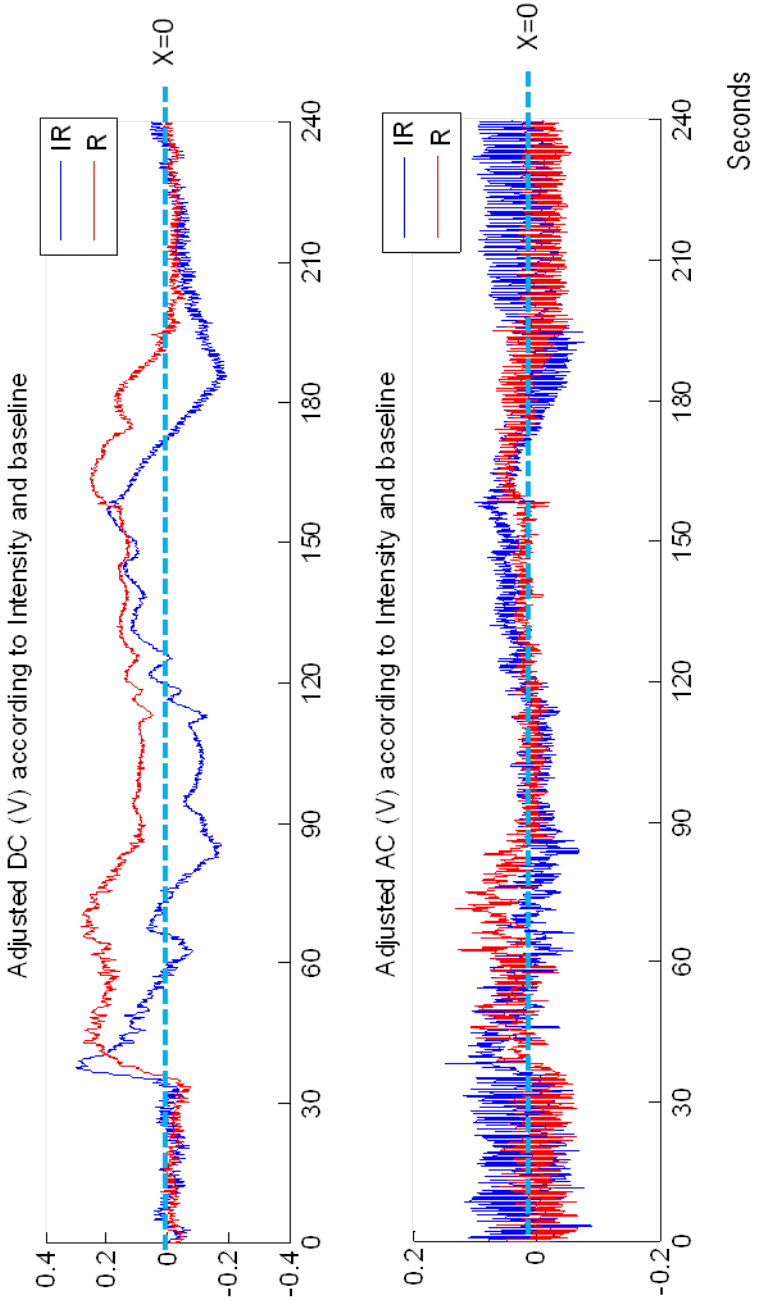

Figure 8.7: Normalized DC components of R(red) and IR(blue) (top panel) and normalized AC components of R(red) and IR(blue) using a 30 second average of R and IR during baseline measurements (bottom panel).

More specifically, an increase in the R plot represents an increase in amount of reduced hemoglobin (Hb), whereas increases in IR (blue) indicate higher amounts of total oxyhemoglobin and reduced hemoglobin (HbO_2 + Hb). The bigger the gap in the DC plot, the greater amount of HbO_2 in blood. Thus, represents less oxygen being absorbed. Because of baseline normalization, the changes are relative to the initial value. Hence, changes in R and IR throughout a test represent higher or lower extraction with respect to the initial condition during the test.

8.5 Measure of Microcirculation Efficacy

Oxygen is carried from the lungs to the rest of body by red blood cells. Blood flows in the body and passes oxygen to the tissues. The amount of oxygen uptake by a tissue is dependent on the oxygen transport factor. When oxygen transport is decreased in healthy individuals, oxygen consumption is maintained by increasing tissue oxygen extraction. Therefore, oxygen extraction is a function of blood flow and oxygen consumption, which indicates the microcirculation efficacy of an individual.

The pulse oximeter used in this study measures extraction by comparing the DC components of R and IR signals. The IR signal is related to the overall blood volume, (HbO_2 + Hb) and the R signal is related to the amount of reduced hemoglobin, (Hb). Differences between these two signals thus represents the amount of oxygenated hemoglobin, HbO_2. Therefore, a higher value of IR signal relative to R signal indicates the amount of extraction. The larger the gap between these two signals, the higher the extraction and vice

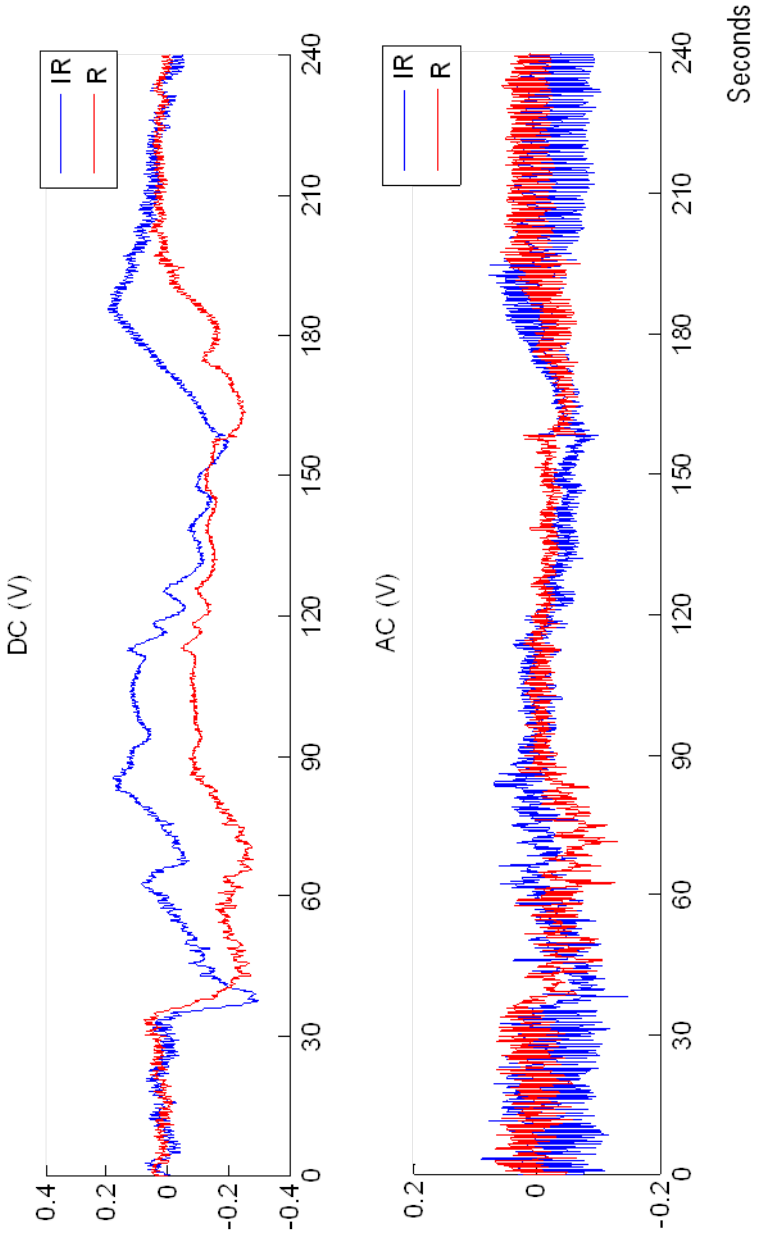

Figure 8.8: DC components of R(red) and IR(blue) (top panel) and DC components of R(red) and IR(blue) after inverting (bottom panel).

versa, for a specific level of cardiac output.

8.6 Summary

Sepsis is a disease of microcirculation, and microcirculation dysfunction is a critical element in sepsis and organ failure. In this chapter, the signals from a pulse oximeter are presented as a means to extract additional information on the absorption of oxygen and thus the efficacy of microcirculation function. The processed signals capture reduced hemoglobin and blood volume (oxyhemoglobin plus reduced hemoglobin) at a particular time relative to its initial condition. Therefore, changes in terms of amount or volume of oxyhemoglobin and deoxyhemoglobin relative to its baseline can also be monitored as a marker of extraction and microcirculation function. Therefore, blood flow and oxygen extraction can be used to measure and assess microcirculation function.

Chapter 9

Pulse Oximeter Validation

In this chapter, several tests on healthy individuals are used to demonstrate and validate pulse oximeter concept discussed in Chapter 8. In particular, vascular occlusion tests (VOT) and physical exercise are used to artificially create changes in extraction to test the concept. The goal is to determine if changes in oxygen extraction, a key feature of sepsis, can be assessed with good resolution under known and well understood perturbations.

In this context, the VOT has been used in research using near-infrared spectroscopy to assess microvascular changes, particularly dynamic tissue oxygen saturation [Bernet et al., 2011; Futier et al., 2011; Mayeur et al., 2011; Bezemer et al., 2009; Gomez et al., 2008]. Results indicate that the VOT permits the determination of tissue metabolic rate, particularly during ischemia [Mayeur et al., 2011; Colier et al., 1995]. Similarly indicative results were found during exercise [Burton et al., 2004; Treacher and Leach, 1998; Martin, 1999]. Additionally, the rate of desaturation determined immediately during post-exercise ischemia have been used for the estimation of individual metabolic rate and tissue oxygen consumption [Boushel et al., 2001].

The use of pulse oximeter data to assess changes in oxygen extraction for an individual can therefore indicate changes in metabolic condition. Thus,

the overall goal appears feasible with simple equipment that allows significant and potentially clinically important additional information to be captured.

9.1 Test Design

In this analysis, several tests have been conducted to validate the pulse oximeter concept discussed in Chapter 8. The tests were done on healthy individuals, and include a vascular occlusion test (VOT) and moderate physical exercise to induce changes in extraction. This study and the use of this data was approved by the University of Canterbury Human Ethics Committee, Christchurch, New Zealand.

9.1.1 Vascular Occlusion Test (VOT)

In this test, subjects were comfortably seated with one arm rested on a table. An initial manual blood pressure measurement was taken on the arm to define baseline perfusion pressure using a sphygmomanometer. A pulse oximeter probe was attached to each subject's finger and subjects were asked not to move their hand or arm during measurements. The sphygmomanometer was then placed on the forearm. A baseline measurement was recorded for 30-60 seconds. The sphygmomanometer was then rapidly inflated until the pressure was 40 mmHg more than baseline systolic pressure to induce the occlusion. Inflation took approximately 10-30 seconds. The sphygmomanometer was then rapidly deflated after 3 minutes of vascular occlusion. The pulse oximeter data was continuously recorded for at least another 3 minutes after the

sphygmomanometer was released.

During the test, DC and AC signals for R and IR absorption were measured. The R signal measures reduced hemoglobin and the IR signal measures the sum of reduced hemoglobin and oxyhemoglobin. During the inflation of the sphygmomanometer, both the R and IR DC signals were expected to decrease over time as less blood was flowing into the occluded area, before reaching constant values indicating a constant blood volume in the occluded area and no blood flow into it. Additionally, no pulsatile waveform should be seen during this time since no pulsation of arterial blood should exist during the occlusion. After the sphygmomanometer was released, the R and IR DC signals should rise immediately above baseline as more blood flows initially into the hand area, followed by blood redistribution and progressive desaturation. This process occurs until the blood flowed has been normalized.

9.1.2 Physical Exercise

For physical exercise tests, subjects were required to run for at least 3 minutes on a short, flat circuit. Pre-exercise measurement was recorded for at least 30 seconds. Post-exercise measurements were also recorded for at least 120 seconds. This process was repeated (exercise and record data) for up to five laps.

In this test, AC R and IR signals are expected to increase during the post-exercise compared to the baseline, due to increases in heart rate. In addition, changes in oxygen extraction are expected during the post-exercise period, as indicated by the difference between the IR signal relative to the R

signal. In particular, the IR DC signal was expected to be higher than the R signal. Depending on workout amount (laps) and intensity, changes in heart rate and cardiac output were assessed by changes in period beat to beat, Δt, the amplitude of the AC signal, and the area under the curve of the DC signal.

9.2 Test Subject

There were 15 healthy volunteers who participated in the vascular occlusion test, and 10 healthy individuals in the physical exercise test. Tables 9.1 and 9.2 show the demographic characteristics of the subjects for the VOT and physical exercise test, respectively.

Table 9.1: Demographic characteristics of the test subjects for vascular occlusion test (VOT).

Demographic characteristic	Median [IQR]
Age (years)	26 [23 - 30]
Gender (%)	
Female	40
Male	60
Dominant hand (%)	
Right	93
Left	7
Weight (kg)	61 [46 - 72]
Height (cm)	166 [155 - 177]
Systolic blood pressure (mmHg)	110 [100 - 110]
Diastolic blood pressure (mmHg)	60 [60 - 64]
Heart rate (beats/minute)	65 [59 - 71]

Table 9.2: Demographic characteristics of the test subjects for physical exercise test.

Demographic characteristic	Median [IQR]
Age (years)	27 [23 - 29]
Gender (%)	
Female	30
Male	70
Weight (kg)	72 [50 - 76]
Height (cm)	178 [157 - 182]
Systolic blood pressure (mmHg)	108 [100 - 110]
Diastolic blood pressure (mmHg)	60 [55 - 70]
Heart rate (beats/minute)	51 [48 - 57]

9.3 Results

9.3.1 Vascular Occlusion Test (VOT)

Figure 9.1 shows the DC and AC components of the R and IR pulse oximeter signals during a VOT on Subject 1. The VOT can be divided into three stages, which are baseline, vascular occlusion, and recovery. Additionally, Figure 9.2 shows the scaled AC components of IR signals on Subject 1 for a 15 second interval in each stage during the test.

In Figure 9.1, the huge drop of DC R and IR signals is observed during vascular occlusion relative to baseline. As the vascular occlusion progressed, the DC IR signal increases slightly, while the DC R signal was almost constant.

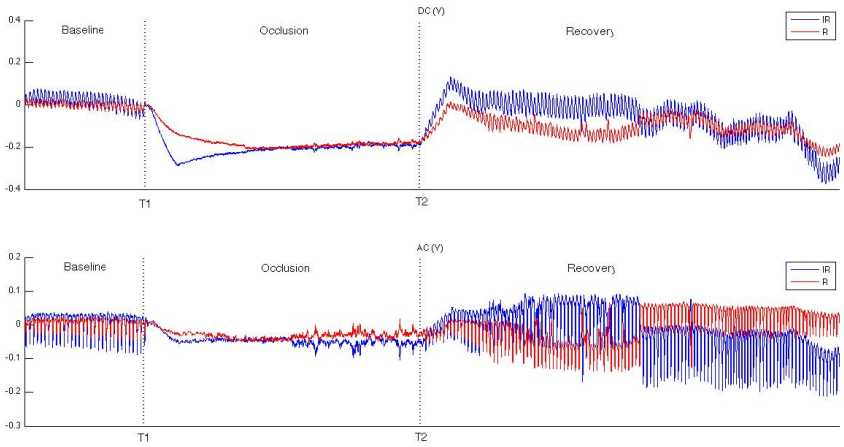

Figure 9.1: DC components of R(red) and IR(blue) on the top panel and AC components of R(red) and IR(blue) on the bottom panel during VOT on Subject 1.

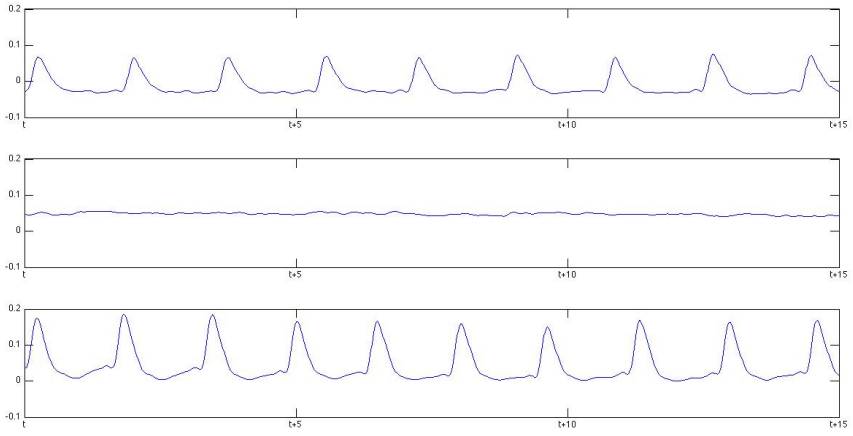

Figure 9.2: Infrared (IR) AC signals of Subject 1 for 15 seconds interval of baseline (top panel), vascular occlusion (middle panel) and recovery (bottom panel).

Both R and IR signals increased immediately after the sphygmomanometer was deflated and there were greater changes in the IR signal compared to the R signal. During the vascular occlusion presented in the middle panel of Figure 9.2, no heart beat was detected, as expected, since blood flow ceased and blood volume redistribution was limited.

Figure 9.3 shows the DC and AC components for R and IR signals during a separate vascular occlusion test on Subject 2. Similarly, Figure 9.4 shows the AC components of IR signals on Subject 2 during the baseline, vascular occlusion and recovery phases for an interval of 15 seconds in each phase. No significant changes are observed in AC component on Subject 2 during baseline and recovery, as shown in top and bottom panels of Figure 9.4, where the heart beat is blocked in the occlusion phase.

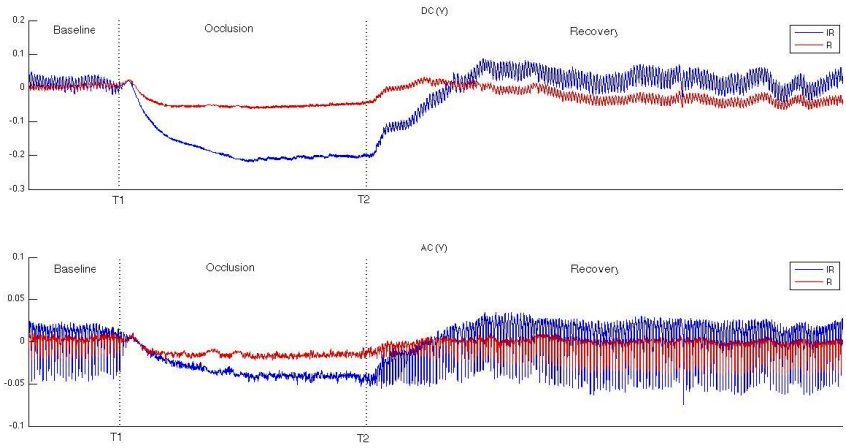

Figure 9.3: DC components of R(red) and IR(blue) on the top panel and AC components of R(red) and IR(blue) on the bottom panel during VOT on Subject 2.

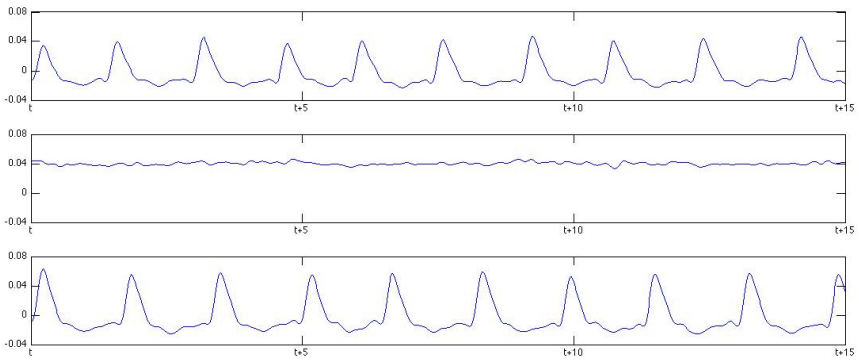

Figure 9.4: Infrared AC signals of Subject 2 for 15 seconds interval of baseline (top panel), vascular occlusion (middle panel) and recovery (bottom panel).

Similarly, Figures 9.5 and 9.6 show another example of the DC and AC components of R and IR signals during a vascular occlusion test on Subject 14. Overall, the AC and DC patterns of all subjects are similar to the patterns shown for Subjects 1, 2 and 14 . However, the changes varied across subjects in terms of lower or higher signals observed during occlusion and recovery, respectively. For example, the DC IR signal was sigificantly decreased during occlusion for Subject 2 relative to its baseline compared to the profile for Subject 1.

Table 9.3 summarizes the baseline and recovery characteristics for all 15 test subjects during the VOT. Overall, amplitude and beat-to-beat interval of AC IR signal are almost the same during baseline and recovery, and no significant changes are observed in heart rate for all test subjects. Median amplitude of AC signals during baseline and recovery are 0.08 and 0.12 volts, respectively. However, rise time, measured as time taken from the release of the sphygmomanometer to the highest peak of recovery, were highly variable across test subjects with a median [IQR] of 14.7 [5.8, 35.8] seconds.

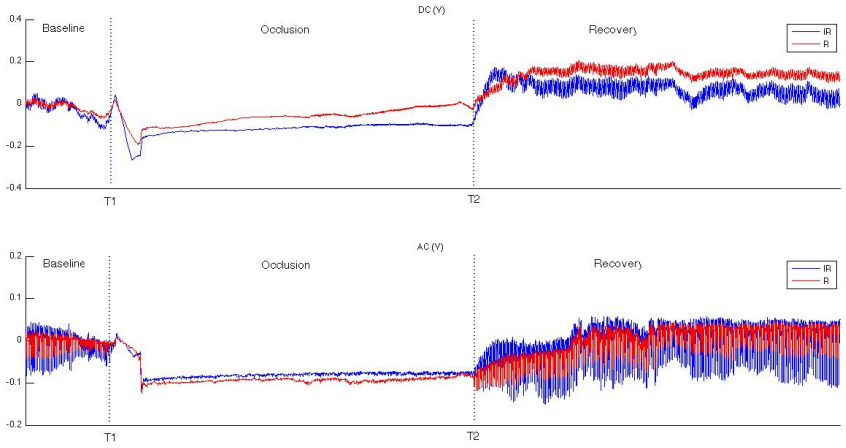

Figure 9.5: DC components of R(red) and IR(blue) on the top panel and AC components of R(red) and IR(blue) on the bottom panel during VOT on Subject 14.

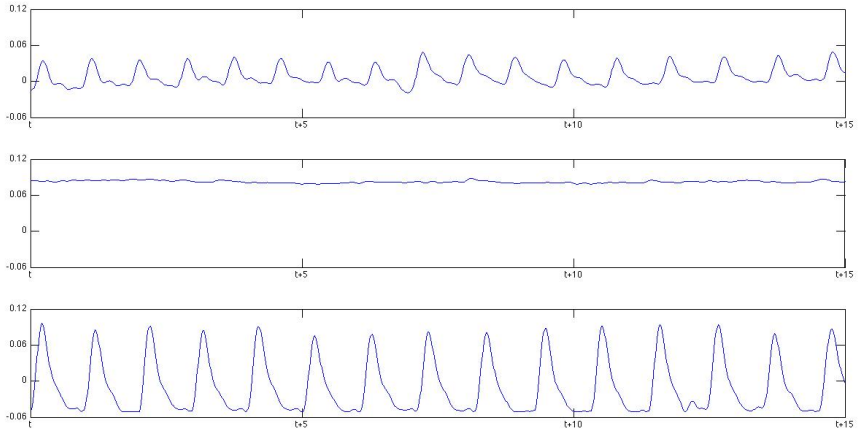

Figure 9.6: Infrared AC signals of Subject 3 for 14 seconds interval of baseline (top panel), vascular occlusion (middle panel) and recovery (bottom panel).

Table 9.3: Average value of AC IR amplitude, beat to beat interval, heart rate and rise time measured during baseline and recovery during VOT for 15 subjects studied.

Subject no	Baseline			Recovery			Rise time (Seconds)
	Amplitude (Volts)	Beat-beat interval (Seconds)	Heart rate (bpm)	Amplitude (Volts)	Beat-beat interval (Seconds)	Heart rate (bpm)	
1	0.06	1.749	34	0.16	1.484	40	16.6
2	0.05	1.543	39	0.08	1.583	38	59.7
3	0.03	0.902	66	0.04	1.068	56	38.7
4	0.17	0.629	95	0.19	0.637	94	5.1
5	0.09	0.804	75	0.10	0.777	77	6.5
6	0.12	0.840	71	0.17	0.938	64	4.7
7	0.07	0.855	70	0.08	0.948	63	14.7
8	0.04	0.959	63	0.09	0.876	68	27.1
9	0.15	0.795	75	0.17	0.822	73	5.5
10	0.09	0.658	85	0.12	0.705	91	16.9
11	0.10	1.147	52	0.19	1.192	50	55.7
12	0.02	0.813	74	0.04	0.879	68	68.8
13	0.14	1.179	51	0.17	1.153	52	8.8
14	0.08	0.996	60	0.10	1.022	59	14.6
15	0.08	0.840	71	0.17	0.947	63	4.9
Median	0.08	0.855	70	0.12	0.947	63	14.7
IQR	0.05-0.12	0.806-1.109	54-75	0.08-0.17	0.836-1.132	53-72	5.8-35.8

Figure 9.7 shows the rise time profile for the 15 test subjects in the VOT. The x-axis represents time in seconds and y-axis represents change in amplitude (Δ Volts). In this context, rise time can be defined as the time required to wash out the stagnant reduced hemoglobin with oxygenated arterial blood during reperfusion.

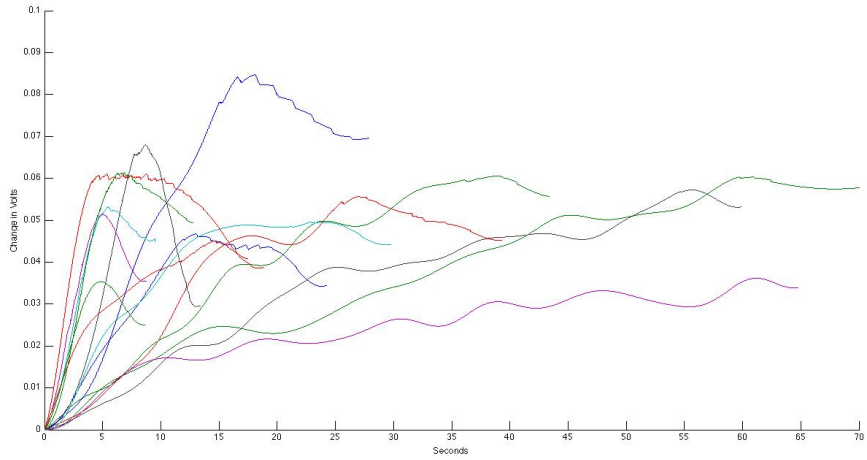

Figure 9.7: Infrared AC signals for 15 subjects studied during the release of sphygmomanometer to the highest peak indicating measure of rise time.

Table 9.4 shows the average value of oxygen extraction in volts and percentage measured during baseline and recovery for all 15 subjects during the VOT. Extraction is measured as the amount of oxygenated hemoglobin, HbO_2, that is the difference between IR and R DC signals. Most of the subjects had increased oxygen extraction at recovery with respect to baseline, as expected. However, the changes in oxygen extraction from baseline to recovery were relatively small, and some individuals had lower oxygen extraction at recovery than at baseline.

Changes in oxygen extraction shown in Table 9.4 are relatively small

Table 9.4: Average value of oxygen extraction at baseline and recovery and change in oxygen extraction for 15 subjects participated in the vascular occlusion test (VOT).

Subject no	HbO_2		HbO_2		Δ HbO_2	% Absolute	% Relative
	(Volts)	(%)	(Volts)	(%)			
1	0.03	60.0	0.05	62.5	+0.02	+2.5	4.2
2	0.02	33.3	0.09	56.3	+0.07	+23.0	69.1
3	0.02	66.7	0.04	100.0	+0.02	+33.3	49.9
4	0.09	52.9	0.08	42.1	-0.01	-10.8	20.4
5	0.04	44.4	0.02	20.0	-0.02	-24.4	55.0
6	0.07	58.3	0.10	58.8	+0.03	+0.5	0.9
7	0.02	28.6	0.02	25.0	+0.00	-3.6	12.6
8	0.02	50.0	0.05	55.6	+0.03	+5.6	11.2
9	0.06	40.0	0.06	35.3	+0.00	-4.7	11.8
10	0.03	33.3	0.02	16.7	-0.01	-16.6	49.9
11	0.09	90.0	0.09	47.4	+0.00	-42.6	47.3
12	0.01	50.0	0.02	50.0	+0.01	+0.0	0.0
13	0.06	42.9	0.08	47.1	+0.02	+4.2	9.8
14	0.04	50.0	0.05	50.0	+0.01	+0.0	0.0
15	0.03	37.5	0.10	58.8	+0.07	+21.3	56.8
Median	0.03	50.0	0.05	50.0	0.01	0.0	12.6
IQR	0.02-0.06	38.1-57.0	0.03-0.09	37.0-58.2	0.00-0.03	-9.3-5.3	5.6-49.9

with a median [IQR] of 0.01 [0.00,0.03] volts. Additionally, the percentage of absolute change is also small with a maximum of 42.6% and median [IQR] of 0.0 [-9.3,5.3] %. However, the relative change has a wider range with a median [IQR] of 12.6 [5.6, 49.9] %.

9.3.2 Physical Exercise

Table 9.5 shows the average amplitude of IR AC signal for the pre-exercise and five post-exercise phases (laps) for 10 test subjects in the physical exercise activity. The IR AC signal also represents the relative amount of blood volume ($HbO_2 + Hb$). Due to health reasons, Subject 4 was unable to complete the test until post-exercise 5. Overall, the amplitude during pre-exercise and post exercise are highly varied across individuals. Additionally, median of the average amplitude are largely increased from pre-exercise to post-exercise 1 and fluctuated from post-exercise 2 to post-exercise 5.

Table 9.6 summarizes the average value of the beat-to-beat interval in seconds and heart rate in beats per minute during pre-exercise and post-exercise phases for the same 10 subjects. Heart rate was significantly increased during post-exercise 1 for all subjects compared to pre-exercise. However, from post-exercise 1 to post-exercise 5, the heart rate continuously increased for some individuals, while for others, the heart rate fluctuated from post-exercise 1 to post-exercise 5. Median and IQR increased from pre-exercise to post-exercise 2 and decreased during post-exercise 3, particularly for 25_{th} percentile. These differences are likely due to relative fitness and condition. In contrast, the first test is a relative shock to the system for all subjects.

Table 9.5: Average amplitude of IR AC in volts measured for 10 subjects during pre-exercise and post-exercises.

No	Pre-exercise (Volts)	Post-exercise 1 (Volts)	Post-exercise 2 (Volts)	Post-exercise 3 (Volts)	Post-exercise 4 (Volts)	Post-exercise 5 (Volts)
1	0.241	0.150	0.209	0.142	0.142	0.079
2	0.027	0.049	0.070	0.103	0.115	0.131
3	0.044	0.077	0.094	0.110	0.047	0.145
4	0.026	0.055	0.064	0.065	-	-
5	0.032	0.063	0.073	0.065	0.053	0.060
6	0.218	0.146	0.052	0.063	0.052	0.052
7	0.092	0.110	0.145	0.120	0.154	0.177
8	0.049	0.066	0.051	0.051	0.091	0.082
9	0.172	0.126	0.089	0.095	0.088	0.068
10	0.169	0.217	0.162	0.196	0.171	0.190
Median	0.071	0.094	0.081	0.099	0.091	0.082
25^{th} percentile	0.032	0.063	0.064	0.065	0.053	0.066
75^{th} percentile	0.172	0.146	0.145	0.120	0.091	0.153

Table 9.6: Average value of beat-to-beat interval (BB) and heart rate (HR) measured during pre-exercise and post-exercises for 10 subjects studied.

No	Pre-exercise		Post-exercise 1		Post-exercise 2		Post-exercise 3		Post-exercise 4		Post-exercise 5	
	BB (Secs)	HR (bpm)	BB (Secs)	HR (bpm)	BB (Secs)	HR (bpm)	BB (Secs)	HR (bpm)	BB (Secs)	HR (bpm)	BB (Secs)	HR (bpm)
1	1.171	51	0.757	79	0.714	84	0.657	91	0.657	91	0.671	99
2	1.057	57	0.571	105	0.557	108	0.557	108	0.543	111	0.543	111
3	1.171	51	0.614	98	0.586	102	0.614	98	0.614	98	0.557	108
4	0.936	64	0.629	95	0.629	95	0.671	89	-	-	-	-
5	1.000	60	0.800	75	0.657	91	0.629	95	0.629	95	0.600	100
6	1.257	48	0.586	102	0.614	98	0.586	102	0.571	105	0.571	105
7	1.214	49	0.757	79	0.714	84	0.729	82	0.743	81	0.786	76
8	1.143	53	0.700	86	0.671	89	0.729	82	0.700	86	0.714	84
9	1.286	47	0.800	75	0.729	82	0.750	80	0.786	76	0.757	79
10	1.314	46	1.014	59	0.971	62	0.829	72	0.829	72	0.786	76
Median	1.171	51	0.729	83	0.664	90	0.664	90	0.657	91	0.671	99
25^{th} percentile	1.067	48	0.614	75	0.614	84	0.614	82	0.603	80	0.568	78
75^{th} percentile	1.257	57	0.800	98	0.664	98	0.729	98	0.754	100	0.764	106

Table 9.7 shows the average value of changes in oxygen extraction in volts and changes in percentage of oxygen extraction for 10 subjects measured during the physical exercise test. Average oxygen extraction was higher during post-exercise 1 compared to pre-exercise for most subjects. Interestingly, only Subjects 3, 7 and 10 had lower oxygen extraction during post-exercise 1 with respect to their pre-exercise. Oxygen extractions were either decreased or increased slightly from post-exercise 2 to post-exercise 5, and largely in a similar range during post-exercise phases. Median and IQR of oxygen extraction show a similar pattern to the median and IQR of heart rate shown in Table 9.6 Again, relative fitness plays a role, as not all volunteers were equally fit.

Figure 9.8 shows the change in cardiac output and change in cardiac output over time throughout the pre-exercise, and post-exercise 1, 2, 3, 4, and 5 for Subject 5. During pre-exercise, very low cardiac output was recorded compared to all post-exercise phases. Cardiac output increased significantly during post-exercise 1 compared to pre-exercise and continue to increase during post-exercise 2. The cardiac output began to drop during post-exercise 3 and continue to drop until post-exercise 5. In the bottom panel of Figure 9.8, there is a clear separation between the change in cardiac output over time for pre-exercise and all post-exercises.

Similarly, Figures 9.9-9.10 show another example of change in cardiac output and change in cardiac output over time throughout the pre-exercise, and post-exercise phases for Subjects 9 and 10. Overall, Subjects 9 and 10 have a similar cardiac output profile as Subject 5. However, Subject 10 has a smaller gap between pre-exercise and other post-exercise phases compared to Subjects 5 and 9 illustrating the variability between individuals and fitness

Table 9.7: Average value of changes in oxygen extraction at pre-exercise and recovery for 10 subjects participated in the physical exercise test.

No	Pre-exercise		Post-exercise 1		Post-exercise 2		Post-exercise 3		Post-exercise 4		Post-exercise 5	
	HbO_2		HbO_2		HbO_2		HbO_2		HbO_2		HbO_2	
	(Volts)	(%)	(Volts)	(%)	(Volts)	(%)	(Volts)	(%)	(Volts)	(%)	(Volts)	(%)
1	0.082	33.8	0.063	42.2	0.066	31.5	0.047	32.9	0.047	32.9	0.020	25.2
2	0.005	17.9	0.018	36.7	0.026	37.4	0.043	41.7	0.044	37.9	0.047	35.8
3	0.022	50.4	0.031	41.0	0.043	45.6	0.041	37.1	0.018	38.0	0.070	48.4
4	0.002	8.7	0.011	19.1	0.020	30.9	0.022	34.1	-	-	-	-
5	0.010	30.7	0.027	42.5	0.027	36.9	0.028	43.3	0.021	39.4	0.024	40.4
6	0.093	42.8	0.064	43.7	0.015	28.2	0.019	29.8	0.021	41.0	0.013	26.0
7	0.041	44.6	0.045	41.3	0.060	41.6	0.055	45.7	0.074	47.7	0.080	45.1
8	0.001	0.9	0.016	23.9	0.020	38.3	0.003	6.7	0.031	33.7	0.035	42.3
9	0.070	40.9	0.055	43.3	0.034	38.7	0.034	36.1	0.039	43.7	0.027	39.6
10	0.072	42.8	0.084	38.8	0.066	41.0	0.082	41.7	0.073	42.7	0.078	41.3
Median	0.032	37.4	0.038	41.2	0.031	37.9	0.038	36.6	0.039	39.4	0.035	40.4
25^{th} percentile	0.005	17.9	0.018	36.7	0.020	31.5	0.022	32.9	0.021	36.9	0.023	33.4
75^{th} percentile	0.072	42.8	0.063	42.5	0.060	41.0	0.047	41.7	0.054	43.0	0.072	43.0

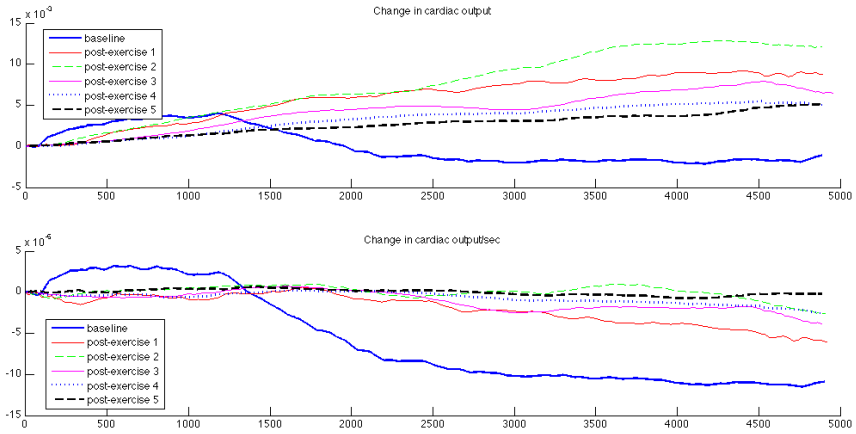

Figure 9.8: Change in cardiac output (top panel) and change in cardiac output over time (bottom panel) from pre-exercise to post-exercise phases 1 to 5 for Subject 5.

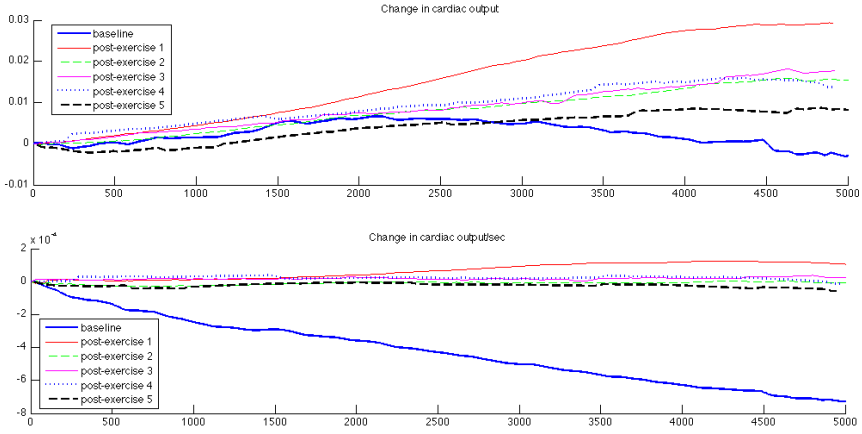

Figure 9.9: Change in cardiac output (top panel) and change in cardiac output over time (bottom panel) from pre-exercise to post-exercise phases 1 to 5 for Subject 9.

levels.

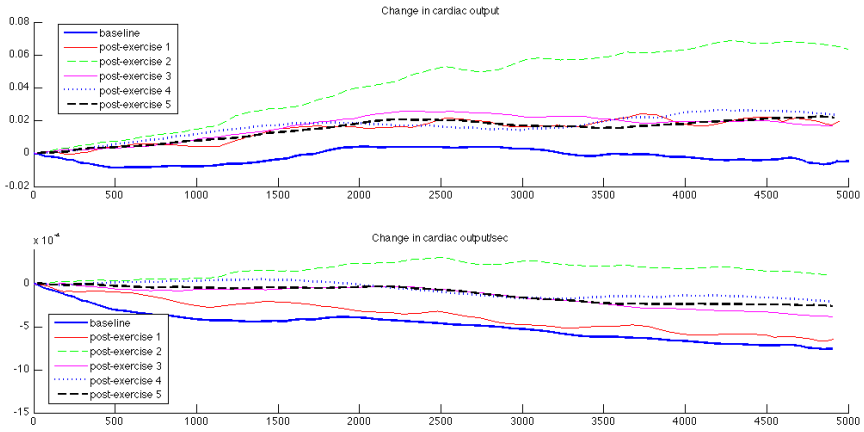

Figure 9.10: Change in cardiac output (top panel) and change in cardiac output over time (bottom panel) from pre-exercise to post-exercise phases 1 to 5 for Subject 10.

9.4 Discussion

9.4.1 Vascular Occlusion Test (VOT)

During vascular occlusion, DC components of both the R and IR signals rapidly decreased as a result of less blood flow into the occluded area and consequently reduced total blood volume. This process continues slowly until total vascular occlusion is achieved. Additionally, small volumes of blood may potentially shift within the vascular compartments as vasomotor tone decreases during this induced ischemia. However, these volume shifts are likely very small in comparison to the total blood volume and highly variable across individual responses.

During this ischemic challenge, the DC IR signals that represent total blood volume, are almost constant for most test subjects. Nevertheless, the blood compartment volumes will vary significantly amongst individuals as capillary integrity, inflow vasomotor tone, and arterial pressure varies. This variability will consequently lead to variability in the effect of the VOT among individuals, as seen for example in Figures 9.1, 9.3 and 9.5. After the sphygmomanometer is deflated, both the R and IR signals immediately increased as a result of the large amount of blood flow into the occluded area as normalization of the blood and tissue occur. However, in general, this description is largely similar for all test subjects, showing that the basic changes expected were visible via these signals.

Generally, the VOT is used to evaluate the response of the system to a pre-determined stress in terms of local metabolic demand and reperfusion response in a healthy individual [Creteur et al., 2007; Pareznik et al., 2006; Doerschug et al., 2007]. However, variation in metabolic rates may exist depending on individual experience during ischemic challenge [Gomez et al., 2008]. For example, in Figure 9.5, the DC R signals were slightly increased after a period of time during vascular occlusion, which indicates that the amount of reduced hemoglobin increased while the total blood remain constant as might be expected as available oxygen is taken up. Interestingly, this behavior was not clearly seen in Subjects 1 and 2. Potentially, this outcome happened as Subject 3 had a longer period of vascular occlusion compared to Subjects 1 and 2 because additional time was needed for proper inflation at the beginning of vascular occlusion. Therefore, there is a potential for greater oxygen uptake by tissue during the longer vascular occlusion process,

as observed in this case.

After cuff pressure is released, total hemoglobin increased rapidly almost to baseline level. In some cases, total hemoglobin increased above the baseline level. This response was followed by a recovery process. The recovery process represents the expected microvasculature response in which the determinants of re-oxygenation includes capillary integrity, local blood volume, local vasomotor tone, perfusion pressure, tissue oxygen saturation and total hemoglobin [Gomez et al., 2008].

Referring to Table 9.3, higher amplitudes of AC IR are observed during recovery compared to baseline for all subjects. This outcome is due to the higher total blood volume during the recovery compared to baseline as an effect of reperfusion after the vascular occlusion process. However, no significant changes in heart rate were observed during these two activities across all subjects. Therefore, where perfusion pressure is assumed to be adequate in this test, the main criteria of microvasculature response is thus total hemoglobin and tissue oxygen saturation, unaffected by changes in cardiac output.

Assessing recovery rates during VOT determines the microcirculatory flow distribution, capillary recruitment and restoration. In addition, rise time has been used to represent microvascular reperfusion in the assessment of oxygen saturation [Bezemer et al., 2009]. In this test, 40% of all subjects had a rise time less than 10 seconds. Another 20% of subject required more than 50 seconds. The remaining 40% were between 10-50 seconds. These results illustrate the dynamic response due to the VOT and represents the patient-specific tissue perfusion response. Therefore, longer response times indicate that the specific subject required more time for microvascular reperfusion due

to different microvasculature tone and response.

Oxygen extraction is expected to change slightly during the VOT due to the greater blood flow during recovery compared to baseline, as seen in Table 9.4. The change in extraction represents the amount of oxygen with hemoglobin, HbO_2. However, in some subjects, higher changes in extraction can be observed. Variation of oxygen extraction are largely due to the effect of the vascular occlusion process differing between individuals.

Overall, the vascular occlusion tests show very similar and expected patterns for R and IR signals and both their AC and DC components across different healthy individuals. Repeating the test in the same individual also results in a similar pattern indicating repeatability across individuals, particularly using the pulse oximeter used in this study. Overall, the VOT results show that the pulse oximeter concept can assess change in extraction due to ischemia, but these change vary across individuals.

9.4.2 Physical Exercise

Generally, much more oxygen and carbon dioxide are exchanged during exercise than at rest as exercise increases oxygen consumption and carbon dioxide production [Martin, 1999]. The increase in oxygen is also due to the increase in both arterial oxygen delivery and tissue oxygen extraction.

The average value of beat-to beat period and heart rate for pre-exercise and different post-exercise phases shown in Table 9.6 clearly indicate that heart rate increased largely from pre-exercise to post-exercise 1, which means

from resting to doing physical activity. Heart rate continued to increase when a person increased intensity of the exercise. For some subjects, heart rate maintained at a certain level and started to decrease for the rest of the post-exercise phases, likely due to fitness level and recovery from the initial start.

Throughout exercise, hemoglobin continues to be fully saturated with oxygen particularly in people with normal respiratory function [Burton et al., 2004]. Additionally, stroke volume, heart rate and cardiac output also increase during activity. However, the increases of heart rate depend on metabolic condition, workload, duration and intensity of the physical activity [Burton et al., 2004]. At certain levels, stroke volume remained constant and further increases of cardiac output are largely due to the increases in heart rate. Hence, these two variables trade off.

The effect of exercise on oxygen extraction in healthy individuals can be seen in Table 9.7. From the results presented, it shows that exercise increases oxygen consumption, as expected. The increases in oxygen extraction are represented by how the content of oxyhemoglobin increases over time during exercise, particularly from pre-exercise to post-exercise 1. However, from post-exercise 3 to post-exercise 5, the changes in oxygen extraction dropped and remained at this range for most subjects. This latter outcome indicates more oxygen combined with hemoglobin in blood cells initially and the amount of oxyhemoglobin reached stability later on as oxygen has been transported into the tissue. Additionally, the variation of exercise intensity and an individual fitness become factors for the resulting changes in oxygen extraction.

In particular, fitter individuals will recover and require less oxygen after the initial exercise shock. Less fit individuals will be unable to maintain effort

and require less oxygen. In both cases, the pulse oximeter signals are able to identify the changes in extraction, which is the main goal, regardless of cause.

In healthy individuals, exercise increases oxygen delivery and extraction from the arterial blood. Furthermore, it also increases arterial-venous oxygen content difference [Martin, 1999]. However, this may not happen to sepsis patients due to microcirculatory dysfunction, such as insufficient amount of oxygen reaching the tissue which affects the organ as well. Thus, in some disease states, oxygen demand may exceed consumption. Overall, the pulse oximeter measurements of extraction presented for the physical exercise test show it is capable of capturing these dynamics.

The changes in cardiac output for activity shown in Figures 9.8-9.10 indicate that cardiac output increases during physical activity as a result of increasing heart rate. However, cardiac output decreases slightly after post-exercise 2 or 3 depending on the metabolic condition and intensity of the physical activity done by individuals. Additionally, increases in cardiac output indicate more oxygen delivers to the exercising muscles [Martin, 1999]. Interestingly, the change in cardiac output is directly related to the change in oxygen extraction. Again, however, this sensor approach was able to assess relative changes in cardiac output, yielding and additional possible use.

9.5 Summary

In this chapter, a pulse oximeter concept was used to assess metabolic condition in healthy individuals. Instead of measuring heart rate and oxygen sat-

uration only, the pulse oximeter was used in this study to extract additional information signals due to absorption of red and infrared light. These data are processed to measure the change in extraction at or near the microvasculature. Vascular occlusion tests and physical exercise are used to investigate and validate the concept on changes in metabolic condition in heathy individuals.

In VOT, pulsatile signal is eliminated during occlusion due to limited blood flows into the occluded area. In addition, recovery process significantly indicate metabolic and microcirculatory condition of an individual by comparing amplitude, period and rise time. No significant changes in oxygen extraction has been observed when comparing baseline and recovery during the VOT.

In addition, heart rate and cardiac output were clearly seen to be increased during physical activity indicating higher oxygen extraction changes particularly from rest to exercise. Both parameters were generally increased when exercise was continuously performed. However, the increased rate varies across studied subjects since it depends on the metabolic change and metabolic requirement of an individual.

In conclusion, the pulse oximeter sensor concept used in this study is capable of extracting valuable information to assess metabolic condition. More importantly, the tests used in this study validated the concept of this pulse oximeter based sensor approach to assess underlying changes in microvasculature response and oxygen extraction. Thus, implementing this concept and method on ICU patients has the potential to aid sepsis diagnosis. Moreover, since pulse oximeters are very widely used in ICU settings, they represent a simple, non-invasive, low-cost means to monitor these patients.

Chapter 10

Conclusions

Hyperglycemia, organ failure and sepsis are common clinical conditions faced in ICU and highly associated with mortality. These conditions are highly correlated since the physiological effects of hyperglycemia lead to organ dysfunction and potentiates the pro-inflammatory response typical in sepsis. Thus, tight glycemic control (TGC) in critical illness has been documented to reduce mortality and sepsis.

Despite positive emerging evidence in favor of TGC in reducing organ failure, sepsis and mortality, reproducing the beneficial results is challenging since most glycemic control protocols are based on clinician experience. This situation is exacerbated by the fact that metabolic condition, nutritional support, and insulin regiments are highly variable across and between patients. Therefore, a physiological model that captures the glucose-insulin system dynamics is a basis for optimal, patient-specific glycemic control.

The physiological model presented in this thesis is robust, adaptable to patient-specific condition, and, most importantly, clinically validated and applicable. This model was validated using independent critical care patient data, is robust to different clinical interventions, and accurately predicts clinical intervention outcomes. Overall, it represents a balanced tradeoff of com-

plexity and non-linearity versus simplicity with respect to other models, which span a range of these tradeoffs. In essence, it is the interaction between model-based insulin sensitivity, S_I, the insulin and nutrition administered, and the patients variability over time that determines glycemic outcome in TGC. The glucose-insulin system model and model-based metric, S_I are fully validated in Chapter 4, for both fitting and prediction error.

The model achieves median fitting error <1% in data from 173 patients (N = 42,941 hours in total) who received insulin while in the ICU and stayed for more than 72 hours. More importantly, the median per-patient one-hour ahead prediction error is a very low 2.80%. A sensitivity study, as part of an internal model validation to assess the reliability of the model, confirms the validity of limiting time-varying parameters to SI only. It is significant that the 75th percentile prediction error is now within the lower bound of typical glucometer measurement errors of 7-12%, which is better than any other reported model. The result confirms that the model used is suitable for developing model-based insulin therapies, and capable of delivering tight blood glucose control, in a real-time model based control framework with a tight prediction error range.

To date, diagnosing sepsis in critical care has been a great challenge. In particular, ad-hoc protocols have been implemented which are largely based on clinical experience. A wider range of scoring systems have also been widely used to represent sepsis condition for diagnosis across different centers. In this thesis, a new scoring system has been developed which is more realistic and clinically and physiologically sensible. Incorporating the new scoring system together with other model-based metric and patients data is expected to aid

sepsis diagnosis, particularly for real-time basis.

However, information on S_I was found to be insufficient to determine the exact sepsis condition of a patient, particularly at moderate sepsis levels (eg SS2=1) which are important for early diagnosis as the condition develops. The result is unfortunate given that the physiological impact of sepsis on metabolic markers, such as S_I, is clear. Several other relevant physiological and clinical variables were also tested. Neural network and statistical analysis conclude that clinical feedback is the only parameter that resulted in higher sensitivity and specificity than is currently obtained.

Sepsis is a disease of the microcirculation. Since information on S_I and other clinical variables are insufficient for sepsis diagnosis on their own, particularly on the cohort used in this study, a pulse oximeter is used in a further study to assess microcirculation function. The pulse oximeter used is able to capture the amount of reduced hemoglobin and oxyhemoglobin. Therefore, the absorption of oxygen and extraction at the microcirculation can be estimated. The pulse oximeter concept has been validated using a vascular occlusion test and physical exercise on several healthy individuals to show it an measure the range and type of changes that might be expected.

In summary, the model presented in this thesis is physiologically relevant for clinical control and has been validated using independent data. Model-based metric and several clinical and physiological variables have been investigated to identify their possibility in becoming sepsis bio-marker. However, the concepts and methods used on pulse oximeter to assess microcirculation and metabolic condition have more promising results. Therefore, relative oxygen extraction can be used as a marker to aid sepsis diagnosis. The overall

work presents a novel, knowledgeable contribution to solving the critical care glycemic control problem, particularly for sepsis diagnosis. Furthermore, implementing the introduced concept and methods can aid sepsis diagnosis in critical care.

Chapter 11

Future Avenues

The models and control methods presented in this thesis provide a framework and background for automating glucose control and sepsis diagnosis in critical care. Insulin sensitivity, S_I, a patient-specific parameter, has accurately represented the severity of illness as discussed in Chapter 3 and and 4. However, the challenges in defining a sepsis specific bio-marker with this metric and other data open the doors for a wider view on diagnosing sepsis as a disease.

11.1 Further Clinical Validation

Timely diagnosis and treatment of sepsis in critical illness requires significant clinical effort, experience and resources. Insulin sensitivity is known to decrease with worsening condition and could thus be used to aid diagnosis. Initial studies in adults have shown insulin sensitivity provides a negative predictive diagnostic for sepsis [Blakemore et al., 2008]. Accurate and timely diagnosis of early onset sepsis remains challenging to the clinician and the laboratory. Thus, real-time, model-fitted insulin sensitivity may provide a novel marker of sepsis in this cohort.

The data from the sepsis study presented in this thesis covers only 30 patients selected based on clinician experience. They were confirmed as having sepsis based on blood culture results taken from blood tests later in the study. Therefore, there is a possibility of mismatch on time recorded for the blood culture results to the computer generated profile of insulin sensitivity that would skew results. More results from a more rigorous clinical trial may increase the sample data and potentially provide better cohort for testing and diagnosis.

11.2 Clinical Implementation

The proposed proof-of-concept study using the pulse oximeter will be a first clinical step towards developing a comprehensive and non-invasive method to detect sepsis at an early stage by assessing microcirculation function. By implementing the concept discussed in Chapter 8 in the ICU, on ongoing project, different responses between non-septic and septic patients can be analyzed to prove the concept clinically.

Long-term implementation of a standard test procedure using a pulse oximeter in intensive care would require developing robust, verified software and hardware. Additionally, critical care nursing is a highly technical profession, and staff are typically proficient with computerised technology. However, any system needs to operate using terminology and workflow patterns familiar to clinical staff to reduce training time and ease implementation.

In addition, the procedure must be standardized and require minimum

clinical effort. Therefore, protocol violations and insufficient staff will not be an issue. The software for monitoring the test may be stored on dedicated bedside computers. Any further embodiment of the software would include its incorporation into standard hospital and laboratory information systems.

Appendix A

Pulse Oximeter Validation

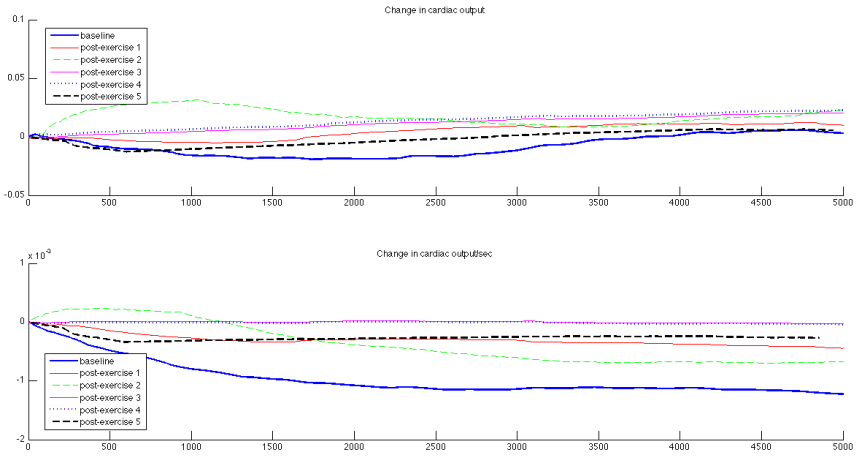

Figure A.1: Change in cardiac output (top panel) and change in cardiac output over time (bottom panel) from pre-exercise to post-exercise phases 1 to 5 for Subject 1.

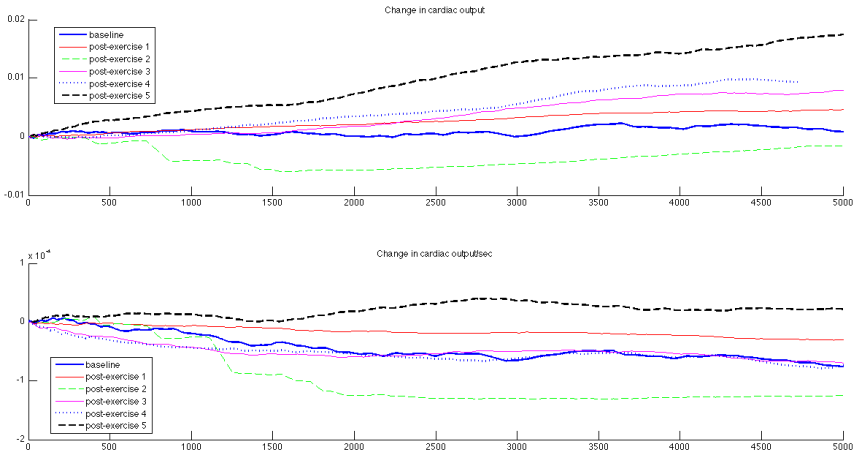

Figure A.2: Change in cardiac output (top panel) and change in cardiac output over time (bottom panel) from pre-exercise to post-exercise phases 1 to 5 for Subject 2.

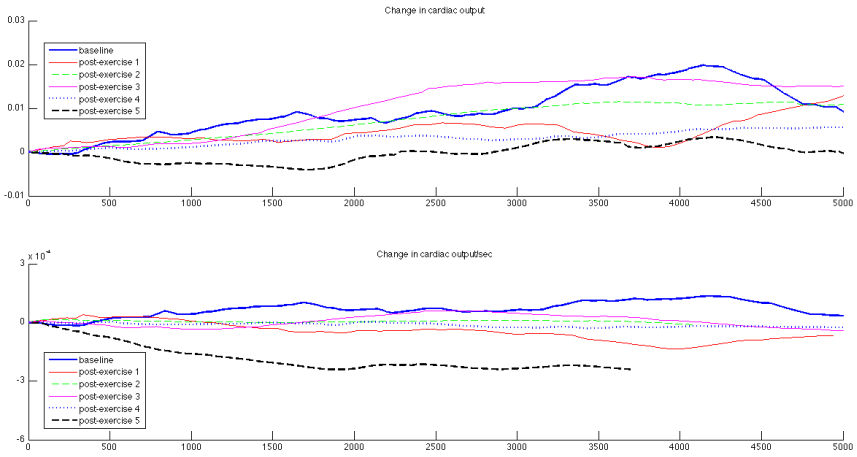

Figure A.3: Change in cardiac output (top panel) and change in cardiac output over time (bottom panel) from pre-exercise to post-exercise phases 1 to 5 for Subject 3.

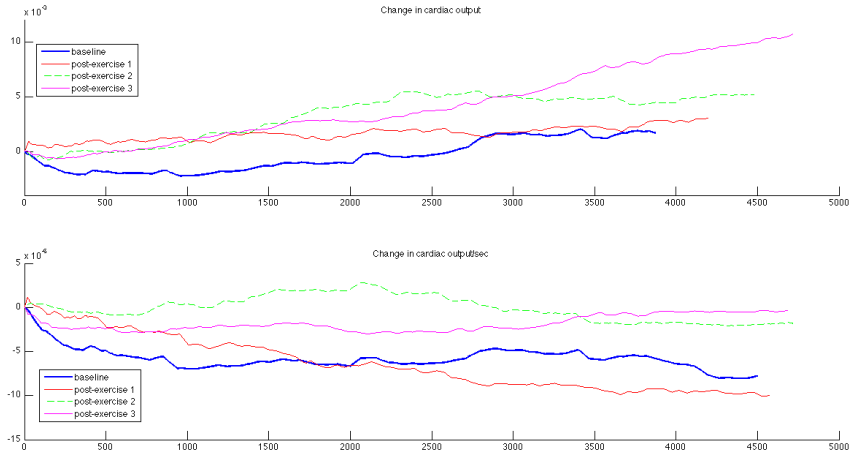

Figure A.4: Change in cardiac output (top panel) and change in cardiac output over time (bottom panel) from pre-exercise to post-exercise phases 1 to 3 for Subject 4.

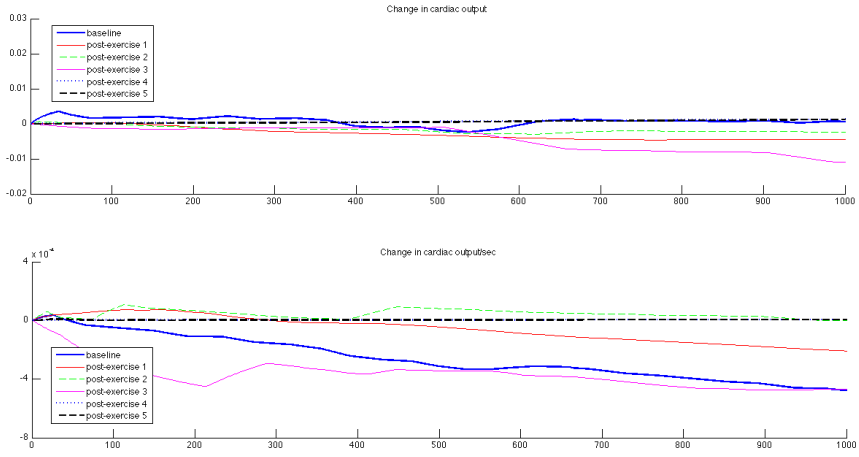

Figure A.5: Change in cardiac output (top panel) and change in cardiac output over time (bottom panel) from pre-exercise to post-exercise phases 1 to 5 for Subject 6.

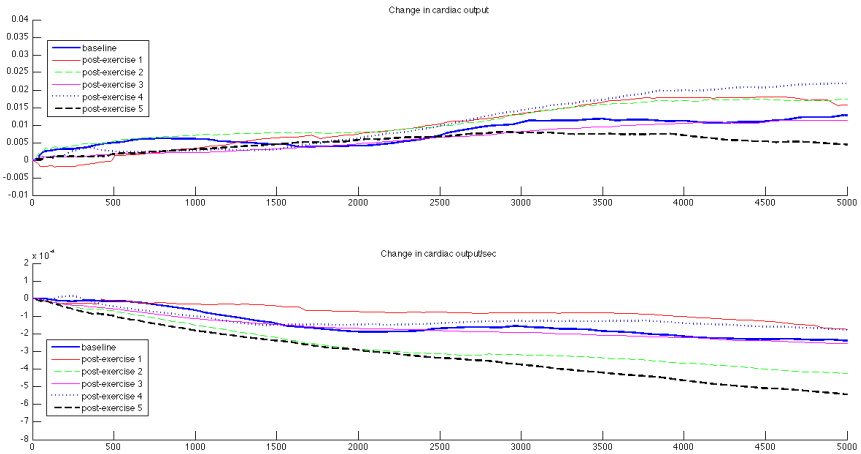

Figure A.6: Change in cardiac output (top panel) and change in cardiac output over time (bottom panel) from pre-exercise to post-exercise phases 1 to 5 for Subject 7.

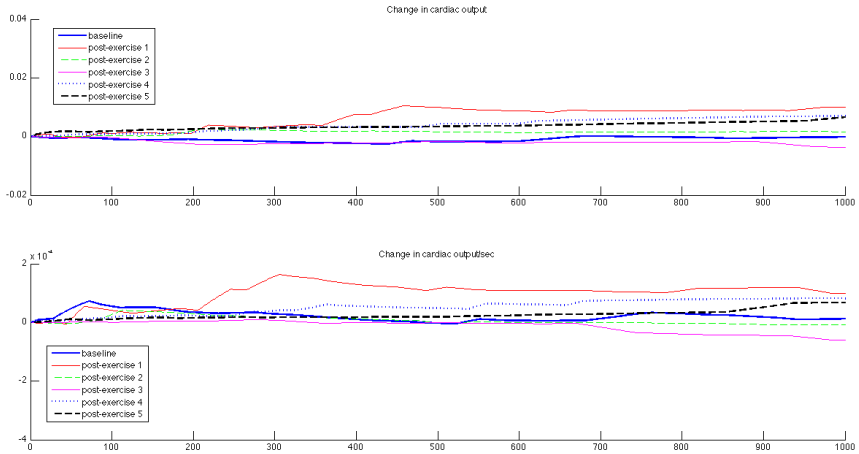

Figure A.7: Change in cardiac output (top panel) and change in cardiac output over time (bottom panel) from pre-exercise to post-exercise phases 1 to 5 for Subject 8.

Bibliography

E. Ackerman, L. C. Gatewood, J. W. Rosevear, and G. D. Molnar. Model studies of blood-glucose regulation. *Bull Math Biophys*, 27:21–37, 1965.

A. O. Agwunobi, C. Reid, P. Maycock, R. A. Little, and G. L. Carlson. Insulin resistance and substrate utilization in human endotoxemia. *J. Clin. Endocrinol. Metab.*, 85:3770–3778, Oct 2000.

C. L. Ahrens, J. F. Barletta, S. Kanji, J. G. Tyburski, R. F. Wilson, J. J. Janisse, and J. W. Devlin. Effect of low-calorie parenteral nutrition on the incidence and severity of hyperglycemia in surgical patients: a randomized, controlled trial. *Crit. Care Med.*, 33:2507–2512, Nov 2005.

N. A. Ali, J. M. O'Brien, K. Dungan, G. Phillips, C. B. Marsh, S. Lemeshow, A. F. Connors, and J. C. Preiser. Glucose variability and mortality in patients with sepsis. *Crit. Care Med.*, 36:2316–2321, Aug 2008.

S. K. Andersen, J. Gjedsted, C. Christiansen, and E. T?nnesen. The roles of insulin and hyperglycemia in sepsis pathogenesis. *J. Leukoc. Biol.*, 75: 413–421, Mar 2004.

D. C. Angus, W. T. Linde-Zwirble, J. Lidicker, G. Clermont, J. Carcillo, and M. R. Pinsky. Epidemiology of severe sepsis in the United States: analysis of incidence, outcome, and associated costs of care. *Crit. Care Med.*, 29: 1303–1310, Jul 2001.

Y. M. Arabi, M. Dehbi, A. H. Rishu, E. Baturcam, S. H. Kahoul, R. J. Brits, B. Naidu, and A. Bouchama. sRAGE in diabetic and non-diabetic critically

ill patients: effects of intensive insulin therapy. *Crit Care*, 15:R203, 2011.

S. M. Ayres. SCCM's new horizons conference on sepsis and septic shock. *Crit. Care Med.*, 13:864–866, Oct 1985.

S. M. Bagshaw, R. Bellomo, M. J. Jacka, M. Egi, G. K. Hart, and C. George. The impact of early hypoglycemia and blood glucose variability on outcome in critical illness. *Crit Care*, 13:R91, 2009.

C. BalcI, H. Sungurtekin, E. Gurses, U. Sungurtekin, and B. Kaptanoglu. Usefulness of procalcitonin for diagnosis of sepsis in the intensive care unit. *Crit Care*, 7:85–90, Feb 2003.

R. A. Balk and R. C. Bone. The septic syndrome. Definition and clinical implications. *Crit Care Clin*, 5:1–8, Jan 1989.

A. V. Barochia, X. Cui, D. Vitberg, A. F. Suffredini, N. P. O'Grady, S. M. Banks, P. Minneci, S. J. Kern, R. L. Danner, C. Natanson, and P. Q. Eichacker. Bundled care for septic shock: an analysis of clinical trials. *Crit. Care Med.*, 38:668–678, Feb 2010.

O. K. Baskurt, A. Temiz, and H. J. Meiselman. Red blood cell aggregation in experimental sepsis. *J. Lab. Clin. Med.*, 130:183–190, Aug 1997.

M. Bassetti, F. Ginocchio, and D. R. Giacobbe. New approaches for empiric therapy in Gram-positive sepsis. *Minerva Anestesiol*, 77:821–827, Aug 2011.

N. Bele, M. Darmon, I. Coquet, J. P. Feugeas, S. Legriel, N. Adaoui, B. Schlemmer, and E. Azoulay. Diagnostic accuracy of procalcitonin in

critically ill immunocompromised patients. *BMC Infect. Dis.*, 11:224, 2011.

R. N. Bergman, Y. Z. Ider, C. R. Bowden, and C. Cobelli. Quantitative estimation of insulin sensitivity. *Am. J. Physiol.*, 236:E667–677, Jun 1979.

R. N. Bergman, L. S. Phillips, and C. Cobelli. Physiologic evaluation of factors controlling glucose tolerance in man: measurement of insulin sensitivity and beta-cell glucose sensitivity from the response to intravenous glucose. *J. Clin. Invest.*, 68:1456–1467, Dec 1981.

R. N. Bergman, D. T. Finegood, and M. Ader. Assessment of insulin sensitivity in vivo. *Endocr. Rev.*, 6:45–86, 1985.

C. Bernet, O. Desebbe, S. Bordon, C. Lacroix, P. Rosamel, F. Farhat, J. J. Lehot, and M. Cannesson. The impact of induction of general anesthesia and a vascular occlusion test on tissue oxygen saturation derived parameters in high-risk surgical patients. *J Clin Monit Comput*, 25:237–244, Aug 2011.

R. Bezemer, A. Lima, D. Myers, E. Klijn, M. Heger, P. T. Goedhart, J. Bakker, and C. Ince. Assessment of tissue oxygen saturation during a vascular occlusion test using near-infrared spectroscopy: the role of probe spacing and measurement site studied in healthy volunteers. *Crit Care*, 13 Suppl 5: S4, 2009.

B. R. Bistrian. Hyperglycemia and infection: which is the chicken and which is the egg? *JPEN J Parenter Enteral Nutr*, 25:180–181, 2001.

A. Blakemore, S. H. Wang, A. Le Compte, G. M Shaw, X. W. Wong, J. Lin, T. Lotz, C. E Hann, and J. G. Chase. Model-based insulin sensitivity as a sepsis diagnostic in critical care. *J Diabetes Sci Technol*, 2:468–477, May

2008.

V. W. Bolie. Coefficients of normal blood glucose regulation. *J Appl Physiol*, 16:783–788, Sep 1961.

R. C. Bone, C. J. Fisher, T. P. Clemmer, G. J. Slotman, C. A. Metz, and R. A. Balk. Sepsis syndrome: a valid clinical entity. Methylprednisolone Severe Sepsis Study Group. *Crit. Care Med.*, 17:389–393, May 1989.

R. C. Bone, R. A. Balk, F. B. Cerra, R. P. Dellinger, A. M. Fein, W. A. Knaus, R. M. Schein, and W. J. Sibbald. Definitions for sepsis and organ failure and guidelines for the use of innovative therapies in sepsis. The ACCP/SCCM Consensus Conference Committee. American College of Chest Physicians/Society of Critical Care Medicine. *Chest*, 101:1644–1655, Jun 1992.

R. Boushel, H. Langberg, J. Olesen, J. Gonzales-Alonzo, J. Bulow, and M. Kjaer. Monitoring tissue oxygen availability with near infrared spectroscopy (NIRS) in health and disease. *Scand J Med Sci Sports*, 11:213–222, Aug 2001.

R. G. Branco, P. C. Garcia, J. P. Piva, C. H. Casartelli, V. Seibel, and R. C. Tasker. Glucose level and risk of mortality in pediatric septic shock. *Pediatr Crit Care Med*, 6:470–472, Jul 2005.

F. M. Brunkhorst, C. Engel, F. Bloos, A. Meier-Hellmann, M. Ragaller, N. Weiler, O. Moerer, M. Gruendling, M. Oppert, S. Grond, D. Olthoff, U. Jaschinski, S. John, R. Rossaint, T. Welte, M. Schaefer, P. Kern, E. Kuhnt, M. Kiehntopf, C. Hartog, C. Natanson, M. Loeffler, and K. Rein-

hart. Intensive insulin therapy and pentastarch resuscitation in severe sepsis. *N. Engl. J. Med.*, 358:125–139, Jan 2008.

M. Burney, J. Underwood, S. McEvoy, G. Nelson, A. Dzierba, V. Kauari, and D. Chong. Early Detection and Treatment of Severe Sepsis in the Emergency Department: Identifying Barriers to Implementation of a Protocol-based Approach. *J Emerg Nurs*, Nov 2011.

D. A. Burton, K. Stokes, and G. M. Hall. Physiological effects of exercise. 4 (6):185–188, 2004.

C. M. Buysse, H. Raat, J. A. Hazelzet, L. C. Vermunt, E. M. Utens, W. C. Hop, and K. F. Joosten. Long-term health-related quality of life in survivors of meningococcal septic shock in childhood and their parents. *Qual Life Res*, 16:1567–1576, Dec 2007.

S. E. Capes, D. Hunt, K. Malmberg, and H. C. Gerstein. Stress hyperglycaemia and increased risk of death after myocardial infarction in patients with and without diabetes: a systematic overview. *Lancet*, 355:773–778, Mar 2000.

T. Cardoso, A. H. Carneiro, O. Ribeiro, A. Teixeira-Pinto, and A. Costa-Pereira. Reducing mortality in severe sepsis with the implementation of a core 6-hour bundle: results from the Portuguese community-acquired sepsis study (SACiUCI study). *Crit Care*, 14:R83, 2010.

S. D. Carrigan, G. Scott, and M. Tabrizian. Toward resolving the challenges of sepsis diagnosis. *Clin. Chem.*, 50:1301–1314, Aug 2004.

E. R. Carson and C. Cobelli. *Modelling methodology for physiology and*

medicine. Academic Press Series in Biomedical Engineering, Academic Press, San Diego, 2001.

A. Caumo, P. Vicini, J. J. Zachwieja, A. Avogaro, K. Yarasheski, D. M. Bier, and C. Cobelli. Undermodeling affects minimal model indexes: insights from a two-compartment model. *Am. J. Physiol.*, 276:E1171–1193, Jun 1999.

J. M. Cavaillon and M. Adib-Conquy. Determining the degree of immunodysregulation in sepsis. *Contrib Nephrol*, 156:101–111, 2007.

F. B. Cerra, M. R. Benitez, G. L. Blackburn, R. S. Irwin, K. Jeejeebhoy, D. P. Katz, S. K. Pingleton, J. Pomposelli, J. L. Rombeau, E. Shronts, R. R. Wolfe, and G. P. Zaloga. Applied nutrition in ICU patients. A consensus statement of the American College of Chest Physicians. *Chest*, 111:769–778, Mar 1997.

J. G. Chase, G. M. Shaw, J. Lin, C. V. Doran, C. Hann, T. Lotz, G. C. Wake, and B. Broughton. Targeted glycemic reduction in critical care using closed-loop control. *Diabetes Technol. Ther.*, 7:274–282, Apr 2005.

J. G. Chase, G. M. Shaw, T. Lotz, A. LeCompte, J. Wong, J. Lin, T. Lonergan, M. Willacy, and C. E. Hann. Model-based insulin and nutrition administration for tight glycaemic control in critical care. *Curr Drug Deliv*, 4:283–296, Oct 2007.

J. G. Chase, A. LeCompte, G. M. Shaw, A. Blakemore, J. Wong, J. Lin, and C. E. Hann. A benchmark data set for model-based glycemic control in critical care. *J Diabetes Sci Technol*, 2:584–594, Jul 2008a.

J. G. Chase, G. Shaw, A. Le Compte, T. Lonergan, M. Willacy, X. W. Wong, J. Lin, T. Lotz, D. Lee, and C. Hann. Implementation and evaluation of the SPRINT protocol for tight glycaemic control in critically ill patients: a clinical practice change. *Crit Care*, 12:R49, 2008b.

J. G. Chase, C. G. Pretty, L. Pfeifer, G. M. Shaw, J. C. Preiser, A. J. Le Compte, J. Lin, D. Hewett, K. T. Moorhead, and T. Desaive. Organ failure and tight glycemic control in the SPRINT study. *Crit Care*, 14: R154, 2010a.

J. G. Chase, F. Suhaimi, S. Penning, J. C. Preiser, A. J. Le Compte, J. Lin, C. G. Pretty, G. M. Shaw, K. T. Moorhead, and T. Desaive. Validation of a model-based virtual trials method for tight glycemic control in intensive care. *Biomed Eng Online*, 9:84, 2010b.

J. G. Chase, A. J. Le Compte, J. C. Preiser, G. M. Shaw, S. Penning, and T. Desaive. Physiological modeling, tight glycemic control, and the ICU clinician: what are models and how can they affect practice? *Ann Intensive Care*, 1:11, 2011a.

J. G. Chase, A. J. Le Compte, F. Suhaimi, G. M. Shaw, A. Lynn, J. Lin, C. G. Pretty, N. Razak, J. D. Parente, C. E. Hann, J. C. Preiser, and T. Desaive. Tight glycemic control in critical care–the leading role of insulin sensitivity and patient variability: a review and model-based analysis. *Comput Methods Programs Biomed*, 102:156–171, May 2011b.

J.G. Chase, G.M. Shaw, X.W. Wong, T. Lotz, J. Lin, and C.E. Hann. Model-based glycaemic control in critical careĽÛÓa review of the state of the possible. *Biomedical Signal Processing and Control*, 1(1):3 – 21,

2006. ISSN 1746-8094. doi: 10.1016/j.bspc.2006.03.002. URL http://www.sciencedirect.com/science/article/pii/S1746809406000061.

F. Chee, T. Fernando, and P. V. van Heerden. Closed-loop glucose control in critically ill patients using continuous glucose monitoring system (CGMS) in real time. *IEEE Trans Inf Technol Biomed*, 7:43–53, Mar 2003a.

F. Chee, T. L. Fernando, A. V. Savkin, and V. van Heeden. Expert PID control system for blood glucose control in critically ill patients. *IEEE Trans Inf Technol Biomed*, 7:419–425, Dec 2003b.

M. J. Chen, H. M. Tseng, Y. L. Huang, W. N. Hsu, K. W. Yeh, T. L. Wu, L. C. See, and J. L. Huang. Long-term outcome and short-term survival of patients with systemic lupus erythematosus after bacteraemia episodes: 6-yr follow-up. *Rheumatology (Oxford)*, 47:1352–1357, Sep 2008.

A. W. Chiu, S. Daniel, H. Khosravani, P. L. Carlen, and B. L. Bardakjian. Prediction of seizure onset in an in-vitro hippocampal slice model of epilepsy using Gaussian-based and wavelet-based artificial neural networks. *Ann Biomed Eng*, 33:798–810, Jun 2005.

C. Cobelli and A. Mari. Validation of mathematical models of complex endocrine-metabolic systems. A case study on a model of glucose regulation. *Med Biol Eng Comput*, 21:390–399, Jul 1983.

C. Cobelli, E. R. Carson, L. Finkelstein, and M. S. Leaning. Validation of simple and complex models in physiology and medicine. *Am. J. Physiol.*, 246:R259–266, Feb 1984.

C. Cobelli, G. Toffolo, and D. M. Foster. Tracer-to-tracee ratio for analysis

of stable isotope tracer data: link with radioactive kinetic formalism. *Am. J. Physiol.*, 262:E968–975, Jun 1992.

C. Cobelli, A. Caumo, and M. Omenetto. Minimal model SG overestimation and SI underestimation: improved accuracy by a Bayesian two-compartment model. *Am. J. Physiol.*, 277:E481–488, Sep 1999.

M. J. Cohen, M. Call, M. Nelson, C. S. Calfee, C. T. Esmon, K. Brohi, and J. F. Pittet. Critical Role of Activated Protein C in Early Coagulopathy and Later Organ Failure, Infection and Death in Trauma Patients. *Ann. Surg.*, Dec 2011.

W. N. Colier, I. B. Meeuwsen, H. Degens, and B. Oeseburg. Determination of oxygen consumption in muscle during exercise using near infrared spectroscopy. *Acta Anaesthesiol Scand Suppl*, 107:151–155, 1995.

G. Colin, O. Nardi, A. Polito, J. Aboab, V. Maxime, B. Clair, D. Friedman, D. Orlikowski, T. Sharshar, and D. Annane. Masseter tissue oxygen saturation predicts normal central venous oxygen saturation during early goal-directed therapy and predicts mortality in patients with severe sepsis. *Crit. Care Med.*, Oct 2011.

J. Creteur, T. Carollo, G. Soldati, G. Buchele, D. De Backer, and J. L. Vincent. The prognostic value of muscle StO2 in septic patients. *Intensive Care Med*, 33:1549–1556, Sep 2007.

H. L. Cronshaw, R. Daniels, A. Bleetman, E. Joynes, and M. Sheils. Impact of the Surviving Sepsis Campaign on the recognition and management of severe sepsis in the emergency department: are we failing? *Emerg Med J*,

28:670–675, Aug 2011.

U. N. Das. Insulin in sepsis and septic shock. *J Assoc Physicians India*, 51: 695–700, Jul 2003.

P. C. Davidson, R. D. Steed, and B. W. Bode. Glucommander: a computer-directed intravenous insulin system shown to be safe, simple, and effective in 120,618 h of operation. *Diabetes Care*, 28:2418–2423, Oct 2005.

G. d. e. l. C. De La Rosa, J. H. Donado, A. H. Restrepo, A. M. Quintero, L. G. Gonzalez, N. E. Saldarriaga, M. Bedoya, J. M. Toro, J. B. Velasquez, J. C. Valencia, C. M. Arango, P. H. Aleman, E. M. Vasquez, J. C. Chavarriaga, A. Yepes, W. Pulido, and C. A. Cadavid. Strict glycaemic control in patients hospitalised in a mixed medical and surgical intensive care unit: a randomised clinical trial. *Crit Care*, 12:R120, 2008.

R. P. Dellinger, J. M. Carlet, H. Masur, H. Gerlach, T. Calandra, J. Cohen, J. Gea-Banacloche, D. Keh, J. C. Marshall, M. M. Parker, G. Ramsay, J. L. Zimmerman, J. L. Vincent, and M. M. Levy. Surviving Sepsis Campaign guidelines for management of severe sepsis and septic shock. *Crit. Care Med.*, 32:858–873, Mar 2004.

R. N. Dickerson. Hypocaloric feeding of obese patients in the intensive care unit. *Curr Opin Clin Nutr Metab Care*, 8:189–196, Mar 2005.

R. N. Dickerson, K. J. Boschert, K. A. Kudsk, and R. O. Brown. Hypocaloric enteral tube feeding in critically ill obese patients. *Nutrition*, 18:241–246, Mar 2002.

J. D. Dickinson and M. H. Kollef. Early and adequate antibiotic therapy in

the treatment of severe sepsis and septic shock. *Curr Infect Dis Rep*, 13: 399–405, Oct 2011.

G. Dimitriadis, B. Leighton, M. Parry-Billings, S. Sasson, M. Young, U. Krause, S. Bevan, T. Piva, G. Wegener, and E. A. Newsholme. Effects of glucocorticoid excess on the sensitivity of glucose transport and metabolism to insulin in rat skeletal muscle. *Biochem. J.*, 321 (Pt 3): 707–712, Feb 1997.

P. D. Docherty, J. G. Chase, T. F. Lotz, and T. Desaive. A graphical method for practical and informative identifiability analyses of physiological models: a case study of insulin kinetics and sensitivity. *Biomed Eng Online*, 10:39, 2011.

K. C. Doerschug, A. S. Delsing, G. A. Schmidt, and W. G. Haynes. Impairments in microvascular reactivity are related to organ failure in human sepsis. *Am. J. Physiol. Heart Circ. Physiol.*, 293:H1065–1071, Aug 2007.

C. V. Doran, J. G. Chase, G. M. Shaw, K. T. Moorhead, and N. H. Hudson. Automated insulin infusion trials in the intensive care unit. *Diabetes Technol. Ther.*, 6:155–165, Apr 2004a.

C. V. Doran, N. H. Hudson, K. T. Moorhead, J. G. Chase, G. M. Shaw, and C. E. Hann. Derivative weighted active insulin control modelling and clinical trials for ICU patients. *Med Eng Phys*, 26:855–866, Dec 2004b.

M. J. Dortch, N. T. Mowery, A. Ozdas, L. Dossett, H. Cao, B. Collier, G. Holder, R. A. Miller, and A. K. May. A computerized insulin infusion titration protocol improves glucose control with less hypoglycemia com-

pared to a manual titration protocol in a trauma intensive care unit. *JPEN J Parenter Enteral Nutr*, 32:18–27, 2008.

M. Egi and R. Bellomo. Reducing glycemic variability in intensive care unit patients: a new therapeutic target? *J Diabetes Sci Technol*, 3:1302–1308, Nov 2009.

M. Egi, R. Bellomo, E. Stachowski, C. J. French, and G. Hart. Variability of blood glucose concentration and short-term mortality in critically ill patients. *Anesthesiology*, 105:244–252, Aug 2006.

M. Egi, R. Bellomo, E. Stachowski, C. J. French, G. K. Hart, C. Hegarty, and M. Bailey. Blood glucose concentration and outcome of critical illness: the impact of diabetes. *Crit. Care Med.*, 36:2249–2255, Aug 2008.

P. Q. Eichacker, C. Natanson, and R. L. Danner. Surviving sepsis–practice guidelines, marketing campaigns, and Eli Lilly. *N. Engl. J. Med.*, 355: 1640–1642, Oct 2006.

M. Elia, A. Ceriello, H. Laube, A. J. Sinclair, M. Engfer, and R. J. Stratton. Enteral nutritional support and use of diabetes-specific formulas for patients with diabetes: a systematic review and meta-analysis. *Diabetes Care*, 28: 2267–2279, Sep 2005.

K. Ellemann, B. Thorsteinsson, S. Fugleberg, B. Feldt-Rasmussen, O. O. Andersen, P. Gr?nbaek, and C. Binder. Kinetics of insulin disappearance from plasma in cortisone-treated normal subjects. *Clin. Endocrinol. (Oxf)*, 26: 623–628, May 1987.

A. Evans, G. M. Shaw, A. Le Compte, C. S. Tan, L. Ward, J. Steel, C. G.

Pretty, L. Pfeifer, S. Penning, F. Suhaimi, M. Signal, T. Desaive, and J. G. Chase. Pilot proof of concept clinical trials of Stochastic Targeted (STAR) glycemic control. *Ann Intensive Care*, 1:38, 2011.

M. Fernandez, A. Gastaldelli, C. Triplitt, J. Hardies, A. Casolaro, R. Petz, P. Tantiwong, N. Musi, E. Cersosimo, E. Ferrannini, and R. A. DeFronzo. Metabolic effects of muraglitazar in type 2 diabetic subjects. *Diabetes Obes Metab*, 13:893–902, Oct 2011.

S. Finfer and S. Heritier. The NICE-SUGAR (Normoglycaemia in Intensive Care Evaluation and Survival Using Glucose Algorithm Regulation) Study: statistical analysis plan. *Crit Care Resusc*, 11:46–57, Mar 2009.

S. J. Finney, C. Zekveld, A. Elia, and T. W. Evans. Glucose control and mortality in critically ill patients. *JAMA*, 290:2041–2047, Oct 2003.

D. E. Fry, L. Pearlstein, R. L. Fulton, and H. C. Polk. Multiple system organ failure. The role of uncontrolled infection. *Arch Surg*, 115:136–140, Feb 1980.

E. Futier, S. Christophe, E. Robin, A. Petit, B. Pereira, J. Desbordes, J. E. Bazin, and B. Vallet. Use of near-infrared spectroscopy during a vascular occlusion test to assess the microcirculatory response during fluid challenge. *Crit Care*, 15:R214, Sep 2011.

P. A. Goldberg, M. D. Siegel, R. S. Sherwin, J. I. Halickman, M. Lee, V. A. Bailey, S. L. Lee, J. D. Dziura, and S. E. Inzucchi. Implementation of a safe and effective insulin infusion protocol in a medical intensive care unit. *Diabetes Care*, 27:461–467, Feb 2004.

D. Goldman, R. M. Bateman, and C. G. Ellis. Effect of sepsis on skeletal muscle oxygen consumption and tissue oxygenation: interpreting capillary oxygen transport data using a mathematical model. *Am. J. Physiol. Heart Circ. Physiol.*, 287:H2535–2544, Dec 2004.

H. Gomez, A. Torres, P. Polanco, H. K. Kim, S. Zenker, J. C. Puyana, and M. R. Pinsky. Use of non-invasive NIRS during a vascular occlusion test to assess dynamic tissue O(2) saturation response. *Intensive Care Med*, 34: 1600–1607, Sep 2008.

F. J. Gonzalez de Molina and R. Ferrer. Appropriate antibiotic dosing in severe sepsis and acute renal failure: factors to consider. *Crit Care*, 15:175, 2011.

D. E. Griesdale, R. J. de Souza, R. M. van Dam, D. K. Heyland, D. J. Cook, A. Malhotra, R. Dhaliwal, W. R. Henderson, D. R. Chittock, S. Finfer, and D. Talmor. Intensive insulin therapy and mortality among critically ill patients: a meta-analysis including NICE-SUGAR study data. *CMAJ*, 180: 821–827, Apr 2009.

A. C. Guyton. *Textbook of medical physiology.* Saunders, United States of America, eighth edition edition, 1991.

A. C. Guyton and J. E. Hall. *Textbook of medical physiology.* Saunders, United States of America, ninth edition edition, 1996.

C. E. Hann, J. G. Chase, J. Lin, T. Lotz, C. V. Doran, and G. M. Shaw. Integral-based parameter identification for long-term dynamic verification of a glucose-insulin system model. *Comput Methods Programs Biomed*, 77:

259–270, Mar 2005.

A. Hasegawa, H. Iwasaka, S. Hagiwara, H. Koga, R. Hasegawa, K. Kudo, J. Kusaka, and T. Noguchi. Anti-inflammatory effects of perioperative intensive insulin therapy during cardiac surgery with cardiopulmonary bypass. *Surg. Today*, 41:1385–1390, Oct 2011.

P. C. Hebert, A. J. Drummond, J. Singer, G. R. Bernard, and J. A. Russell. A simple multiple system organ failure scoring system predicts mortality of patients who have sepsis syndrome. *Chest*, 104:230–235, Jul 1993.

M. A. Hemels, A. van den Hoogen, M. A. Verboon-Maciolek, A. Fleer, and T. G. Krediet. Shortening the Antibiotic Course for the Treatment of Neonatal Coagulase-Negative Staphylococcal Sepsis: Fine with Three Days? *Neonatology*, 101:101–105, Sep 2011.

D. K. Heyland, W. Hopman, H. Coo, J. Tranmer, and M. A. McColl. Long-term health-related quality of life in survivors of sepsis. Short Form 36: a valid and reliable measure of health-related quality of life. *Crit. Care Med.*, 28:3599–3605, Nov 2000.

P. Hicks, D. J. Cooper, S. Webb, J. Myburgh, I. Seppelt, S. Peake, C. Joyce, D. Stephens, A. Turner, C. French, G. Hart, I. Jenkins, and A. Burrell. The Surviving Sepsis Campaign: International guidelines for management of severe sepsis and septic shock: 2008. An assessment by the Australian and New Zealand intensive care society. *Anaesth Intensive Care*, 36:149–151, Mar 2008.

H. Hirasawa, S. Oda, and M. Nakamura. Blood glucose control in patients

with severe sepsis and septic shock. *World J. Gastroenterol.*, 15:4132–4136, Sep 2009.

I. B. Hirsch and M. Brownlee. Should minimal blood glucose variability become the gold standard of glycemic control? *J. Diabetes Complicat.*, 19: 178–181, 2005.

M. Holub and J. Zavada. Clinical aspects of sepsis. *Contrib Microbiol*, 17: 12–30, 2011.

R. Hovorka, F. Shojaee-Moradie, P. V. Carroll, L. J. Chassin, I. J. Gowrie, N. C. Jackson, R. S. Tudor, A. M. Umpleby, and R. H. Jones. Partitioning glucose distribution/transport, disposal, and endogenous production during IVGTT. *Am. J. Physiol. Endocrinol. Metab.*, 282:992–1007, May 2002.

R. Hovorka, V. Canonico, L. J. Chassin, U. Haueter, M. Massi-Benedetti, M. Orsini Federici, T. R. Pieber, H. C. Schaller, L. Schaupp, T. Vering, and M. E. Wilinska. Nonlinear model predictive control of glucose concentration in subjects with type 1 diabetes. *Physiol Meas*, 25:905–920, Aug 2004.

Kuo-lin Hsu, Hoshin Vijai Gupta, and Soroosh Sorooshian. Artificial neural network modeling of the rainfall-runoff process. *Water Resour. Res.*, 31(10): 2517–2530, 1995.

C. Ince. The microcirculation is the motor of sepsis. *Crit Care*, 9 Suppl 4: S13–19, 2005.

C. Ince and M. Sinaasappel. Microcirculatory oxygenation and shunting in sepsis and shock. *Crit. Care Med.*, 27:1369–1377, Jul 1999.

P. U. Iyer. Nutritional support in the critically ill child. *Indian J Pediatr*, 69: 405–410, May 2002.

L. S. Jefferson, Cherrington A. D., and Goodman H. M. *Handbook of Physiology. Section 7: The Endocrine System*, volume II. Oxford, United States of America, 2001.

E. Jeremitsky, L. A. Omert, C. M. Dunham, J. Wilberger, and A. Rodriguez. The impact of hyperglycemia on patients with severe brain injury. *J Trauma*, 58:47–50, Jan 2005.

A. Jubran. Pulse oximetry. *Crit Care*, 3:R11–R17, 1999.

A. Jubran. Pulse oximetry. *Intensive Care Med*, 30:2017–2020, Nov 2004.

R. Juneja, C. P. Roudebush, S. A. Nasraway, A. A. Golas, J. Jacobi, J. Carroll, D. Nelson, V. J. Abad, and S. J. Flanders. Computerized intensive insulin dosing can mitigate hypoglycemia and achieve tight glycemic control when glucose measurement is performed frequently and on time. *Crit Care*, 13: R163, 2009.

R. Khan, L. A. Kirschenbaum, C. Larow, and M. E. Astiz. The effect of resuscitation fluids on neutrophil-endothelial cell interactions in septic shock. *Shock*, 36:440–444, Nov 2011.

S. Kibe, K. Adams, and G. Barlow. Diagnostic and prognostic biomarkers of sepsis in critical care. *J. Antimicrob. Chemother.*, 66 Suppl 2:33–40, Apr 2011.

H. Kim, E. Son, J. Kim, K. Choi, C. Kim, W. Shin, and O. Suh. Association

of hyperglycemia and markers of hepatic dysfunction with dextrose infusion rates in Korean patients receiving total parenteral nutrition. *Am J Health Syst Pharm*, 60:1760–1766, Sep 2003.

W. A. Knaus, D. P. Wagner, and J. Lynn. Short-term mortality predictions for critically ill hospitalized adults: science and ethics. *Science*, 254:389–394, Oct 1991.

B. J. Krajicek, Y. C. Kudva, and H. A. Hurley. Potentially important contribution of dextrose used as diluent to hyperglycemia in hospitalized patients. *Diabetes Care*, 28:981–982, Apr 2005.

J. S. Krinsley. Association between hyperglycemia and increased hospital mortality in a heterogeneous population of critically ill patients. *Mayo Clin. Proc.*, 78:1471–1478, Dec 2003.

J. S. Krinsley. Effect of an intensive glucose management protocol on the mortality of critically ill adult patients. *Mayo Clin. Proc.*, 79:992–1000, Aug 2004.

J. S. Krinsley. Glycemic variability: a strong independent predictor of mortality in critically ill patients. *Crit. Care Med.*, 36:3008–3013, Nov 2008.

J. S. Krinsley. Glycemic variability and mortality in critically ill patients: the impact of diabetes. *J Diabetes Sci Technol*, 3:1292–1301, Nov 2009.

J. A. Krishnan, P. B. Parce, A. Martinez, G. B. Diette, and R. G. Brower. Caloric intake in medical ICU patients: consistency of care with guidelines and relationship to clinical outcomes. *Chest*, 124:297–305, Jul 2003.

A. Kumar, D. Roberts, K. E. Wood, B. Light, J. E. Parrillo, S. Sharma, R. Suppes, D. Feinstein, S. Zanotti, L. Taiberg, D. Gurka, A. Kumar, and M. Cheang. Duration of hypotension before initiation of effective antimicrobial therapy is the critical determinant of survival in human septic shock. *Crit. Care Med.*, 34:1589–1596, Jun 2006.

A. M. Laird, P. R. Miller, P. D. Kilgo, J. W. Meredith, and M. C. Chang. Relationship of early hyperglycemia to mortality in trauma patients. *J Trauma*, 56:1058–1062, May 2004.

C. Lam, K. Tyml, C. Martin, and W. Sibbald. Microvascular perfusion is impaired in a rat model of normotensive sepsis. *J. Clin. Invest.*, 94:2077–2083, Nov 1994.

L. Langouche, I. Vanhorebeek, D. Vlasselaers, S. Vander Perre, P. J. Wouters, K. Skogstrand, T. K. Hansen, and G. Van den Berghe. Intensive insulin therapy protects the endothelium of critically ill patients. *J. Clin. Invest.*, 115:2277–2286, Aug 2005.

L. Langouche, S. Vander Perre, P. J. Wouters, A. D'Hoore, T. K. Hansen, and G. Van den Berghe. Effect of intensive insulin therapy on insulin sensitivity in the critically ill. *J. Clin. Endocrinol. Metab.*, 92:3890–3897, Oct 2007.

S. Laver, S. Preston, D. Turner, C. McKinstry, and A. Padkin. Implementing intensive insulin therapy: development and audit of the Bath insulin protocol. *Anaesth Intensive Care*, 32:311–316, Jun 2004.

A. Lavrentieva, S. Papadopoulou, J. Kioumis, E. Kaimakamis, and M. Bitzani. PCT as a diagnostic and prognostic tool in burn patients. Whether time

course has a role in monitoring sepsis treatment. *Burns*, Oct 2011.

A. Le Compte, J. G. Chase, A. Lynn, C. Hann, G. Shaw, X. W. Wong, and J. Lin. Blood glucose controller for neonatal intensive care: virtual trials development and first clinical trials. *J Diabetes Sci Technol*, 3:1066–1081, Sep 2009.

E. D. Lehmann and T. Deutsch. A physiological model of glucose-insulin interaction in type 1 diabetes mellitus. *J Biomed Eng*, 14:235–242, May 1992.

E. Lelkes, B. R. Unsworth, and P. I. Lelkes. Reactive oxygen species, apoptosis and altered NGF-induced signaling in PC12 pheochromocytoma cells cultured in elevated glucose: an in vitro cellular model for diabetic neuropathy. *Neurotox Res*, 3:189–203, Apr 2001.

M. M. Levy, M. P. Fink, J. C. Marshall, E. Abraham, D. Angus, D. Cook, J. Cohen, S. M. Opal, J. L. Vincent, and G. Ramsay. 2001 SCCM/ESICM/ACCP/ATS/SIS International Sepsis Definitions Conference. *Crit. Care Med.*, 31:1250–1256, Apr 2003.

K. S. Lewis, S. L. Kane-Gill, M. B. Bobek, and J. F. Dasta. Intensive insulin therapy for critically ill patients. *Ann Pharmacother*, 38:1243–1251, 2004.

J. Li, B. Carr, M. Goyal, and D. F. Gaieski. Sepsis: the inflammatory foundation of pathophysiology and therapy. *Hosp Pract (Minneap)*, 39:99–112, Aug 2011.

J. Lin, J. G. Chase, G. M. Shaw, T. F. Lotz, C. E. Hann, C. V. Doran, and D. S. Lee. Long term verification of glucose-insulin regulatory system model

dynamics. *Conf Proc IEEE Eng Med Biol Soc*, 1:758–761, 2004.

J. Lin, D. Lee, J. G. Chase, G. M. Shaw, A. Le Compte, T. Lotz, J. Wong, T. Lonergan, and C. E. Hann. Stochastic modelling of insulin sensitivity and adaptive glycemic control for critical care. *Comput Methods Programs Biomed*, 89:141–152, Feb 2008.

J. Lin, J. D. Parente, J. G. Chase, G. M. Shaw, A. J. Blakemore, A. J. Lecompte, C. Pretty, N. N. Razak, D. S. Lee, C. E. Hann, and S. H. Wang. Development of a model-based clinical sepsis biomarker for critically ill patients. *Comput Methods Programs Biomed*, 102:149–155, May 2011a.

J. Lin, N. N. Razak, C. G. Pretty, A. Le Compte, P. Docherty, J. D. Parente, G. M. Shaw, C. E. Hann, and J. Geoffrey Chase. A physiological Intensive Control Insulin-Nutrition-Glucose (ICING) model validated in critically ill patients. *Comput Methods Programs Biomed*, 102:192–205, May 2011b.

Jessica Lin, Dominic Lee, J. Geoffrey Chase, Geoffrey M. Shaw, Christopher E. Hann, Thomas Lotz, and Jason Wong. Stochastic modelling of insulin sensitivity variability in critical care. *Biomedical Signal Processing and Control*, 1(3):229 – 242, 2006. ISSN 1746-8094. doi: 10.1016/j.bspc.2006.09.003. URL http://www.sciencedirect.com/science/article/pii/S1746809406000462.

T. Lonergan, A. Le Compte, M. Willacy, J. G. Chase, G. M. Shaw, X. W. Wong, T. Lotz, J. Lin, and C. E. Hann. A simple insulin-nutrition protocol for tight glycemic control in critical illness: development and protocol comparison. *Diabetes Technol. Ther.*, 8:191–206, Apr 2006.

T. F. Lotz, J. G. Chase, K. A. McAuley, D. S. Lee, J. Lin, C. E. Hann, and J. I. Mann. Transient and steady-state euglycemic clamp validation of a model for glycemic control and insulin sensitivity testing. *Diabetes Technol. Ther.*, 8:338–346, Jun 2006.

T. F. Lotz, J. G. Chase, K. A. McAuley, G. M. Shaw, X. W. Wong, J. Lin, A. Lecompte, C. E. Hann, and J. I. Mann. Monte Carlo analysis of a new model-based method for insulin sensitivity testing. *Comput Methods Programs Biomed*, 89:215–225, Mar 2008.

F. R. Machado and B. F. Mazza. Improving mortality in sepsis: analysis of clinical trials. *Shock*, 34 Suppl 1:54–58, Sep 2010.

K. Malmberg. Prospective randomised study of intensive insulin treatment on long term survival after acute myocardial infarction in patients with diabetes mellitus. DIGAMI (Diabetes Mellitus, Insulin Glucose Infusion in Acute Myocardial Infarction) Study Group. *BMJ*, 314:1512–1515, May 1997.

K. Malmberg, A. Norhammar, H. Wedel, and L. Ryden. Glycometabolic state at admission: important risk marker of mortality in conventionally treated patients with diabetes mellitus and acute myocardial infarction: long-term results from the Diabetes and Insulin-Glucose Infusion in Acute Myocardial Infarction (DIGAMI) study. *Circulation*, 99:2626–2632, May 1999.

A. Mari. Assessment of insulin sensitivity and secretion with the labelled intravenous glucose tolerance test: improved modelling analysis. *Diabetologia*, 41:1029–1039, Sep 1998.

A. Mari, G. Pacini, E. Murphy, B. Ludvik, and J. J. Nolan. A model-based method for assessing insulin sensitivity from the oral glucose tolerance test. *Diabetes Care*, 24:539–548, Mar 2001.

P. E. Marik and M. Raghavan. Stress-hyperglycemia, insulin and immunomodulation in sepsis. *Intensive Care Med*, 30:748–756, May 2004.

P. E. Marik and J. Varon. Early goal-directed therapy: on terminal life support? *Am J Emerg Med*, 28:243–245, Feb 2010.

J. C. Marshall, D. J. Cook, N. V. Christou, G. R. Bernard, C. L. Sprung, and W. J. Sibbald. Multiple organ dysfunction score: a reliable descriptor of a complex clinical outcome. *Crit. Care Med.*, 23:1638–1652, Oct 1995.

J. C. Marshall, R. P. Dellinger, and M. Levy. The Surviving Sepsis Campaign: a history and a perspective. *Surg Infect (Larchmt)*, 11:275–281, Jun 2010.

G. S. Martin, D. M. Mannino, S. Eaton, and M. Moss. The epidemiology of sepsis in the United States from 1979 through 2000. *N. Engl. J. Med.*, 348: 1546–1554, Apr 2003.

L. Martin. *Exercise Physiology. Chapter 12: Pulmonary Physiology in Clinical Practice*. 1999.

P. S. Martins, E. G. Kallas, M. C. Neto, M. A. Dalboni, S. Blecher, and R. Salomao. Upregulation of reactive oxygen species generation and phagocytosis, and increased apoptosis in human neutrophils during severe sepsis and septic shock. *Shock*, 20:208–212, Sep 2003.

T. Masters. *Neural, novel and hybrid algorithms for time series prediction.*

John Wiley and Sons, Inc., United States of America, 1995.

C. Mayeur, S. Campard, C. Richard, and J. L. Teboul. Comparison of four different vascular occlusion tests for assessing reactive hyperemia using near-infrared spectroscopy. *Crit. Care Med.*, 39:695–701, Apr 2011.

K. C. McCowen, A. Malhotra, and B. R. Bistrian. Stress-induced hyperglycemia. *Crit Care Clin*, 17:107–124, Jan 2001.

I. A. Meynaar, L. Dawson, P. L. Tangkau, E. F. Salm, and L. Rijks. Introduction and evaluation of a computerised insulin protocol. *Intensive Care Med*, 33:591–596, Apr 2007.

S. T. Micek, E. C. Welch, J. Khan, M. Pervez, J. A. Doherty, R. M. Reichley, J. Hoppe-Bauer, W. M. Dunne, and M. H. Kollef. Resistance to empiric antimicrobial treatment predicts outcome in severe sepsis associated with Gram-negative bacteremia. *J Hosp Med*, 6:405–410, Sep 2011.

B. A. Mizock. Alterations in fuel metabolism in critical illness: hyperglycaemia. *Best Pract. Res. Clin. Endocrinol. Metab.*, 15:533–551, Dec 2001.

N. T. Mowery, O. L. Gunter, R. M. Kauffmann, J. J. Diaz, B. C. Collier, and A. K. May. Duration of Time on Intensive Insulin Therapy Predicts Severe Hypoglycemia in the Surgically Critically Ill Population. *World J Surg*, Nov 2011.

A. Natali, A. Gastaldelli, S. Camastra, A. M. Sironi, E. Toschi, A. Masoni, E. Ferrannini, and A. Mari. Dose-response characteristics of insulin action on glucose metabolism: a non-steady-state approach. *Am. J. Physiol. Endocrinol. Metab.*, 278:794–801, May 2000.

H. B. Nguyen, W. S. Kuan, M. Batech, P. Shrikhande, M. Mahadevan, C. H. Li, S. Ray, and A. Dengel. Outcome effectiveness of the severe sepsis resuscitation bundle with addition of lactate clearance as a bundle item: a multi-national evaluation. *Crit Care*, 15:R229, Sep 2011.

M. Oddo, M. D. Schaller, T. Calandra, and L. Liaudet. [New therapeutic strategies in severe sepsis and septic shock]. *Rev Med Suisse Romande*, 124: 329–332, Jun 2004.

R. O'Neill, J. Morales, and M. Jule. Early Goal-directed Therapy (EGDT) for Severe Sepsis/Septic Shock: Which Components of Treatment are More Difficult to Implement in a Community-based Emergency Department? *J Emerg Med*, May 2011.

C. Pachler, J. Plank, H. Weinhandl, L. J. Chassin, M. E. Wilinska, R. Kulnik, P. Kaufmann, K. H. Smolle, E. Pilger, T. R. Pieber, M. Ellmerer, and R. Hovorka. Tight glycaemic control by an automated algorithm with time-variant sampling in medical ICU patients. *Intensive Care Med*, 34:1224–1230, Jul 2008.

G. Pacini and R. N. Bergman. MINMOD: a computer program to calculate insulin sensitivity and pancreatic responsivity from the frequently sampled intravenous glucose tolerance test. *Comput Methods Programs Biomed*, 23: 113–122, Oct 1986.

R. Pareznik, R. Knezevic, G. Voga, and M. Podbregar. Changes in muscle tissue oxygenation during stagnant ischemia in septic patients. *Intensive Care Med*, 32:87–92, Jan 2006.

R. S. Parker, F. J. Doyle, and N. A. Peppas. A model-based algorithm for blood glucose control in type I diabetic patients. *IEEE Trans Biomed Eng*, 46:148–157, Feb 1999.

R. S. Parker, F. J. Doyle, and N. A. Peppas. The intravenous route to blood glucose control. *IEEE Eng Med Biol Mag*, 20:65–73, 2001.

J. E. Parrillo, M. M. Parker, C. Natanson, A. F. Suffredini, R. L. Danner, R. E. Cunnion, and F. P. Ognibene. Septic shock in humans. Advances in the understanding of pathogenesis, cardiovascular dysfunction, and therapy. *Ann. Intern. Med.*, 113:227–242, Aug 1990.

G. W. Patel, N. Roderman, H. Gehring, J. Saad, and W. Bartek. Assessing the effect of the Surviving Sepsis Campaign treatment guidelines on clinical outcomes in a community hospital. *Ann Pharmacother*, 44:1733–1738, Nov 2010.

J. F. Patino, S. E. de Pimiento, A. Vergara, P. Savino, M. Rodriguez, and J. Escallon. Hypocaloric support in the critically ill. *World J Surg*, 23: 553–559, Jun 1999.

A. Perel. Bench-to-bedside review: the initial hemodynamic resuscitation of the septic patient according to Surviving Sepsis Campaign guidelines–does one size fit all? *Crit Care*, 12:223, 2008.

T. M. Perl, L. Dvorak, T. Hwang, and R. P. Wenzel. Long-term survival and function after suspected gram-negative sepsis. *JAMA*, 274:338–345, Jul 1995.

M. Piagnerelli, K. Z. Boudjeltia, M. Vanhaeverbeek, and J. L. Vincent. Red

blood cell rheology in sepsis. *Intensive Care Med*, 29:1052–1061, Jul 2003.

G. Pillonetto, G. Sparacino, P. Magni, R. Bellazzi, and C. Cobelli. Minimal model S(I)=0 problem in NIDDM subjects: nonzero Bayesian estimates with credible confidence intervals. *Am. J. Physiol. Endocrinol. Metab.*, 282: E564–573, Mar 2002.

G. Pillonetto, G. Sparacino, and C. Cobelli. Numerical non-identifiability regions of the minimal model of glucose kinetics: superiority of Bayesian estimation. *Math Biosci*, 184:53–67, Jul 2003.

J. Plank, J. Blaha, J. Cordingley, M. E. Wilinska, L. J. Chassin, C. Morgan, S. Squire, M. Haluzik, J. Kremen, S. Svacina, W. Toller, A. Plasnik, M. Ellmerer, R. Hovorka, and T. R. Pieber. Multicentric, randomized, controlled trial to evaluate blood glucose control by the model predictive control algorithm versus routine glucose management protocols in intensive care unit patients. *Diabetes Care*, 29:271–276, Feb 2006.

P. Povoa, A. M. Teixeira-Pinto, and A. H. Carneiro. C-reactive protein, an early marker of community-acquired sepsis resolution: a multi-center prospective observational study. *Crit Care*, 15:R169, Jul 2011.

J. C. Preiser and P. Devos. Clinical experience with tight glucose control by intensive insulin therapy. *Crit. Care Med.*, 35:S503–507, Sep 2007.

J. C. Preiser, P. Devos, S. Ruiz-Santana, C. Melot, D. Annane, J. Groeneveld, G. Iapichino, X. Leverve, G. Nitenberg, P. Singer, J. Wernerman, M. Joannidis, A. Stecher, and R. Chiolero. A prospective randomised multi-centre controlled trial on tight glucose control by intensive insulin therapy in adult

intensive care units: the Glucontrol study. *Intensive Care Med*, 35:1738–1748, Oct 2009.

C. Pretty, J. G. Chase, J. Lin, G. M. Shaw, A. Le Compte, N. Razak, and J. D. Parente. Impact of glucocorticoids on insulin resistance in the critically ill. *Comput Methods Programs Biomed*, 102:172–180, May 2011.

S. A. Price, D. A. Spain, M. A. Wilson, P. D. Harris, and R. N. Garrison. Subacute sepsis impairs vascular smooth muscle contractile machinery and alters vasoconstrictor and dilator mechanisms. *J. Surg. Res.*, 83:75–80, May 1999.

R. L. Prigeon, M. E. R?der, D. Porte, and S. E. Kahn. The effect of insulin dose on the measurement of insulin sensitivity by the minimal model technique. Evidence for saturable insulin transport in humans. *J. Clin. Invest.*, 97: 501–507, Jan 1996.

D. Qi and B. Rodrigues. Glucocorticoids produce whole body insulin resistance with changes in cardiac metabolism. *Am. J. Physiol. Endocrinol. Metab.*, 292:E654–667, Mar 2007.

P. Ravishankaran, A. M. Shah, and R. Bhat. Correlation of interleukin-6, serum lactate, and C-reactive protein to inflammation, complication, and outcome during the surgical course of patients with acute abdomen. *J. Interferon Cytokine Res.*, 31:685–690, Sep 2011.

G. Reggiori, G. Occhipinti, A. De Gasperi, J. L. Vincent, and M. Piagnerelli. Early alterations of red blood cell rheology in critically ill patients. *Crit. Care Med.*, 37:3041–3046, Dec 2009.

E. Rivers, B. Nguyen, S. Havstad, J. Ressler, A. Muzzin, B. Knoblich, E. Peterson, and M. Tomlanovich. Early goal-directed therapy in the treatment of severe sepsis and septic shock. *N. Engl. J. Med.*, 345:1368–1377, Nov 2001.

R. A. Rizza, L. J. Mandarino, and J. E. Gerich. Dose-response characteristics for effects of insulin on production and utilization of glucose in man. *Am. J. Physiol.*, 240:E630–639, Jun 1981.

J. A. Roberts, M. S. Roberts, A. Semark, A. A. Udy, C. M. Kirkpatrick, D. L. Paterson, M. J. Roberts, P. Kruger, and J. Lipman. Antibiotic dosing in the 'at risk' critically ill patient: Linking pathophysiology with pharmacokinetics/pharmacodynamics in sepsis and trauma patients. *BMC Anesthesiol*, 11:3, 2011.

Y. Sakr, M. J. Dubois, D. De Backer, J. Creteur, and J. L. Vincent. Persistent microcirculatory alterations are associated with organ failure and death in patients with septic shock. *Crit. Care Med.*, 32:1825–1831, Sep 2004.

J. I. Salluh and T. Lisboa. C-reactive protein in community-acquired sepsis: you can teach new tricks to an old dog. *Crit Care*, 15:186, Sep 2011.

S. Samarasinghe. *Neural networks for applied sciences and engineering.* Auerbach Publications, Taylor and Francis Group, United States of America, 2007.

Y. U. Sarikabadayi, O. Aydemir, C. Aydemir, N. Uras, S. S. Oguz, O. Erdeve, and U. Dilmen. Umbilical cord oxidative stress in infants of diabetic mothers and its relation to maternal hyperglycemia. *J. Pediatr. Endocrinol. Metab.*,

24:671–674, 2011.

M. Savioli, M. Cugno, F. Polli, P. Taccone, G. Bellani, P. Spanu, A. Pesenti, G. Iapichino, and L. Gattinoni. Tight glycemic control may favor fibrinolysis in patients with sepsis. *Crit. Care Med.*, 37:424–431, Feb 2009.

B. Schrag, P. Roux-Lombard, D. Schneiter, P. Vaucher, P. Mangin, and C. Palmiere. Evaluation of C-reactive protein, procalcitonin, tumor necrosis factor alpha, interleukin-6, and interleukin-8 as diagnostic parameters in sepsis-related fatalities. *Int J Legal Med*, Jul 2011.

P. Schuetz, W. Albrich, and B. Mueller. Procalcitonin for diagnosis of infection and guide to antibiotic decisions: past, present and future. *BMC Med*, 9: 107, 2011.

L. Shan, P. P. Hao, and Y. G. Chen. Efficacy and safety of intensive insulin therapy for critically ill neurologic patients: a meta-analysis. *J Trauma*, 71: 1460–1464, Nov 2011.

R. E. Shangraw, F. Jahoor, H. Miyoshi, W. A. Neff, C. A. Stuart, D. N. Herndon, and R. R. Wolfe. Differentiation between septic and postburn insulin resistance. *Metab. Clin. Exp.*, 38:983–989, Oct 1989.

R. Shulman, S. J. Finney, C. O'Sullivan, P. A. Glynne, and R. Greene. Tight glycaemic control: a prospective observational study of a computerised decision-supported intensive insulin therapy protocol. *Crit Care*, 11:R75, 2007.

W. J. Sibbald and J. L. Vincent. Round table conference on clinical trials for the treatment of sepsis. *Crit. Care Med.*, 23:394–399, Feb 1995.

P. Sidenius. The axonopathy of diabetic neuropathy. *Diabetes*, 31:356–363, Apr 1982.

N. Sivayoham, A. Rhodes, T. Jaiganesh, N. van Zyl Smit, S. Elkhodhair, and S. Krishnanandan. Outcomes from implementing early goal-directed therapy for severe sepsis and septic shock : a 4-year observational cohort study. *Eur J Emerg Med*, Sep 2011.

P. E. Spronk, D. F. Zandstra, and C. Ince. Bench-to-bedside review: sepsis is a disease of the microcirculation. *Crit Care*, 8:462–468, Dec 2004.

B. Suberviola, A. Castellanos-Ortega, A. Gonzalez-Castro, L. A. Garcia-Astudillo, and B. Fernandez-Miret. Prognostic value of procalcitonin, C-reactive protein and leukocytes in septic shock. *Med Intensiva*, Nov 2011.

F. Suhaimi, A. Le Compte, J. C. Preiser, G. M. Shaw, P. Massion, R. Radermecker, C. G. Pretty, J. Lin, T. Desaive, and J. G. Chase. What makes tight glycemic control tight? The impact of variability and nutrition in two clinical studies. *J Diabetes Sci Technol*, 4:284–298, Mar 2010.

B. E. Sumpio, J. T. Riley, and A. Dardik. Cells in focus: endothelial cell. *Int. J. Biochem. Cell Biol.*, 34:1508–1512, Dec 2002.

F. S. Taccone, D. de Backer, P. F. Laterre, H. Spapen, T. Dugernier, I. Delattre, P. Wallemacq, J. L. Vincent, and F. Jacobs. Pharmacokinetics of a loading dose of amikacin in septic patients undergoing continuous renal replacement therapy. *Int. J. Antimicrob. Agents*, 37:531–535, Jun 2011a.

F. S. Taccone, M. Hites, M. Beumier, S. Scolletta, and F. Jacobs. Appropriate antibiotic dosage levels in the treatment of severe sepsis and septic shock.

Curr Infect Dis Rep, 13:406–415, Oct 2011b.

G. Takahashi, N. Matsumoto, T. Shozushima, C. Onodera, S. Kan, S. Akitomi, K. Hoshikawa, T. Kikkawa, M. Kojika, Y. Inoue, K. Suzuki, G. Wakabayashi, and S. Endo. Retrospective study on the effect of tight glucose control in postoperative sepsis patients using an artificial pancreas. *J Infect Chemother*, Jun 2011.

J. Textoris, S. Wiramus, C. Martin, and M. Leone. Antibiotic therapy in patients with septic shock. *Eur J Anaesthesiol*, 28:318–324, May 2011.

A. N. Thomas, A. E. Marchant, M. C. Ogden, and S. Collin. Implementation of a tight glycaemic control protocol using a web-based insulin dose calculator. *Anaesthesia*, 60:1093–1100, Nov 2005.

G. Toffolo, W. T. Cefalu, and C. Cobelli. Beta-cell function during insulin-modified intravenous glucose tolerance test successfully assessed by the C-peptide minimal model. *Metab. Clin. Exp.*, 48:1162–1166, Sep 1999.

G. Toffolo, M. Campioni, R. Basu, R. A. Rizza, and C. Cobelli. A minimal model of insulin secretion and kinetics to assess hepatic insulin extraction. *Am. J. Physiol. Endocrinol. Metab.*, 290:E169–E176, Jan 2006.

P. Toft and E. Tonnesen. Immune-modulating interventions in critically ill septic patients: pharmacological options. *Expert Rev Clin Pharmacol*, 4: 491–501, Jul 2011.

D. F. Treacher and R. M. Leach. Oxygen transport-1. Basic principles. *BMJ*, 317(7168):1302–1306, 11 1998.

M. Tromp, D. H. Tjan, A. R. van Zanten, S. E. Gielen-Wijffels, G. J. Goekoop, M. van den Boogaard, C. M. Wallenborg, H. S. Biemond-Moeniralam, and P. Pickkers. The effects of implementation of the Surviving Sepsis Campaign in the Netherlands. *Neth J Med*, 69:292–298, Jun 2011.

E. L. Tsalik, L. B. Jaggers, S. W. Glickman, R. J. Langley, J. C. van Velkinburgh, L. P. Park, V. G. Fowler, C. B. Cairns, S. F. Kingsmore, and C. W. Woods. Discriminative Value of Inflammatory Biomarkers for Suspected Sepsis. *J Emerg Med*, Nov 2011.

S. K. Turi and D. Von Ah. Implementation of Early Goal-directed Therapy for Septic Patients in the Emergency Department: A Review of the Literature. *J Emerg Nurs*, Jul 2011.

M. Turina, D. E. Fry, and H. C. Polk. Acute hyperglycemia and the innate immune system: clinical, cellular, and molecular aspects. *Crit. Care Med.*, 33:1624–1633, Jul 2005.

R. Uusitalo-Sepp L, P. Koskinen, A. Leino, H. Peuravuori, T. Vahlberg, and E. M. Rintala. Early detection of severe sepsis in the emergency room: Diagnostic value of plasma C-reactive protein, procalcitonin, and interleukin-6. *Scand. J. Infect. Dis.*, 43:883–890, Dec 2011.

B. Vallet. Endothelial cell dysfunction and abnormal tissue perfusion. *Crit. Care Med.*, 30:S229–234, May 2002.

G. Van den Berghe, P. Wouters, F. Weekers, C. Verwaest, F. Bruyninckx, M. Schetz, D. Vlasselaers, P. Ferdinande, P. Lauwers, and R. Bouillon. Intensive insulin therapy in the critically ill patients. *N. Engl. J. Med.*, 345:

1359–1367, Nov 2001.

G. Van den Berghe, P. J. Wouters, R. Bouillon, F. Weekers, C. Verwaest, M. Schetz, D. Vlasselaers, P. Ferdinande, and P. Lauwers. Outcome benefit of intensive insulin therapy in the critically ill: Insulin dose versus glycemic control. *Crit. Care Med.*, 31:359–366, Feb 2003.

G. Van den Berghe, A. Wilmer, G. Hermans, W. Meersseman, P. J. Wouters, I. Milants, E. Van Wijngaerden, H. Bobbaers, and R. Bouillon. Intensive insulin therapy in the medical ICU. *N. Engl. J. Med.*, 354:449–461, Feb 2006a.

G. Van den Berghe, A. Wilmer, I. Milants, P. J. Wouters, B. Bouckaert, F. Bruyninckx, R. Bouillon, and M. Schetz. Intensive insulin therapy in mixed medical/surgical intensive care units: benefit versus harm. *Diabetes*, 55:3151–3159, Nov 2006b.

Sherman J. Vander, A. and D.. Luciano. *Human Physiology: The Mechanisms of Body Function.* McGraw-Hill, New York, eighth edition edition, 2001.

I. Vanhorebeek, L. Langouche, and G. Van den Berghe. Tight blood glucose control: what is the evidence? *Crit. Care Med.*, 35:496–502, Sep 2007a.

I. Vanhorebeek, L. Langouche, and G. Van den Berghe. Tight blood glucose control with insulin in the ICU: facts and controversies. *Chest*, 132:268–278, Jul 2007b.

V. M. Victor, M. Rocha, and M. De la Fuente. Immune cells: free radicals and antioxidants in sepsis. *Int. Immunopharmacol.*, 4:327–347, Mar 2004.

V. M. Victor, J. V. Espulgues, A. Hernandez-Mijares, and M. Rocha. Oxidative stress and mitochondrial dysfunction in sepsis: a potential therapy with mitochondria-targeted antioxidants. *Infect Disord Drug Targets*, 9: 376–389, Aug 2009.

J. L. Vincent, R. Moreno, J. Takala, S. Willatts, A. De Mendonca, H. Bruining, C. K. Reinhart, P. M. Suter, and L. G. Thijs. The SOFA (Sepsis-related Organ Failure Assessment) score to describe organ dysfunction/failure. On behalf of the Working Group on Sepsis-Related Problems of the European Society of Intensive Care Medicine. *Intensive Care Med*, 22:707–710, Jul 1996.

J. L. Vincent, A. de Mendonca, F. Cantraine, R. Moreno, J. Takala, P. M. Suter, C. L. Sprung, F. Colardyn, and S. Blecher. Use of the SOFA score to assess the incidence of organ dysfunction/failure in intensive care units: results of a multicenter, prospective study. Working group on "sepsis-related problems" of the European Society of Intensive Care Medicine. *Crit. Care Med.*, 26:1793–1800, Nov 1998.

A. Virkamaki and H. Yki-Jarvinen. Mechanisms of insulin resistance during acute endotoxemia. *Endocrinology*, 134:2072–2078, May 1994.

D. Vlasselaers, I. Milants, L. Desmet, P. J. Wouters, I. Vanhorebeek, I. van den Heuvel, D. Mesotten, M. P. Casaer, G. Meyfroidt, C. Ingels, J. Muller, S. Van Cromphaut, M. Schetz, and G. Van den Berghe. Intensive insulin therapy for patients in paediatric intensive care: a prospective, randomised controlled study. *Lancet*, 373:547–556, Feb 2009.

J. A. Wagner, H. Langenfeld, L. Klett, and S. Stork. Activated protein C in

patients with septic shock: a consecutive case series. *Int J Clin Pharm*, Nov 2011.

A. J. Walkey, R. S. Wiener, J. M. Ghobrial, L. H. Curtis, and E. J. Benjamin. Incident stroke and mortality associated with new-onset atrial fibrillation in patients hospitalized with severe sepsis. *JAMA*, 306:2248–2254, Nov 2011.

F. Weekers, A. P. Giulietti, M. Michalaki, W. Coopmans, E. Van Herck, C. Mathieu, and G. Van den Berghe. Metabolic, endocrine, and immune effects of stress hyperglycemia in a rabbit model of prolonged critical illness. *Endocrinology*, 144:5329–5338, Dec 2003.

C. Weissman. Nutrition in the intensive care unit. *Crit Care*, 3:67–75, 1999.

A. P. Wheeler and G. R. Bernard. Treating patients with severe sepsis. *N. Engl. J. Med.*, 340:207–214, Jan 1999.

W. J. Wiersinga. Current insights in sepsis: from pathogenesis to new treatment targets. *Curr Opin Crit Care*, 17:480–486, Oct 2011.

R. R. Wolfe, J. R. Allsop, and J. F. Burke. Glucose metabolism in man: responses to intravenous glucose infusion. *Metab. Clin. Exp.*, 28:210–220, Mar 1979.

R. R. Wolfe, D. N. Herndon, F. Jahoor, H. Miyoshi, and M. Wolfe. Effect of severe burn injury on substrate cycling by glucose and fatty acids. *N. Engl. J. Med.*, 317:403–408, Aug 1987.

X. W. Wong, J. G. Chase, G. M. Shaw, C. E. Hann, T. Lotz, J. Lin, I. Singh-Levett, L. J. Hollingsworth, O. S. Wong, and S. Andreassen. Model predic-

tive glycaemic regulation in critical illness using insulin and nutrition input: a pilot study. *Med Eng Phys*, 28:665–681, Sep 2006a.

X. W. Wong, I. Singh-Levett, L. J. Hollingsworth, G. M. Shaw, C. E. Hann, T. Lotz, J. Lin, O. S. Wong, and J. G. Chase. A novel, model-based insulin and nutrition delivery controller for glycemic regulation in critically ill patients. *Diabetes Technol. Ther.*, 8:174–190, Apr 2006b.

G. Xi, X. Shen, L. A. Maile, C. Wai, K. Gollahon, and D. R. Clemmons. Hyperglycemia Enhances IGF-I-Stimulated Src Activation via Increasing Nox4-Derived Reactive Oxygen Species in a PKCëę-Dependent Manner in Vascular Smooth Muscle Cells. *Diabetes*, Dec 2011.

Y. J. Yang, J. H. Youn, and R. N. Bergman. Modified protocols improve insulin sensitivity estimation using the minimal model. *Am. J. Physiol.*, 253:595–602, Dec 1987.